CONTRIBUTORS TO THIS VOLUME

Matteo Adinolfi, John Crolla, Harry C. Dietz, Régen Drouin, Vincent J. Hearing, Jr. Gerald P. Holmquist, James R. Lupski, Francesco Ramirez, Claude-Lise Richer, Benjamin B. Roa, Lynn S. Sakai, Richard A. Spritz

Edited by
H. Harris and
K. Hirschhorn

22

Advances in HUMAN GENETICS

ADVANCES IN HUMAN GENETICS 22

CONTRIBUTORS TO THIS VOLUME

Matteo Adinolfi
Division of Medical & Molecular Genetics
United Medical and Dental Schools
Guy's and St. Thomas's Hospitals
London Bridge, London, England

John Crolla
Wessex Regional Genetics Laboratory
Salisbury District Hospital
Salisbury, Wiltshire, England

Harry C. Dietz
Departments of Pediatrics, Medicine,
and Molecular Biology and Genetics
Johns Hopkins School of Medicine
Baltimore, Maryland

Régen Drouin
Research Unit in Human and
Molecular Genetics
Saint Francis of Assisi Hospital
Research Center
Laval University, Montreal, Quebec, Canada

Vincent J. Hearing, Jr.
Laboratory of Cell Biology
National Cancer Institute
National Institutes of Health
Bethesda, Maryland

Gerald P. Holmquist
Division of Biology
Beckman Research Institute of the City of Hope
Duarte, California

James R. Lupski
Departments of Molecular and Human
Genetics,
Pediatrics and Human Genome Center
Baylor College of Medicine
Houston, Texas, and Texas Children's Hospital
Houston, Texas

Francesco Ramirez
Brookdale Center for Molecular Biology
Mount Sinai School of Medicine
New York, New York

Claude-Lise Richer
Department of Anatomy
University of Montreal,
Montreal, Quebec, Canada, and
Department of Pathology and Pediatric
Research Center
Saint Justine Hospital, Montreal, Quebec,
Canada

Benjamin B. Roa
Department of Molecular and Human Genetics
Baylor College of Medicine
Houston, Texas

Lynn S. Sakai
Shriners Hospital for Crippled Children
and Department of Biochemistry
and Molecular Biology
Oregon Health Sciences University
Portland, Oregon

Richard A. Spritz
Departments of Medical Genetics and
Pediatrics
University of Wisconsin
Madison, Wisconsin

ADVANCES IN HUMAN GENETICS 22

Edited by

Harry Harris

Former Harnwell Professor of Human Genetics
Late of University of Pennsylvania, Philadelphia

and

Kurt Hirschhorn

Herbert H. Lehman Professor and Chairman of Pediatrics
Mount Sinai School of Medicine of The City University of New York

Springer Science+Business Media, LLC

The Library of Congress catalogued the first volume of this title as follows:

Advances in human genetics. 1–
New York, PLenum Press, 1970–
(1) v. illus. 24-cm.
Editors: V. 1– H. Harris and K. Hirschhorn.
1. Human genetics—Collected works. I. Harris, Harry, ed. II. Hirschhorn, Kurt, 1926– joint ed.

QH431.A1A32 573.2'1 77-84583

ISBN 978-1-4757-9064-1 ISBN 978-1-4757-9062-7 (eBook)
DOI 10.1007/978-1-4757-9062-7

Originally published by Plenum Press, New York in 1994.
Softcover reprint of the hardcover 1st edition 1994

HARRY HARRIS, M.D.

September 1919–July 1994

It is with great sadness that I note the passing of my dear friend and co-editor, **Harry Harris, M.D.** He, more than anyone in the field, was the ultimate symbol of Human Biochemical Genetics. His numerous contributions over the years developed and clarified the concept of biochemical polymorphism to demonstrate genetic individuality and uniqueness of all human beings. His careful study of biochemical variation included, as well, the clarification of a number of inborn errors of metabolism. In that, he was the natural heir of Garrod, who was one of his heroes.

I first met Harry when I was a Fellow in Human Genetics and visited him at the London Hospital where he had begun his work on electrophoresis and chromatography to demonstrate individual variation in enzymes. I spent two magnificent Sabbaticals with him, the first at Kings College Medical School and the second at the Galton Laboratory. These experiences allowed me to appreciate Harry as one of the truly great minds in the field of Human Genetics.

This series, *Advances in Human Genetics*, was founded during a discussion with the late Alan Liss, at that time the Vice President of Plenum Press, during an informal conversation on a beach in Cape Cod. While Harry, always a skeptic, expressed doubts that we could fill even a single volume, the response of all in the field led to the 110 contributions in the 22 volumes so far published. This current volume is dedicated to his memory. It is in his memory that I will continue to work on additional volumes of the series, and I am most gratified that Robert J. Desnick, Ph.D., M.D., Chairman of the Department of Human Genetics at Mount Sinai School of Medicine, will join me as the new co-editor in this effort.

—KH

ARTICLES PLANNED FOR FUTURE VOLUMES

Biochemical Defects in Immunodeficiency • *Rochelle Hirschhorn*
Advances in Prenatal Genetic Diagnosis • *John C. Hobbins and Maurice J. Mahoney*
Malformation Syndromes Caused by Single Gene Defects • *Judith G. Hall*
Genetic Screening Using the Tay Sachs Model • *Michael M. Kaback*
Genetics of Hormone Receptors and Their Abnormalities • *Jesse Roth and Simeon I. Taylor*
Theory and Practice of Gene Mapping, Including Multipoint Linkage Analysis •*Eric S. Lander*
Organization and Genetics of Satellite DNA Families in the Human Genome •
Huntington F. Willard
Primary Sex Determination and Its Aberrations in Man • *Malcolm A. Ferguson-Smith*
The Molecular Genetics of Polycystic Kidney Disease • *Stephen T. Reeders*
Triplet Amplification • *C. Thomas Caskey and Huda Zoghbi*

CONTENTS OF EARLIER VOLUMES

VOLUME 1 (1970)
Analysis of Pedigree Data • *J. H. Edwards*
Autoradiography in Human Cytogenetics • *Orlando J. Miller*
Genetics of Immunoglobulins • *H. Hugh Fudenberg and Noel E. Warner*
Human Genetics of Membrane Transport with Emphasis on Amino Acids •
Charles R. Scriver and Peter Hechtman
Genetics of Disorders of Intestinal Digestion and Absorption • *Jean Frézal and Jean Rey*

VOLUME 2 (1971)
Glucose-6-Phosophate Dehydrogenase • *Henry N. Kirkman*
Albinism • *Carl J. Witkop, Jr.*
Acatalasemia • *Hugo Aebi and Hedi Suter*
Chromosomes and Abortion • *D. H. Carr*
A Biochemical Genetic View of Human Cell Culture • *William J. Mellman*

VOLUME 3 (1972)
Prenatal Detection of Genetic Disorders • *Henry I. Nadler*
Ganglioside Storage Diseases • *John S. O' Brien*
Induced Chromosomal Aberrations in Man • *Arthur D. Bloom*
Linkage Analysis Using Somatic Cell Hybrids • *Frank H. Ruddle*
The Structure and Function of Chromatin • *David E. Comings*

VOLUME 4 (1973)
Genetic Screening • *Harvey L. Levy*
Human Population Structure • *Chris Cannings and L. Cavalli-Sforza*
Status and Prospects of Research in Hereditary Deafness • *Walter E. Nance and*
Freeman E. McConnell
Congenital Adrenal Hyperplasia • *Maria I. New and Lenore S. Levine*
Cytogenetic Aspects of Human Male Meiosis • *Maj Hultén and J. Lindsten*

VOLUME 5 (1975)
The Chondrodystrophies • *David L. Rimoin*
New Techniques in the Study of Human Chromosomes: Methods and Applications • *Bernard Dutrillaux and Jerome Lejeune*
The Thalassemias: Models for Analysis of Quantitative Gene Control • *David Kabat and Robert D. Koler*
Spontaneous Mutation in Man • *Friedrich Vogel and Rüdiger Rathenberg*
Genetic Screening Legislation • *Philip Reilly*

VOLUME 6 (1976)
Vitamin-Responsive Inherited Metabolic Disorders • *Leon E. Rosenberg*
Inherited Deficiency of Hypoxanthine-Guanine Phosphoribosyltransferase in X-Linked Uric Aciduria • *J. Edwin Seegmiller*
Hereditary Hemolytic Anemia Due to Enzyme Defects of Glycolysis • *Sergio Piomelli and Laurence Corash*
Population Structure of the Åland Islands, Finland • *James H. Mielke, Peter L. Workman, Johan Fellman, and Aldur W. Eriksson*
Population Genetics amd Health Care Delivery: The Quebec Experience • *Claude Laberge*

VOLUME 7 (1976)
Biochemical Genetics of Carbonic Anhydrase • *Richard E. Tashian and Nicholas D. Carter*
Human Behavior Genetics • *Barton Childs, Joan M. Finucci, Malcolm S. Preston, and Ann E. Pulver*
Mammalian X-Chromosome Inactivation • *Stanley M. Gartler and Robert J. Andina*
Genetics of the Complement System • *Chester A. Alper and Fred S. Rosen*
Selective Systems in Somatic Cell Genetics • *Ernest H. Y. Chu and Sandra S. Powell*

VOLUME 8 (1977)
Genetics and Etiology of Human Cancer • *Alfred G. Knudson, Jr.*
Population Genetics Theory in Relation to the Neutralist-Selectionist Controversy • *Warren J. Ewens*
The Human α–Amylases • *A. Donald Merrit and Robert C. Karn*
The Genetic Aspects of Facial Abnormalities • *Robert J. Gorlin and William S. Boggs*
Some Facts and Fancies Relating to Chromosome Structure in Man • *H. J. Evans*

VOLUME 9 (1979)
Chromosome and Neoplasia • *David G. Harnden and A. M. R. Taylor*
Terminological, Diagnostic Nosological, and Anatomical-Developmental Aspects of Developmental Defects in Man • *John M. Opitz, Jürgen Herrmann, James C. Pettersen, Edward T. Bersu, and Sharon C. Colacino*
Human Alphafetoprotein 1956-1978 • *Matteo Adinolfi*
Genetic Mechanisms Contributing to the Expression of the Human Hemoglobin Loci • *William P. Winter, Samir M. Hanash, and Donald L. Rucknagel*
Genetic Aspects of Folate Metabolism • *Richard W. Erbe*

VOLUME 10 (1980)

Biochemistry and Genetics of the ABO, Lewis, and P Blood Group Systems • *Winifred M. Watkins*

HLA— A Central Immunological Agency of Man • *D. Bernard Amos and D. D. Kostyu*

Linkage Analysis in Man • *P. Michael Conneally and Marian L. Rivas*

Sister Chromatid Exchanges • *Samuel A. Latt, Rhona R. Schreck, Kenneth S. Loveday, Charlotte P. Dougherty, and Charles F. Shuler*

Genetic Disorders of Male Sexual Differentiation • *Kaye R. Fichman, Barbara R. Migeon, and Claude J. Migeon*

VOLUME 11 (1981)

The Pi Polymorphism: Genetic, Biochemical, and Clinical Aspects of Human α-Antitrypsin • *Magne K. Fagerhol and Diane Wilson Cox*

Segregation Analysis • *R. C. Elston*

Genetic, Metabolic, and Biochemical Aspects of the Prophyrias • *Shigeru Sassa and Attallah Kappas*

The Molecular Genetics of Thalassemia • *Stuart H. Orkin and David G. Nathan*

Advances in the Treatment of Inherited Metabolic Diseases • *Robert J. Desnick and Gregory A. Gravowski*

VOLUME 12 (1982)

Genetic Disorders of Collagen Metabolism • *David W. Hollister, Peter H. Beyers, and Karen A. Holbrook*

Advances in Genetics in Dermatology • *Howard P. Baden and Philip A. Hooker*

Haptoglobin: The Evolutionary Product of Duplication, Unequal Crossing over, and Point Mutation • *Barbara H. Bowman and Alexander Kurosky*

Models of Human Genetic Disease in Domestic Animals • *D. F. Patterson, M. E. Haskins, and P. F. Jezyk*

Mapping the Human Genome, Cloned Genes, DNA Polymorphisms, and Inherited Disease • *Thomas B. Shows, Alan Y. Sakaguchi, and Susan L. Naylor*

VOLUME 13 (1983)

The Genetics of Blood Coagulation • *John B. Graham, Emily S. Barrow, Howard M. Reisner, and Cora-Jean S. Edgell*

Marker (X)-Linked Mental Retardation • *Gillian Turner and Patricia Jacobs*

Human Antibody Genes: Evolutionary and Molecular Genetic Perspectives • *Jay W. Ellison and Leroy E. Hood*

Mutations Affecting Trace Elements in Humans and Animals: A Genetic Approach to an Understanding of Trace Elements • *D. M. Danks and J. Camakaris*

Phenylketonuria and Its Variants • *Seymour Kaufman*

VOLUME 14 (1985)

Cytogenetics of Pregnancy Wastage • *Andre Boué, Alfred Gropp, and Joëlle Boué*

MuMutation in Human Populations • *James F. Crow and Carter Denniston*

Genetic Mutations Affecting Human Lipoprotein Metabolism • *Vassilis I. Zannis and Jan L. Breslow*

Glucose-6-Phosphate Dehydrogenase • *L. Luzzato and G. Battistuzzi*

Steroid Sulfatase Deficiency and the Genetics of the Short Arm of the Human X Chromosome • *Larry J. Shapiro*

VOLUME 15 (1986)

Chromosomal Abnormalities in Leukemia and Lymphoma: Clinical and Biological Significance • *Michelle M. Le Beau and Janet D. Rowley*

An Algorithm for Comparing Two-Dimensional Electrophoretic Gels, with Particular Reference to the Study of Mutation • *Michael M. Skolnick and James V. Neel*

The Human Argininosuccinate Synthetase Locus and Citrullinemia • *Arthur L. Beaudet, William E. O'Brian, Hans-Georg O. Bock, Svend O. Freytag, and Tsung-Sheng Su*

Molecular Genetics of the Human Histocompatibility Complex • *Charles Auffray and Jack L. Strominger*

Genetics of Human Alcohol and Aldehyde Dehydrogenases • *Moyra Smith*

VOLUME 16 (1987)

Genetics of Lactose Digestion in Humans • *Gebhard Flatz*

Perspectives in the Teaching of Human Genetics • *Ronald G. Davidson and Barton Childs*

Investigation of Genetic Linkage in Human Families • *Ray White and Jean-Mark Lalouel*

Chronic Granulomatous Disease • *John T. Curnutte and Bernard M. Babior*

Genetics of Steroid Receptors and Their Disorders • *Leonard Pinksky and Morris Kaufman*

VOLUME 17 (1988)

Chorionic Villus Sampling • *James D. Goldberg and Mitchell S. Globus*

The Molecular Genetics of Hemophilia A and B in Man: Factor VIII and Factor IX Deficiency • *Stylianos E. Antonarakis*

Cloning of the Duchenne/Becker Muscular Dystrophy Locus • *Anthony P. Monaco and Louis M. Kunkel*

Trisomy 21: Molecular and Cytogenetic Studies of Nondisjunction • *Gordon D. Stewart, Terry J. Hassold, and David M. Kurnit*

Molecular Gentics of Human Salivary Proteins and Their Polymorphisms • *Edwin A. Azen and Nobuyo Maeda*

VOLUME 18 (1989)

The Molecular Basis of HLA-Disease Association • *J. I. Bell, J. A. Todd, and H. O. McDevitt*

Chromosome Instability Syndromes • *Maimon M. Cohen and Howard P. Levy*

Lacticademia: Biochemical, Clinical and Genetic Considerations • *Brian H. Robinson*

A Comprehensive and Critical Assessment of Overgrowth and Overgrowth Syndromes • *M. Michael Cohen, Jr.*

Genetics of Growth Hormone and Its Disorders • *John A. Phillips III and Cindy L. Vnencak-Jones*

VOLUME 19 (1990)

The Lethal Osteochondrodysplasias • *Jürgen Spranger and Pierre Maroteaux*

Mutations in Type I Procollagen Genes that Cause Osteogenesis Imperfecta • *Darwin J. Prockop, Clinton T. Baldwin, and Constantinos D. Constantinou*

Structural Defects in Inherited and Giant Platelet Disorders • *James G. White*

Genetic Aspects of Immunoglobulin A Deficiency • *Charlotte Cunningham-Rundles*

Oxidative Phosphorylation Diseases: Disorders of Two Genomes • *John M. Shoffner IV and Douglas C. Wallace*

VOLUME 20 (1991)

Clinical and Molecular Genetics of Congenital Adrenal Hyperplasia Due to 21-Hydroxylase Deficiency • *Yves Morel and Walter L. Miller*

Genetic Aspects of Amyloidosis • *Daniel R. Jacobson and Joel N. Buxbaum*

Huntington's Disease • *James F. Gusella*

Biochemical and Molecular Genetics of Cystic Fibrosis • *Lap-Chee Tsui and Manuel Buchwald*

Molecular Genetics of von Recklinghausen Neurofibromatosis • *Margaret R. Wallace and Francis S. Collins*

VOLUME 21 (1993)

Peroxisomal Diseases • *Hugo W. Moser*

X-Linked Immunodeficiencies • *Jennifer M. Puck*

Genetic Mutations Affecting Human Lipoproteins, Their Receptors, and Their Enzymes • *Vassilis I. Zannis, Dimitris Kardassis, and Eleni Economou Zanni*

Genetic Aspects of Cancer • *Audrey D. Goddard and Ellen Solomon*

Gaucher Disease: Enzymology, Genetics, and Treatment • *Gregory A. Grabowski*

Preface to Volume 1

During the last few years the science of human genetics has been expanding almost explosively. Original papers dealing with different aspects of the subject are appearing at an increasingly rapid rate in a very wide range of journals, and it becomes more and more difficult for the geneticist and virtually impossible for the nongeneticist to keep track of the developments. Furthermore, new observations and discoveries relevant to an overall understanding of the subject result from investigations using very diverse techniques and methodologies and originating in a variety of different disciplines. Thus, investigations in such various fields as enzymology, immunology, protein chemistry, cytology, pediatrics, neurology, internal medicine, anthropology, and mathematical and statistical genetics, to name but a few, have each contributed results and ideas of general significance to the study of human genetics. Not surprisingly it is often difficult for workers in one branch of the subject to assess and assimilate findings made in another. This can be a serious limiting factor on the rate of progress.

Thus, there appears to be a real need for critical review which summarizes the positions reached in different areas, and it is hoped that *Advances in Human Genetics* will help to meet this requirement.

Each of the contributors has been asked to write an account of the position that has been reached in the investigations of a specific topic in one of the branches of human genetics. The reviews are intended to be critical and to deal with the topic in depth from the writer's own point of view. It is hoped that the articles will provide workers in other branches of the subject, and in related disciplines, with a detailed account of the results so far obtained in the particular area, and help them to assess the relevance of these discoveries to aspects of their own work, as well as to the science as a whole. The reviews are also intended to give the reader some idea of the nature of the technical and methodological problems involved, and to indicate new directions stemming from recent advances.

The contributors have not been restricted in the arrangement or organization

of their material or in the manner of its presentation, so that the reader should be able to appreciate something of the individuality of approach which goes to make up the subject of human genetics, and which, indeed, gives it much of its fascination.

HARRY HARRIS
The Galton Laboratory
University College London

KURT HIRSCHHORN
Division of Medical Genetics
Department of Pediatrics
Mount Sinai School of Medicine

Preface to Volume 10

This is the tenth volume of *Advances in Human Genetics* and some fifty different reviews covering a very wide range of topics have now appeared. Many of the earlier articles still stand as valuable sources of reference. But the subject continues to move forward at an increasing speed and its vitality is indicated by its remarkable recruitment of young investigators. New areas of research which could hardly have been envisaged only a few years ago have emerged, and quite unexpectedly discoveries have been made in parts of the subject which only recently had come to be thought as fully explored. So there continues to be a need for authoritative and critical reviews intended to keep workers in the various branches of this seemingly ever-expanding subject fully informed about the progress that is being made and also, of course, to provide a ready and accessible account of new developments in human genetics for those whose primary interests are in other fields of biological and medical research.

We see no reason to alter the general policy which was outlined in the preface to the first volume. We believe that it has served our readers well. The subject seems to us to be just as exciting and intellectually stimulating and rewarding as it did when this series was first started. We expect the next decade of research in human genetics to be as innovative and productive as the last and our aim is to record its progress in *Advances in Human Genetics*.

HARRY HARRIS
University of Pennsylvania, Philadelphia

KURT HIRSCHHORN
Mount Sinai School of Medicine of the City University of New York

Contents

Chapter 1

Genetic Disorders of Pigmentation

Richard A. Spritz and Vincent J. Hearing, Jr.

Introduction 1
The Mammalian Pigmentary System 2
Disorders of Melanocyte Function 8
Albinism 8
Type I (Tyrosinase-Deficient) OCA (MIM #203100) 8
Type II (Tyrosinase-Positive) OCA (MIM #203200) 15
Type IV (Brown) OCA (MIM #203290) 19
X-linked Recessive Ocular Albinism, Nettleship-Falls Type (OA1; MIM #300500) 20
Disorders of Melanocyte Development: Piebaldism and Waardenburg Syndrome 21
Piebaldism (MIM #172800) 21
Waardenburg Syndrome (MIM #193500) 26
Other Cloned Genes Affecting Pigmentation in the Mouse 29
Mottled 30
Pallid 30
Pearl 31
Microphthalmia 31
Dilute 32
Extension 32
Agouti 32
Slaty 33

Silver 34
References 34

Chapter 2

High-Resolution Replication Bands Compared with Morphologic G- and R-Bands

Régen Drouin, Gerald P. Holmquist, and Claude-Lise Richer

Introduction 47
Arrest of DNA Replication by DNA Synthesis Inhibitors 51
BrdUrd Incorporation and S-Phase 53
BrdUrd Detection 58
Fluorochrome-Photolysis-Giemsa Staining Technique 59
BrdUrd Antibody-Binding (BAB) Technique 68
Comparative Band Pattern Analysis 70
Replication Band Patterns 70
Replication Band Patterns versus Morphologic Band Patterns 73
Juxtacentromeric Area 85
C-band Area 85
Telomeric Area 86
Inactive X-Chromosome 87
Homolog Discordance 88
Lateral Asymmetry 90
R/G Transition and 3C Pause 92
Quantification of R-, G- and C-band Chromatin 93
Condensation and Replication: Two Interrelated Phenomena 95
Features of R- and G-bands 99
Conclusion 100
Acknowledgments 101
References 101

Chapter 3

Molecular Genetics of Charcot-Marie-Tooth Neuropathy

Benjamin B. Roa and James R. Lupski

Introduction 117

Pathological Features 118
Charcot-Marie-Tooth Disease 118
Inherited Primary Peripheral Neuropathies Related to CMT 119
Genetic Heterogeneity of Charcot-Marie-Tooth Disease 120
Gene Dosage as a Novel Mechanism for CMT Type 1A 121
DNA Duplication as the Major Cause of CMT1A 121
The Region Duplicated in CMT1A is Flanked by Large Regions of Homology 122
Evidence Supporting the Gene Dosage Model for CMT1A 124
The *PMP22* Gene in Charcot-Marie-Tooth Disease and Inherited Primary Peripheral Neuropathy 128
PMP22 and Charcot-Marie-Tooth Disease Type 1A 128
PMP22 and the Dejerine-Sottas Syndrome 129
PMP22 and Hereditary Neuropathy with Liability to Pressure Palsies 129
Genes Associated with Other Forms of CMT 132
The Myelin Protein Zero (*MPZ*) Gene and CMT1B 132
MPZ and Dejerine-Sottas Syndrome 133
The *Cx32* Gene and X-linked CMT 133
Implications of CMT Studies on Peripheral Nerve Biology 133
Genetic Diagnosis for CMT and Associated Neuropathies 135
Detection of the CMT1A Duplication 135
Mutation Analysis of Genes Associated with CMT 138
Molecular Insights Related to the CMT1A Duplication 139
CMT1A Duplication and HNPP Deletion at the 17p11.2p12 Region 139
Homologous Recombination in Model Systems 140
DNA Rearrangements Associated with Disease Phenotypes 141
Conclusions 143
Acknowledgments 145
References 145

Chapter 4

Marfan's Syndrome and Other Microfibrillar Diseases

Harry C. Dietz, Francesco Ramirez, and Lynn Y. Sakai

Introduction 153
Elastic Fibers and Microfibrils 154
Organization and Distribution 155

Composition 157
Fibrillins 161
Protein Structure 161
Gene Structure 166
Microfibrillar Assembly 166
Marfan's Syndrome 168
Clinical Features 168
Clinical Management 172
Fibrillin Mutations 173
Intrafamilial Variability 178
Marfan-Like Conditions 180
Conclusions and Future Prospectives 181
Acknowledgments 182
References 182

Chapter 5

Nonisotopic *in Situ* Hybridization
Clinical Cytogenetics and Gene Mapping Applications

Matteo Adinolfi and John Crolla

Introduction 187
The Probes 190
Detection by NISH of Chromosomal Disorders in Metaphase Spreads .. 194
Translocations and Isochromosomes 195
Marker Chromosomes 198
Deletions and Duplications 204
Detection by NISH of Chromosomal Abnormalities in Cells in Interphase 215
Prenatal Tests on Cells in Interphase by NISH 215
Detection of Mosaicism 221
Radiation Induced Chromosomal Damage 222
Somatic Pairing 223
NISH and the Mapping of the Human Genome 223
Metaphase Mapping 224
Interphase Mapping 227
Cancer and NISH Analysis of Chromosomal Defects 228
Evolution 232

Conclusions 234
Acknowledgments 235
References 235

Index 257

ADVANCES IN HUMAN GENETICS 22

Chapter 1

Genetic Disorders of Pigmentation

Richard A. Spritz

Departments of Medical Genetics and Pediatrics
University of Wisconsin
Madison, WI 53706

Vincent J. Hearing, Jr.

Laboratory of Cell Biology
National Cancer Institute
National Institutes of Health
Bethesda, MD 20892

INTRODUCTION

Disorders of pigmentation were among the first genetic disorders recognized in humans. The distinctive phenotypes of oculocutaneous albinism (OCA) and piebaldism were known to the ancient Greeks and Romans, and the typical clinical features, modes of inheritance, and genetic heterogeneity of these disorders are apparent even in classical descriptions (Lucian, 1905; Pliny, 1942; Gellius, 1952). Similar phenotypes were recognized early in the mouse, and the availability of inbred lines carrying characterized mutations has made the mouse an invaluable tool for studies of genetic disorders of pigmentation. Absent catalytic activity of tyrosinase in the skin of albino animals was one of the first enzymatic deficiencies recognized (Durham, 1904), and as early as 1908 Garrod suggested that albinism might be an inborn error of metabolism (Garrod, 1908).

Despite their venerable histories, genetic disorders of pigmentation have only recently yielded to modern molecular analytic techniques. Many of the associated

Advances in Human Genetics, Volume 22, edited by Henry Harris and Kurt Hirschhorn. Plenum Press, New York, 1994.

genes have now been cloned. In many cases identification of the human gene occurred only subsequent to analysis of the corresponding mouse locus, and several others genes associated with pigmentation disorders in the mouse have yet to be linked to abnormalities in humans. Our greatly improved understanding of the biochemical and molecular basis of genetic disorders of pigmentation has permitted the development of a much more accurate diagnostic nosology than was possible from only clinical and biochemical studies. This improved understanding provides the opportunity for much more accurate diagnosis, carrier detection, and prenatal diagnosis of these disorders, especially in selected families and high-risk ethnic groups. In addition, improved understanding of the biochemical and genetic causes of these disorders challenges us to develop novel and specific therapies—biochemical, pharmacologic, and perhaps, eventually, DNA–based.

Genetic disorders of pigmentation can be classified in two general categories: disorders of melanocyte function and disorders of melanocyte development. Disorders of melanocyte function are associated with generalized hypopigmentation from reduced melanin per melanocyte, whereas disorders of melanocyte development are associated with heterogeneous pigmentation patterns resulting from abnormal distribution of normally pigmented melanocytes. In the following discussion, MIM numbers for each disorder are from Online Mendelian Inheritance in Man (1994).

The Mammalian Pigmentary System

Melanocytes constitute only a small part of the cell population in the skin and eyes of mammals, but they are the only cells that produce melanin, accounting for virtually all of the visible pigmentation of those tissues. Melanin has a variety of important functions—as a cosmetic entity participating in protective coloration and in sexual attraction within species, as a barrier protecting against ultraviolet (UV) radiation, as a scavenger of cytotoxic radicals and metabolic intermediates; and as a participant in developmental processes, particularly of the nervous system. Skin melanocytes are highly dendritic cells that originate during development as melanoblasts in the neural crest; melanocytes in the retina derive from the optic cup. The melanoblasts subsequently migrate to three principal locations: the epidermal/dermal border of the skin, the hair bulbs in the dermis of the skin, and the iris, choroid, and retina of the eyes (Montagna and Ellis, 1958; Kawamura *et al.*, 1971; Montagna and Parakkal, 1974; Fitzpatrick, 1981; Bennett, 1991; Montagna *et al.*, 1991; Hearing and King, 1994). For pigmentation to proceed normally, many complex events and interactions must occur with precision during development and differentiation. Melanocytes must differentiate appropriately as

melanoblasts in the neural crest, the signal for migration must be given at the correct time, and movement of melanoblasts towards their eventual destination must begin. To achieve uniform pigmentation, melanoblasts must not only disperse correctly, but must subsequently receive the appropriate signal to stop migrating, establish themselves, proliferate and differentiate appropriately, and function correctly. The signals necessary to achieve all of these events depend on a number of genes, some expressed by the melanoblasts and/or melanocytes, others by other cell types. Since the ultimate patterns of pigmentation in the skin and hair depend on other cellular constituents, such as keratinocytes, genes that regulate those other cell types can also indirectly affect pigmentation. More than 150 different mutations that affect pigmentation have been identified in the mouse, and these have been mapped to more than 60 distinct genetic loci (Silvers, 1979; Lyon and Searle, 1989). A number of these genes have now been cloned and a discussion follows (see Table I).

Within the melanocyte, the pigment biosynthetic machinery is confined to membrane-bound organelles called melanosomes. Premelanosomes emerge from the smooth endoplasmic reticulum as membrane-bound vesicles devoid of the factors required for melanin synthesis (Hearing *et al.*, 1992; Mishima, 1992; Kameyama *et al.*, 1993; Shibata *et al.*, 1993). These factors, which include tyrosinase and other melanogenic enzymes, are synthesized on ribosomes and transported through the rough endoplasmic reticulum and Golgi apparatus, where their post-translational processing and glycosylation takes place. The enzymes are then secreted within coated vesicles into the cytoplasm and transported to the premelanosomes, where they fuse with its limiting membrane. The melanogenic enzymes orient within the melanosomal membrane with their catalytic domains inwards, and once activated, melanogenesis begins. Melanin is deposited on the internal fibers of the melanosome, and the opacity of the organelle gradually increases until all substructure is obscured, leaving just an electron dense mature melanin granule visible. As melanization proceeds, the melanosomes move steadily away from the perinuclear region to the periphery of the melanocyte, and are then transported to keratinocytes, where they subsequently degrade.

The basic biochemical outline of melanin production from the amino acid tyrosine has been known for some time; however, the comparative complexity of melanin biosynthesis *in vivo* has only been recognized relatively recently (reviewed in Hearing and Tsukamoto, 1991; Urabe *et al.*, 1993). Tyrosinase is the only enzyme absolutely essential for melanin formation *in vitro*; when tyrosine is incubated in the presence of tyrosinase and a suitable cofactor, visible melanin is produced within minutes. As shown in Fig. 1, tyrosinase catalyzes the first step of melanin biosynthesis, the hydroxylation of tyrosine to 3,4-dihydroxyphenyl

TABLE I. Human Pigmentation Disorders and Homologous Mouse Genes and Functions

Human disorder	Mouse locus (symbol)	Protein encoded	Function in pigmentation
		Disorders of melanocyte function	
Type I OCA, AROA	Albino (*c*)	Tyrosinase	Tyrosine hydroxylase, DOPA and DHI oxidase
Type II OCA, AROA, Prader-Willi & Angelman Syndromes	Pink-eyed dilution (*p*)	Transport protein*	Membrane structure and/or function*
Type IV OCA*	Brown (*b*)	TRP-1	DHICA oxidase
X-linked Ocular albinism	Unknown	Unknown	Unknown
		Disorders of melanocyte development	
Piebaldism	White spotting (*W*)	c-Kit tyrosine kinase receptor	Migration, proliferation and/or survival of melanoblasts
Waardenburg syndrome	Splotch (*Sp*)	Transcription factor	Melanoblast development in the neural tube*
		Incompletely characterized cloned genes affecting pigmentation	
Menkes' disease	Mottled (*mo*)*	Copper-transporting ATPase*	Unknown, possibly tyrosinase copper regulation
Hermansky-Pudlak Syndrome	Pallid (*pa*)* Pearl (*pe*)*	Membrane stability factor*	Organellogenesis*, esp lysosomes, platelets and melanosomes
Unknown	Steel (*Sl*)	Steel factor	Ligand for the *W* locus product (cf. above)
Unknown	Microphthalmia (*mi*)	Transcription factor	Melanocyte function and/or viability
Unknown	Dilute (*d*)	Myosin-related protein	Dendrite formation and/or structure, or melanosome movement*
Unknown	Extension (*e*)	MSH receptor	Hormonal regulation of melanogenesis
Unknown	Agouti (*a*)	Paracrine signalling protein	Regulation of eumelanogenesis versus pheomelanogenesis
Unknown	Slaty (*slt*)	TRP-2	DOPAchrome tautomerase
Unknown	Silver (si)	Pmel-17	Melanosomal matrix protein*

*Putative homologues.

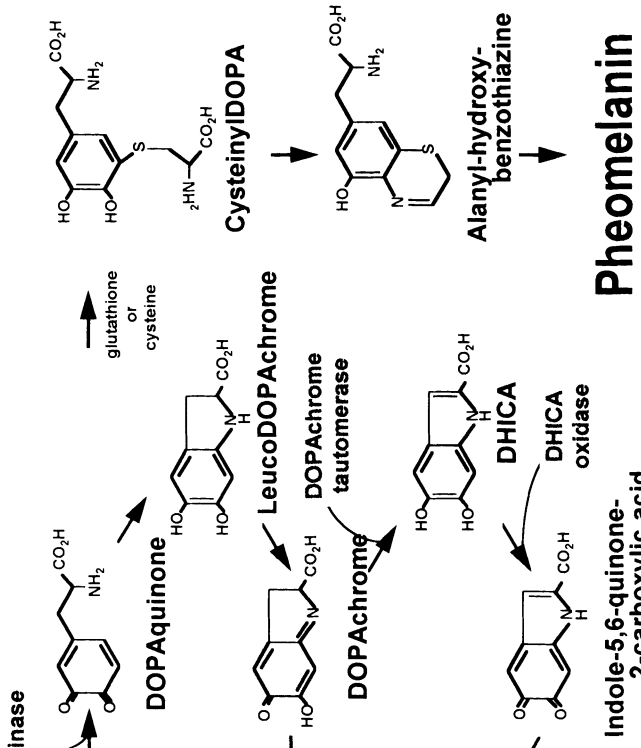

Fig. 1. Schematic of melanin biosynthetic pathway. The relations involved in the biosynthetic pathway of melanin pigments are shown, as originally proposed by Lerner and Fitzpatrick (1950), and later modified by Korner and Pawelek (1982); *cf.* Hearing and Tsukamoto (1991), Hearing and King (1994) for reviews and relevant references.

alanine (DOPA); this first reaction is the most critical since its spontaneous rate is negligible. DOPA can readily autooxidize to DOPAquinone even in the absence of tyrosinase (although tyrosinase can also catalyze this reaction), and then continue through the pathway by cyclizing to sequentially form the indole ring structures leucoDOPAchrome and DOPAchrome. DOPAchrome in turn spontaneously decarboxylates to produce 5,6-dihydroxyindole (DHI), which rapidly oxidizes to produce indole-5,6-quinone. Melanin was initially thought to be a high molecular weight homogeneous biopolymer consisting exclusively of an indole-5,6-quinone backbone, but it is now known that physiological melanins are much more heterogeneous and incorporate other intermediates in the pathway as well. The reactions outlined above which lead to the formation of indole-5,6-quinone will take place spontaneously in a test tube, but *in vivo* several other biological factors influence these reactions. These include other enzymes (such as DOPAchrome tautomerase and 5,6-dihydroxyindole-2-carboxylic acid (DHICA) oxidase), the availability of reactive sulfhydryls (such as glutathione and/or cysteine), melanogenic inhibitors, and perhaps even other regulatory elements. These enzymes have been characterized biochemically, and the corresponding genes encoding several of these (tyrosinase, DOPAchrome tautomerase, and DHICA oxidase) have been cloned and are discussed in more detail below.

Two basic types of melanin can be produced in mammalian melanocytes, eumelanin and pheomelanin. Eumelanin is black and/or brown, pheomelanin is red and/or yellow (Prota, 1986, 1988a,b, 1992; Pawelek, 1991). The decision to produce one or the other type of melanin is made immediately following the production of DOPAquinone. If sulfhydryls such as cysteine or glutathione are available, they stoichiometrically react with DOPAquinone to generate cysteinyl-DOPAs, which then undergo a series of reactions that result in the cyclization of a second, nonindole ring and polymerization into a higher molecular weight complex, pheomelanin. Little is known about the enzymatic modulation of the pheomelanin pathway. However, two genes, *extension* and *agouti*, that modulate the pheomelanin versus eumelanin switch, at least in mice, have now been cloned; these are also discussed below.

The second major post-tyrosinase regulatory point in the melanogenic pathway occurs following the production of DOPAchrome. As noted above, DOPAchrome can spontaneously decarboxylate to form DHI. However, in the presence of certain divalent metal cations and the enzyme DOPAchrome tautomerase, the carboxylated intermediate DHICA will be produced. Since DHI and DHICA are not interconvertible, this step determines the carboxyl content of the resulting melanin. Other enzymes that function distal to DHI and DHICA have also been described. DHICA oxidase accelerates the oxidation of DHICA into melanins, and

stabilin can act as an inhibitor or stabilizer of DHI and DHICA, preventing their further metabolism into melanins. Several inhibitors of melanogenesis endogenous to melanocytes may also regulate pigment production.

Ocular pigmentation results from melanocyte function in the choroid, iris and retina, and the melanins there are thought to function primarily as a photoprotective barrier. Ocular melanocytes are relatively dormant: rates of melanogenesis are quite low after fetal development, and the pigment produced is not secreted, but remains within the melanocyte. In contrast, melanocytes in the skin are highly secretory. Hair color results from melanins produced by melanocytes within hairbulbs that are subsequently transferred to keratinocytes and incorporated into the growing hair shafts. With age, hairbulb melanocytes often become dormant and cease their production of pigment, resulting in the characteristic graying of hair associated with aging. Skin color is dependent upon melanocytes that reside primarily at the junction of the dermis and epidermis. The pigment granules secreted are taken up by neighboring keratinocytes (the predominant cell type in the epidermis), which then further process them, degrading and redistributing them either into smaller pieces and/or into larger complexes that eventually result in visible skin color. Although melanocytes in the epidermis proliferate slowly if at all, the surrounding keratinocytes are highly proliferative and gradually move upward towards the surface of the skin with their accumulated pigment. In humans, the number of epidermal melanocytes per unit area is remarkably similar between races; phenotypic differences in skin color depend primarily on the quantity and distribution of the melanin "packets" or "dust" in the keratinocytes at or near the skin surface.

The intimate association of the melanocyte and its neighboring keratinocytes has historically been referred to as the "epidermal melanin unit"; however, we now know that melanocytes also continually interact with other cell types in the dermis and epidermis. Although epidermal melanocytes have characteristic basal levels of melanogenesis particular to each individual, they are highly responsive cells that continually sample their environment and modulate their levels of proliferation or melanogenesis accordingly. Interactions of melanocytes with their environment are numerous and complex; growth factors, hormones, cytokines and a variety of other stimuli such as ultraviolet light affect rates of melanogenesis and/or the proliferative nature of melanocytes. Melanocytes express numerous cell surface receptors that allow them to interact with other cells in their microenvironment, including keratinocytes and Langerhans cells in the epidermis, as well as factors produced exogenously by cells present in the dermis, including endothelial, mast, and inflammatory cells (Pawelek, 1985; Pawelek *et al.*, 1992). Additionally, in various disease conditions and other "abnormal" states the skin can be

infiltrated by other types of cells, such as lymphocytes or macrophages, or by foreign cells penetrating a breach in the skin. These cells can secrete various factors that bind to melanocyte receptors and can modulate melanogenic activity. Therefore, pigmentation is often of prognostic value to the clinician since it can be a highly visible indicator of the status of the health of that tissue. Thus, the melanocyte is involved in a highly dynamic interrelationship with many different cell types in its immediate environment, all of which participate in determining the level of its melanogenic activity.

DISORDERS OF MELANOCYTE FUNCTION

Albinism

Albinism is a heterogeneous group of disorders of melanocyte function, manifest principally by generalized hypopigmentation. In oculocutaneous albinism (OCA) pigment is reduced or absent in the skin, hair, and eyes, whereas in ocular albinism (OA) visual involvement is accompanied by relatively normal pigmentation of the skin and hair. However, all forms of human albinism are oculocutaneous, involving both the eyes and the integument to at least some extent; thus, the distinction between OCA and OA is largely artificial.

The role played by melanin in the developing visual system is not known. However, if pigment production is reduced below some critical level, regardless of its genetic cause, the result is a stereotypic set of defects of neuronal migration in the visual pathways, with consequent low vision, nystagmus, and strabismus in affected individuals. In general, the severity of the visual defects correlates with the severity of the pigmentation deficit in the eye. OCA has traditionally been classified as "tyrosinase-deficient" (type I) or "tyrosinase-positive" (type II) based on biochemical assay of hairbulb tyrosinase. Furthermore, several additional tyrosinase-positive types of OCA have been distinguished on clinical grounds. Both X–linked and autosomal recessive forms of OA have been recognized. However, elucidation of the molecular basis of these disorders has led to improved understanding of their true relationships and to more accurate classification based on molecular criteria.

Type I (Tyrosinase-Deficient) OCA (MIM #203100)

Type I OCA is an autosomal recessive disorder resulting from deficient catalytic activity of tyrosinase (monophenol monooxygenase; monophenol,

L-dopa:oxygen oxidoreductase; EC 1.14.18.1), a copper-containing enzyme that catalyzes the first two steps, and at least one subsequent step, in the melanin biosynthetic pathway (Lerner *et al.*, 1949; Lerner and Fitzpatrick 1950; Tripathi *et al.*, 1992a). Expression of tyrosinase is absolutely necessary for pigment production, although other control points in the pathway are also critical to the regulation of melanogenesis *in vivo*, as discussed above. Freshly epilated hair-bulbs from patients with type I OCA accumulate little to no melanin pigment following *in vitro* incubation in tyrosine or dopa, the classic assay for this disorder (Kugelman and van Scott, 1961). In humans at least two different subtypes of type I OCA, types IA and IB, have been distinguished clinically. In type IA (tyrosinase-negative) OCA, the classic, most severe form of the disorder, tyrosinase activity is completely absent, and there is no detectable melanin pigment in the skin, hair, or eyes. Visual acuity is greatly decreased, usually to approximately 20/400, and nystagmus, strabismus, and photophobia are usually severe. In type IB ("yellow mutant"), initially recognized in the Amish (Nance *et al.*, 1970), tyrosinase activity is greatly reduced, and although there is little or no apparent melanin pigment at birth, progressive melanization may occur during childhood and adult life. Types IA and IB OCA have long been recognized to be allelic, based on the existence of apparent type IA/IB compound heterozygotes who exhibit a phenotype approximately intermediate between those of the two homozygous forms (Hu *et al.*, 1980).

The cloning of the human tyrosinase gene (*TYR*) and its analysis in patients with type I OCA has demonstrated that an allelic series of tyrosinase gene mutations accounts for both type IA and type IB OCA, and a large number of different mutations of the tyrosinase gene have now been identified. The *TYR* gene consists of five exons spanning more than 50 kb of genomic DNA on the long arm of human chromosome 11 (Giebel *et al.*, 1991b). Tyrosinase is translated as a 529-amino acid polypeptide, from which an 18-amino acid hydrophobic leader peptide is cleaved to yield the mature tyrosinase protein (Kwon *et al.*, 1987b; Wittbjer *et al.*, 1989). An apparent transmembrane domain near the carboxyl terminus of the polypeptide indicates that tyrosinase is membrane bound, perhaps on the inner surface of the melanosome. Among Caucasians, two codons, 192 and 402, are commonly dimorphic (Giebel and Spritz, 1990; Tripathi *et al.*, 1991), encoding either of two alternative amino acid residues at each site. As a result, there are four slightly different alternative normal tyrosinase isoforms, which differ significantly in their stabilities and thus also in their net catalytic activities (Tripathi *et al.*, 1991). However, the occurrence of these four tyrosinase isoforms does not correlate with the apparent pigmentation phenotype in Caucasians.

Human type I OCA was first shown to be genetically linked to the *TYR*

structural gene by analysis of large families with OCA using *TYR* gene restriction fragment length polymorphisms (Giebel *et al.*, 1990; Spritz *et al.*, 1990). Subsequently, specific *TYR* gene mutations were demonstrated in patients with type I OCA by nucleotide sequence analyses of *TYR* cDNAs cloned from cultured melanocytes (Tomita *et al.*, 1989) and *TYR* genomic segments amplified from patient DNA by use of the polymerase chain reaction (PCR) (Giebel *et al.*, 1990; Spritz *et al.*, 1990). As shown in Figure 2 and Table II, at least 60 different pathologic mutations of the *TYR* gene have been identified to date in patients with various forms of type I OCA (reviewed in Oetting and King, 1993; Spritz, 1993b; Spritz, 1994a). These include missense mutations that result in amino acid substitutions, nonsense mutations that result in premature termination of translation, frameshifts, and mutations that interfere with normal pre-mRNA splicing.

A number of these mutations have been subjected to functional analysis by expression in transfected cells, permitting correlation of the resultant tyrosinase enzymatic activity with the associated clinical phenotypes. As expected, the nonsense frameshift, and missense mutations that completely abolish tyrosinase catalytic activity are associated with type IA OCA (Tomita *et al.*, 1989; Kikuchi *et al.*, 1990; Takeda *et al.*, 1990; Tripathi *et al.*, 1991, 1992a). However, missense mutations that result in greatly reduced, but not abolished, enzymatic activity are specifically associated with type IB OCA (Giebel *et al.*, 1991c,d; Tripathi *et al.*, 1991, 1992a). In particular, the V275F, P406L, and R422Q missense substitutions,

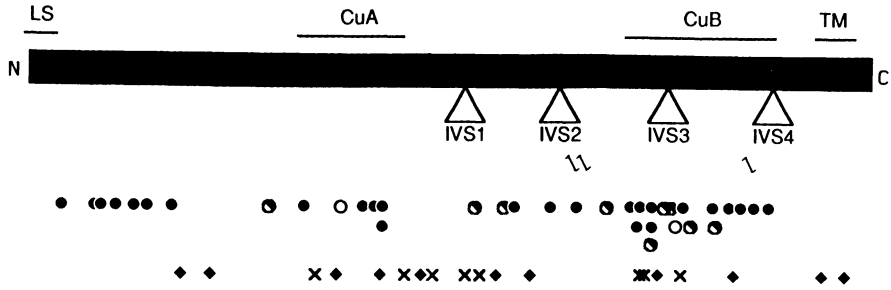

Fig. 2. Locations of known *TYR* gene mutations associated with type I (tyrosinase-deficient) OCA. The blackened box denotes the 529-amino acid tyrosinase polypeptide. The 18-amino acid amino-terminal leader sequence (LS), the two regions of sequence homology with hemocyanins (CuA and CuB), and the transmembrane domain (TM) are indicated. The positions of the four intervening sequences (IVSs) are indicated. Blackened circles indicate the sites of type IA OCA missense substitutions; half blackened circles indicate the sites of type IB OCA missense substitutions; unblackened circles indicate the sites of polymorphic amino acids 192 and 402. Blackened diamonds indicate the sites of frameshifts; ×'s indicate the sites of nonsense mutations; zig-zags indicate the sites of splice consensus mutations. Many of the indicated mutations represent our unpublished data, and are not included in Table II.

and also the R402Q polymorphism, result in unstable tyrosinase polypeptides, with temperature-sensitive catalytic activities that are greatly reduced at 37°C compared to 31°C, both *in vivo* (King *et al.*, 1991) and *in vitro* (Giebel *et al.*, 1991c; Tripathi *et al.*, 1991; Tripathi *et al.*, 1992a). As shown in Fig. 2, the nonsense and frameshift mutations are randomly distributed throughout the tyrosinase coding region. However, most of the missense substitutions associated with type IA OCA cluster in two regions of the polypeptide (King *et al.*, 1991; Tripathi *et al.*, 1992b): near the amino terminus of the mature tyrosinase polypeptide (codons 21–89) and near the center of the tyrosinase polypeptide (codons 371–448). This latter region corresponds closely to the so-called "Cu B" region of tyrosinase. This is one of two regions of the tyrosinase polypeptide that exhibit amino acid sequence homology to arachnid, crustacean, and molluscan hemocyanins (Lerch, 1988), proteins which, like tyrosinase, also complex with atomic copper. However, involvement of the Cu B region in copper binding by tyrosinase has yet to be demonstrated experimentally, and the only amino acid substitution we have found that involves one of the putative copper-binding histidines (Martinez *et al.*, 1985) (H390D) is associated with a particularly mild OCA phenotype (unpublished data).

In Caucasians, no single mutant *TYR* allele accounts for a significant fraction of the total; therefore, in the absence of parental consanguinity most patients are compound heterozygotes for different mutant alleles. Patients with type IA OCA have two type IA OCA alleles, whereas patients with type IB OCA may have either two type IB alleles or one type IB and one type IA allele. Patients with type IB OCA exhibit considerable phenotypic heterogeneity (even among patients with similar genotypes), the likely result of factors that modulate pigmentation epistatic to tyrosinase. In fact, we have found that approximately one-third of Caucasian patients diagnosed with type II (tyrosinase-positive) OCA based on clinical and biochemical criteria have been incorrectly diagnosed, and have pathologic *TYR* gene mutations that would be expected to only modestly reduce tyrosinase catalytic activity (Tripathi *et al.*, 1992b; unpublished data). Furthermore, we have recently identified mutations of the *TYR* gene in several patients with autosomal recessive ocular albinism (AROA; MIM #203310), previously thought to be a distinct entity. The range of phenotypes associated with type IB OCA alleles is thus surprisingly broad, from apparent type IA OCA, to apparent type II OCA, to AROA. This underscores the need for molecular diagnosis to accurately distinguish these disorders.

We have studied several examples of type I OCA occurring in two successive generations of a kindred (Giebel *et al.*, 1990, 1991c; unpublished data). All of these cases were found to result from pseudodominance, an affected individual having inadvertently married an unrelated carrier. It would be of great interest to determine whether this phenomenon might account for some or all of the reported

TABLE II. Published Mutations and Polymorphisms of the *TYR* Gene Associated with Type I Oculocutaneous Albinism

Mutation	Base substitution[a]	OCA type	Population	Frequency	Reference
P21S	CCT (Pro)→TCT (Ser)	IA	Caucasian	Rare	Tripathi *et al.*, 1992b
D42G	GAC (Asp)→GGC (Gly)	IA	Caucasian	Rare	King *et al.*, 1991
G47D	GGC (Gly)→GAC (Asp)	IA	Caucasian	Rare	Oetting *et al.*, 1991a
			Puerto Rican	Rare	Oetting *et al.*, 1993b
			Moroccan Jewish	0.83	Gershoni-Baruch *et al.*, 1994
C55Y	TGT (Cys)→TAT (Tyr)	IA	Caucasian	Rare	King *et al.*, 1991
R77Q	CGG (Arg)→CAG (Gln)	IA	Japanese	?	Kikuchi *et al.*, 1990; Takeda *et al.*, 1990
P81L	CCT (Pro)→CTT (Leu)	IA	Caucasian	~0.10	Giebel *et al.*, 1990
C89R	TGC (Cys)→CGC (Arg)	IA	Black	?	Spritz *et al.*, 1991
M96insA	ATG (Met)→AATG	IA	Caucasian	Rare	Oetting *et al.*, 1991b
R115delGA	AGA (Arg)→A--	IA	Indo-Pakistani	? Rare	Oetting *et al.*, 1993a
P152S	CCC (Pro)→TCC (Ser)	IB?	Jewish	Rare	Gershoni-Baruch *et al.*, 1994
F176I	TTT (Phe)→ATT (Ile)	IA	Caucasian	Rare	Oetting and King, 1992
W178X	TGG (Trp)→TAG (TER)	IA	Afghan	?	Giebel *et al.*, 1991a
G191delG	GGA (Gly)→-GA	IA	Caucasian	Rare	Oetting *et al.*, 1991b
Y192S	TCT (Ser)→TAT (Tyr)	Poly	All but Oriental	0.48	Giebel and Spritz, 1990
A206T	GCT (Ser)→ACT (Thr)	IA	Caucasian	Rare	King *et al.*, 1991
L216M	TTG (Leu)→ATG (Met)	IA	Hispanic	?	Oetting *et al.*, 1993b
R217W	CGG (Arg)→TGG (Trp)	IA	Caucasian	Rare	Tripathi *et al.*, 1992b
R217Q	CGG (Arg)→CAG (Gln)	IA	Caucasian	Rare	Oetting and King, 1992
R217delC	CGG (Arg)→-GG	IA	Jewish	Rare	Gershoni-Baruch *et al.*, 1994
W236X	TGG (Trp)→TAG (TER)	IA	Black	?	Oetting *et al.*, 1993b
C244delTG	TGT (Cys)→--T	IA	Caucasian	Rare	Oetting *et al.*, 1991b
V275F	GTC (Val)→TTC (Phe)	IB	Caucasian	~0.05	Giebel *et al.*, 1991d

R278X	CGA (Arg)→TGA (TER)	IA	Guyanan	Unknown	Tripathi *et al.*, 1993
			Jewish	Rare	Gershoni-Baruch *et al.*, 1994
L288S	TTA (Leu)→TCA (?) (Ser)	?	?	?	Oetting *et al.*, 1994
L288delT	TTA (Leu)→-TA	IA	Korean	?	Spritz, 1993b
R299H	CGT (Arg)→CAT (His)	IA	Caucasian	Rare	Tripathi *et al.*, 1992b
			Arab	Rare?	Gershoni-Baruch *et al.*, 1994
P310insC	CCA (Pro)→CCCA	IA	Japanese	?	Tomita *et al.*, 1989
E328Q	GAA (Glu)→CAA (Gln)	IA	Indo-Pakistani	? Rare	Tripathi *et al.*, 1993
G346E	GGA (Gly)→GAA (Glu)	?	?	?	Oetting *et al.*, 1994
G346X	GGA (Gly)→TGA (TER)	IA	?	?	Oetting *et al.*, 1994
A355Q	GCG (Ala)→CCG (Pro)	IB	Caucasian	Rare	Spritz, 1993b
A355E	GCG (Ala)→GAG (?) (Glu)	?	?	?	Oetting *et al.*, 1994
N371T	AAT (Asn)→ACT (Thr)	IA	Caucasian	Rare	Oetting *et al.*, 1991a
T373K	ACA (Thr)→AAA (Lys)	IA	Caucasian	~0.10	Spritz *et al.*, 1990
			Libyan Jewish	? Common	Gershoni-Baruch *et al.*, 1994
Q376X	CAG (Gln)→TAG (TER)	IA	Indo-Pakistani	? Rare	Tripathi *et al.*, 1993
N382K	AAC (Asn)→AAA (Lys)	IA	Caucasian	Rare	Oetting *et al.*, 1991b
D383N	GAT (Asp)→AAT (Asn)	IA	Caucasian	~0.04	Spritz *et al.*, 1990
L388delT	CTT (Leu)→CT-	IA	Caucasian	Rare	Tripathi *et al.*, 1992b
H390D	CAT (His)→GAT (Asp)	IB	Caucasian	Rare	Spritz, 1993b
V393F	GTT (Val)→TTT (?) (Phe)	?	?	?	Oetting *et al.*, 1994
R402Q	CGA (Arg)→CAA (Gln)	Poly	All but Oriental	0.15	Tripathi *et al.*, 1991
R402X	CGA (Arg)→TGA (TER)	IA	Arab	? Common	Gershoni-Baruch *et al.*, 1994
			Caucasian	Rare	Gershoni-Baruch *et al.*, 1994
R403S	AGG (Arg)→AGT (Ser)	IA	Caucasian	Rare	Tripathi *et al.*, 1992b
P406L	CCT (Pro)→CTT (Leu)	IB	Caucasian	Rare	Giebel *et al.*, 1991d
G419R	GGA (Gly)→AGA (Arg)	IA	Caucasian	Rare	King *et al.*, 1991
			Indo-Pakistani	?	Tripathi *et al.*, 1993

(*Continued*)

TABLE II. ***(Continued)***

Mutation	Base substitution[a]	OCA type	Population	Frequency	Reference
R422Q	CGG (Arg)→CAG (Gln)	IB	Caucasian	Rare	Giebel *et al.*, 1991c
P431L	CCA (Pro)→CTA (Leu)	IA	Indo-Pakistani	? Rare	Tripathi *et al.*, 1993
F438-F439delCTTT	TTCTTT (PhePhe)→TT----	IA	Caucasian	Rare	Oetting and King, 1992
G446S	GGC (Gly)→AGC (Ser)	IA	Caucasian	Rare	Tripathi *et al.*, 1992b
D448N	GAC (Asp)→AAC (Asn)	IA	Caucasian	Rare	Tripathi *et al.*, 1992b
Q453X	CAA (Gln)→TAA (TER)	IA	Caucasian	Rare	Oetting and King, 1992
T489insT	ACT (Thr)→ACTT	IA	Caucasian	Rare	Chintamaneni *et al.*, 1991a
R501insC	CGT (Arg)→CCGT	IA	Caucasian	Rare	Giebel *et al.*, 1991d
IVS2 -7T→A	tgaacagGA→agaacagGA	IB	Jewish	Rare	Gershoni-Baruch *et al.*, 1994
			Caucasian	Rare	Gershoni-Baruch *et al.*, 1994

[a]Poly, nonpathologic amino acid polymorphism; upper case, coding sequence; lower case, intervening sequence (IVS).

cases of "autosomal dominant OCA," which has previously been considered to be a distinct entity (MIM #126070).

The lack of predominant mutant *TYR* alleles among Caucasian patients with type I OCA complicates efforts at molecular diagnosis or carrier detection, except in selected families. However, one specific mutant allele has been identified in the Amish (P406L; Giebel *et al.*, 1991d), one mutant allele (G47D) strongly predominates in patients from Puerto Rico (Oetting *et al.*, 1993b) and in Moroccan Jews (Gershoni-Baruch *et al.*, 1994), and the G419R substitution may comprise about half of mutant alleles among Indo-Pakistani patients (Tripathi *et al.*, 1993). In these populations, therefore, genetic screening procedures can be targeted for the appropriate predominant mutant *TYR* alleles.

Type II (Tyrosinase-Positive) OCA (MIM #203200)

Type II (tyrosinase-positive) OCA is an autosomal recessive disorder with a phenotype similar to but typically less severe than that of type I OCA, although the two disorders display considerable clinical overlap. Infants with type II OCA may have little or no apparent melanin pigment at birth. However, during early to mid-childhood most patients with type II OCA acquire modest amounts of pigment, predominantly yellow-red pheomelanins. The ultimate peripheral pigmentation phenotype can be extremely variable, ranging from one similar to type IA OCA to virtually normal. The visual deficits are also usually less severe in type II OCA than in type I; the visual acuity of patients with type II OCA is typically in the 20/60 to 20/200 range, with only moderate nystagmus. Furthermore, in type II OCA visual acuity and nystagmus may improve during childhood and even during adolescence, with ultimate visual acuity reaching approximately 20/40 to 20/70. Rarely, nystagmus may even disappear entirely and visual acuity may be normal (Summers *et al.*, 1991).

As described above, molecular analysis has shown that a significant fraction of Caucasian patients thought to have "tyrosinase-positive" OCA actually have clinically mild forms of type IB OCA. However, the existence of a true type II OCA, genetically distinct from type I OCA, has long been known from several instances of matings between parents, one with type I OCA and the other with type II OCA, that have produced normally pigmented children (Witkop *et al.*, 1989).

Recently, we identified the gene responsible for type II OCA in humans and have characterized mutations of this gene in a number of patients with type II OCA (Rinchik *et al.*, 1993; Lee *et al.*, 1994b,c). This success resulted from the coalescence of several seemingly unrelated lines of data. First, we isolated a

human *P* cDNA (Rinchik *et al.*, 1993), which proved to correspond to the pink-eyed dilution (*p*) locus of mouse (Gardner *et al.*, 1992; Rinchik *et al.*, 1993). Mice homozygous for *p* mutations exhibit a phenotype very similar to that of humans with type II OCA, and the human *P* gene is located in chromosome segment 15q11-q13, the same region to which human type II OCA was mapped on the basis of linkage analysis (Ramsay *et al.*, 1992). This is essentially the same chromosomal region that is commonly deleted in patients with the Prader–Willi (PWS; MIM #176270) and Angelman (AS; MIM #105830) syndromes (reviewed in Nicholls, 1993), both of which are often associated with significant hypopigmentation (Butler, 1989). Furthermore, approximately one percent of PWS and AS patients exhibit the phenotype of classic type II OCA, a frequency similar to the expected prevalence of carriers of type II OCA. In addition to *P* being a candidate for type II OCA, these data suggested that hypopigmentation in PWS and AS might stem from large proximal chromosome 15q deletions that include *P*, and that the atypical PWS/AS patients with OCA might be hemizygous for inherited *P* gene mutations on the nondeleted chromosome.

To test these hypotheses, we first analyzed the *P* gene in one patient with PWS plus type II OCA, and we found that the patient was hemizygous for a maternally inherited mutant *P* allele containing a partial gene deletion (Rinchik *et al.*, 1993). To identify point mutations of the *P* gene in patients with type II OCA, we characterized the *P* genomic locus, which consists of 25 exons spanning approximately 150 kb of DNA on proximal 15q (Lee *et al.*, 1994a). Based on this, we have subsequently identified 22 different additional abnormalities of the *P* gene in a number of other patients with various forms of type II OCA, including two other patients with type II OCA and PWS (Lee *et al.*, 1994b,c). As shown in Table III and Fig. 3, these abnormalities include partial gene deletions, two small in-frame deletions, three frameshifts, one splice junction mutation, twelve missense substitutions, and one double missense substitution. Although none of these mutations are strongly predominant, we have observed the V443I substitution in several Caucasian and black patients, suggesting that this may be a relatively prevalent mutant allele. Interestingly, we have found abnormalities of the *P* gene in only 6 of 14 Caucasian patients with "tyrosinase-positive OCA," none of whom have mutations in their *TYR* genes (unpublished data). As will be discussed below, at least some of these patients may have mutations of a putative third OCA locus. In contrast, we (Lee *et al.*, 1994c) and others (Durham-Pierre *et al.*, 1994) have found pathologic mutations of the *P* gene in all of the African–American patients with type II OCA studied, consistent with complete linkage of type II OCA to 15q markers in South African black patients (Ramsay *et al.*, 1992; Kedda *et al.*, 1994).

TABLE III. Published Mutations of the *P* Gene Associated with Type II Oculocutaneous Albinism

Mutation	Base substitution[b]	OCA type	Population	Frequency	Reference
del L206-P211	6 codon deletion	II	black	? Common	Lee et al., 1994c
N273K/W274V	AACTGG (AsnTrp) → AAGGTC (LysVal)	II	black	?	Lee et al., 1994c
F385I	TTT (Phe)→ATT (Ile)	II	black	?	Lee et al., 1994c
M395L	ATG (Met)→CTG (Leu)	II	black	?	Lee et al., 1994c
del M425	ATG (Met)→---	Mild II or AROA	black	?	Lee et al., 1994c
V443I	GTC (Val)→ATC (Ile)	II	Caucasian, black	? Common	Lee et al., 1994b,c
A481T	GCC (Ala)→ACC (Thr)	AROA	Caucasian	?	Lee et al., 1994b
A654delG	GCT (Ala)→-CT	II	Indo-Pakistani	?	Lee et al., 1994b
W679R	TGG (Trp)→CGG (Arg)	II	black	?	Lee et al., 1994c
P743L	CCG (Pro)→CTG (Leu)	II	Caucasian, black	?	Lee et al., 1994b,c
IVS17 +1G→T	AAGgtaccc→AAGttaccc	II	Caucasian	?	Lee et al., 1994b

AROA, autosomal recessive ocular albinism; upper case, coding sequence; lower case, intervening sequence (IVS).

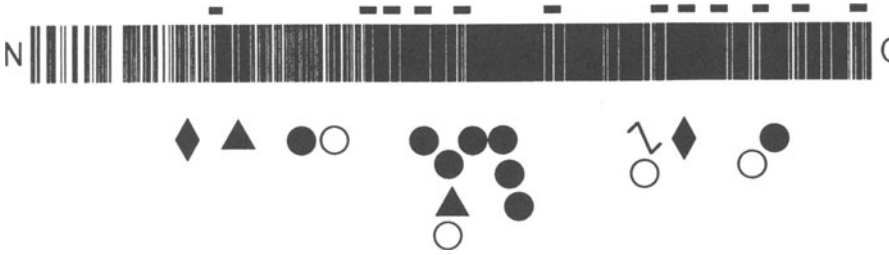

Fig. 3. Locations of known *P* gene mutations associated with type II (tyrosinase-positive) OCA. The box denotes the 838-amino-acid P polypeptide. Black vertical bars indicate segments of amino acid identity between the human (Rinchik *et al.*, 1993) and mouse (Gardner *et al.*, 1992) P polypeptides. Horizontal bars overline indicate the twelve putative transmembrane domains. Blackened triangles indicate the sites of in-frame deletions; other symbols are as described in the legend to Fig. 2. Many of the indicated mutations represent our unpublished data, and are not included in Table III.

This unexpected difference between Caucasian and black patients with tyrosinase-positive OCA may be the result of historically different selection pressures on these two populations.

The range of phenotypes associated with pathologic mutations of the *P* gene in humans is very broad. Individuals homozygous for frameshift mutations, which would be expected to totally abolish function, exhibit a phenotype almost as severe as type IA OCA (Lee *et al.*, 1994b). At the other end of the range, mutations of *P* appear to account for at least some cases of AROA (MIM #203310). We have characterized two such patients. One was a compound heterozygote for a splice junction mutation, which would be expected to abolish function, and a missense mutation, A481T (Lee *et al.*, 1994b). The other was a compound heterozygote for a large gene deletion and a small deletion of a single codon (Lee *et al.*, 1994c). Both exhibited normally pigmented skin and hair but had typical ocular features of AROA. We have detected additional *P* gene mutations of the *P* and *TYR* genes in several other patients with AROA; however, we failed to detect mutations of either the *TYR* or *P* genes in some others, suggesting that AROA is heterogeneous.

Although the *P* gene product has not yet been characterized experimentally, it is thought to play an important role in eumelanotic pigmentation. In mice, *P* mRNA is only expressed *in vivo* in melanocytes that synthesize eumelanin; melanocytes that specifically synthesize pheomelanin do not express *P* (Rinchik *et al.*, 1993). The predicted human P polypeptide includes a total of 12 transmembrane domains, in an arrangement characteristic of proteins that transport

small molecules such as amino acids. This suggests that the P protein may be an integral component of the melanosomal membrane, possibly involved in the transport of tyrosine, the immediate precursor to melanin biosynthesis. This would be consistent with the observation that pigmentation of melanocytes from humans with type II OCA and from homozygous *p* mutant mice is greatly increased by incubation in excess exogenous tyrosine (reviewed in Silvers, 1979; Witkop *et al.*, 1989). More important, this suggests that treatment with exogenous tyrosine or other agents may offer an approach to pharmacologic therapy for patients with type II OCA.

Type IV (Brown) OCA (MIM #203290)

Originally described in patients from Nigeria, "brown OCA" is associated with moderate hypopigmentation of the skin, hair, and eyes, and modest ocular dysfunction. Brown OCA has long been considered a possible human homologue of brown (*b*) mutant mice, which exhibit brown coat color (Silvers, 1979; Lyon and Searle, 1991). Patients with so-called "brown OCA" are tyrosinase-positive, and are not clinically distinguishable from patients with milder forms of type II OCA. Thus, the issue of allelism between human "brown OCA" and type II OCA remains open. Recently, however, some evidence for hypopigmentation in association with abnormalities of the human *b* locus (*TYRP*; MIM #115501) has begun to emerge.

A cDNA for mouse *b* was the first member of the tyrosinase gene family to be (inadvertently) cloned (Shibahara *et al.*, 1986), and was subsequently shown to represent the *b* locus, rather than tyrosinase itself (Jackson, 1988; Bennett *et al.*, 1990). The amino acid sequence of the *b* gene product is remarkably similar to that of tyrosinase, and hence was named "tyrosinase-related protein" (TRP-1); it corresponds to a melanosomal protein previously termed "gp75" (Vijayasaradhi *et al.*, 1990). In the mouse, *b* locus mutations result in the production of brown rather than black melanin, and recent biochemical studies suggest that TRP-1 corresponds to DHICA oxidase (Jimenez-Cervantes *et al.*, 1994; Winder *et al.*, 1994).

The homologous human gene (*TYRP*) has been cloned (Cohen *et al.*, 1990) and mapped to chromosome segment 9p22–p23 (Chintamaneni *et al.*, 1991b; Murty *et al.*, 1992). There has been no human *TYRP* mutation conclusively identified thus far. However, Wagstaff (1993) demonstrated deletion of *TYRP* in two patients with the 9p-syndrome plus moderate hypopigmentation, and in one patient with "brown OCA" Boissy and coworkers (1993) found virtually no *TYRP*

mRNA and no detectable TRP-1. This patient may thus have true "brown OCA," and eventual molecular analyses of his *TYRP* gene will be of considerable interest.

X-Linked Recessive Ocular Albinism, Nettleship-Falls Type (OA1; MIM #300500)

Ocular albinism of the Nettleship-Falls type (OA1) is an X-linked recessive disorder with clinical characteristics similar to AROA. In affected males mild cutaneous hypopigmentation is accompanied by hypopigmentation of the iris and retina and foveal hypoplasia, resulting in reduced visual acuity, photophobia, nystagmus, and strabismus. Electron microscopy of skin melanocytes of affected individuals demonstrates melanin macroglobules, often termed "macromelanosomes," in some but not all cases. Carrier females may exhibit a heterogeneous distribution of retinal pigmentation, sometimes referred to as a "tigroid" or "mud-spattered" pattern, which is thought to indicate X-inactivation.

At the time of this writing, the OA1 gene had not yet been identified. However, efforts at positional cloning are far advanced. The gene was assigned to chromosome segment Xp22.3 based on genetic linkage studies, with a localization most likely between markers DXS143 and DXS85 (Bergen *et al.*, 1990, 1991; Schnur *et al.*, 1991; Charles *et al.*, 1992). Sunohara *et al.* (1986) described a patient with three apparent X-linked recessive disorders; OA1, X-linked ichthyosis, and Kallmann's syndrome, indicating that these three genes may be in close physical proximity and deleted in this patient (Andria *et al.*, 1987). Furthermore, the colocalization of both OA1 and "X-linked ocular albinism and deafness" (OASD; MIM #300650) to Xp22.3 suggests that OASD may also result from a microdeletion that includes the OA1 gene (Winship *et al.*, 1993). By detailed mapping of the X chromosomal deletions in the patient reported by Sunohara *et al.* (1986) and a second, similar patient, Wapenaar *et al.* (1993) localized the OA1 locus to a 200-kilobase interval, between markers 210B5-R and A187H6-41A. They assembled a 2.6-megabase yeast artificial chromosome (YAC) contig spanning this region, part of a larger YAC contig spanning chromosome segment Xp22 (Schaefer *et al.*, 1993). It seems likely that these YACs will be useful reagents for the eventual isolation of the OA1 gene.

Interestingly, the OA1 locus is located with 1–2 Mb of the gene for "microphthalmia with linear skin defects" (MLS; MIM #309801) (Wapenaar *et al.*, 1993). Although there is not a clear homologue to human OA1 in the mouse, homology between the human and mouse X-chromosomal maps suggests that the mouse "lined" mutation (*Li*) might be a chromosomal deletion encompassing MLS and possibly also OA1 (Lyon and Searle, 1989).

DISORDERS OF MELANOCYTE DEVELOPMENT: PIEBALDISM AND WAARDENBURG SYNDROME

Piebaldism and Waardenburg syndrome are distinct inherited disorders characterized in part by striking areas of congenital depigmentation. These disorders contrast with albinism, in which relatively homogeneous hypopigmentation results from defects of melanocyte function, and with vitiligo, in which acquired areas of depigmentation result from reduced melanocyte survival. In piebaldism the abnormal distribution of pigment results from abnormal distribution of melanocytes during development, most likely due to defective proliferation of melanoblasts prior to migration to the dermis during embryogenesis. In piebaldism the pigmentary anomalies constitute the principal clinical manifestation, whereas in Waardenburg syndrome deafness and dystopia canthorum (lateral displacement of the eyes) are also of major clinical importance. The elucidation of the molecular defects underlying piebaldism and Waardenburg syndrome provide additional examples of the use of human and mouse genetics in combination to dissect the molecular basis of genetic diseases.

Piebaldism (MIM #172800)

Piebaldism is an autosomal dominant disorder of melanocyte development characterized clinically by congenital patches of white skin (leukoderma) and white hair (poliosis), principally located on the scalp, forehead, ventral chest and abdomen, and extremities (Keeler, 1934; Froggat, 1951; Cooke, 1952). In contrast to vitiligo, with which it is frequently confused, in piebaldism the depigmented patches are present from birth and are generally static in shape and distribution, although limited filling in sometimes occurs, especially in milder cases. Hirschprung disease is occasionally also present, but most affected individuals display only the pigmentary anomaly. Piebaldism is relatively rare, although its actual frequency is not known. Because of its distinctive phenotype, piebaldism, sometimes incorrectly called "partial albinism," was one of the first autosomal dominant genetic disorders recognized (Morgan, 1786; Lucian, 1905), and was one of the first genetic disorders for which a pedigree was presented (reviewed in Froggat, 1951). Histologically, the depigmented patches lack most or all melanocytes (Breathnach *et al.*, 1965; Jimbow *et al.*, 1975), although areas of increased pigmentation may occur at the boundaries of, or even within, the regions of hypopigmentation. Melanocytes in the skin and hairbulbs derive embryologically from the neural crest, and piebaldism has thus been considered to be a

lineage–specific disorder of neural crest development, most likely involving defective melanoblast proliferation, migration, or survival (Murphy *et al.*, 1992; Steel *et al.*, 1992).

The critical clues to the molecular basis of human piebaldism came from studies of a similar disorder of mice, "dominant white spotting" (*W*) (reviewed in Spritz, 1993a, 1994b). Mouse dominant white spotting, which is associated with defects of pigmentation, hematopoiesis, and germ-cell development (reviewed in Silvers, 1979; Lyon and Searle, 1989), was found to result from deletions or point mutations of the c-*kit* protooncogene (Chabot *et al.*, 1988; Geissler *et al.*, 1988; Reith *et al.*, 1990; Tan *et al.*, 1990; reviewed in Morrison-Graham and Takahashi, 1993). c-*kit*, originally identified in the genome of the HZ4-feline sarcoma virus (Besmer *et al.*, 1986), encodes the cell-surface receptor for an embryonic growth factor, variously called "steel factor" (SLF), "mast cell growth factor," "stem cell factor," and "KL" (kit ligand) in the literature (Copeland *et al.*, 1990; Flanagan and Leder, 1990; Huang *et al.*, 1990; Zsebo *et al.*, 1990; Murphy *et al.*, 1992; reviewed in Morrison-Graham and Takahashi, 1993). The KIT receptor is expressed by melanocytes, whereas SLF is expressed by other, as yet undefined, cell types. SLF is the product of the steel (*Sl*) locus of mice, and both *Sl* and *W* mutant mice display similar piebald-like phenotypes. However, *Sl* mutant melanocytes develop normally when transplanted to normal skin (since normal ligand is available) whereas *W* mutant melanocytes (with an inherently defective receptor) do not. The human piebaldism locus was mapped to chromosome segment 4q12 on the basis of several patients with piebaldism and *de novo* chromosomal translocations or deletions involving this region (Funderburk and Crandall, 1974; Lacassie *et al.*, 1977; Hoo *et al.*, 1986; Yamamoto *et al.*, 1989). Subsequently, the human *KIT* gene was mapped to approximately the same chromosomal location (Yarden *et al.*, 1987; d'Auriol *et al.*, 1988), suggesting that human piebaldism might, like mouse "dominant white spotting," also result from abnormalities of the *KIT* gene.

The KIT protein is a member of the tyrosine kinase family of transmembrane receptors. As illustrated in Fig. 4, the KIT polypeptide consists of an amino-terminal extracellular ligand-binding receptor domain composed of five immunoglobulin-type repeats, a short transmembrane domain, and an intracellular domain consisting of a bipartite tyrosine kinase domain followed by a carboxyl–terminal tail. The stoichiometry of interaction between SLF and the extracellular domain of the KIT receptor is not certain, but is thought to be monovalent (Lev *et al.*, 1992). On binding SLF, the KIT receptor dimerizes within the cell membrane (Lev *et al.*, 1992), activating its intracellular tyrosine kinase. This, in turn, results in autophosphorylation of specific tyrosine residues within the KIT kinase domain, enhancing the binding of various proteins, including phosphatidylinositol 3′

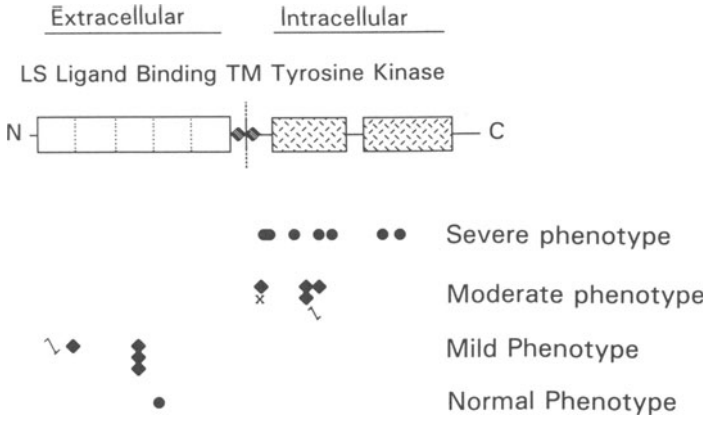

Fig. 4. Locations of known *KIT* gene mutations associated with piebaldism. The amino-terminal extracellular leader sequence (LS) and pentarepetitive ligand-binding domain, the transmembrane domain (TM), and the intracellular bipartite tyrosine kinase domain are indicated. Symbols are as described in the legends to Figs. 2 and 3. Many of the indicated mutations represent our unpublished data, and are not included in Table IV.

kinase and phospholipase Cγl, which act as downstream mediators of the mitogenic signal in the KIT–dependent pathway of signal transduction (reviewed in Morrison-Graham and Takahashi 1993). In the mouse, KIT function is required both immediately prior to melanoblast migration and also postnatally (Nishikawa *et al.*, 1991), and we have shown that KIT function is required for proliferation, although not survival, of human melanocytes in culture (Spritz *et al.*, 1994a). It seems likely, therefore, that white spotting in both human piebaldism and mouse

TABLE IV. Published Mutations of the *KIT* Gene Associated with Piebaldism

Mutation	Base substitution[a]	Phenotype	Reference
E85delG	GAA (Glu)→-AA	Mild	Spritz *et al.*, 1992c
N250-S251delCAGT	AACAGT (AsnSer)→AA----	Mild	Spritz *et al.*, 1993a
E561insG	GAG (Glu)→GGAG	Variable	Spritz *et al.*,1992b
E583K	GAG (Glu)→AAG (Lys)	Severe	Fleischman, 1992
F584L	TTT (Phe)→TTG (Leu)	Severe	Spritz *et al.*, 1992b
K642delAA	AAA (Lys)→A--	Variable	Spritz *et al.*, 1992b
G664R	GGG (Gly)→AGG (Arg)	Severe	Giebel and Spritz, 1991
R791G	AGA (Arg)→GGA (Gly)	Severe	Spritz *et al.*, 1993b
G812V	GGT (Gly)→GTT (Val)	Severe	Spritz *et al.*, 1993b
IVS12 +1G→A	AAGgtaagt→AAGataagt	Variable	Spritz *et al.*, 1992c

[a]Upper case, coding sequence; lower case, intervening sequence (IVS).

W results from deficient proliferation of melanoblasts prior to migration during development.

The human *KIT* gene consists of 21 exons spanning more than 70 kb at chromosome segment 4q12 (Giebel *et al.*, 1992; Vandenbark *et al.*, 1992), part of a cluster of genes encoding type III receptor tyrosine kinases, organized *PDGFRA-KIT-KDR* (Spritz *et al.*, 1994b). The first direct evidence for the involvement of *KIT* mutations in human piebaldism came from Giebel and Spritz (1991), who studied an extended kindred with piebaldism and identified a missense mutation, G664R, within the highly conserved intracellular tyrosine kinase domain, and demonstrated linkage with a lod score in excess of 6 with no recombinants. Further support came from analyses of two additional patients, one with a cytogenetic deletion of 4q12–q21.1 (Yamamoto *et al.*, 1989), in both of whom *KIT* and *PDGFRA* were found to be deleted (Fleischman *et al.*, 1991; Spritz *et al.*, 1992a). As shown in Table IV and Fig. 4, a total of 14 different point mutations of the *KIT* gene have now been identified in different families with piebaldism. Interestingly, as illustrated in Fig. 4, these mutations can be classified into three general groups, each group tending to be associated with piebald phenotypes of differing severity. Thus, a hierarchical paradigm of pathologic human *KIT* mutations appears to account for a graded series of dominant phenotypes in human piebaldism.

The first group of *KIT* gene mutations consists of missense substitutions. A total of 7 missense mutations have been identified (Table IV), all located within the highly conserved tyrosine kinase domain and almost all involving amino acid residues that have been particularly conserved. Several of these human *KIT* substitutions correspond closely to the positions of similar mutations in various strains of *W* mutant mice (reviewed in Morrison-Graham and Takahashi, 1993), underscoring the importance of these sites to function of the KIT receptor. In fact, the human E583K mutation corresponds precisely to the mouse W^{37} mutation (Fleischman, 1992). All of these *KIT* missense substitutions are associated with relatively severe piebald phenotypes. This is a consequence of the fact that the KIT kinase is only activated on dimerization of the receptor, and KIT receptor heterodimers consisting of one normal KIT polypeptide and one abnormal KIT polypeptide are inactive. Thus, patients heterozygous for these "dominant-negative" *KIT* missense mutations have only one-fourth of the normal amount of KIT receptor dimer, and accordingly they exhibit relatively severe piebald phenotypes.

In contrast, the second group of *KIT* mutations completely eliminates the production of KIT protein by the mutant gene. Patients heterozygous for these "loss of function" mutant alleles thus express half of the normal amount of KIT receptor, resulting in haploinsufficiency for KIT-dependent signal transduction.

These *KIT* mutations are thus associated with relatively mild piebald phenotypes, in which the depigmented patches are usually small and poliosis is often absent, although affected individuals frequently experience early graying of the hair. In fact, some members of families with *KIT* mutations of this type have been so mildly affected that the clinical diagnosis was only made subsequent to DNA diagnosis. We have identified three different mutations of this type; two proximally located frameshifts and a nonsense mutation (see Table IV). Interestingly, we detected one of these frameshifts, codons 250-251 ΔCAGT, in three different, unrelated families with mild piebaldism (Spritz *et al.*, 1993a), suggesting that this recurrent *KIT* gene mutation may account for a significant fraction of human piebaldism, especially among clinically milder cases.

The third group of patients with piebaldism exhibits a rather variable phenotype, ranging from extremely mild to quite severe, even among affected members of an individual family. We have identified four different *KIT* mutations of this type; three frameshifts and a splice junction mutation (see Table IV). As shown in Fig. 4, all of these would result in premature termination of translation, truncating the nascent KIT polypeptide distally within the intracellular tyrosine kinase domain. Clearly, these mutations would abolish expression of normal KIT polypeptide from this allele. However, the truncated KIT receptors apparently can still bind SLF and even form dimers, dominant negatively inhibiting function of the normal KIT polypeptide (Lev *et al.*, 1992). It is likely, however, that both the truncated KIT polypeptides and the incompletely translated *KIT* mRNA are relatively unstable. Therefore, these mutations probably reduce KIT function to an amount between one-fourth and one-half of normal, accounting for the intermediate and highly variable piebald phenotype.

Thus, piebaldism is associated with reduced function of the KIT receptor, resulting in decreased KIT-dependent signal transduction and abnormal distribution of melanoblasts during embryologic development. Interestingly, we have found only a single missense substitution within the extracellular ligand-binding domain of the KIT receptor, and this appears to constitute a normal polymorphic variant with no pathologic consequences (unpublished data). As noted above, this region of the KIT polypeptide consists principally of five immunoglobulin-like repeat domains, and it is therefore possible that this region may be at least in part functionally redundant. Accordingly, many amino acid substitutions in this portion of the KIT polypeptide may have little or no effect on ligand binding, and thus may have little or no phenotypic effect. However, the extracellular portion of the KIT polypeptide is also thought to contain the segments that mediate receptor dimerization, and it seems likely that pathologic amino acid substitutions of residues involved in this process may be encountered in the future.

Overall, we have identified pathologic point mutations of the *KIT* in approximately two-thirds of the patients with piebaldism studied to date. About half of the remaining patients have complete or partial deletions of the *KIT* gene. The rest may have occult *KIT* point mutations not detected by SSCP/heteroduplex screening, and genetic linkage analyses in three of these families showed complete linkage of the piebald trait to *KIT* intragenic markers (unpublished data). None of these patients have abnormalities of the *MGF* gene (the human *Steel* gene homologue), suggesting that, in contrast with mice, mutations of this gene may not result in the piebald phenotype in humans. The possible roles that the adjacent *PDGFRA* and *KDR* genes might play in the phenotypes of some of these patients is also not known. The mouse "patch" (*Ph*) mutation, which results in a dominant white spotting phenotype similar to that of *W*, comprises a deletion that includes the *pdgfra* gene but not c-*kit* (Smith *et al.*, 1991; Stephenson *et al.*, 1991). Although white spotting in *Ph* mice might result either from deletion of the *pdgfra* gene itself or from inhibitory effects of the large chromosomal deletion on expression of the nearby c-*kit* gene, it thus seems possible that some cases of human piebaldism might result from mutations in *PDGFRA*.

Waardenburg Syndrome (MIM #193500)

Waardenburg syndrome, first described in 1951 by a Dutch ophthalmologist (Waardenburg, 1951), is an autosomal dominant disorder characterized clinically by piebald-like pigmentary anomalies of the skin and hair, pigmentary abnormalities of the iris (heterochromia iridis), lateral displacement of the inner canthi of the eyes (dystopia canthorum), and sensorineural deafness (Waardenburg, 1951; DiGeorge *et al.*, 1960). Waardenburg syndrome occurs with an overall frequency of 1 to 2 per hundred thousand, and accounts for at least 0.5% of cases of congenital deafness. All of the abnormalities in Waardenburg syndrome involve the neural crest, and both Hirschsprung's disease (Currie *et al.*, 1986; Ariturk *et al.*, 1992) and neural tube defects (Bergleiter and Harris, 1992; Carezani–Gavin *et al.*, 1992; Chatkupt *et al.*, 1993; Kromberg and Krause, 1993) occur at increased frequencies among affected individuals. Waardenburg syndrome has thus been considered a more general disorder of neural crest development than piebaldism. Three subtypes of Waardenburg syndrome have been clinically distinguished; Waardenburg syndrome type I (*WS1*) is the classic form, Waardenburg syndrome type II (*WS2*; MIM #193510) lacks dystopia canthorum, and Waardenburg syndrome type III (*WS3*; Klein–Waardenburg syndrome; MIM #148820) is associated with limb abnormalities as well as dystopia canthorum.

Elucidation of the molecular basis of human Waardenburg syndrome was facilitated by studies of a similar disorder of mouse, "Splotch" (*Sp*) (reviewed in Pierpont and Erickson, 1993; Spritz, 1993a). *Splotch* mutations typically result in piebald-like patches of unpigmented skin and hair (Epstein *et al.*, 1991, 1993; Goulding *et al.*, 1991; Moase and Trasler, 1992; Goulding *et al.*, 1993; Vogan *et al.*, 1993), probably due to delayed migration of melanoblasts or to a reduction in their number so that melanoblasts fail to reach the affected regions before hair follicles develop. The murine *Splotch* (*Sp*) locus encodes a developmental gene known as *Pax-3*, one of a family of so-called "paired box" genes involved in embryological development (Burri *et al.*, 1989). Although the exact function of the *Pax-3* gene product is not yet known, it is thought to be a transcription factor critical for activating melanoblasts to begin migration from the neural crest. The human PAX3 polypeptide contains four principal structural motifs: the "paired box" domain, a homeobox domain, a conserved octapeptide, and a serine-threonine-proline-rich carboxyl segment (Fig. 5). The 128–amino acid paired box domain, from which the name of the gene is derived, and the 60–amino acid homeobox domain are both highly conserved amino acid sequence motifs present in a number of mammalian and *Drosophila* genes involved in controlling segmentation. These motifs form a helix-turn-helix structure and are both thought to mediate DNA binding.

The murine *Splotch* locus was mapped to chromosome 1, in a region that is homologous to part of human chromosome 2q, and the mouse Sp^{2H} mutation was then found to consist of a deletion in the paired box domain of *Pax-3* (Epstein

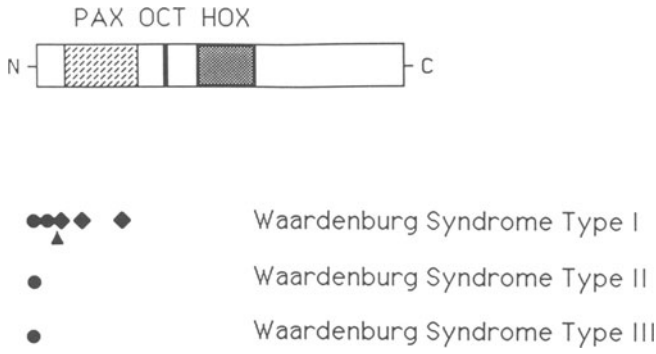

Fig. 5. Locations of known *PAX3* gene mutations associated with Waardenburg syndrome. The paired box domain (PAX), conserved octapeptide (OCT), and the homeobox domain (HOX) are indicated. Symbols are as described in the legends to Figs. 2 and 3.

et al., 1991). The human Waardenburg syndrome gene was first localized to the distal long arm of chromosome 2 on the basis of a patient with an chromosomal inversion of 2q35–q37.3 (Ishikiriyama *et al.*, 1989), and subsequent genetic linkage analyses demonstrated linkage between *WS1* and markers in this region (Foy *et al.*, 1990; Asher *et al.*, 1991), suggesting that human Waardenburg syndrome and mouse Splotch might be homologous. Although only a portion of the human *PAX3* gene had been characterized, Tassabehji and coworkers (1992) and Baldwin and coworkers (1992) quickly identified point mutations in several patients with *WS1*, and demonstrated that these mutations were genetically linked to the Waardenburg phenotype in these families.

As shown in Fig. 5 and Table V, six different mutations of the *PAX3* gene have now been reported in patients with *WS1*. These include an in-frame deletion within the paired box domain (Tassabehji *et al.*, 1992), three frameshifts (Morell *et al.*, 1992; Tassabehji *et al.*, 1993), and two missense substitutions, both located within the paired box domain (Baldwin *et al.*, 1992; Hoth *et al.*, 1993). Furthermore, Hoth *et al.* (1993) identified an additional missense mutation, N47H, in a family with so-called *WS3*, demonstrating that *WS1* and *WS3* are allelic; these clinically distinct disorders result from different abnormalities of *PAX3*. By genetic linkage analysis of 41 families, Farrer and coworkers (1992) determined that mutations at the *WS1* locus on distal chromosome 2, apparently the *PAX3* gene, account for about half of cases of *WS1*. This implies the existence of at least one additional gene for *WS1* located elsewhere in the genome.

TABLE V. Published Mutations of the *PAX3* Gene Associated with Waardenburg Syndrome

Mutation	Base substitution[a]	Phenotype	Reference
N47H	AAC (Asn)→CAC (His)	*WS3*	Hoth *et al.*, 1993
G48A	GGC (Gly)→GCC (Ala)	*WS2*	Tassabehji *et al.*, 1993
P50L	CCG (Prog)→CTG (Leu)	*WS1*	Baldwin *et al.*, 1992
R56L	CGC (Arg)→CTC (Leu)	*WS1*	Hoth *et al.*, 1993
M62-I67 0	ATGGCCCACCACGGCATCCGG (MetAlaHisHisGlyIleArg)→ A----------GG (Arg)	*WS1*	Tassbehji *et al.*, 1992
I64delA	ATA (Ile)→AT-	*WS1*	Tassabehji *et al.*, 1993
R89-T93del	AGGTACCAGGAGACT (ArgTyrGlnGluThr)→A--	*WS1*	Morell *et al.*, 1993
H186-S187delCA*	CACAGC (HisSer)→CA--GC	*WS1*	Tassabehji *et al.*, 1993

[a]Upper case, coding sequence; lower case, intervening sequence (IVS).

Two groups recently reported refined map data for the human *PAX3* gene. Tsukamoto and coworkers (1992b) showed that the distal chromosome 2q inversion associated with *WS1*, described above, interrupted exons 2 and 3 of the *PAX3* gene, and they suggested that the *PAX3* gene is located within chromosome segment 2q35. Similarly, Lu-Kuo *et al.* (1993) showed that the *PAX3* gene is deleted in a patient with Waardenburg syndrome and a distal chromosome 2 deletion (Kirkpatrick *et al.*, 1992), and they mapped the *PAX3* gene to 2q36.1–q36.2. These two map assignments are actually quite close, probably within the limits of cytogenetic resolution.

The issue of whether or not *WS2* is allelic with other forms of Waardenburg syndrome is not entirely clear. Recently, Hughes and coworkers (1994) reported localization of the gene *WS2* to chromosome segment 3p12–p14.1, in close proximity to *MITF*, the human homolog of the mouse *microphthalmia* gene (Tachibana *et al.*, 1994). As discussed below, *mi* mutant mice exhibit pigmentary abnormalities and hearing loss, suggesting that *MITF* is a good candidate gene for WS2. Tassabehji *et al.* (1993) reported a *PAX3* missense substitution in a family that they considered to have *WS2*; however, clinical photographs of this family are suggestive of mild dystopia canthorum, and thus *WS1*. Farrer and coworkers (1992) found no evidence of linkage between chromosome 2 markers and *WS2*, indicating that this disorder usually does not result from mutations of *PAX3*.

In a surprising turn of events, Barr and coworkers (1993) recently showed that the *PAX3* gene is rearranged in the chromosome 2;13 translocation consistently observed in cases of alveolar rhabdomyosarcoma (MIM #268220), an aggressive solid tumor of childhood. In three such tumors the chromosome 2 breakpoints are located within the fourth intervening sequence of the *PAX3* gene, juxtaposing the upstream *PAX3* DNA binding motifs, including the paired box domain, conserved octapeptide, and homeobox domain, to a specific gene located on chromosome 13q14. As a result, an abundant novel mRNA is transcribed, most likely encoding a novel fusion protein that interferes with the normal controls of striated muscle cell proliferation. Thus, the *PAX3* gene appears to lead a double life: inherited loss of function mutations result in Waardenburg syndrome and acquired gain of function mutations result in alveolar rhabdomyosarcoma.

OTHER CLONED GENES AFFECTING PIGMENTATION IN THE MOUSE

In addition to the correlation of human pigmentary disorders with cloned genes discussed above, a number of mouse loci with mutant phenotypes that

include aberrant pigmentation have also been cloned that have not yet been definitively associated with human disorders (see Table I). However, it seems likely that at least some of these mouse loci do have counterparts in human genetic disease, and may provide clues that will prove instrumental for identifying the human gene defects.

Mottled

The mouse mottled (*mo*) locus is associated with a semidominant mutant phenotype involving a variegated pattern of pigmentation, wavy vibrissae and coat, mild skeletal and neurological abnormalities, and abnormalities of collagen and elastin (Silvers, 1979; Lyon and Searle, 1989). The murine gene is located on the X chromosome, and is thought to encode a protein involved in the metabolism of copper, an essential component of tyrosinase. Altered pigment production in *mo* mice might thus result from decreased melanogenic function of tyrosinase (Holstein *et al.*, 1979). Mouse *mottled* is thought to be homologous to human Menkes disease (MIM #309400), an X-linked recessive genetic disorder of copper transport (Camakaris *et al.*, 1980) characterized by hypopigmentation, defective keratinization of the hair, and neurologic and bone abnormalities. This gene has recently been cloned and found to encode a copper transporting ATPase, as expected (Chelly *et al.*, 1993; Mercer *et al.*, 1993; Vulpe *et al.*, 1993).

Pallid

The mouse pallid (*pa*) locus is associated with a homozygous mutant phenotype of significant hypopigmentation, otoliths, reduced activity of several lysosomal enzymes, a storage pool deficiency of blood platelets, and slightly reduced viability of homozygotes (Silvers, 1979; Lyon and Searle, 1989). There are abnormal aggregates of subcellular organelles, including melanosomes and lysosomes (Theriault and Hurley, 1970; Ito *et al.*, 1982), and reduced number and content of platelet dense granules, resulting in a prolonged bleeding time. Pallid mice also have a severe deficiency of α1–antitrypsin activity (Martorana *et al.*, 1993), although the cause remains unknown. The murine *pa* gene has been cloned (White *et al.*, 1992), and although as yet uncharacterized, the *pa* gene product may be required for stabilization of subcellular organelle membranes, analogous to factors required for stabilizing plasma membranes. Mouse *pa* may be homologous to at least some cases of the human Hermansky-Pudlak syndrome (MIM #203300).

Pearl

Pearl (*pe*) mutant mice exhibit a phenotype characterized by slight eye hypopigmentation and dilute coat color associated with reduced activities of several lysosomal enzymes and a bleeding diathesis due to a platelet storage pool deficiency (Silvers, 1979; Lyon and Searle, 1989). Mouse *pe* may thus also be homologous to some cases of human Hermansky-Pudlak syndrome (MIM #203300). The *pe* mutation arose spontaneously and frequently reverts to wild type, suggesting that the mutation may involve an insertion or tandem duplication. The *pe* gene is located on mouse chromosome 13, and the recent isolation of closely linked markers may facilitate future efforts at positional cloning (Rikke *et al.*, 1993).

Microphthalmia

The mouse microphthalmia (*mi*) locus is associated with a mutant phenotype that can include microphthalmia, hypopigmentation, various abnormalities of neural crest development, deficient mast cells, and osteopetrosis (Silvers, 1979; Lyon and Searle, 1989). The *mi* gene product is thus apparently required for normal eye and ear development, and also for fertility and hematopoiesis, and is required to transduce signals from the CSF1 and SLF receptors (respectively, the *FMS* and *KIT* gene products) (Dubreuil *et al.*, 1991). The mouse *mi* gene encodes a novel member of the basic–helix–loop–helix–leucine zipper family of transcription factors (Hodgkinson *et al.*, 1993)—proteins that have a variety of roles in regulating gene expression, cellular proliferation and differentiation—consistent with the pleiotropic phenotypic effects of *mi* mutations. Lamoreux *et al.* (1992) have reported that in the mouse *mi* mutations correlate with the vitiligo phenotype. Although superficially similar to piebaldism, in vitiligo melanocytes are normally distributed and functional at early ages and pigmentation is normal. Over time, however, melanocytes in defined areas cease to function, probably due to melanocyte death, and involvement of the affected areas progresses, often until the individual is completely depigmented. The human homologue to the mouse *mi* gene was recently cloned (*MITF*) (Tachibana *et al.*, 1994), and it will be of interest to determine whether this gene is involved in the pathogenesis of vitiligo in humans.

Furthermore, as discussed above, the *MITF* gene is a good candidate for human *WS2* (Hughes *et al.*, 1994), although abnormalities of *MITF* have yet to be identified in this disorder.

Dilute

The mouse dilute (*d*) locus is associated with diluted coat color (Silvers, 1979; Lyon and Searle, 1989). The dendrites of melanocytes in *d/d* mice are relatively poorly developed, and the distribution of melanosomes is impaired, with clumping in the perinuclear region, although their ultrastructure appears normal. The murine *d* gene has been cloned, and encodes a protein clearly related to myosin (Mercer *et al.*, 1991; Sanders *et al.*, 1992). The *d* gene product may somehow participate in the progressive movement of melanosomes from the perinuclear region to the dendrites of the melanocyte, which is essential for the subsequent transfer of melanosomes to keratinocytes and thus to pigmentation of skin and hair.

Extension

The mouse extension (*e*) locus is associated with a mutant phenotype in which there is exclusive production of either eumelanin or pheomelanin (Silvers, 1979; Lyon and Searle, 1989). Both the murine and human *e* genes have been cloned and shown to encode the melanocyte specific cellular receptor for melanocyte-stimulating hormone (MSH) (Mountjoy *et al.*, 1992; Gantz *et al.*, 1993; Robbins *et al.*, 1993; Magenis *et al.*, 1994). The *e* gene product is one of a family of melanocortin (e.g., MSH and ACTH) receptors that define a subfamily of receptors coupled to a guanine nucleotide-binding (G) protein, and the relationship between this function and the mutant phenotypes has not yet been elucidated. The *e* locus MSH receptor is specifically expressed by melanocytes, whereas the other receptors in this family are expressed by other types of cells and are probably required for other types of functions in nonmelanocytic tissues, including the brain, pituitary, and immune system.

Agouti

The agouti (*a*) locus in mice regulates the production of eumelanin versus pheomelanin by a yet unknown mechanism, as well as controlling a variety of other phenotypic parameters including obesity, susceptibility to neoplasia, and diabetes. Its effect on pigmentation is somehow coordinated with the opposing action of MSH from exogenous sources, that is, from cells peripheral to the melanocyte (cf. discussion of *e* locus above). The *a* gene has now been cloned, and it encodes a unique, 131-amino acid protein with a leader sequence and a cysteine–

rich carboxy terminus (Bultman *et al.*, 1992; Miller *et al.*, 1993). The *a* gene product appears to be a paracrine signalling protein, which controls melanin production primarily within hair follicles. A number of mutant alleles of the agouti locus have been identified that result in a variety of pleiotropic effects, and several are lethal when homozygous. Recent studies (Vrieling *et al.*, 1994; Yen *et al.*, 1994) suggest that the apparent complexity of the *a* locus is due to effects on a number of regulatory elements that control a single coding sequence, regulating an animal's temporal or geographic gene expression. At least one of these mutations (yellow, A^y) is a deletion that removes a different coding sequence adjacent to *a*, and the lethality is not due to the loss of *a* itself (Duhl *et al.*, 1994; Michaud *et al.*, 1994). Another mutation, lethal nonagouti (a^x) is a deletion involving regulatory regions of the *a* gene, and may affect pigmentation by removing an *a* enhancer region, while the lethality is due to deletion of yet another adjacent gene, encoding S-adenosylhomocysteine hydrolase (Miller *et al.*, 1994). There is propensity for homozygous nonagouti to revert to two other dominant *a* alleles, termed black-and-tan (a^t) and white bellied agouti (a^W), at relatively high frequency. All three of these *a* alleles (*a*, a^t and a^W) have insertions into the *a* gene at precisely the same location in the first exon (Bultman *et al.*, 1994). The relatively high frequency of reversion results from excision of these inserted sequences via homologous recombination. The distinct insertions present in those alleles apparently elicit their various effects on pigmentation by affecting the expression of alternatively processed forms of the *a* mRNA.

Slaty

Slaty (*slt*) mutant mice exhibit a phenotype characterized by slight dilution of coat pigment (Silvers, 1979; Lyon and Searle, 1991). Both the mouse and human *slt* genes have been cloned (Jackson *et al.*, 1992; Yokoyama *et al.*, 1994), and shown to encode a melanocyte-specific protein related to tyrosinase, termed TRP–2. TRP–2 has features in common with the *brown* locus (TRP–1) and tyrosinase proteins, including a transmembrane region, highly conserved putative copper binding sites, two conserved cysteine–rich domains, potential glycosylation sites, and a signal peptide. Interestingly, there is evidence that TRP–2 requires iron for catalytic function rather than copper, as tyrosinase does (Chakraborty *et al.*, 1991, 1992). The function of TRP-2 has now been established as DOPAchrome tautomerase (Hearing *et al.*, 1992; Tsukamoto *et al.*, 1992a; Yokoyama *et al.*, 1994), the enzyme that regulates that melanogenic pathway following the production of DOPAchrome. The biological importance of the regulation of DHICA versus DHI production in melanocytes by DOPAchrome tautomerase is as yet unknown,

although the phenotypic properties of melanins produced in the presence or absence of TRP2 are markedly distinct (Orlow *et al.*, 1992) and they also have significantly different cytotoxic properties (Urabe *et al.*, 1994).

Silver

Silver (*si*) mutant mice exhibit a phenotype characterized by variable pigmentation (Silvers, 1979; Lyon and Searle, 1991) associated with a reduced number of pigment granules and somewhat reduced melanocyte survival (Spanakis *et al.*, 1992). Pmel 17-1, an anonymous melanocyte cDNA marginally related to tyrosinase, has been mapped to the *si* locus of mice (Kwon *et al.*, 1991). The function of the putative silver protein is unknown, although its expression is restricted to melanocytes and its abundance correlates well with pigmentation (Kwon *et al.*, 1987a). The silver protein appears to be closely related to a melanosomal matrix protein initially identified in chicken melanocytes (Jimbow *et al.*, 1988; Mochii *et al.*, 1991; Orlow *et al.*, 1993), suggesting that it may have an integral function in melanosomal structure.

REFERENCES

Andria, G., Ballabio, A., and Parenti, G., 1987, X-linked ichthyosis due to steroid sulfatase deficiency associated with hypogonadism and anosmia, *Ann. Neurol.* **22:**98.

Ariturk, E., Tosyali, N., and Ariturk, N., 1992, A case of Waardenburg syndrome and aganglionosis, *Turk. J. Pediatr.* **34:**111–114.

Asher, J.H., Jr., Morell, R., and Friedman, T.B., 1991, Waardenburg syndrome (WS): The analysis of a single family with a WS1 mutation showing linkage to RFLP markers on human chromosome 2q, *Am. J. Hum. Genet.* **48:**43–52.

Baldwin, C.T., Hoth, C.F., Amos, J.A., Da Silva, E.O., and Milunsky, A., 1992, An exonic mutation in the *HuP2* paired domain gene causes Waardenburg syndrome, *Nature* **355:**637–638.

Barr, F.G., Galili, N., Holick, J., Biegelo, J.A., Rovera, G., and Emanuel, B.S., 1993, Rearrangement of the PAX3 paired box gene in the pediatric solid tumor alveolar rhabdomyosarcoma, *Nature Genetics* **3:**113–117.

Bennett, D.C., 1991, Color genes, oncogenes and melanocyte differentiation, *J. Cell. Sci.* **98:**135–139.

Bennett, D.C., Huszar, D., Laipis, P.J., Jaenisch, R., and Jackson, I.J., 1990, Phenotypic rescue of mutant brown melanocytes by a retrovirus carrying a wild type tyrosinase–related protein gene, *Development* **110:**471–475.

Bergen, A.A.B., Sammans, C., Van Dorp, D.B., Ferguson-Smith, M.A., Gal, A., and Bleeker-Wagemakers, E.M., 1990, Localization of the X-linked ocular albinism gene (OA1) between DXS278/DXS237 and DXS143/DXS16 by linkage analysis, *Ophthalmic Pediatr. Genet.* **11:** 165–170.

Bergen, A.A.B., Samanns, C., Schuurman, E.J.M., Van Osch, L., Van Dorp, D.B., Pinckers, A.J.L.G., Bakker, E., Gal, A., Van Ommen, G.J.B., and Bleeker-Wagemakers, E.M., 1991,

Multipoint linkage analysis in X-linked ocular albinism of the Nettleship-Falls type, *Hum. Genet.* **88:**162–166.

Bergleiter, M.L., and Harris, D.J., 1992, Waardenburg syndrome and meningocele, *Am. J. Med. Genet.* **44:**541.

Besmer, P., Murphy, J.E., George, P.C., Qiu, F., Bergold, P.J., Lederman, L., Snyder, H.W., Jr., Brodeur, D., Zuckerman, E.E., and Hardy, W.S., 1986, A new acute transforming feline retrovirus and the relationship of its oncogene v-*kit* with the protein kinase gene family, *Nature* **320:**415–421.

Boissy, R.E., Zhao, H., Austin, L.M., Nordlund, J.J., and King, R.A., 1993, Melanocytes from an individual with brown oculocutaneous albinism lack expression of TRP-1, the product of the human homolog of the murine brown locus, *Am. J. Hum. Genet.* **53**(Suppl.):160.

Breathnach, A.S., Fitzpatrick, T.B., and Wyllie, L.M.A., 1965, Electron microscopy of melanocytes in a case of human piebaldism, *J. Invest. Dermatol.* **45:**28–37.

Bultman, S.J., Michaud, E.J., and Woychik, R.P., 1992, Molecular characterization of the mouse *agouti* locus, *Cell* **71:**1195–1204.

Bultman, S.J., Klebig, M.L., Michaud, E., Sweet, H.O., Davisson, M.T., and Woychik, R.P., 1994, Molecular analysis of reverse mutations from nonagouti (*a*) to black-and-tan (a^t) and white-bellied agouti (A^W) reveals alternative forms of *agouti* transcripts, *Genes Dev.* **8:**481–490.

Burri, M., Tromvoukis, Y., Bopp, D., Frigerio, G., and Noll, M., 1989, Conservation of the paired domain in metazoans and its structure in three isolated human genes, *EMBO J.* **8:**1183–1190.

Butler, M.G., 1989, Hypopigmentation: A common feature of Prader-Labhart-Willi syndrome, *Am. J. Hum. Genet.* **45:**140–146.

Camakaris, J., Danks, D.M., Ackland, L., Cartwright, E., Borger, P., and Cotton, R.G.H., 1980, Altered copper metabolism in cultured cells from human Menkes' syndrome and mottled mouse mutants, *Biochem. Genet.* **18:**117–131.

Carezani-Gavin, M., Slarren, S.K., and Steege, T., 1992, Waardenburg syndrome associated with meningomyelocele, *Am. J. Med. Genet.* **42:**135.

Chabot, B., Stephenson, D.A., Chapman, V.M., Besmer, P., and Bernstein, A., 1988, The proto-oncogene c-*kit* encoding a transmembrane tyrosine kinase receptor maps to the mouse *W* locus, *Nature* **335:**88–90.

Chakraborty, A.K., and Pawelek, J.M., 1991, Evidence that DOPAchrome conversion factor is a metalloenzyme, *Pigment Cell Res.* **4:**132–133.

Chakraborty, A.K., Orlow, S.J., and Pawelek, J.M., 1992, Evidence that DOPAchrome tautomerase is a ferrous iron-binding glycoprotein, *FEBS Lett.* **302:**126–128.

Charles, S.J., Moore, A.T., and Yates, J.R.W., 1992, Genetic mapping of X-linked ocular albinism: Linkage analysis in British families, *J. Med. Genet.* **29:**552–554.

Chatkupt, S., Chatkupt, S., and Johnson, W.G., 1993, Waardenburg syndrome and myelomeningocele in a family, *J. Med. Genet.* **30:**83–84.

Chelly, J., Tumer, Z., Tonnesen, T., Petterson, A., Ishikawa-Brudh, Y., Tommerup, N., Horn, N., and Monaco, A.P., 1993, Isolation of a candidate gene for Menkes disease that encodes a potential heavy metal binding protein, *Nature Genetics* **3:**14–19.

Chintamaneni, C.D., Halaban, R., Kobayashi, Y., Witkop, C.J., Jr., and Kwon, B.S., 1991a, A single base insertion in the putative transmembrane domain of the tyrosinase gene as a cause for tyrosinase-negative oculocutaneous albinism, *Proc. Natl. Acad. Sci. USA* **88:**5272–5276.

Chintamaneni, C.D., Ramsay, M., Colman, M.A., Fox, M.F., Pickard, R.T., and Kwon, B.S., 1991b, Mapping the human CAS2 gene, the homolog of the mouse brown (*b*) locus, to human chromosome 9p22-pter, *Biochem. Biophys. Res. Commun.* **178:**227–235.

Cohen, T., Muller, R.M., Tomita, Y., and Shibahara, S., 1990, Nucleotide sequence of the cDNA encoding human tyrosinase-related protein, *Nucl. Acids Res.* **18:**2807–2808.

Cooke, J.V., 1952, Familial white skin spotting (piebaldness) ('partial albinism') with white forelock, *J. Pediatr.* **41:**1–12.

Copeland, N.G., Gilbert, D.J., Cho, B.C., Donovan, P.J., Jenkins, N.A., Cosman, D., Anderson, D., Lyman, S.D., and Williams, D.E., 1990, Mast cell growth factor maps near the steel locus on mouse chromosome 10 and is deleted in a number of steel alleles, *Cell* **63:**175–183.

Currie, A.B.M., Haddad, M., Honeyman, M., and Boddy, S-A.M., 1986, Associated developmental abnormalities of the anterior end of the neural crest: Hirschsprung's disease-Waardenburg's syndrome, *J. Pediatr. Surg.* **21:**248–250.

d'Auriol, L., Mattei, M.G., Andre, C., and Galibert, F., 1988, Localization of the human c-kit protooncogene on the q11–q12 region of chromosome 4, *Hum. Genet.* **78:**374–376.

DiGeorge, A.M., Olmsted, R.W., and Harley, R.D., 1960, Waardenburg syndrome, *J. Pediatr.* **57:**649–669.

Dubreuil, P., Forrester, L., Rottapel, R., Reedijk, M., Fujita, J., and Bernstein, A., 1991, The c-*fms* gene complements the mitogenic defect in mast cells derived from mutant *W* mice but not *mi* (microphthalmia) mice, *Proc. Natl. Acad. Sci. USA* **88:**2341–2345.

Duhl, D.M.J., Vrieling, H., Stevens, M.E., Saxon, P.J., Miller, M.W., Epstein, C.J., and Barsh, G.S., 1994, Pleiotropic effects of the mouse *lethal yellow* (A^y) mutation explained by deletion of a maternally expressed gene and the simultaneous production of *agouti* fusion RNAs, *Development*, in press.

Durham, F.M., 1904, On the presence of tyrosinases in the skins of some pigmented vertebrates, *Proc. R. Soc. (Lond.)* **74:**310–313.

Durham-Pierre, D., Gardner, J.M., Nakatsu, Y., King, R.A., Francke, U., Ching, A., Aquaron, R., del Marmol, V., and Brilliant, M.H.(1994).African origin of an intragenic deletion of the human *P* gene in tyrosinase positive oculocutaneous albinism. *Nature Genet.* **7:**176–179.

Epstein, D.J., Vekemans, M., and Gros, P. 1991, Splotch (Sp2H), a mutation affecting development of the mouse neural tube, shows a deletion within the paired homeodomain of Pax-3, *Cell* **67:** 767–774.

Epstein, D.J., Vogan, K.J., Trasler, D.G., and Gros, P., 1993, A mutation within intron 3 of the Pax-3 gene produces aberrantly spliced mRNA transcripts in the splotch (Sp) mouse mutant, *Proc. Natl. Acad. Sci. USA* **90:**532–536.

Farrer, L.A., Grundfast, K.M., Amos, J., Arnos, K.S., Asher, J.H., Jr., Beighton, P., Diehl, S.R., Fex, J., Foy, C., Friedman, T.B., Greenberg, J., Hoth, C., Marazita, M., Milunsky, A., Morell, R., Nance, W., Newton, V., Ramesar, R., San Agustin, T.B., Skare, J., Steens, C.A., Wagner, R.G., Jr., Wilcox, E.R., Winship, I., and Read, A.P., 1992, Waardenburg syndrome (WS) type I is caused by defects at multiple loci, one of which is near ALPP on chromosome 2: First report of the WS consortium, *Am. J. Hum. Genet.* **50:**902–913.

Fitzpatrick, T.B., 1981, *Biology and Diseases of Dermal Pigmentation*, pp.3–18, University of Tokyo Press, Tokyo.

Flanagan, J.G., and Leder, P., 1990, The kit ligand: A cell surface molecule altered in steel mutant fibroblasts, *Cell* **63:**185–194.

Fleischman, R.A., Saltman, D.L., Stastny, V., and Zneimer, S., 1991, Deletion of the c-*kit* protooncogene in the human developmental defect piebald trait, *Proc. Natl. Acad. Sci. USA* **88:**10885–10889.

Fleischman, R.A., 1992, Human piebald trait resulting from a dominant negative mutant allele of the c-*kit* membrane receptor gene, *J. Clin. Invest.* **89:**1713–1717.

Foy, C., Newton, V.E., Wellesley, D., Harris, R., and Read, A.P., 1990, Assignment of WS1 locus to human 2q37 and possible homology between Waardenburg syndrome and the Splotch mouse, *Am. J. Hum. Genet.* **46:**1017–1023.

Froggat, P., 1951, An outline with bibliography of human piebaldism, *Ir. J. Med. Sci.* **398:**86–94.

Funderburk, S.J., and Crandall, B.F., 1974, Dominant piebald trait in a retarded child with a reciprocal translocation and small intercalary deletion, *Am. J. Hum. Genet.* **26:**715–722.

Gantz, I., Miwa, H., Konda, Y., Shimoto, Y., Tashiro, T., Watson, S.J., DelValle, J., and Yamada, T., 1993, Molecular cloning, expression, and gene localization of a fourth melanocortin receptor, *J. Biol. Chem.* **268:**15174–15179.

Gardner, J.M., Nakatsu, Y., Gondo, Y., Lee, S., Lyon, M.F., King, R.A., and Brilliant, M.H., 1992, The mouse pink-eyed dilution gene: Association with human Prader-Willi and Angelman syndromes, *Science* **257:**1121–1124.

Garrod, A.E., 1908, The Croonian lectures on inborn errors of metabolism: Lecture I, *Lancet* **2:**1–7.

Geissler, E.N., Ryan, M.A., Housman, D.E., 1988, The dominant-white spotting (W) locus of the mouse encodes the c-*kit* proto-oncogene, *Cell* **55:**185–192.

Gellius, 1952, *The Attic Nights of Aulus Gellius*, Book 9 (J.C. Rolfe, trans.), Harvard University Press, Cambridge.

Gershoni-Baruch, R., Rosenmann, A., Droetto, S., Holmes, S., Tripathi, R.K., Spritz, R.A., 1994, Mutations of the tyrosinase gene in patients with oculocutaneous albinism from various ethnic groups in Israel, *Am. J. Hum. Genet.* **54:**586–594.

Giebel, L.B., and Spritz, R.A., 1990, RFLP for MboI in the human tyrosinase (TYR) gene detected by PCR, *Nucl. Acids Res.* **18:**3103.

Giebel, L.B., and Spritz, R.A., 1991, Mutation of the c-kit (mast/stem cell growth factor receptor) proto-oncogene in human piebaldism, *Proc. Natl. Acad. Sci. USA* **88:**8696–8699.

Giebel, L.B., Strunk, K.M., King, R.A., Hanifin, J.M., and Spritz, R.A., 1990, A frequent tyrosinase gene mutation in classic, tyrosinase-negative (type IA) oculocutaneous albinism, *Proc. Natl. Acad. Sci. USA* **87:**3255–3258.

Giebel, L.B., Musarella, M.A., and Spritz, R.A., 1991a, A nonsense mutation in the tyrosinase gene of Afghan patients with tyrosinase negative (type IA) oculocutaneous albinism, *J. Med. Genet.* **28:**464–467.

Giebel, L.B., Strunk, K.M., and Spritz, R.A., 1991b, Organization and nucleotide sequences of the human tyrosinase gene and a truncated tyrosinase-related segment, *Genomics* **9:**435–445.

Giebel, L.B., Tripathi, R.K., King, R.A., and Spritz, R.A., 1991c, A tyrosinase gene missense mutation in temperature-sensitive type I oculocutaneous albinism. A human homologue to the Siamese cat and the Himalayan mouse, *J. Clin. Invest.* **87:**1119–1122.

Giebel, L.B., Tripathi, R.K., Strunk, K.M., Hanifin, J.M., Jackson, C.E., King, R.A., and Spritz, R.A., 1991d, Tyrosinase gene mutations associated with type IB ("yellow") oculocutaneous albinism, *Amer. J. Hum. Gen.* **48:**1159–1167.

Giebel, L.B., Strunk, K.M., Holmes, S.A., and Spritz, R.A., 1992, Organization and nucleotide sequence of the human *KIT* (mast/stem cell growth factor receptor) proto-oncogene, *Oncogene* **7:**2207–2217.

Goulding, M.D., Chalepakis, G., Deutsch, U., Erselius, J.R., and Gruss, P., 1991, Pax-3, a novel murine DNA binding protein expressed during early neurogenesis, *EMBO J.* **10:**1135–1147.

Goulding, M.D., Sterrer, S., Fleming, J., and Balling, R., 1993, Analysis of the *Pax-3* gene in the mouse mutant splotch, *Genomics* **17:**355–363.

Hearing, V.J., and King, R.A., 1994, Determinants of skin color: Melanocytes and melanization. In: *Pigmentation and Pigmentary Abnormalities* (N. Levine, ed.), pp.3–18, CRC Press, New York.

Hearing, V.J., and Tsukamoto, K., 1991, Enzymatic control of pigmentation in mammals, *FASEB J.* **5:**2902–2909.

Hearing, V.J., Tsukamoto, K., Urabe, K., Kameyama, K., Montague, P.M., and Jackson, I.J., 1992, Functional properties of cloned melanogenic proteins, *Pigment Cell Res.* **5:**264–270.

Hodgkinson, C.A., Moore, K.J. Nakayama, A., Steingrimsson, E., Copeland, N.G., Jenkins, N.A., and Arnheiter, H., 1993, Mutations at the mouse microphthalmia locus are associated with defects in a gene encoding a novel basic-helix-loop-helix-zipper protein, *Cell* **74:**395–404.

Holstein, T.J., Fung, R.Q., Quevedo, W.C.J., and Bienieki, T.C., 1979, Effect of altered copper metabolism induced by mottled alleles and diet on mouse tyrosinase, *Proc. Soc. Exp. Biol. Med.* **162:**264–268.

Hoo, J.J., Haslam, R.H.A., and van Orman, C., 1986, Tentative assignment of piebald trait gene to chromosome band 4q12, *Hum. Genet.* **73:**230–231.

Hoth, C.F., Milunsky, A., Lipsky, N., Sheffer, R., Clarren, S.K., and Baldwin, C.T., 1993, Mutations in the paired domain of the human PAX-3 gene cause Klein-Waardenburg syndrome (WS-III) as well as Waardenburg syndrome type I (WS1), *Am. J. Hum. Genet.* **52:**455–462.

Hu, F., Hanifin, J.M., Prescott, G.H., and Tongue, A.C., 1980, Yellow mutant albinism: Cytochemical, ultrastructural, and genetic characterization suggesting multiple allelism, *Am. J. Hum. Genet.* **32:**387–395.

Huang, E., Nocka, K., Beler, D.R., Chu, T.Y., Buck, J., Lahm, H.W., Wellner, D., Leder, P., and Besmer, P., 1990, The hematopoietic growth factor KL is encoded by the *Sl* locus and is the ligand of the c-*kit* receptor, the gene product of the *W* locus, *Cell* **63:**225–233.

Hughes, A.E., Newton, V.E., Liu, X.Z., Read, A.P., 1994, A gene for Waardenburg syndrome type 2 maps close to the human homolog of the *micropthalmia* gene at chromosome 3p12-p14.1, *Nature Genetics* **7:**509–512.

Ishikiriyama, S., Tonoki, H., Shibuya, Y., Chin, S., Harada, N., Abe, K., and Niikawa, N., 1989, Waardenburg syndrome type I in a child with de novo inversion (2)(q35q37.3), *Am. J. Med. Genet.* **33:**505–507.

Ito, M., Hashimoto, K., and Organisciak, D.T., 1982, Ultrastructural, histochemical and biochemical studies of the melanin metabolism in pallid mouse eye, *Curr. Eye Res.* **2:**13–28.

Jackson, I.J., 1988, A cDNA encoding tyrosinase-related protein maps to the brown locus in mice, *Proc. Natl. Acad. Sci. USA* **85:**4392–4396.

Jackson, I.J., Chambers, D.M., Tsukamoto, K., Copeland, N.G., Gilbert, D.J., Jenkins, N.A., and Hearing, V.J., 1992, A second tyrosinase-related protein, TRP2, maps to and is mutated at the mouse slaty locus, *EMBO J.* **11:**527–535.

Jimbow, K., Fitzpatrick, T.B., Szabo, G., and Hori, Y., 1975, Congential circumscribed hypomelanosis: a characterization based on electron microscopic study of tuberous sclerosis, nevus depigmentosus, and piebaldism, *J. Invest. Dermatol.* **64:**50–62.

Jimbow, K., Yamana, K., Akutsu, Y., and Maeda, K., 1988, Nature and biosynthesis of structural matrix protein in melanosomes: melanosomal structural protein as differentiation antigen for neoplastic melanocytes, *Prog. Clin. Biol. Res.* **256:**169–182.

Jiminez-Cervantes, C., Solano, F., Kobayashi, T., Urabe, K., Hearing, V.J., Lozano, J.A., and García-Borrón, J.C., 1994, A new enzymatic function in the melanogenic pathway. *J. Biol. Chem.* **269**:17993–18001.

Kameyama, K., Takemura, T., Hamada, Y., Sakai, C., Kondoh, S., Nishiyama, S., Urabe, K., and Hearing, V.J., 1993, Pigment production in murine melanoma cells is regulated by tyrosinase, tyrosinase-related protein 1 (TRP1), DOPAchrome tautomerase (TRP2) and a melanogenic inhibitor, *J. Invest. Dermatol.* **100:**126–131.

Kawamura, K., Fitzpatrick, T.B., and Seiji, M., 1971, *Biology of Normal and Abnormal Melanocytes*, University Park Press, Baltimore, pp.1–411.

Kedda, M.A., Stevens, G., Manga, P., Viljoen, C., Jenkins, T., and Ramsay, M., 1994, The tyrosinase-positive oculocutaneous albinism gene shows locus homogeneity on chromosome 15q11–q13 and evidence of multiple mutations in South African Negroids, *Am. J. Hum. Genet.* **54:**1078–1084.

Keeler, C.E., 1934, The heredity of a congenital white spotting in Negroes, *J. Am. Med. Assoc.* **103:**179–180.

Kikuchi, H., Hara, S., Ishiguro, S., Tamai, M., and Watanabe, M., 1990, Detection of point mutation in the tyrosinase gene of a Japanese albino patient by a direct sequencing of amplified DNA, *Hum. Genet.* **85:**123–124.

King, R.A., Mentink, M.M., and Oetting, W.S., 1991, Nonrandom distribution of missense mutations within the human tyrosinase gene in type I (tyrosinase-related) oculocutaneous albinism, *Mol. Biol. Med.* **8:**19–29.

Kirkpatrick, S.J., Kent, C.M., Laxova, R., and Sekhon, G.S., 1992, Waardenburg syndrome type I in a child with deletion (2)(q35q36.2), *Am. J. Med. Genet.* **44:**699–700.

Korner, A.M., and Pawelek, J., 1982, Mammalian tyrosinase catalyzes three reactions in the biosynthesis of melanin, *Science* **217:**1163–1165.

Kromberg, J.G.R., and Krause, A., 1993, Waardenburg syndrome and spina bifida, *Am. J. Med. Genet.* **45:**536–537.

Kugelman, T.P., and van Scott, E.J., 1961, Tyrosinase activity in melanocytes of human albinos, *J. Invest. Dermatol.* **37:**73–76.

Kwon, B.S., Halaban, R., Kim, G.S., Usack, L., Pomerantz, S.H., and Haq, A.K., 1987a, A melanocyte-specific complementary DNA clone whose expression is inducible by melanotropin and isobutylmethyl xanthine, *Mol. Biol. Med.* **4:**339–355.

Kwon, B.S., Haq, A.K., Pomerantz, S.H., and Halaban, R., 1987b, Isolation and sequence of a putative cDNA clone for human tyrosinase that maps at the mouse c-albino locus, *Proc. Natl. Acad. Sci. USA* **84:**7473–7477.

Kwon, B.S., Chintamaneni, C.D., Kozak, C.A., Copeland, N.G., Gilbert, D.J., Jenkins, N.A., Barton, D.E., Francke, U., Kobayashi, Y., and Kim, K.K., 1991, A melanocyte-specific gene, Pmel 17, maps near the silver coat color locus on mouse chromosome 10 and is in a syntenic region on human chromosome 12, *Proc. Natl. Acad. Sci. USA* **88:**9228–9232.

Lacassie, Y., Thurmon, T.F., Tracy, M.D., and Pelias, M.Z., 1977, Piebald trait in a retarded child with interstitial deletion of chromosome 4, *Am. J. Hum. Genet.* **29:**641–642.

Lamoreux, M.L., Boissy, R.E., Womack, J.E., and Nordlund, J.J., 1992, The vit gene maps to the Mi (Microphthalmia) locus of the laboratory mouse, *J. Hered.* **83:**435–439.

Lee, S.-T., Nichols, R.D., Jong, M.T.C., and Spritz, R.A, 1994a, Organization and sequence of the human *P* gene and identification of a new family of transport pump proteins, *Genomics*, in press.

Lee, S-T., Strunk, K.M., Bundey, S., Laxova, R., Musarella, M., and Spritz, R.A., 1994b, Mutations of the *P* gene in oculocutaneous albinism, ocular albinism, and Prader-Willi syndrome plus albinism, *New Engl. J. Med.* **330:**529–534.

Lee, S.-T., Nicholls, R.D., Schnur, R.E., Guida, L.C., Lu-Kuo, J., Spinner, N.B., Zackai, E.H., and Spritz, R.A., 1994c, Diverse mutations of the *P* gene among African-Americans with type II (tyrosine-positive) oculocutaneous albinism (OCA2). *Hum. Molec. Genet.*, in press.

Lerch, K., 1988, Protein and active-site structure of tyrosinase, *Adv. Pigment Cell Res. Prog. Clin. Biol. Res.* **256:**85–98.

Lerner, A.B., Fitzpatrick, T.B., 1950, Biochemistry of melanin formation, *Physiol. Rev.* **30:**91–126.

Lerner, A.B., Fitzpatrick, T.B., Calkins, E., Summerson, W.H., 1949, Mammalian tyrosinase: Preparation and properties, *J. Biol. Chem.* **178:**185–195.

Lev, S., Yarden, Y., and Givol, D., 1992, Dimerization and activation of the kit receptor by monovalent and bivalent binding of the stem cell factor, *J. Biol. Chem.* **267:**15970–15977.

Lucian, 1905, *The Works of Lucian of Samosata*, Vol.1 [Fowler, H.W., trans.], Clarendon Press, Oxford.

Lu-Kuo, J., Ward, D.C., and Spritz, R.A., 1993, Fluorescence *in situ* hybridization mapping of 25 markers on distal human chromosome 2q surrounding the human Waardenburg syndrome, type I (WS1) locus (*PAX3* gene), *Genomics* **16:**173–179.

Lyon, M., and Searle, A.G., 1989, *Genetic Variants and Strains of the Laboratory Mouse*, Oxford University Press, Oxford.

Magenis, R.E., Smith, L., Nadeau, H.J., Johnson, K.R., Mountjoy, K.G., and Cone, R.D., 1994, Mapping of the ACTH, MSH, and neural (MC3 and MC4) melanocortin receptors in the mouse and human, *Genomics*, in press.

Martinez, J.H., Solano, F., Garcia-Borron, J.C., Iborra, J.L., and Lozano, J.A., 1985, The involvement of histidine at the active site of Harding-Passey mouse melanoma tyrosinase, *Biochem. Int.* **11:** 729–738.

Martorana, P.A., Brand, T., Gardi, C., and van Even, P., 1993, The pallid mouse. A model of genetic α1-antitrypsin deficiency, *Lab. Invest.* **68:**233–241.

Mercer, J.A., Seperack, P.K., Strobel, M.C., Copeland, N.G., and Jenkins, N.A., 1991, Novel myosin heavy chain encoded by murine dilute coat color locus, *Nature* **349:**709–713.

Mercer, J.F.B., Livingston, J., Hall, B., Paynter, J.A., Begy, C., Chandrasekharappa, S., Lockhart, P., Grimes, A., Bhave, M., Siemieniak, D., and Glover, T.W., 1993, Isolation of a partial candidate gene for Menkes disease by positional cloning, *Nature Genetics* **3:**20–25.

Michaud, E.J., Bultman, S.J., Klebig, M.L., van Vugt, M.J., Stubbs, L.J., Russell, L.B., and Woychik, R.P., 1994, A molecular model for the genetic and phenotypic characteristics of the mouse lethal yellow (A^y) mutation, *Proc. Natl. Acad. Sci. USA* **91:**2562–2566.

Miller, M.W., Duhl, D.M.J., Vrieling, H., Cordes, S.P., Ollmann, M.M., Winkes, B.M., and Barsh, G.S., 1993, Cloning of the mouse *agouti* gene predicts a secreted protein ubiquitously expressed in mice carrying the *lethal yellow* mutation, *Genes and Dev.* **7:**454–467.

Miller, M.W., Winkes, B.M., Duhl, D.M.J., Arredondo-Vega, F., Saxon, P.J., Wolff, G.L., Epstein, C.J., Hershfield, M.S., and Barsh, G.S., 1994, The mouse *lethal nonagouti* (a^x) mutation deletes the *S-adenosylhomocysteine hydrolase* (*Ahcy*) gene, *EMBO J.* **13:**1806–1816.

Mishima, Y., 1992, A post-melanosomal era: control of melanogenesis and melanoma growth, *Pigment Cell Res.* (Suppl. 2)**:**3–16.

Moase, C.E., and Trasler, D.G., 1992, Splotch locus mouse mutants: models for neural tube defects and Waardenburg syndrome type I in humans, *J. Med. Genet.* **29:**145–151.

Mochii, M., Agata, K., and Eguchi, G., 1991, Complete sequence and expression of a cDNA encoding a chicken 115-kDa melanosomal matrix protein, *Pigment Cell Res.* **4:**41–47.

Montagna, W., and Ellis, R.A., 1958, *The Biology of Hair Growth*, Academic Press, New York, pp. 1–358.

Montagna, W., and Parakkal, P.F., 1974, *The Structure and Function of Skin*, Academic Press, New York, pp.1–433.

Montagna, W., Kligman, A.M., Carlisle, K.S., 1991, *Atlas of Normal Human Skin*, Springer-Verlag, pp.1–422.

Morell, R., Friedman, T.B., Moelijopawiro, S., Hartono, Soewito, and Asher, J.H., Jr., 1992, A frameshift mutation in the HUP2 paired domain of the probable human homolog of murine *PAX-3* is responsible for Waardenburg syndrome type I in an Indonesian family, *Hum. Mol. Genet.* **1:**243–247.

Morgan, J., 1786, Some accounts of motley colored or pye Negro girl and mulatto boy, *Trans. Am. Philos. Soc.* (Phila) **2:**392–395.

Morrison-Graham, K., and Takahashi, Y., 1993, Steel factor and c-*kit* receptor: from mutants to a growth factor system, *BioEssays* **15:**77–83.

Mountjoy, K.G., Robbins, L.S., Mortrud, M.T., and Cone, R.D., 1992, The cloning of a family of genes that encode the melanocortin receptors, *Science* **257:**1248–1251.

Murphy, M., Reid, K., Williams, D.E., Lyman, S.D., and Bartlett, P.F., 1992, Steel factor is required for maintenance, but not differentiation, of melanocyte precursors in the neural crest, *Devel. Biol.* **153:**396–401.

Murty, V.V.V.S., Bouchard, B., Mathew, S., Vijayasaradhi, S., and Houghton, A.N., 1992, Assignment of the human *TYRP* (*brown*) locus to chromosome region 9p23 by nonradioactive *in situ* hybridization, *Genomics* **13:**227–229.

Nance, W.E., Jackson, C.E., and Witkop, C.J., Jr., 1970, Amish albinism: A distinctive autosomal recessive phenotype, *Am. J. Hum. Genet.* **22:**579–586.

Nicholls, R.D., 1993, Genomic imprinting and uniparental disomy in Angelman and Prader-Willi syndromes: A review, *Am. J. Med. Genet.* **46:**16–25.

Nishikawa, S., Kusakabe, M., Yoshinaga, K., Ogawa, M., Hayashi, S-I., Kunisada, T., Era, T., Sakakura, T., and Nishikawa, S-I., 1991, *In utero* manipulation of coat color formation by a monoclonal anti-c-*kit* antibody: two distinct waves of c-*kit* dependency during melanocyte development, *EMBO J.* **10:**2111–2118.

Oetting, W.S., and King, R.A., 1992, Molecular analysis of type IA (tyrosinase negative) oculocutaneous albinism, *Hum. Genet.* **90:**258–262.

Oetting, W.S., King, R.A., 1993, Molecular basis of type I (tyrosinase related) oculocutaneous albinism: Mutations and polymorphisms of the human tyrosinase gene, *Hum. Mutation* **2:**1–6.

Oetting, W.S., Handoko, K.Y., Mentink, M.M., Paller, A.S., White, J.G., King, R.A., 1991a, Molecular analysis of an extended family with type IA (tyrosinase-negative) oculocutaneous albinism, *J. Invest. Dermatol.* **97:**15–19.

Oetting, W.S., Mentink, M.M., Summers, C.G., Lewis, R.A., White, J.G., and King, R.A., 1991b, Three different frameshift mutations of the tyrosinase gene in type IA oculocutaneous albinism, *Am. J. Hum. Genet.* **49:**199–206.

Oetting, W.S., Fryer, J.P., and King, R.A., 1993a, A dinucleotide deletion (−ΔGA115) in the tyrosinase gene responsible for type I-A (tyrosinase negative) oculocutaneous albinism in a Pakistani individual, *Hum. Molec. Genet.* **2:**1047–1048.

Oetting, W.S., Witkop, C.J., Brown, S.A., Colomer, R., Fryer, J.P., Bloom, K.E., and King, R.A., 1993b, A frequent mutation in the tyrosinase gene associated with type I-A (tyrosinase-negative) oculocutaneous albinism in Puerto Rico, *Am. J. Hum. Genet.* **52:**17–23.

Oetting, W.S., Fryer, J.P., Oofuji, Y., Middendorf, L.R., Brumbaugh, J.A., Summers, C.G., King, R.A., 1994, Analysis of tyrosinase gene mutations using direct automated infrared fluorescence DNA sequencing of amplified exons, *Electrophoresis* **15:**159–164.

Online Mendelian Inheritance in Man, OMIM (TM) 1994, [database online], The Johns Hopkins University, Baltimore, Maryland.

Orlow, S.J., Osber, M.P., and Pawelek, J.M., 1992, Synthesis and characterization of melanins from dihydroxyindole-2-carboxylic acid and dihydroxyindole, *Pigment Cell Res.* **5:**113–121.

Orlow, S.J., Zhou, B.K., Boissy, R.E., and Pifko-Hirst, S., 1993, Identification of a mammalian melanosomal matrix glycoprotein, *J. Invest. Dermatol.* **101:**141–144.

Pawelek, J.M., 1985, Studies on the Cloudman melanoma cell line as a model for the action of MSH, *Yale J. Biol. Med.* **58:**571–578.

Pawelek, J.M., 1991, After DOPAchrome? *Pigment Cell Res.* **4:**53–62.

Pawelek, J.M., Chakraborty, A.K., Osber, M.P., Orlow, S.J., Min, K., Rosenzweig, K.E., and Bolognia, J., 1992, Molecular cascades in UV-induced melanogenesis: A central role for melanotropins? *Pigment Cell Res.* **5:**348–356.

Pierpont, J.W., and Erickson, R.P., 1993, Facts on PAX, *Am. J. Hum. Genet.* **52:**451–454.

Pliny, 1942, *The Natural History of Pliny: Plinius Secundus the Elder*. Book 7. Rackman H., trans., Harvard University Press, Cambridge.

Prota, G., 1986, Pigment cell metabolism: Chemical and enzymatic control, in: *Cutaneous Melanoma* (U. Veronesi and N. Cascinelli, eds.), Academic Press, New York, pp. 233–241.

Prota, G., 1988a, Progress in the chemistry of melanins and related metabolites, *Med. Res. Rev.* **8:** 525–556.

Prota, G., 1988b, Some new aspects of eumelanin chemistry, *Prog. Clin. Biol. Res.* **256:**101–124.

Prota, G., 1992, *Melanins and Melanogenesis*, Academic Press, New York, pp. 1–290.

Ramsay, M., Colman, M-A., Stevens, G., Zwane, E., Kromberg, J., Farrall, M., and Jenkins, T., 1992, The tyrosinase-positive oculocutaneous albinism locus maps to chromosome 15q11.2–q12, *Am. J. Hum. Genet.* **51:**879–884.

Reith, A.D., Rottapel, R., Giddens, E., Brady, C., Forrester, L., and Bernstein, A., 1990, W mutant mice with mild or severe developmental defects contain distinct point mutations in the kinase domain of the c-kit receptor, *Genes Dev.* **4**:390–400.

Rikke, B.A., Pinto, L.H., Gorin, M.B., and Hardies, S.C., 1993, *Mus spretus*-specific LINE-1 DNA probes applied to the cloning of the murine *pearl* locus, *Genomics* **15**:291–296.

Rinchik, E.M., Bultman, S.J., Horsthemke, B., Lee, S.T., Strunk, K.M., Spritz, R.A., Avidano, K.M., Jong, M.T.C., and Nicholls, R.D., 1993, A gene for the mouse pink-eyed dilution locus and for human type II oculocutaneous albinism, *Nature* **361**:72–76.

Robbins, L.S., Nadeau, J.H., Johnson, K.R., Kelly, M.A., Roselli-Rehfuss, L., Baack, E., Mountjoy, K.G., and Cone, R.D., 1993, Pigmentation phenotypes of variant extension locus alleles result from point mutations that alter MSH receptor function, *Cell* **72**:827–834.

Sanders, G., Lichte, B., Meyer, H.E., and Kilimann, M.W., 1992, cDNA encoding the chicken ortholog of the mouse dilute gene product. Sequence comparison reveals a myosin I subfamily with conserved C-terminal domains, *FEBS Lett.* **311**:295–298.

Schaefer, L., Ferrero, G.B., Grillo, A., Bassi, M.T., Roth, E.J., Wapenaar, M.C., Van Ommen, G.J.B., Mohandas, T.K., Rocchi, M., Zoghbi, H.Y., and Ballabio, A., 1993, A high resolution deletion map of human chromosome Xp22, *Nature Genetics* **4**:272–279.

Schnur, R.E., Nussbaum, R.L., Anson-Cartwright, L., McCowell, C., Worton, R.G., and Musarella, M.A., 1991, Linkage analysis in X-linked ocular albinism, *Genomics* **9**:605–613.

Shibahara, S., Tomita, Y., Sakakura, T., Nager, C., Chaudhuri, B., and Muller, R., 1986, Cloning and expression of cDNA encoding mouse tyrosinase, *Nucl. Acids Res.* **14**:2413–2427.

Shibata, T., Prota, G., and Mishima, Y., 1993, Non-melanosomal regulatory factors in melanogenesis, *J. Invest. Dermatol.* **100**:274S–280S.

Silvers, W.K., 1979, *The Coat Colors of Mice*. Springer-Verlag, New York.

Smith, E.A., Seldin, M.F., Martinez, L., Watson, M.L., Choudhury, G.G., Lalley, P.A., Pierce, J., Aaronson, S., Barker, J., Naylor, S.L., and Sakaguchi, A.Y., 1991, Mouse platelet-derived growth factor receptor α gene is deleted in W^{19H} and patch mutations on chromosome 5, *Proc. Natl. Acad. Sci. USA* **88**:4811–4815.

Spanakis, E., Lamina, P., and Bennett, D.C., 1992, Effects of the developmental colour mutations silver and recessive spotting on proliferation of diploid and immortal mouse melanocytes in culture, *Development* **114**:675–680.

Spritz, R.A., 1993*a*, Molecular basis of piebaldism and Waardenburg syndrome, *Current Opinion in Dermatology*, 78–84.

Spritz, R.A., 1993, Molecular genetics of oculocutaneous albinism, *Semin. Dermatol.* **12**:167–172.

Spritz, R.A., 1994a, Molecular genetics of oculocutaneous albinism, *Hum. Molec. Genet.* **3**:1469–1475.

Spritz, R.A., 1994b, The molecular basis of human piebaldism, *J. Invest. Dermatol.*, in press.

Spritz, R.A., Strunk, K.M., Giebel, L.B., and King, R.A., 1990, Detection of mutations in the tyrosinase gene in a patient with Type IA oculocutaneous albinism, *New Eng. J. Med.* **322**:1724–1728.

Spritz, R.A., Strunk, K.M., Hsieh, C.L., Sekhon, G.S., and Francke, U., 1991, Homozygous tyrosinase gene mutation in an American black with tyrosinase-negative (type IA) oculocutaneous albinism, *Amer. J. Hum. Gen.* **48**:318–324.

Spritz, R.A., Droetto, S., and Fukushima, Y., 1992a, Deletion of the *KIT* and *PDGFRA* genes in a patient with piebaldism, *Amer. J. Med. Gen.* **44**:492–495.

Spritz, R.A., Giebel, L.B., and Holmes, S.A., 1992b Dominant negative and loss of function mutations of the c-*kit* (mast/stem cell growth factor receptor) proto-oncogene in human piebaldism, *Amer. J. Hum. Gen.* **50**:261–269.

Spritz, R.A., Holmes, S.A., Ramesar, R., Greenberg, J., Curtis, D., and Beighton, P., 1992c, Mutations of the *KIT* (mast/stem cell growth factor receptor) proto-oncogene account for a continuous range of phenotypes in human piebaldism, *Amer. J. Hum. Gen.* **51**:1058–1065.

Spritz, R.A., Holmes, S.A., Berg, S.Z., Nordlund, J.J., and Fukai, K., 1993a, A recurrent deletion in the *KIT* (mast/stem cell growth factor receptor) gene is a frequent cause of human piebaldism, *Hum. Molec. Genet.* **2:**1499–1500.

Spritz, R.A., Holmes, S.A., Itin, P., and Küster, W., 1993b, Novel mutations of the *KIT* (mast/stem cell growth factor receptor) proto-oncogene in human piebaldism, *J. Invest. Dermatol.* **101:** 22–25.

Spritz, R.A., Ho, L., and Strunk, K.M., 1994a, Inhibition of proliferation of human melanocytes by a *KIT* antisense oligodeoxynucleotide: Implications for human piebaldism and mouse dominant white spotting (*W*), *J. Invest. Dermatol.* **103:**148–150.

Spritz, R.A., Strunk, K.M., Lee, S-T., Lu-Kuo, J.M., Ward, D.C., LePaslier, D., Altherr, M.R., Dorman, T.E., and Moir, D.T., 1994b, A YAC contig spanning a cluster of human type III receptor protein tyrosine kinase genes (*PDGFRA-KIT-KDR*) in chromosome segment 4q12, *Genomics* **22:**431–436.

Steel, K.P., Davidson, D.R., and Jackson, I.J., 1992, TRP2/DT, a new early melanoblast marker, shows that steel growth factor (c-kit ligand) is a survival factor, *Development* **115:**1111–1119.

Stephenson, D.A., Mercola, M., Anderson, E., Wang, C., Stiles, C.D., Bowen-Pope, D.F., and Chapman, V.M., 1991, Platelet-derived growth factor receptor α-subunit gene (*Pfgfra*) is deleted in the mouse patch (*Ph*) mutation, *Proc. Natl. Acad. Sci. USA* **88:**6–10.

Summers, C.G., Creel, D., Townsend, D., and King, R.A., 1991, Variable expression of vision in sibs with albinism, *Am. J. Med. Genet.* **40:**327–331.

Sunohara, N., Sakuragawa, N., Satoyoshi, E., Tanae, A., and Shapiro, L.J., 1986, A new syndrome of anosmia, ichthyosis, hypogonadism, and various neurological manifestations with deficiency of steroid sulfatase and arylsulfatase C, *Ann. Neurol.* **19:**174–181.

Tachibana, M., Perez-Jurado, L.A., Nakayama, A., Hodgkinson, C.A., Li, X., Schneider, M., Miki, T., Fex, J., Francke, U., and Arnheiter, H., 1994, Cloning of *MITF*, the human homolog of the mouse *microphthalmia* gene, and assignment to human chromosome 3, region p14.1–p12.3, *Hum. Molec. Genet.* **3:**553–558.

Takeda, A., Tomita, Y., Matsunaga, J., Tagami, H., and Shibahara, S., 1990, Molecular basis of tyrosinase-negative oculocutaneous albinism, *J. Biol. Chem.* **265:**17792–17797.

Tan, J.C., Nocka, K., Ray, P., Traktman, P., and Besmer, P., 1990, The dominant W^{42} *spotting* phenotype results from a missense mutation in the c-*kit* receptor kinase, *Science* **247:**209–212.

Tassabehji, M., Read, A.P., Newton, V.E., Harris, R., Balling, R., Gruss, P., Strachan, T., 1992, Waardenburg syndrome patients have mutations in the human homolog of the *Pax-3* paired box gene, *Nature* **355:**635–636.

Tassabehji, M., Read, A.P., Newton, V.E., Patton, M., Gruss, P., Harris, R., Strachan, T., 1993, Mutations in the *PAX3* gene causing Waardenburg syndrome type 1 and type 2, *Nature Genetics* **3:**26–30.

Theriault, L.L., Hurley, L.S., 1970, Ultrastructure of developing melanosomes in C57 black and pallid mice, *Devel. Biol.* **23:**261–275.

Tomita, Y., Takeda, A., Okinaga, S., Tagami, H., Shibahara, S., 1989, Human oculocutaneous albinism caused by single base insertion in the tyrosinase gene, *Biochem. Biophys. Res. Commun.* **164:**990–996.

Tripathi, R.K., Giebel, L.B., Strunk, K. M., Spritz, R.A., 1991, A polymorphism of the human tyrosinase gene that is associated with temperature-sensitive enzymatic activity, *Gene Expression* **1:**103–110.

Tripathi, R.K., Hearing, V.J., Urabe, K., Aroca, P., Spritz, R.A., 1992a, Mutational mapping of the catalytic activities of human tyrosinase, *J. Biol. Chem.* **267:**23707–23712.

Tripathi, R.K., Strunk, K.M., Giebel, L.B., Weleber, R.G., Spritz, R.A., 1992b, Tyrosinase gene mutations in type I (tyrosinase-deficient) oculocutaneous albinism define two clusters of missense substitutions, *Amer. J. Med. Gen.* **43:**865–871.

Tripathi, R.K., Bundey, S., Musarella, M.A., Droetto, S., Strunk, K.M., Holmes, S., Spritz, R.A., 1993, Mutations of the tyrosinase gene in Indo-Pakistani Patients with type I (tyrosinase-deficient) oculocutaneous albinism (OCA), *Am. J. Hum. Genet.* **53:**1173–1179.

Tsukamoto, K., Jackson, I.J., Urabe, K., Montague, P.M., Hearing, V.J., 1992a, A second tyrosinase-related protein, TRP2, is a melanogenic enzyme termed DOPAchrome tautomerase, *EMBO J.* **11:**519–526.

Tsukamoto, K., Tohma, T., Ohta, T., Yamakawa, K., Fukushima, Y., Nakamura, Y., Niikawa, N., 1992b, Cloning and characterization of the inversion breakpoint at chromosome 2q35 in a patient with Waardenburg syndrome type I, *Hum. Molec. Genet.* **1:**315–317.

Urabe, K., Aroca, P., Hearing, V.J., 1993, From gene to protein: Determination of melanin synthesis, *Pigment Cell Res.* **6:**186–192.

Vandenbark, G.R., DeCastro, C.M., Taylor, H., Dew-Knight, S., Kaurman, R.E., 1992, Cloning and structural analysis of the human c-*kit* gene. *Oncogene* **7:**1259–1266.

Vijayasaradhi, S., Bouchard, B., Houghton, A.N., 1990, The melanoma antigen gp75 is the human homolog of the mouse *b* (brown) locus gene product, *J. Exp. Med.* **171:**1375–1380.

Vogan, K.J., Epstein, D.J., Trasler, D.G., Gros, P., 1993, The *splotch-delayed* (*Spd*) mouse mutant carries a point mutation within the paired box of the *Pax-3* gene, *Genomics* **17:**364–369.

Vrieling, H., Duhl, D.M.J., Millar, S.E., Miller, K.A., Barsh, G.S., 1994, Differences in dorsal and ventral pigmentation result from regional expression of the mouse *agouti* gene, *Proc. Natl. Acad. Sci. USA* **91:**5667–5671.

Vulpe, C., Levinson, B., Whitney, S., Packman, S., Gitschier, J., 1993, Isolation of a candidate gene for Menkes disease and evidence that it encodes a copper-transporting ATPase, *Nature Genetics* **3:** 7–13.

Waardenburg, P.J., 1951, A new syndrome combining developmental anomalies of the eyelids, eyebrows and nose root with pigmentary defects of the iris and head hair with congenital deafness, *Am. J. Hum. Genet.* **3:**195–253.

Wagstaff, J., 1993, A translocation-associated deletion defines a critical region for the 9p-syndrome, *Am. J. Hum. Genet.* **53**, (Suppl.), 619.

Wapenaar, M.C., Bassi, M.T., Schaefer, L., Grillo, A., Ferrero, G.B., Chinault, A.C., Ballabio, A., and Zoghbi, H.Y., 1993, The genes for X-linked ocular albinism (OA1) and microphthalmia with linear skin defects (MLS): Cloning and characterization of the critical regions, *Hum. Molec. Genet.* **2:**947–957.

White, R.A., Peters, L.L., Adkison, L.R., Korsgren, C., Cohen, C.M., and Lux, S.E., 1992, The murine *pallid* mutation is a platelet storage pool disease associated with the protein 4.2 (pallidin) gene, *Nature Genetics* **2:**80–83.

Winder, A.J., Kobayashi, T., Tsukamoto, K., Urabe, K., Aroca, P., Kameyama, K., Hearing, V.J., 1994, The tyrosinase gene family: Interactions of melanogenic proteins to regulate melanogenesis, *Biochem. J.*, in press.

Winship, I.M., Babaya, M., Ramesar, R.S., 1993, X-linked ocular albinism and sensorineural deafness: Linkage to Xp23.3, *Genomics* **18:**444–445.

Witkop, C.J., Jr., Quevedo, W.C., Jr., Fitzpatrick, T.B., and King, R.A., 1989, Albinism, in: *The Metabolic Basis of Inherited Disease* (C.R. Scriver, A.L. Beaudet, W.S. Sly, and D. Valle, eds.), McGraw-Hill, New York, pp. 2905–2947.

Wittbjer, A., Dahlback, B., Odh, G., Rosengren, A-M., Rosengren, E., and Rorsman, H., 1989, Isolation of human tyrosinase from cultured melanoma cells, *Acta. Derm. Venereol.* (Stokh.) **69:**125–131.

Yamamoto, Y., Nishimoto, H., and Ikemoto, S., 1989, Interstitial deletion of the proximal long arm of chromosome 4 associated with father-child incompatibility within the Gc-system: Probable reduced gene dosage effect and partial piebald trait, *Am. J. Med. Genet.* **32:**520–523.

Yarden, Y., Kuang, W-J., Yang-Feng, T., Coussens, L., Munemitsu, S., Dull, T.J., Chen, E.,

Schlessinger, J., Francke, U., Ullrich, A., 1987, Human proto-oncogene c-*kit*: A new cell surface receptor tyrosine kinase for an unidentified ligand, *EMBO J.* **6**:3341–3351.

Yen, T.T., Gill, A.M., Frigeri, L.G., Barsh, G.S., and Wolff, G.L., 1994, Obesity, diabetes, and neoplasia in yellow A^{vy}/– mice: Ectopic expression of the *agouti* gene, *FASEB J.* **8**:479–488.

Yokoyama, K., Suzuki, H., Yasumoto, K., Tomita, Y., and Shibahara, S., 1994, Molecular cloning and functional analysis of a cDNA coding for human DOPAchrome tautomerase/tyrosinase-related protein-2, *Biochim. Biophys. Acta.* **121**:317–321.

Zsebo, K.M., Williams, D.A., Geissler, E.N., Broudy, V.C., Martin, F.H., Atkins, H.L., Hsu, R.Y., Birkett, N.C., Okino, K.H., Murdock, D.C., Jacobsen, F.W., Langley, K.E., Smith, K.A., Takeishi, T., Cattanach, B.M., Galli, S.J., and Suggs, S.V., 1990, Stem cell factor is encoded at the *Sl* locus of the mouse and is the ligand for the c-*kit* tyrosine kinase receptor, *Cell* **63**:213–224.

Chapter 2

High-Resolution Replication Bands Compared with Morphologic G- and R-bands

Régen Drouin* and Gerald P. Holmquist

Division of Biology
Beckman Research Institute of the City of Hope
Duarte, California 91010-0269

Claude-Lise Richer

Department of Anatomy
University of Montreal, Montreal, Quebec, Canada H3C 3J7, and
Department of Pathology and Pediatric Research Center
Saint Justine Hospital, Montreal, Quebec, Canada H3T 1C5

INTRODUCTION

Replication banding using 5-bromo-2′-deoxyuridine (BrdUrd) has traditionally yielded band patterns with extensive cell-to-cell variation, including variation between homologous chromosomes in the same cell. With the discovery that cycling cells can be blocked at the R/G transition (the time at which R-band synthesis is complete and G-band synthesis has yet to begin), either R-bands or G-bands can be selectively substituted with BrdUrd. This new method (named in this review as the "Thymidine-BrdUrd permutation culture method") coupled with an improved fluorochrome-photolysis-Giemsa (FPG) staining method that

Present address: Research Unit in Human and Molecular Genetics, Saint Francis of Assisi Hospital Research Center, Laval University, Québec City, Quebec, Canada G1L 3L5

Advances in Human Genetics, Volume 22, edited by Henry Harris and Kurt Hirschhorn. Plenum Press, New York, 1994.

reveals only unsubstituted chromatin, provides preparations with replication band patterns as reproducible and with the same resolution as patterns from standard trypsin-Giemsa banding. In this chapter, we will review the basic cell physiology of how R/G transition blocking and replication banding work and compare replication band patterns with classical band patterns.

In mammals, bidirectional replication of replicons begins at replication origins. Clusters of contiguous replicons begin replication at one time and complete synthesis in one to two hours. Such a cluster is a replication band (Latt, 1975; Holmquist, 1988). Usually, replication bands are visualized by introducing the thymidine analog BrdUrd during a particular interval of the DNA synthesis phase, the S-phase of the cell cycle and collecting cells at the subsequent metaphase. DNA that replicates during this interval incorporates BrdUrd instead of thymidine. BrdUrd substitution can be detected in a metaphase replication band by several methods (see p. 59). The replication times of 277 metaphase replication bands have been determined after pulse labeling cells with BrdUrd and dividing the S-phase into eighteen contiguous time intervals (Dutrillaux *et al.*, 1976). For all but one band, R-bands replicate in one of the nine early intervals while G-bands and C-bands (see Table I for abbreviations) replicate in one of the nine late intervals (Holmquist, 1992).

The R-band/G-band transition behaves much like a cell cycle checkpoint. Several inhibitors of DNA synthesis arrest cells at both the beginning of S-phase, the G_1/S-phase transition, and at the R/G transition. After release of inhibition, cells arrested at the R/G transition burst into metaphase 4 to 5 hours later, long before cells arrested at the G_1/S-phase transition. If cells are fixed during the first burst, then only metaphases from cells previously arrested at the R/G transition are obtained. This metaphase burst can be timed exactly and the cytogeneticist can select a time to fix the burst when most of its cells are in prophase (a stage where chromosomes are very extended). The dynamics of utilizing the R/G transition arrest during cell culture are such that the cytogeneticist can choose one of two methods: (1) before the R/G transition, introduce BrdUrd into only the R–bands, or (2) after the R/G transition, introduce BrdUrd into only the G– and C–bands of subsequently observed metaphases. For visualization by transmission light microscopy (LM), cytogeneticists can then stain the unsubstituted chromatin by the FPG technique or stain the substituted chromatin by the BrdUrd antibody binding (BAB) technique. Using only the FPG technique, BrdUrd substitution before the R/G transition produces a GBG–band pattern almost identical to that of GTG–bands and exactly complementary to the RBG-band pattern obtained when BrdUrd substitution occurs after the R/G transition.

Chromosome bandings serve two major purposes: chromosome identifica-

TABLE I. Classification of Chromosome Bands and Definition of the Letter Codes Used to Describe Banding Techniques Discussed in this Chapter

G-bandings	
1. Morphologic or structural type	
GAG[a]	**G**-bands by **A**cetic saline using **G**iemsa
GTG[a]	**G**-bands by **T**rypsin using **G**iemsa
QFQ[a]	**Q**-bands by **F**luorescence using **Q**uinacrine
2. Replication or dynamic type	
GBG[a]	**G**-bands by **B**rdUrd using **G**iemsa
GBI	**G**-bands by **B**rdUrd using **I**mmunological staining
GB-AP	**G**-bands by **B**rdUrd using **A**ntibody and **P**eroxidase
GB-AF	**G**-bands by **B**rdUrd using **A**ntibody and **F**luoresceine
GB-AAu	**G**-bands by **B**rdUrd using **A**ntibody and gold (**Au**)
GB-APA	**G**-bands by **B**rdUrd using **A**ntibody and **P**rotein **A**
R-bandings	
1. Morphologic or structural type	
RHG[a]	**R**-bands by **H**eating using **G**iemsa
THG[a]	**T**-bands by **H**eating using **G**iemsa
2. Replication or dynamic type	
RBG[a]	**R**-bands by **B**rdUrd using **G**iemsa
RBI	**R**-bands by **B**rdUrd using **I**mmunological staining
RB-AP	**R**-bands by **B**rdUrd using **A**ntibody and **P**eroxidase
RB-AF	**R**-bands by **B**rdUrd using **A**ntibody and **F**luoresceine
RB-AAu	**R**-bands by **B**rdUrd using **A**ntibody and gold (**Au**)
RB-APA	**R**-bands by **B**rdUrd using **A**ntibody and **P**rotein **A**
C-bandings	
CBG[a]	**C**-bands by **B**arium hydroxide using **G**iemsa
Special bandings	

[a]Approved by ISCN (1985)

tion, including numerical and structural chromosome aberrations, and visualization of underlying chromosome organization. For identification, a band can be defined as a segment of chromatid distinct from its adjacent segments by its lighter or darker staining (Prieur *et al.*, 1973). For analysis of chromosome organization, a chromosome band designates a chromatid segment that presents distinct functional and structural characteristics resulting in specific staining properties after various banding techniques (Drouin *et al.*, 1991a). These different staining properties constitute the chromatin flavor of each band. Chromatin flavor describes the cytological reactivity of a band to each of several techniques (Holmquist, 1990a, 1992). The two major sets of mammalian euchromatic chromosome bands are loosely called G-bands and R-bands.

Chromosome banding techniques can be classified in two groups: morphologic or structural and dynamic or replication (Table I) (Richer and Drouin, 1990). The former reveals an inherent pattern of chemical heterogeneity that exists along the length of the chromosomes. Chromatin structure, proteins, and protein–DNA interactions along with base composition are the major factors responsible for the differential Giemsa staining after various morphologic banding techniques. The basis of the heterogeneity observed after different treatments (for instance, trypsinization or heat treatment) and the mechanisms of these bandings are still poorly understood (reviewed by Sumner, 1990). The dynamic or replication techniques, rely upon incorporation of a base analog, usually the thymidine analog, BrdUrd, into DNA during the synthesis phase. The principles, the basis, and the mechanisms of dynamic banding techniques are fairly well known.

Resolution will henceforth refer to band level, meaning the number of resolvable bands per haploid genome, and will be designated by a subscript. For example, a $GTG^{+}_{1,250}$ band would designate a single band positively stained by the trypsin and Giemsa technique when a total of 1,250 different bands can be observed. There is an association between the mitotic stage and the band level (Table II). Resolution increases with the length of chromosomes used. It varies with the mitotic stage (Table II). It does not refer to either the culture methods or the blocking agents used; some S-phase blocking protocols, like methotrexate, often yield mostly low-resolution mitoses, while the traditional technique using Colcemid as a blocking agent sometimes yields high-resolution mitoses.

TABLE II. Correspondence Between Band Level and Mitotic Stage for Human Chromosomes[a]

Mitotic stages	Band level (Bands per haploid set)
Late prophase	>1000
Early prometaphase	850–999
Late prometaphase	700–849
Early metaphase	550–699
Middle metaphase	400–549
Late metaphase	<400

[a]These numbers are the ones generally accepted, but no one has ever shown precisely the correspondence between a band level and a specific mitotic stage.

ARREST OF DNA REPLICATION BY DNA SYNTHESIS INHIBITORS

Two key events occur during the cell division cycle in eukaryotes: DNA replication (synthesis phase) and nuclear division (mitotic phase). These are usually separated by gaps or preparatory phases, called G_1 before DNA replication and G_2 before nuclear division (Fig. 1). Cell synchronization methods were developed to phase an otherwise asynchronous population of growing cells and are used by cytogeneticists to increase the percentage of metaphase cells harvested. Colchicine or Colcemid stops the cells at the end of the metaphase. Such mitoses are arrested in late metaphase when the chromosomes are very condensed and short ($bands_{300-400}$, Table II). Chromosomes harvested at late prophase are essential for high-resolution cytogenetics. To increase the percentage of cells showing $bands_{550-1,250}$, cytogeneticists usually use S–phase synchronization techniques.

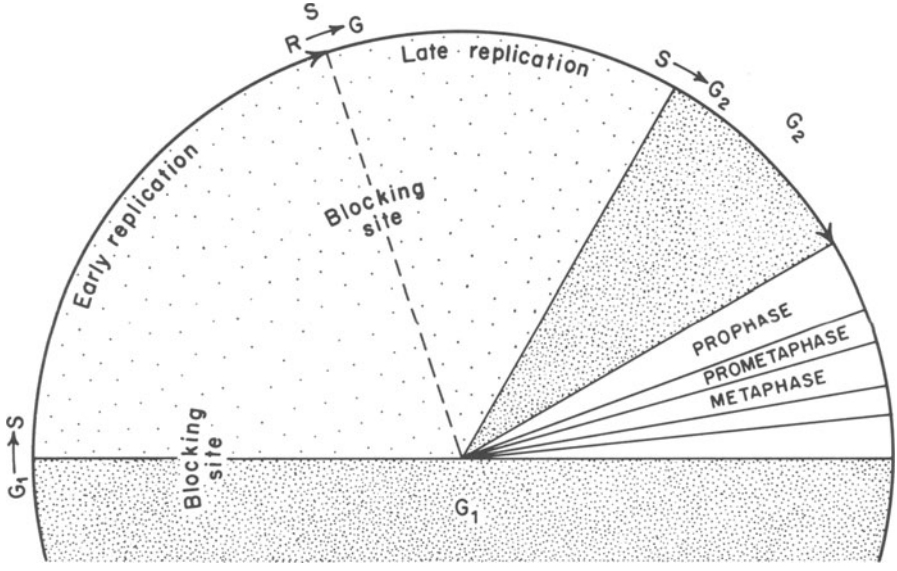

Fig. 1. Schematic representation of the cell cycle, emphasizing the S-phase. The relative duration of these phases has been determined for human lymphocytes: eight to ten hr for S (but can be as short as six hr or as long as 12 hr), two to four hr for G_2 ($S + G_2 = 10$ to 14 hr) and three to six hr for G_1 (Cave, 1966a,b; Takagi and Sandberg, 1968; Grzeschik *et al.*, 1975; Dutrillaux and Fosse, 1976; Kaluzewski, 1982). The G_1 period is the most variable and the one the most affected by the cellular environment. Three indicated transition points are G_1/S, R/G and S/G_2. S-phase blocking agents used in cytogenetics arrest DNA synthesis at the G_1/S and R/G transitions. The mitotic phases indicated are those during which the chromosomes can be harvested.

These techniques have three stages: (1) presynchronization, (2) synchronization by blocking of DNA synthesis, and (3) release. To an exponentially growing cell population, a DNA synthesis inhibitor is added to block and accumulate as many cells as possible during S-phase. The blocking agent is then removed and the released cell wave is harvested when the wave reaches late prophase. The effects on the cell cycle of a number of agents that arrest DNA synthesis have been established: amethopterin or methotrexate (Rueckert and Mueller, 1960; Petersen, 1964; Steffen and Stolzmann, 1969; Stampe Villadsen and Zeuthen, 1970), 5-fluoro-2′-deoxyuridine (FdUrd) (Eidinoff and Rich, 1959; Rueckert and Mueller, 1960; Hsu, 1964; Priest *et al.*, 1967) and an excess of thymidine (Xeros, 1962; Bootsma *et al.*, 1964) or an excess of BrdUrd (Meuth and Green, 1974). The agents subsequently adopted for cytogenetic purposes are methotrexate (Epplen *et al.*, 1976; Yunis, 1976), FdUrd (Nakagome, 1977; Webber and Garson, 1983), 5-fluorouracil (FU) (Rønne, 1984a,b) (intracellularly converted to FdUrd), an excess of thymidine (Schempp *et al.*, 1978; Viegas-Péquignot and Dutrillaux, 1978), and high concentrations of BrdUrd (Schempp *et al.*, 1978; Dutrillaux and Viegas-Péquignot, 1981). These compounds all inhibit DNA synthesis by disturbing the *de novo* synthesis of one pyrimidine base. Methotrexate and FdUrd starve cells for thymidine; methotrexate is a potent competitive inhibitor of dihydrofolate reductase, which is necessary for the conversion of deoxyuridylate to thymidylate (Bertino, 1963; Werkheiser, 1963), whereas FdUrd is a strong inhibitor of the enzyme thymidylate synthetase (Cohen *et al.*, 1958; Hartmann and Heidelberger, 1961). An excess of thymidine (Morris and Fischer, 1963; Morris *et al.*, 1963; Gentry *et al.*, 1965; Bjursell and Reichard, 1973) or high concentrations of BrdUrd (Meuth and Green, 1974; Ashman and Davidson, 1981) cause depletion of the deoxycytidine triphosphate (dCTP) pool. High thymidine and high BrdUrd concentrations induce feedback inhibition of cellular ribonucleotide reductase, an enzyme that catalyzes the reduction of cytidine diphosphate to deoxycytidine diphosphate (Reichard, 1988). Since the dCTP pool decreases rapidly after addition of an excess of thymidine or BrdUrd (Ashman and Davidson, 1981; Wilkinson and McKenna, 1989) and since the dNTP pool suffices for only a few minutes of replication (Reichard, 1988), DNA replication should stop quickly after the addition of an excess of thymidine or BrdUrd. Whether it does so is unknown.

These DNA synthesis inhibition regimens reportedly slow a cell's rate of progression through S-phase with particular blocking points at the G_1/S border and the R/G transition. Methotrexate (Rueckert and Mueller, 1960; Zeuthen, 1968), and FdUrd (Rueckert and Mueller, 1960; Priest *et al.*, 1967) both cause accumulation of cells at the G_1/S transition. Using methotrexate, others reported no specific blocking point but rather a general stoppage during methotrexate treatment and a

progression through the cell cycle without synchronization (Savage and Prasad, 1988). High concentrations of thymidine cause approximately 50% of the cells to accumulate at the G_1/S border, while the remainder halt at various points in S-phase (Bootsma *et al.*, 1964). High thymidine concentrations do not prevent the entry into S-phase but prolong the time during which cells remain in S-phase by inhibiting the rate of DNA synthesis by up to 90% (Bjursell and Reichard, 1973). Cytogenetic data from experiments using methotrexate, FdUrd, or thymidine, support blocking at both the G_1/S block point (Epplen *et al.*, 1976; Nakagome, 1977; Vogel *et al.*, 1978, 1985; Yunis and Chandler, 1978; Schmidt, 1980; Kaluzewski, 1982) and at the R/G transition (Fig. 1) (Viegas-Péquignot and Dutrillaux, 1978; Camargo and Cervenka, 1980; Meer *et al.*, 1981; Rønne, 1984a,b, 1985; Drouin *et al.*, 1990).

In summary, we believe that known inhibitors of DNA synthesis block at two major points, the G_1/S transition and the R/G transition; these represent times when major groups of replicon clusters begin replication (Figs. 1 and 2). Why the R/G transition, also called the 3C pause, is so sensitive to blocking is not understood (reviewed by Holmquist, 1987, 1988). The metabolic inhibition of the initiation of the replication forks is believed to be much easier than the inhibition of continued elongation of existing replication forks (Painter, 1982), which would allow cells already in early S–phase to progress to the R/G transition and stop.

BrdUrd INCORPORATION AND S-PHASE

When BrdUrd is administered to cells during the first or last half of S-phase, a full early– or late–replication pattern can be seen in chromosomes from the subsequent mitotic cells. Early replication of the R-bands and late replication of the G– and C–bands has been demonstrated with cycling asynchronous cells using a terminal BrdUrd pulse or a terminal thymidine pulse (Table III). These replication band patterns showed much intercellular variation and discordant patterns between homologs (Grzeschik *et al.*, 1975; Kim *et al.*, 1975; Latt, 1975; Kondra and Ray, 1978), which can be reduced or eliminated by cell synchronization.

Release of lymphocytes from DNA synthesis inhibition (Fig. 2) results in two synchronous waves of cells progressing to mitosis. The first burst of mitotic activity occurs after four to four-and-a-half hr (Richer *et al.*, 1983a; Drouin *et al.*, 1988a) and represents cells released from the R/G transition block. The second burst occurs 10 to 14 hr after the release (Schempp *et al.*, 1978; Schmidt, 1980; Kaluzewski, 1982; Schwemmle *et al.*, 1989) and represents cells released from the G_1/S transition block. Release times varying from four to 14 hr have been reported

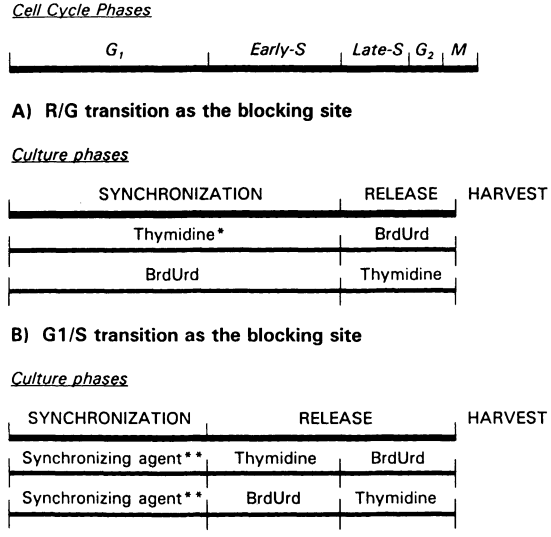

Incorporation of BrdUrd in S-Phase	Band pattern after	
	FPG	BAB
Late	R	G
Early	G	R
Late	R	G
Early	G	R

* Methotrexate and fluorodeoxyuridine have also been used.
** Thymidine, fluorodeoxyuridine, hydroxyurea and methotrexate have been used.

Fig. 2. Relationships between cell cycle, blocking sites, BrdUrd incorporation during the S-phase, and the replication band patterns. R/G (protocol A) and G_1/S (protocol B) transition points are the two blocking points used in replication banding. To harvest the cells blocked at the G_1/S transition (protocol B), a long release time and the presence of low concentrations of thymidine followed by BrdUrd during specific intervals or vice versa are necessary, while a short release time and only thymidine or BrdUrd are necessary to harvest the cells blocked at the R/G transition (protocol A). The thymidine-BrdUrd permutation (TBP) culture method is illustrated by the protocol A. The permutation point, when thymidine and BrdUrd are exchanged, is marked by the vertical line between thymidine and BrdUrd or BrdUrd and thymidine and is aligned with the one separating early and late S-phase.

(Table IV), and we presume the investigators using release periods between four and eight hr harvested cells blocked at the previous R/G transition or during the early part of S-phase, whereas investigators using release periods between 11 and 14 hr harvested cells previously blocked at the G_1/S transition (Table IV). While low BrdUrd concentrations, < 3 μg/ml, have no effect on the S-phase duration, concentrations between 10 and 50 μg/ml noticeably delay the cell cycle (Dutrillaux and Fosse, 1976; Dutrillaux *et al.*, 1976; Kaluzewski, 1982). Using cells blocked at the R/G transition, the time between release and metaphase is about 30 minutes longer for release in the presence of 30 μg/ml BrdUrd than for release in the presence of 3 μg/ml thymidine (Richer *et al.*, 1983a; Drouin *et al.*, 1988a).

For replication banding of cells blocked at the G_1/S border, two releasing

TABLE III. Selected Reports Showing Early Replication of R-bands and Late Replication of G- and C-bands of Human Chromosomes by Adding BrdUrd to an Asynchronous Cell Population

References	Cells studied	Pulse	BrdUrd detection methods
Dutrillaux *et al.*, 1973, 1976	Lymphocytes	Terminal thymidine	Acridine orange staining
Dutrillaux and Fosse, 1974		Terminal BrdUrd	
Dutrillaux, 1975a,b, 1977		Middle BrdUrd	
Latt, 1973, 1974, 1975	Lymphocytes	Terminal thymidine Terminal BrdUrd	Hoechst 33258 staining
Epplen *et al.*, 1975	Skin fibroblasts	Terminal thymidine	FPG[a]
Epplen and Vogel, 1975	Amniotic fluid cells		
Grzeschik *et al.*, 1975	Lymphocytes	Terminal thymidine	FPG
Kim *et al.*, 1975	Lymphocytes	Terminal BrdUrd	FPG
Kondra and Ray, 1978	Fibroblasts	Terminal thymidine	FPG
Sheldon and Nichols, 1981	Renal epithelium Lung fibroblasts	Terminal BrdUrd	FPG
Shafer *et al.*, 1982	Lymphocytes	Terminal thymidine Terminal BrdUrd	FPG
Vogel *et al.*, 1986	Lymphocytes	Terminal BrdUrd	BAB[b]
Aghamohammadi and Savage, 1990	Lymphocytes	BrdUrd	Modified FPG (reverse staining)

[a]FPG: Fluorochrome-Photolysis-Giemsa staining.
[b]BAB: BrdUrd Antibody Binding technique.

conditions, a low concentration of BrdUrd and a low concentration of thymidine must be exchanged at or near the R/G transition (Fig. 2, protocol B). This approach has two major drawbacks. First, some synchrony is lost because of the long release time. Second, the moment when the synchronized cells reach the R/G transition must be approximated. This method yields preparations with much cell-to-cell variation and homolog discordance (Schempp and Vogel, 1979; Schempp, 1980).

For replication banding of cells blocked at the R/G transition, one needs only to release cells in the presence of a low concentration of the alternate base (Fig. 2, protocol A). Only the R-bands or the G- and C-bands, but never a combination of both, should incorporate BrdUrd. The thymidine-BrdUrd permutation (TBP) culture method reliably permits complementary BrdUrd incorporation, that is, either in R-bands or in G- and C-bands. This method designates either of two protocols: thymidine block and release in presence of BrdUrd, or BrdUrd block and release in presence of thymidine, either exogenously added thymidine or endogenously generated dTTP. This TBP culture method produces a 10% mitotic index burst at four to four-and-a-half hr post-release without using Colcemid (Drouin *et al.*, 1988a; Lemieux *et al.*, 1990).

TABLE IV. Reports Showing Early Replication of R-bands and Late Replication of G- and C-bands of Human Chromosomes by Using BrdUrd and S-phase Synchronization

References	Cells studied	Blocking agent (μg/ml)[a,b]	Releasing regimen (μg/ml)[a]	Releasing time (hr)	Colcemid (μg/ml)[a]	BrdUrd detection methods
Nakagome, 1977	Diploid cell line W138	F, 0.1	T, 1.45 then B, 50	11	× 1 hr	AO or H staining
Schempp *et al.*, 1978	Amniotic fluid cells	T, 450	B, 10 F, 0.5	14	0.05 × 2 hr	FPG
		B, 600	T, 4.8			
Viegas-Péquignot and Dutrillaux, 1978	Lymphocytes	T, 300	B, 10	6–8		AO staining
Camargo and Cervenka, 1980	Lymphocytes	M, 0.5	B, 30 F, 0.1 U, 2	5–6	0.07 × 0.25–1 hr	FPG
Pai and Thomas, 1980	Lymphocytes	M, 0.05	B, 25	5–5.5	0.1–0.2 × 0.25 hr	AO staining
Schmidt, 1980	Lymphocytes	M, 0.05	[c]	14	× 2 hr	FPG
Dutrillaux and Viegas-Péquignot, 1981	Lymphocytes	B, 200	T, 0.3	6–7		FPG
Meer *et al.*, 1981	Lymphocytes	M, 0.05	B, 20 F, 0.1	5	0.33 × 0.5 hr	FPG
Schollmayer *et al.*, 1981	Lymphocytes	T, 300	B, 50	5–8		AO staining
Kaluzewski, 1982	Lymphocytes	M, 0.1	B, 10	13.5	0.2 × 2 hr	FPG
Scheres *et al.*, 1982	Lymphocytes	T, 300	B, 36	6.5		BF staining
Webber and Garson, 1983	Bone marrow cells	F, 0.025 U, 0.1	B, 6	7–8	0.1 × 1 hr	FPG

Elejalde *et al.*, 1984	Lymphocytes	M, 0.05	B, 23 F, 0.12 U, 2.35	5	0.5 × 0.5 hr	FPG
Rønne, 1984b	Bone marrow cells	FU, 0.125	B, 30 H, 50	7–8	0.15 × 1 hr	FPG
Schwartz and Palmer, 1984	Lymphocytes	M, 0.05	B, 30 F, 0.1 U, 25 C, 1.4	4.75–5.05		FPG
Lin *et al.*, 1985	Lymphocytes	B, 200	T, 2.25	5	0.05 × 0.17 hr	FPG
Rønne, 1985	Lymphocytes	M, 0.05 FU, 0.25	B, 30 H, 50	5	0.15 × 1 hr	FPG
Lemieux *et al.*, 1987	Bone marrow cells	B, 200	T, 3	5		FPG
Drouin *et al.*, 1988a	Lymphocytes	T, 300	B, 30	4.25		FPG
Lemieux and Richer, 1989	Retinoblastoma cells	B, 200	T, 3	4		FPG
Qu *et al.*, 1989	Amniotic fluid cells	B, 200	T, 3	6.5–7		FPG
Lemieux *et al.*, 1990	Lymphocytes	B, 200	T, 3	4.5		FPG
Savary *et al.*, 1991, 1992	Lymphocytes Bone marrow cells Chorionic villi Amniotic fluid cells	T, 300 B, 200	B, 10 T, 3	7		FPG & BAB

[a] μg/ml of culture medium.

[b] B, BrdUrd; F, fluorodeoxyuridine; C, cytidine; M, methotrexate or amethopterine; T, thymidine; FU, fluorouracil; U, uridine; AO, acridine orange; BF, basic fuchsin; H, Hoechst 33258; FPG, Fluorochrome-Photolysis-Giemsa staining; BAB, BrdUrd Antibody Binding technique.

[c] T, 7 μg/ml followed by B, 25 μg/ml.

To assess the percentage of mitotic cells that the TBP culture method had previously arrested at the R/G transition, the mitotic cells were classified according to their replication band patterns as belonging to one of five replication stages for methotrexate blocked cells released in presence of BrdUrd as described by Camargo and Cervenka (1980, 1982). Their earliest replication stages, I and II, represent cells that incorporated BrdUrd during more than half of their S-phase because they had not reached the R/G transition at the time of release; stage III represents cells that were exactly at the R/G transition at the time of release and show a fully-developed RBG-band pattern; the later replication stages IV and V represent cells that incorporated BrdUrd during a short time at the end of the S-phase because they passed the R/G transition. After the TBP culture method using a thymidine block, 1% of mitotic cells were in stages I or II, 90–95% were in stage III, and 5–10% were in stages IV or V (Drouin *et al.*, 1990, 1991a). The TBP culture method using a BrdUrd block yields about 75 to 80% of the mitotic cells with identical fully developed GBG-band patterns (Drouin *et al.*, 1990). When the release time is extended, more cells blocked somewhere between the G_1/S transition and R/G transition are harvested, causing intercellular band pattern variations and a reduction of analyzable mitoses. In summary, the TBP culture method reliably yields chromosomes from which it is possible to produce replication band patterns as reproducible as those from GTG-banding.

When BrdUrd is added during the release period, the blocking agent can be thymidine, methotrexate or FU–FdUrd (Table IV). Indeed, methotrexate (Drouin *et al.*, 1988a and FU (Rønne, 1984a,b, 1985) also arrest many cells at the R/G transition, because a majority of resulting mitoses show a fully-developed RBG-band pattern. However, either an excess of thymidine (Drouin *et al.*, 1988a) or an excess of BrdUrd (Lemieux *et al.*, 1987) produces a higher mitotic index and is more effective than methotrexate or FU at blocking DNA synthesis at the R/G transition. Presumably, thymidine and BrdUrd are less toxic because they only interfere with DNA synthesis by depleting the dCTP pool. Methotrexate and FU-FdUrd disturb cell metabolism to a great extent, methotrexate creating a folate deficiency (Bertino, 1963; Werkheiser, 1963) and FU-FdUrd by interfering with protein synthesis (Heidelberger, 1975).

BrdUrd DETECTION

The dynamic or replication bandings are based on the addition or removal of BrdUrd during the S–phase of the cells studied later in mitosis. This segmentary and unifilar BrdUrd substitution pattern can be differentially stained by three main

classes of methods. For the first class of methods, fluorochromes like acridine orange (Dutrillaux *et al.*, 1973), Hoechst 33258 (Latt, 1973) and 4′-6-diamidino-2-phenylindole (DAPI) (Lin *et al.*, 1976a) were used to reveal BrdUrd substitution, their fluorescence being quenched by BrdUrd-substituted DNA. Only acridine orange (Viegas-Péquignot and Dutrillaux, 1978; Pai and Thomas, 1980; Schollmayer *et al.*, 1981) has enough contrast to reveal dynamic band patterns at high band levels. The second class of methods, best exemplified by the FPG technique, relies on Giemsa staining following specific post-fixation treatments. The third class involves direct BrdUrd detection by immunochemical methods using an anti-BrdUrd antibody.

Fluorochrome-Photolysis-Giemsa Staining Technique

The Fluorochrome-Photolysis-Giemsa staining technique (FPG) (Fig. 3), originally called fluorescence-plus-Giemsa technique, was devised to differentiate unifilarly substituted (TB) chromatids from their sister bifilarly substituted (BB) chromatids after two rounds of BrdUrd incorporation (Perry and Wolff, 1974). For replication banding, one must distinguish TB chromatid segments from unsubstituted TT segments after BrdUrd incorporation during part of the S-phase.

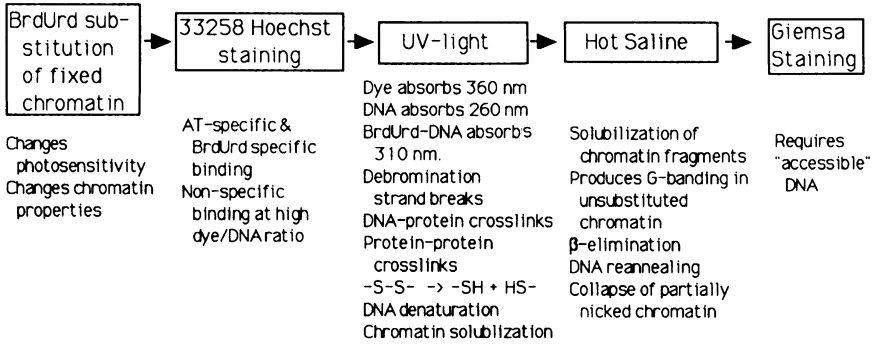

Fig. 3. Five elements are involved in the FPG technique (written in the boxes). Following BrdUrd substitution, there are four possible procedural steps in the FPG technique to produce replication band patterns. The consequences of the substitution and the molecular mechanisms attributed to each step are indicated. UV irradiation of substituted chromosomes produces: (1) debromination of BrdUrd-substituted DNA leading to single-strand breaks (Hutchinson, 1973); (2) DNA-protein (Han *et al.*, 1975; Kornhauser, 1976; Schiaffonati *et al.*, 1978) and protein-protein crosslinking (Martinson *et al.*, 1976; Gantt *et al.*, 1979; Hancock and Sumner, 1982); and (3) breakage of disulphide protein bonds (Buys and Stienstra, 1980; Buys and Osinga, 1981).

The FPG technique acts upon two changes caused by BrdUrd substitution into chromosomal DNA. BrdUrd substitution both renders DNA more photosensitive and alters DNA-protein interactions. Banding mechanisms work upon these two changes to enhance visual differentiation of BrdUrd–substituted chromatin from unsubstituted chromatin. These two mechanisms involve selective photolysis of substituted chromatin, and alterations of DNA-protein (chromatin) structure caused by BrdUrd substitution. The first mechanism relies mainly on selective photolysis of BrdUrd-DNA into small pieces with subsequent dissolution of these pieces. It is rather independent of DNA-protein interactions. The second mechanism can be generalized as BrdUrd-dependent alterations of DNA-protein interactions that affect either dissolution or subsequent Giemsa staining.

The four steps involved in differentiating replication bands by the FPG technique are shown in Fig. 3, along with the molecular mechanisms attributed to each step. Table V shows that investigators using quite different conditions for each step have nonetheless arrived at satisfactory differentiation.

Staining Differentiation by Giemsa Staining

Several different mechanisms have been proposed to explain why, after trypsinization, GTG-bands become refractory to Giemsa staining even though no DNA and very little protein is extracted during the banding procedure (Comings, 1975a; van Duijn *et al.*, 1985; Holmquist and Motara, 1987; Sumner, 1990). These studies show that DNA must be present for positive Giemsa staining but that protein denaturation conditions such as trypsinization or hot saline can easily alter methanol-acetic acid fixed chromatin and differentially mask the Giemsa stainability of its DNA. The various published FPG protocols, designed to reveal replication bands and sister chromatid differentiation (Table V), often include protein denaturation conditions and hot saline treatments such as those used for RHG and GAG banding, which are particularly effective at altering chromatin to differentially mask Giemsa staining of its DNA. The FPG conditions (Lemieux *et al.*, 1987; Lemieux and Richer, 1989; Drouin *et al.*, 1988a) (Table V) recommended for GBG or RBG banding were designed to exclusively utilize the photolysis mechanism while avoiding masking effects of conditions that denature proteins.

Staining Differentiation by Selective Photolysis of BrdUrd-Substituted DNA

1. The fluorochrome, Hoechst 33258, a nonintercalating dye, has two modes of binding. The primary tight noncovalent binding occurs at a low dye/DNA-phosphate ratio, shows base specificity, and is salt-insensitive, while the second-

ary weak binding occurs at a high dye/DNA ratio, shows no base dependence, involves a highly cooperative side stacking mode of binding, and is abolished at high salt levels (Bontemps *et al.*, 1975; Latt and Wohlleb, 1975; Stokke and Steen, 1985, 1986; Jorgenson *et al.*, 1988). At a low dye/DNA ratio, Hoechst exhibits a strong specificity for AT base pairs (Bontemps *et al.*, 1975; Comings 1975b; Latt and Wohlleb, 1975; Müller and Gautier, 1975) and fits snugly into the minor groove of the double helix when four AT base pairs are adjacent (Mikhailov *et al.*, 1981; Martin and Holmes, 1983; Harshman and Dervan, 1985; Pjura *et al.*, 1987; Jorgenson *et al.*, 1988; Teng *et al.*, 1988; Härd *et al.*, 1990). Hoechst binds duplex DNA with a five fold greater affinity for poly(dA–BrdUrd) than for poly(dA–dT) (Latt and Wohlleb, 1975; Jorgenson *et al.*, 1988). For more selective binding to BrdUrd–DNA, a low concentration ($\leq$ 15 μg/ml) of Hoechst diluted in water is recommended for replication banding (Richer and Drouin, 1990).

2. Without a photosensitizer, incorporation of BrdUrd sensitizes DNA to nicking by UV light in proportion to the extent of replacement of thymine by BrdUrd (Hutchinson, 1973; Hutchinson and Köhnlein, 1980). UV induces bromine photodissociation of BrdUrd, leaving uracil with a free radical at the C5 position. While forming uracil, a hydrogen atom is extracted from the adjacent C2′ of the deoxyribose of the nucleoside on the 5′ side of the debrominated base; this causes the DNA single-strand break (Hutchinson, 1973; Hutchinson and Köhnlein, 1980). These nicks can be prevented if hydrogen donors such as sulphydryl groups (-SH) instead of the deoxyribose furnish the H^+ (Hutchinson, 1973; Hutchinson and Köhnlein, 1980). Nicking is maximal at 313 nm (Hutchinson, 1973; Hutchinson and Köhnlein, 1980) instead of at the 260 nm absorption maximum of unsubstituted DNA. In unifilarly substituted DNA, the B-strand is 100–1,000 fold more sensitive to photoinduced strand nicks than the T–strand (Hutchinson, 1973), leading to the fragmentation of the B–strand into much smaller pieces than the T-strand.

3. Hoechst 33258 sensitizes BrdUrd-substituted DNA to 360 nm UV–induced nicking (Stetten *et al.*, 1976; Rosenstein *et al.*, 1980). When Hoechst binds to DNA, it shifts the absorption maximum of the dye from 338 nm to 360 nm (Comings, 1975b; Latt and Wohlleb, 1975; Jorgenson *et al.*, 1988). The 360 nm light is absorbed by the dye, not by the free DNA. This allows a great degree of selectivity in producing DNA nicks only where dye is bound; the 360 nm excitation of bound fluorochrome leads to the ejection of an electron, which is captured by the BrdUrd causing the loss of the bromine (Rahn and Sellin, 1992). This represents a redox reaction whereby the excited Hoechst oxidizes BrdUrd and is itself reduced (Härd *et al.*, 1990). Thus, compared with 313 nm UV irradiation in the absence of dye, Hoechst combined with 360 nm UV light enhances the efficiency with which the debromination occurs and increases the amount of

TABLE V. Variations of the Fluorochrome-Photolysis-Giemsa (FPG) technique

References	Photosensitizer (fluorochrome) (μg/ml)[a]	UV treatment (photolysis)[b]	Heat treatment[c]	Staining (Giemsa) (%)
Perry and Wolff, 1974	H, 0.5 × 12 min	Sunlight, H_2O, × 24 hr	2×SSC or H_2O, 60°C × 2 hr	G, 3
Korenberg and Freedlender, 1974			1 M NaH_2PO_4 pH 8, 87–89°C × 0.17 hr	G, 5
Angell and Jacobs, 1975, 1978	H, 5 × 60 min	200 W mercury vapor lamp, H_2O, × 1–3 min at 40 cm	2×SSC, 60°C × 2 hr	G, 3
Epplen *et al.*, 1975	H, 0.5 × 10 min	Germicidal UV light, 254 nm; SB pH 6; × 0.33–0.5 hr at 15 cm	2×SSC, 63°C × 1.5 hr	G, 7
Goto *et al.*, 1975, 1978	H, 5 × 15 min	BL, 360 nm; McI pH 7.5–8.5; × 0.25 hr at 5 cm		G, 2
Grzeschik *et al.*, 1975	H, 200 × 2 sec	UV light treatment; H_2O; × 1 hr	2×SSC, 62°C × 1 hr	G, 5
Willard, 1977	H, 0.5	UV light, 254 nm; McI pH 7; × 0.67 hr at 5 cm	2×SCC, 60°C × 0.75 hr	G, 3
Emanuel, 1978	H, 2[d]	UV light; 0.5×SSC + H; × 4 hr at 2.5–7.5 cm	0.5×SSC, 60°C × 1 hr	G, 4
Gibas and Limon, 1978	H, 5 × 10 min	HBO-200 mercury lamp; PB pH 7; × 1 hr at 50 cm	2×SSC, 62°C × 1 hr	G, 2
Kondra and Ray, 1978	H, 5 × 15 min	UV light; McI pH 4.5; × overnight at 60 cm	PB 1 M pH 8, 84–85°C × 0.17 hr	G, 4
Ghosh *et al.*, 1979	H, 5 × 120 min	Germicidal lamp, 254 nm; H_2O; × 10 hr at 50 cm	2×SSC, 60°C × 2 hr	G, 2
Gagné, 1980	H, 0.5[d]	UV light; H_2O + H; × 0.25–0.33 hr at 45 cm	H_2O, 62°C × 2 hr	G, 1
Ockey, 1980	H, 1	Germicidal UV light, 254 nm; PBS pH 7.3; × overnight	2×SSC, 60°C × 1 hr, followed by 2×SSC, 80°C × 1 hr	G, 2
Schmidt, 1980	H, 0.5 × 15 min	UV light, NaCl, × 1 hr		G
Buys *et al.*, 1981	DAPI, 0.5[d]	Osram HBO 200 W mercury lamp, 290 nm; McI pH 7 containing DAPI; × 1 min at 17 cm		G, 5

Dutrillaux and Viegas-Péquignot, 1981	H, 1 × 15 min	HBO 200 mercury vapor lamp, 2×SSC, × 0.5–1.5 hr at 30 cm	2×SSC, 60°C × 1.5 hr (for GBG); EBSS pH 5.1, 87°C × 5–20 sec (for RBG)	G, 1.5
Meer *et al.*, 1981	H, 2.5 × 10 min	UV light, PB pH 5.5, × 0.5 hr	2×SSC, 59°C × 1 hr	G, 5
Sheldon and Nichols, 1981	H, 5 × 12 min	Germicidal lamp, 254 nm; SB pH 6.8; × 1.5 hr	H_2O, 60°C × 0.5 hr	G, 10
Camargo and Cervenka, 1982	H, 150 × 5–10 min	Mercury vapor lamp, McI pH 7, × 0.5 hr at 25 cm	2×SSC, 60–62°C, × 0.25–0.33 hr	G, 2
Schempp and Müller, 1982	H, 0.25 × 10 min	UV light, 2×SSC, × 0.5 hr	2×SSC, 60°C × 1.5 hr	G, 8
Shafer *et al.*, 1982	H, 55 × 10 min	BL, PB 1 M pH 7.1, × 0.25 hr at 5 cm	2×SSC, 60°C × 0.083 hr	G, 2
Webber and Garson, 1983		UV light, PB pH 6.8, × 0.25 hr at 5.5 cm	2×SSC, 60°C × 0.33 hr	G, 10
Ieshima *et al.*, 1984	H, 50 × 15 min	UV light on a hot plate at 60°C, 2×SSC, × 1.33 hr at 17 cm		G, 3
Lin *et al.*, 1985	H, 1 × 15 min	BL, 2×SSC, × 1 hr at 2.5 cm		G, 7
Lemieux *et al.*, 1987	H, 0.1 × 15 min	BL, 2×SSC, × 4 hr at 1.5 cm		G, 1
Drouin *et al.*, 1988a	H, 2.5 × 15 min	BL, 2×SSC, × 2–2.5 hr at 2 cm		G, 1
Lemieux and Richer, 1989	H, 2.5 × 15 min	BL, 2×SSC, × 4 hr at 1 cm		G, 4
Qu *et al.*, 1989	H, 10 × 15 min	BL, 2×SSC, × 3 hr at 2 cm		G, 4
Savage, 1990	H, 1–200 × 5–10 min	Mercury vapor street light, 2×SSC, × 0.5–0.67 hr at 30–33 cm		G, 5
Savary *et al.*, 1991	H, 10 × 20 min	BL, 2×SSC, × 1.5 hr at 10 cm	2×SSC, 60°C × 2 hr (for GBG); EBSS pH 5.1, 87°C × 0.083 hr (for RBG)	G, 1.5
Rønne, 1992	H, 1 × 30 min	BL, 2×SSC containing H, × 0.5 hr at 2.5 cm	2×SSC, 65°C × 1 hr	G, 5

[a]SB, Sorensen buffer; PB, phosphate buffer; McI, McIlvaine buffer; 2×SSC, standard saline citrate, used at pH 7.0; PBS, phosphate buffer saline; EBSS, Earle's balanced salt solution; BL, black light, the maximum emission wavelength is at 360 nm; H, Hoechst 33258; G, Giemsa.

[b]Article protocols may specify the type of UV lamp used, its maximum emission wavelength; the type and pH of the solution with which the slides were mounted; the duration of UV irradiation, and the distance between the slides and the UV lamp.

[c]This includes the solution in which the heat treatment was done, the temperature and the duration of the heat treatment.

[d]The fluorochrome was added to the mounting solution for the UV irradiation.

breaks per bromine lost. It has been shown that combined Hoechst-UV treatment can cause double-strand breaks even though only one DNA strand is BrdUrd–substituted (Limoli and Ward, 1993). The frequency of double-strand breaks is proportional to the level of BrdUrd substitution. This would happen when the released bromine reacts to either produce an alkali-labile site (Krasin and Hutchinson, 1978) or causes an actual single-strand break by abstracting an H atom from a deoxyribose on the opposite strand leading to a double-strand break (Limoli and Ward, 1993). DAPI, which has the same characteristics as Hoechst, can also act as a BrdUrd–DNA photosensitizer (Buys *et al.*, 1981, 1986; Buys and van der Veen, 1982).

4. At the chromosome level, the preferential fragmentation and extraction of BrdUrd–substituted DNA by Hoechst-UV treatments have been documented using the Feulgen reaction and using radio-labeled nucleotides (Goto *et al.*, 1975, 1978; Sugiyama *et al.*, 1976; Ockey, 1980; Safronov *et al.*, 1981; Webber *et al.*, 1981; Jan *et al.*, 1984). A black light lamp provides the most efficient light source for photolysis because its peak emission wavelength is at 360 nm (Goto *et al.*, 1978; Chen and Lin, 1985; Drouin *et al.*, 1988a). The pH of the mounting solution should be between 7 and 8.5 and the temperature of the slides during UV exposure should be about 60°C (Goto *et al.*, 1978; Chen and Lin, 1985). This temperature can be easily achieved by using high-wattage lamps and putting the slides very close to the lamps (Chen and Lin, 1985; Drouin *et al.*, 1988a).

5. Using monoclonal anti-BrdUrd antibodies in transmission electron microscopy (TEM), we observed that staining with Hoechst 33258 diluted in water followed by black light irradiation resulted in complete absence of immunochemical banding (no gold bands) (Drouin *et al.*, 1989b). An extensive loss of antigenic sites by DNA extraction was postulated; this conclusion is supported by observations by mean of scanning electron microscopy (SEM) (Takayama and Taniguchi, 1986), and by the banding obtained from TEM, which shows that BrdUrd-substituted bands are less opaque to the electrons than unsubstituted ones following the Hoechst-UV treatment (Drouin *et al.*, 1989b). This extensive loss of material suggests that the UV irradiation causes not only the loss of DNA fragments but also the loss of crosslinked chromosomal proteins.

6. UV irradiation assists chromatin dissolution by a variety of effects, some of which result in DNA denaturation. The irradiation treatment heats the slide considerably (Perry and Wolff, 1974). UV treatment (254 nm) for 14 to 20 hr generates single-stranded regions in the chromosomal DNA allowing binding of polyclonal antinucleoside antibodies (Schreck *et al.*, 1974). Working with mouse antihuman DNA monoclonal antibodies, specific for single-stranded DNA, Mezzanotte *et al.* (1989b) confirmed that the Hoechst-UV treatment (254–366 nm)

produces single-stranded DNA in unifilarly substituted DNA. However, in our experiments, black light exposure alone for two-and-a-half hours did not produce DNA denaturation (Drouin *et al.*, 1989b). Hoechst binding increases the Tm of DNA by 15–25°C (Comings, 1975b), countering the effects of UV-induced denaturation.

7. Hot saline treatment (about 60°C) helps to solubilize degraded BrdUrd-DNA and, as demonstrated by Ockey (1980) and Webber *et al.* (1981), is necessary only when the Hoechst-UV treatment is not optimum (Table V). In addition, some authors used 5 N HCl incubation (González-Gil and Navarrete, 1982; Cortés and Andersson, 1987) or trypsin digestion (Scheid, 1976), to complete DNA breakdown, denature DNA fragments and remove the fragments. The hot saline treatment, which can produce a morphologic G–band pattern (Eiberg, 1973), may collapse the partially nicked BrdUrd-DNA, as verified by SEM (Jack *et al.*, 1989).

8. BrdUrd-substituted chromatin is lightly stained with Giemsa following a hot alkaline saline treatment (Korenberg and Freedlender, 1974; Burkholder, 1978, 1979, 1982; Sakanishi and Takayama, 1977; Takayama and Sakanishi, 1978). This treatment selectively denatures BrdUrd-DNA and preferentially solubilizes, by hydrolysis, BrdUrd-DNA with minimal extraction of chromosomal proteins (Burkholder, 1979, 1982).

Staining Differentiation by Altering the Structure of BrdUrd-Substituted Chromatin

1. BrdUrd-substituted chromosomes and chromatin differ significantly from their unsubstituted counterparts with respect to several structural and physical parameters which include a higher thermal stability, and increased supercoiling (Augenlicht *et al.*, 1974; David *et al.*, 1974; Lapeyre and Bekhor, 1974; Simpson and Seale, 1974). The Van der Waals radius of bromine (0.195 nm) is smaller than that of the methyl group of thymine (0.2 nm) and the bromine is more electronegative than the methyl group (Hutchinson and Köhnlein, 1980). This may contribute to the enhanced affinity of proteins, mainly the positively charged histones, for the BrdUrd-DNA (Gordon *et al.*, 1976; Lin *et al.*, 1976b; Matthes *et al.*, 1977; Schwartz, 1977; Fasy *et al.*, 1980).

2. When chromatin contains BrdUrd, the amount of DNA-protein crosslinking induced by UV light (254 and 313 nm) is increased in proportion to the extent of BrdUrd substitution (Weintraub, 1973; Lin and Riggs, 1974; Schiaffonati *et al.*, 1978). However, the amount of crosslinking that occurs in unifilarly and bifilarly substituted chromatids remains the same (Schiaffonati *et al.*, 1978). As much as 80% of the DNA can be crosslinked to approximately 10% of the total chromo-

somal proteins. Of this 10%, two-thirds of the crosslinked proteins are nonhistone proteins and the remaining one third are histones (Schiaffonati *et al.*, 1978). The selective BrdUrd-substituted DNA-protein crosslinking increases by a factor of 5 when irradiation is changed from 254 nm to 313 nm probably because of the higher absorption of 313 nm radiation in BrdUrd-substituted DNA (Weintraub, 1973). This specific crosslinking involves the loss of bromine and the formation of a covalent bond to the C5 position of the uracil ring (Hutchinson and Köhnlein, 1980). The same mechanism is probably responsible for the extensive DNA-protein crosslinking that occurs after 360 nm UV light irradiation of BrdUrd-DNA, and only in the presence of a low concentration of Hoechst 33258 (Guo *et al.*, 1986).

3. The selective UV-induced DNA-protein crosslinking both blocks access of enzymes [DNase I and II (Burkholder, 1982; Jan *et al.*, 1985), restriction endonucleases (Bianchi *et al.*, 1984, 1985), exonuclease III, or S1 nuclease (Mezzanotte *et al.*, 1989a)], and prevents the extraction of cut DNA following such digestions.

4. DNA-protein interactions can be altered so that staining patterns are the reverse of the usual. For example, BrdUrd-substituted chromatids stain darkly and unsubstituted chromatid segments stain lightly with standard Giemsa staining following hot acid treatment of the chromosomes (Burkholder, 1978, 1979, 1982; Takayama and Sakanishi, 1977; Sakanishi and Takayama, 1978). The hot acid treatment concomitantly denatures the unsubstituted DNA and preferentially extracts the less tightly bound histone 1 of the unsubstituted chromatin causing dispersion of histone 1 depleted DNA outside the boundaries of the chromosomes (Burkholder, 1979, 1982). This explains the higher protein content of BrdUrd-substituted chromatin after acetic acid-methanol fixation of chromosomes (Buys *et al.*, 1982). Alternatively, Giemsa staining in various conditions of salinity with high pH stains the BB chromatid darker than the TB chromatid (Alves and Jonasson, 1978; Takayama and Sakanishi, 1979; Takayama and Tachibana, 1980) suggesting that the staining conditions differentially modify bifilarly substituted chromatin structure allowing the Giemsa to bind.

5. The UV-induced breakage of disulphide bonds (max $\approx$250 nm for simple organic disulphide) leading to formation of sulphydryl groups appears to be higher in the BrdUrd-substituted chromatin than in unsubstituted chromatin (Buys and Stienstra, 1980; Buys and Osinga, 1981). Furthermore, the breakage of disulphide bonds loosens the chromatin structure, thus altering the spatial arrangement of binding sites for Giemsa, leading to lighter staining of this chromatid (Wolff and Bodycote, 1977).

6. If replicating cells are exposed to BrdUrd, both chromatids will have

homogeneous unifilarly substituted DNA (TB–TB). The template strand still contains only thymidine (T strand), while the nascent strand will be BrdUrd-substituted (B strand). A second cycle in the presence of BrdUrd allows chromatid differentiation (TB–BB), the first letter of each pair designating the template strand and the second one designating the nascent strand. During the second cycle, addition of thymidine instead of BrdUrd also allows chromatid differentiation (TT–BT). Contrary to expectations of how BrdUrd substitution affects FPG staining, unifilarly substituted TB and BT chromatids respond differently to identical FPG treatments designed to maximize differences in chromatin structure, TB chromatids being darkly stained and BT chromatids being lightly stained (Speit, 1984; Speit and Haupter, 1985). Mezzanotte *et al.* (1989b), using monoclonal antibodies to single- and double-stranded DNA, showed that, after identical FPG treatment, TB chromatids contained mostly double-strand fragments, whereas BT chromatids contained mostly single-strand fragments. BT and BB chromatids are lightly stained with Giemsa (Speit, 1984; Speit and Haupter, 1985) and show the same ultrastructural features with SEM after the same FPG treatment, but these morphologic features are different from the ones seen with TB chromatids (Jack *et al.*, 1989). TB chromatids are either darkly stained in TB-BB sister chromatid differentiation (SCD) or weakly stained in TT–TT and TB–TB differentiation (replication banding). Considering all the mechanisms formerly discussed, the FPG technique should not be able to distinguish between TB and BT chromatids. The molecular basis of this differentiation is unknown, but, apparently, BrdUrd in the template strand causes more extreme chromatin alterations than BrdUrd in the nascent strand and the FPG techniques used display this as differential Giemsa staining.

FPG Conclusion

A variety of published methods successfully produce an acceptable FPG technique (Table V) by a variety of different mechanisms (Fig. 3). For example, the Hoechst plus black light irradiation method will favor the photolysis mechanism, while germicidal lamp irradiation will favor the DNA-protein interaction class of mechanisms. Thus, replication bands can be revealed with selective BrdUrd-substituted chromatin loss, or without loss but by masking of DNA stainability, or by any combination of these two extremes. Many methods used for SCD, especially those relying on alteration of chromatin structure, were never successfully applied to replication banding because they produce fuzzy ill-defined bands.

To reveal the thinnest replication bands with maximal resolution of band boundaries, conditions that favor the photolysis mechanism are recommended; these require a high level of BrdUrd substitution. BrdUrd, added to the culture medium, can be incorporated very efficiently, since up to 90% of the thymidine can be replaced by BrdUrd in the nascent strand with a concentration of 30 μg/ml (10^{-4} M), and 60% of thymidine replacement can be achieved with a concentration of only 3 μg/ml (10^{-5} M) (Schwartz and Kirsten, 1974; Stetten *et al.*, 1976; Schiaffonati *et al.*, 1978; Severin and Ohnemus, 1982). Hence, 45 to 55% thymidine replacement by BrdUrd (1 μg/ml) is sufficient to demonstrate SCD (Richer *et al.*, 1987) whereas at least 75% substitution (10 μg/ml) is necessary to reveal replication bands (Drouin *et al.*, 1988a). Exclusive photolysis requires that Hoechst 33258 and black-light UV act synergistically to preferentially photolyse BrdUrd-substituted DNA and that the conditions for BrdUrd-DNA photolysis be so optimal that all substituted DNA is solubilized during photolysis, making a subsequent hot salt extraction step unnecessary (Lemieux *et al.*, 1987; Lemieux and Richer, 1989; Drouin *et al.*, 1988a) (Table V). The avoidance of the hot salt treatment obviates the creation of DNA-protein interactions that make insoluble chromatin inaccessible to Giemsa. The result (Fig. 4) is a Giemsa staining of only unsubstituted DNA.

BrdUrd Antibody-Binding (BAB) Technique

The immunochemical detection system utilizes a specific antibody, usually a mouse monoclonal anti-BrdUrd antibody (Gratzner, 1982), which binds to an accessible epitope, BrdUrd, in single-stranded DNA. A secondary antibody when needed is an antimouse immunoglobulin (IgG), either unlabeled or labeled with fluoresceine, peroxidase, gold or any other suitable labeling system. Hence, replication bands can be visualized in light microscopy (LM) with FITC, peroxidase-3,3′–diaminobenzidine (DAB), or alkaline phosphatase (Vogel *et al.*, 1986, 1989; Karube and Watanabe, 1988) and in transmission electron microscopy (TEM) either with gold (which can be coupled with streptavidin, antibody, protein A or protein G) (Drouin *et al.*, 1988b, 1989a; Vogel *et al.*, 1990; Fetni *et al.*, 1991) or with proteins (A or G) (Fetni *et al.*, 1992). The BAB technique shows BrdUrd-substituted bands positively stained while the FPG technique shows them as negatively stained; thus the same BrdUrd regimen will yield complementary band patterns using the different detection techniques (Figs. 2 and 4). For more technical details, the readers should refer to Richer and Drouin (1990).

The BAB technique is an extremely sensitive method for detection of BrdUrd in chromosomes, at least 20 times more sensitive than the FPG technique (Speit

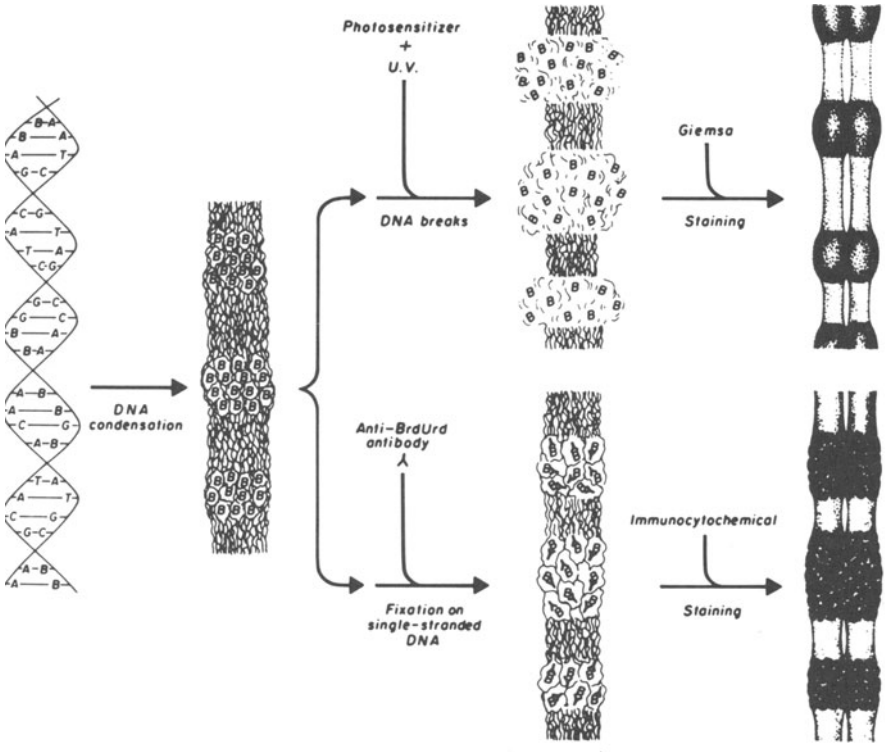

Fig. 4. Molecular model for FPG and BAB (BrdUrd antibody binding) techniques. Specific DNA fragments are BrdUrd-substituted during S-phase. Chromosome condensation permits clustering of substituted DNA into specific bands. The synergistic action of a photosensitizer and UV light selectively breaks the substituted DNA, depolymerizing and solubilizing it, leaving unsubstituted DNA as the only substance remaining to be stained by Giemsa. Alternatively, the DNA is denatured to allow the binding of the anti-BrdUrd antibody, which can be revealed with a labeled antimouse immunoglobulin (anti-IgG) antibody. The FPG technique shows the BrdUrd-substituted bands as negatively stained while the BAB technique shows them positively stained; thus the same BrdUrd incorporation regimen can yield complementary band patterns.

and Vogel, 1986; Tucker *et al.*, 1986; Shiraishi and Ohtsuki, 1987). BrdUrd substitution levels as low as 0.5% to 2.0% of thymine replacement in a single DNA strand is sufficient for a signal (Pinkel *et al.*, 1985; Natarajan *et al.*, 1986; Vogel *et al.*, 1989). The BAB technique is specific in that unsubstituted chromosomes are never stained.

While the exact epitope for the anti-BrdUrd antibody is undetermined, a substituent on C-5 of uridine and the deoxyribose component are both required for antibody recognition (Miller *et al.*, 1986) (Fig. 4). The epitope is inaccessible

when the DNA is double-stranded (Gratzner, 1982; Dolbeare *et al.*, 1983; Miller *et al.*, 1986). Mild denaturation conditions that produce only partial DNA denaturation are adequate for antibody accessibility only to the less condensed interphase chromatin (Gratzner, 1982; Dolbeare *et al.*, 1983; Morstyn *et al.*, 1983; Moran *et al.*, 1985; Vanderlaan *et al.*, 1986). The highly condensed chromatin of mitotic chromosomes requires stronger denaturation conditions to expose the epitope to the antibody. On fixed chromosomes, HCl (Morstyn *et al.*, 1983; Raza *et al.*, 1985; Natarajan *et al.*, 1986; Karube and Watanabe, 1988), NaOH (Speit and Vogel, 1986; Vogel *et al.*, 1986; Latos-Bielenska *et al.*, 1987; Shiraishi and Ohtsuki, 1987; Drouin *et al.*, 1988b), boiling water (Tucker *et al.*, 1986), and formamide (Pinkel *et al.*, 1985; Tucker *et al.*, 1986; Drouin *et al.*, 1989b) have been used to expose the epitope. Exonuclease III, effective in digesting one of the two strands of chromosomal DNA, produces good replication banding with the BAB technique (Fetni *et al.*, 1995). Formamide denaturation gives more consistent results with better preserved chromosome morphology (Drouin *et al.*, 1989b) than do other DNA denaturing agents. The extent to which the epitope is removed or remains inaccessible after these procedures is unknown.

COMPARATIVE BAND PATTERN ANALYSIS

Replication Band Patterns

In euchromatin, the replication band patterns $GBG_{450\text{–}1,000}$ and $GBI_{450\text{–}1,000}$ (Table I) are absolutely identical, and display a 100% band-for-band identity matching (Figs. 5 and 6, Fetni *et al.*, 1995). Similarly, $RBG_{450\text{–}1,250}$- and $RBI_{450\text{–}1,250}$-band patterns (Figs. 5 and 6, Fetni *et al.*, 1995) are absolutely identical. GBG and RBG are obtained with the FPG technique, while GBI and RBI are obtained with the BAB technique. Since GBI and RBI can be produced for LM or TEM analysis, the same congruency was noted in TEM as in LM (Drouin *et al.*, 1988b, 1989a). Using chromosomes from human lymphocytes and bone marrow at a lower band level, Savary *et al.* (1992) confirmed the strict similarity between $GBI_{450\text{–}550}$ and $GBG_{450\text{–}550}$ as well as between $RBI_{450\text{–}550}$ and $RBG_{450\text{–}550}$.

In euchromatin, the replication band patterns $GBG_{450\text{–}1,000}$ and $GBI_{450\text{–}1,000}$ display a 100% band-for-band complementary matching to $RBG_{450\text{–}1,250}$ and $RBI_{450\text{–}1,250}$ band patterns (Figs. 5–7; Drouin *et al.*, 1989a, 1990; Fetni *et al.*, 1995). The only overlapping observed is at band junctions and can be explained by the optical halo effect imparting more visual substance to bands positively stained by each technique (Drouin and Richer, 1985). The paired patterns GBG and RBG

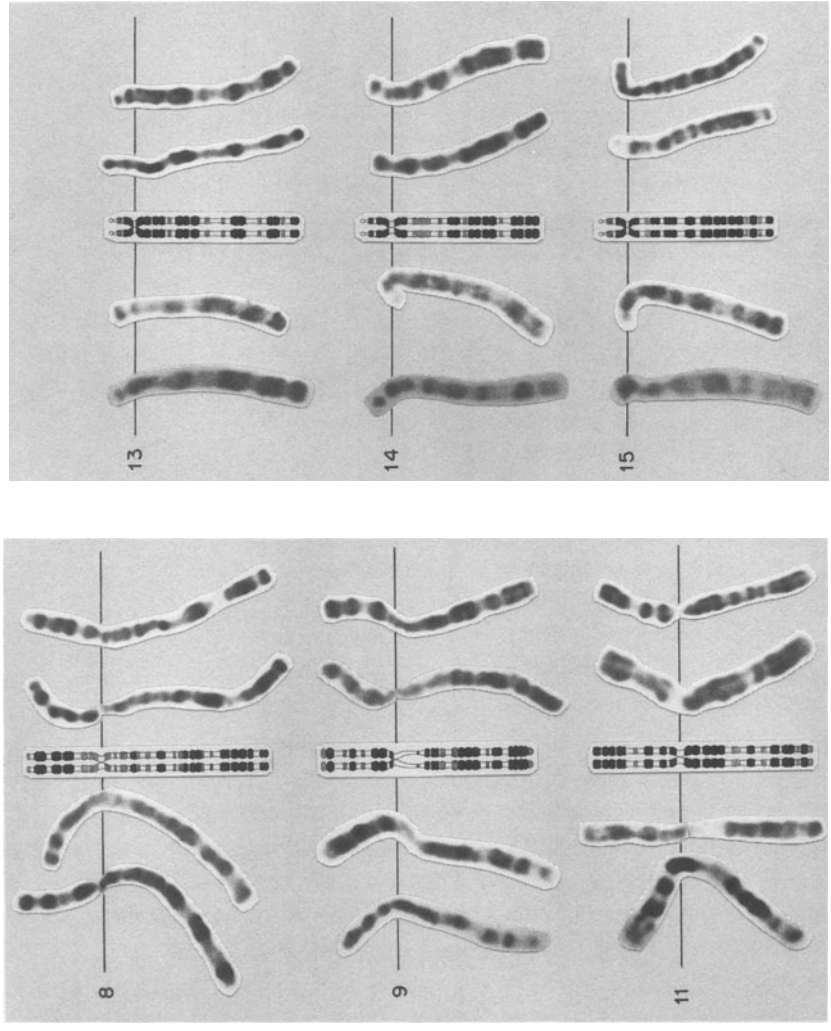

Fig. 5. High-resolution combined partial karyotypes showing chromosomes 8, 9, 11, 13, 14, and 15 at 800–1200 bands/genome resolution. From left to right GBG, GB-AP, $RBG_{1,250}$ idiogram, RB-AP, and RBG. Chromosomes are from Fetni *et al.* (1995). Idiograms are from Drouin and Richer (1989).

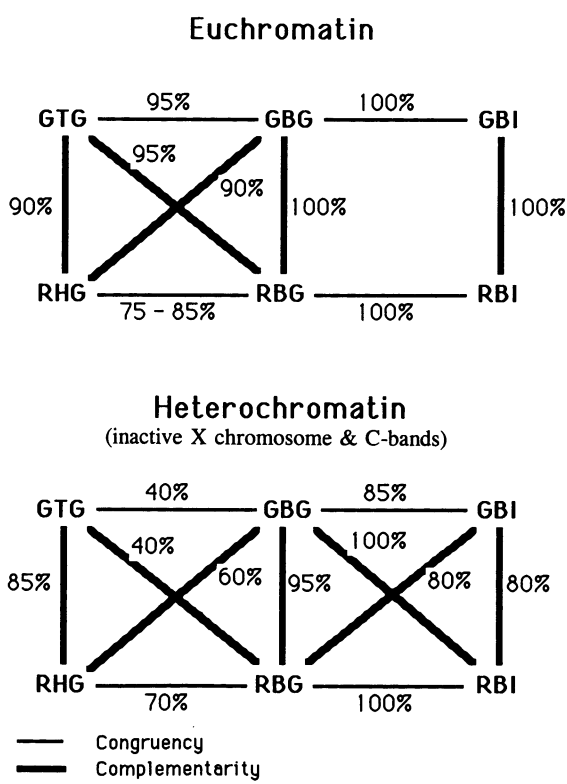

Fig. 6. A summary of the percentage of congruence (horizontal lines) and complementary (vertical and diagonal lines) between various bandings$_{1,000-1,250}$. See Drouin *et al.* (1991a) for technical details.

allow every part of each chromosome to be stained positively. Each euchromatic chromosome segment is either GBG$^+$ or RBG$^+$; a given segment is never positively or negatively stained by both bandings.

If the extensive similarities and complementarities mentioned above are correct, then all the following statements must also be true:

1. In euchromatin and at 1,250 bands/genome resolution, a set of bands, R–bands, replicate in their entirety before the artificially imposed block at the R/G transition seen in Figs. 1 and 2.
2. The remaining and complementary set of all euchromatic bands, the G-bands, replicate in their entirety after the R/G transition block is released.

3. The TBP culture method reliably allows complementary BrdUrd incorporation, in either R–bands or G–bands.
4. The FPG technique, which mostly utilizes the photolysis-dissolution mechanism (Lemieux *et al.*, 1987; Lemieux and Richer, 1989; Drouin *et al.*, 1988a in Table V), stains all unsubstituted bands positively and all BrdUrd-substituted bands negatively.
5. The BAB technique, as developed for either LM or TEM, stains all BrdUrd-substituted bands positively and all unsubstituted bands negatively.

Replication Band Patterns versus Morphologic Band Patterns

In euchromatin, $GTG_{600–1,000}$- and $GBG_{600–1,000}$-band patterns are almost identical (Fig. 7) (Meer *et al.*, 1981; Lemieux *et al.*, 1990; Savary *et al.*, 1991). They display 95% band-for-band identity matching (Fig. 6) with some minor differences being observed in the telomeric regions of 5p, 8q, 11q, 13q and 20q (Fig. 7, Table VI) (Lemieux *et al.*, 1990). Other groups confirmed telomeric differences for 5p (Savary *et al.*, 1991) and 11q (Scheres *et al.*, 1982). At lower band levels, spanning the two chromatids, there is a slight difference in that GBG bands characteristically appear as sharp twin dots and hence differ somewhat from GTG bands that look linear (Lemieux *et al.*, 1990). As expected, the RBG-band pattern is almost exactly complementary (reverse, 95%) to the GTG-band pattern (Figs. 6 and 7).

After analysis of hundreds of chromosomes, idiograms for RHG_{850}-banded chromosomes (Richer *et al.*, 1983b) and $RBG_{1,250}$-banded chromosomes (Fig. 8; Drouin and Richer, 1989) were made. While constructing these idiograms, we found that, in euchromatin, $RHG_{550–850}$- and $RBG_{550–1,250}$-band patterns shows 75% to 85% band-for-band identity matching (Figs. 6 and 7) (Drouin *et al.*, 1991a). These dissimilarities diminish with decreasing band levels and vary from one chromosome region to another (Fig. 7). For example, 5p, the distal third of 6q, the distal third of 8q, and the distal half of 13q show striking dissimilarities between RBG– and RHG–band patterns; the proximal third of 1p, 3q, 15q and 16q show less obvious differences; while 6p, 7p, 14q and 20q appear quite identical after RHG and RBG bandings (Fig. 7). Several bands that are uncharacteristically RHG^+-RBH^- or RHG^--RBG^+ are listed in Table VI. Savary *et al.* (1991), studying lower band level chromosomes, did not find as many differences, except for the telomeric area 5p, 6p, and 10q. The unexpected 15 to 25% noncongruency between the RHG– and the RBG-band patterns depends upon three factors:

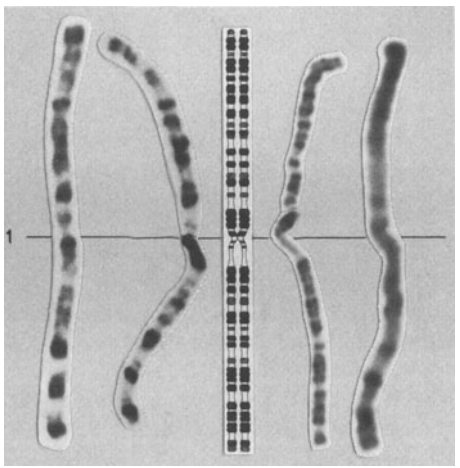
1

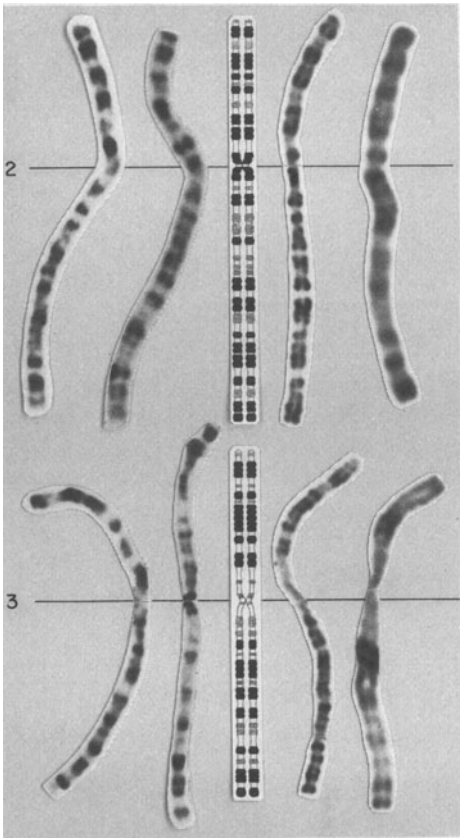
2
3

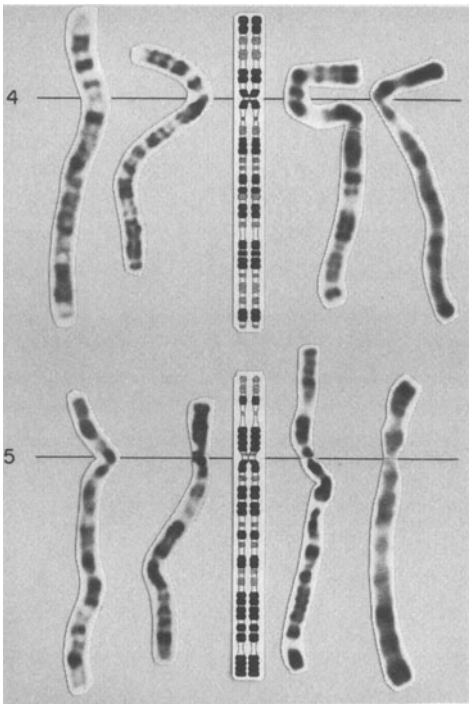
4
5

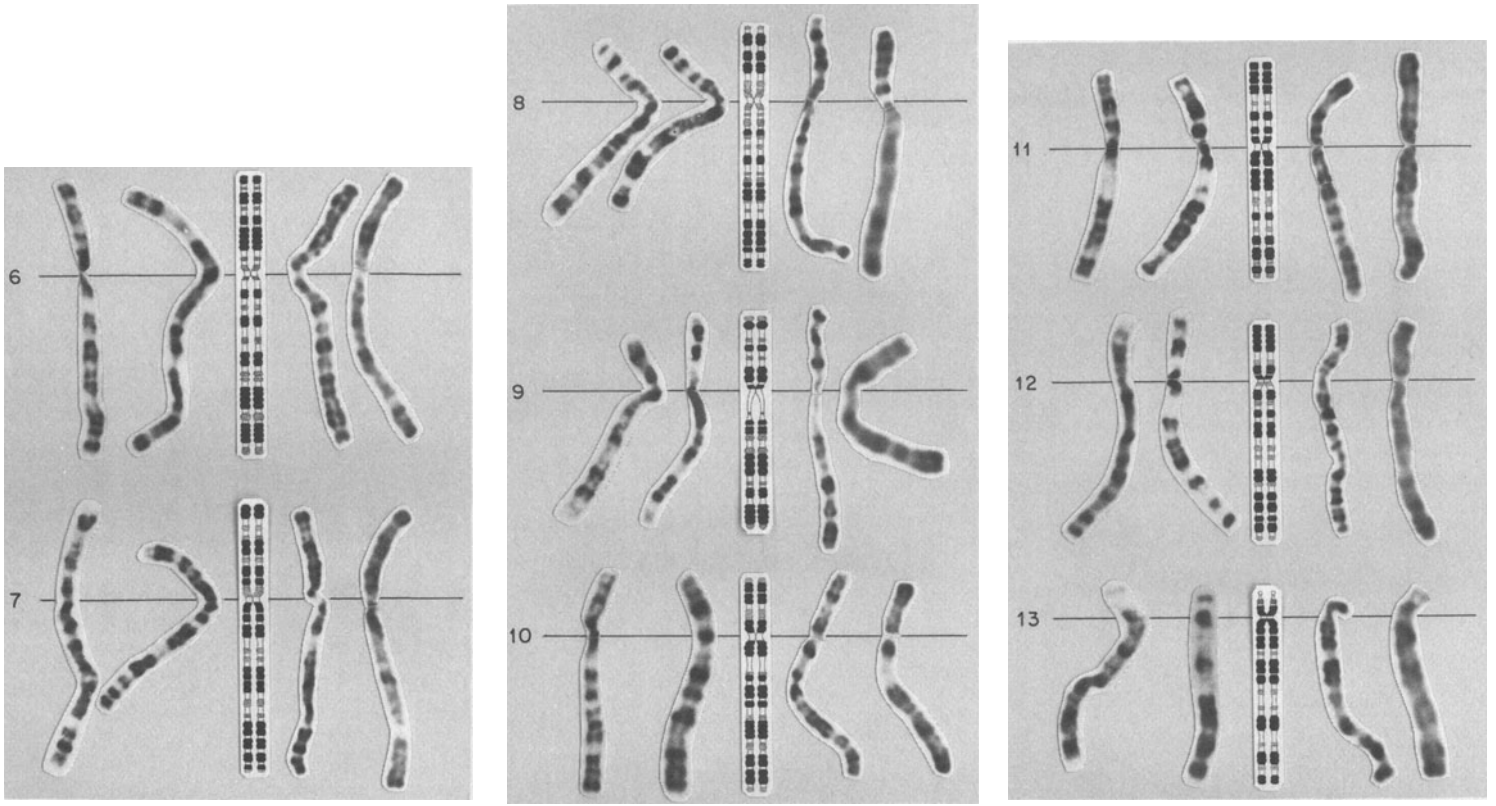

Fig. 7. High-resolution combined haploid karyotypes$_{850\text{–}1,250}$. From left to right: GTG, GBG, RBG$_{1,250}$ idiogram, RBG, and RHG. Some photographs were cut to straighten the chromosomes in order to facilitate band comparison. Chromosomes are from Richer *et al.* (1983b); Drouin and Richer (1989); Drouin *et al.* (1990, 1991a); Lemieux *et al.* (1990). Idiograms are from Drouin and Richer (1989).

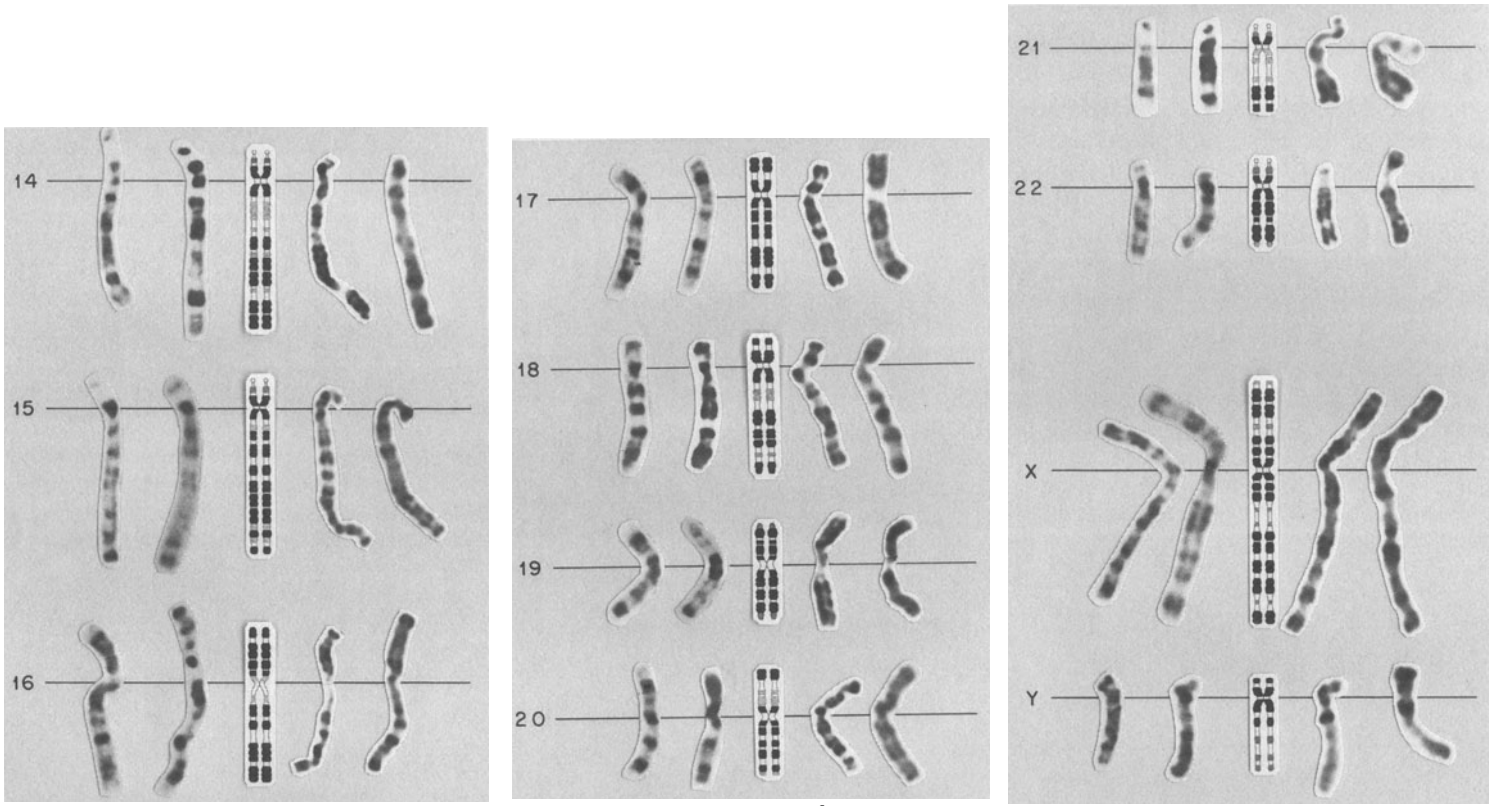

Fig. 7. (*Continued*)

TABLE VI. Cytological Characteristics of Several Bands

	GTG	GBG	RHG	RBG
Common characteristics				
2p25.11	−	−	+	+
6q14.3	+	+	−	−
12p13.1	−	−	+	+
13q31.1	+	+	−	−
Uncommon characteristics				
4q35.21	+	+	+	−
5p15.32	−	+	−	−
11q25.2	−	+	+	−
17q24.2	−	−	−	+
19q13.431	+	+	+	−

(1) staining features of banding, (2) replication time of bands, and (3) BrdUrd-dependent condensation delay.

The morphological $GTG_{550\text{–}1000}$- and $RHG_{550\text{–}850}$-band patterns display less than 90% complementarity matching (Fig. 6) (Drouin and Richer, 1985; Drouin *et al.*, 1991a). Complementarity varies from one chromosome region to another. 7q, 8p, 9p, 20p, 20q and 21q are complementary, while the proximal third of 1p, the distal part of 4q, and the distal halves of 17q, 19p and 19q show several noncomplementary areas (Fig. 7). Examples of GTG^+- RHG^+ and GTG^--RHG^- bands are listed in Table VI.

$RBG^+{}_{550\text{–}1,250}$ bands appear sharp and crisp, whereas $RHG^+{}_{550\text{–}850}$ bands appear fuzzy (Fig. 7; Drouin *et al.*, 1991a; Savary *et al.*, 1991). Over 70% of the RBG^+ bands are darkly stained, while 30%, though positively stained, appear paler (Figs. 7, 8). RHG banding produces a higher percentage of grey bands than does RBG banding and, consequently, confers a paler overall appearance to RHG-banded chromosomes (Figs. 7 and 8). By comparing the RBG (Drouin and Richer, 1989) and RHG (Richer *et al.*, 1983b) idiograms, one sees that most pale $RBG^+{}_{1,250}$ bands are also pale $RHG^+{}_{850}$ bands. The remaining pale and grey $RHG^+{}_{850}$ bands correspond to dark $RBG^+{}_{1,250}$ bands. RHG banding produces a much better contrast at low band level than at high band level, while RBG banding reveals the finest and sharpest bands at high band levels. Grey bands fading into one another without precise delimitation are characteristic of morphologic GTG- and RHG-band patterns at high band levels. These cytological properties hinder comparisons between morphological and replication bandings and could account for some noncongruence. We found that a hot saline treatment following the black light treatment makes RBG banding look more like RHG banding (Drouin and Richer, unpublished data).

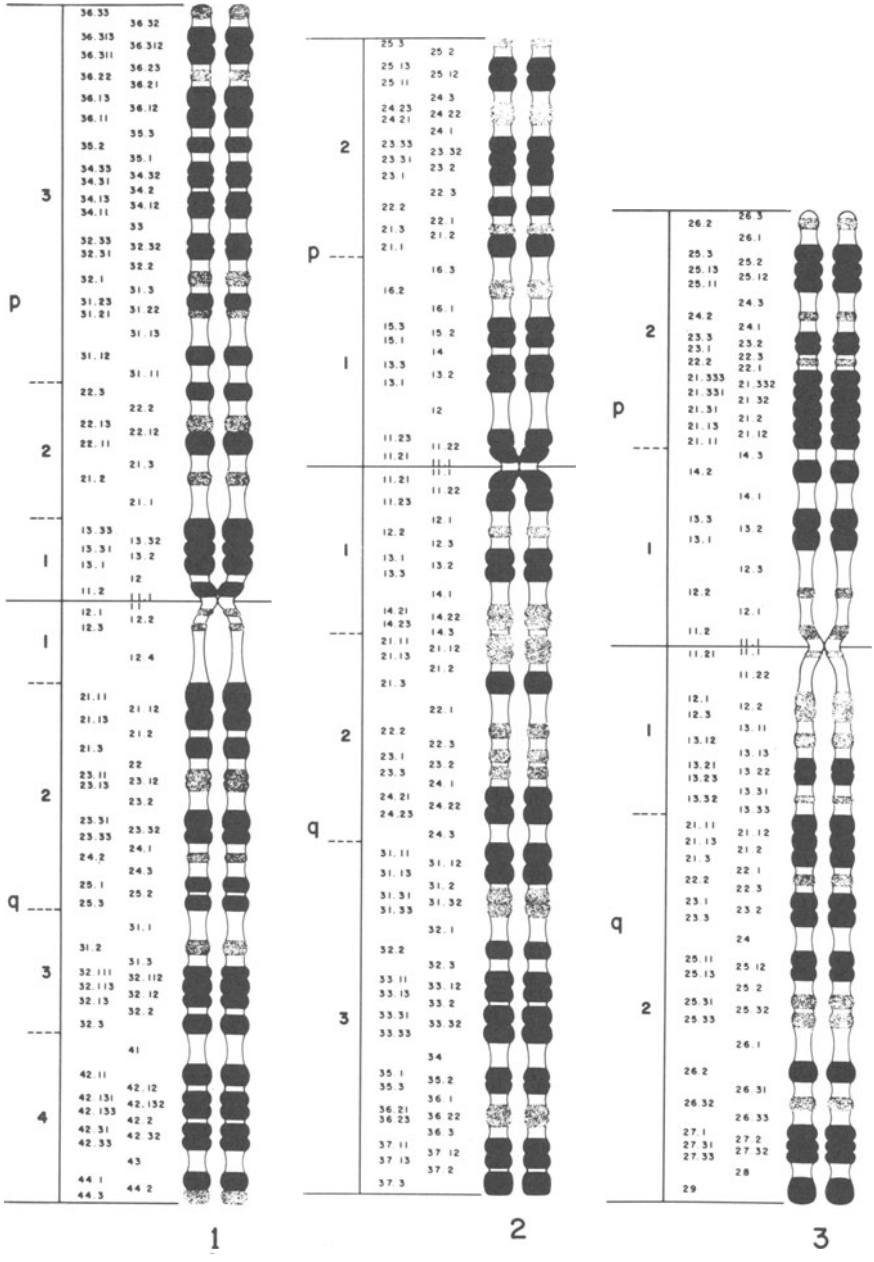

Fig. 8

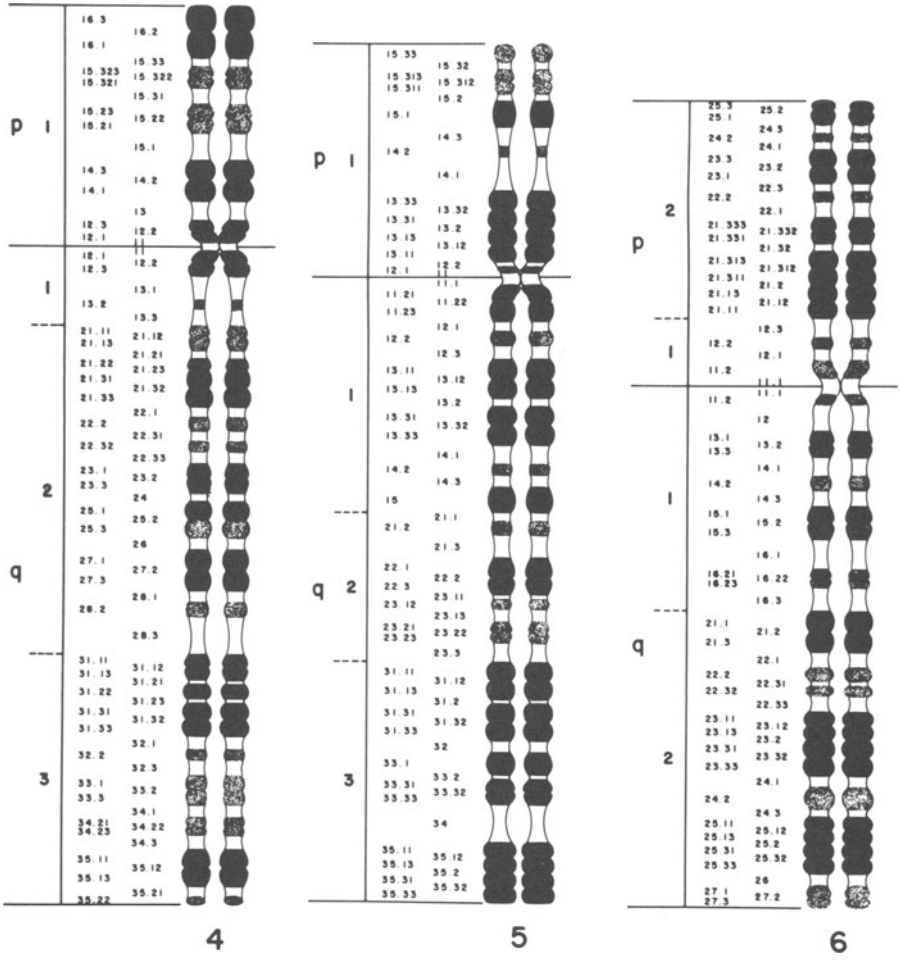

Fig. 8. Idiograms (Drouin and Richer, 1989; with permission) and nomenclature of $RBG_{1,250}$-banded chromosomes representing the relative position, the specific size, and the characteristic staining intensity of each band. Technical protocols for chromosome and band measurements, idiogram construction and band numbering, which is an extension of the ISCN (1985), were detailed in Drouin and Richer (1989).

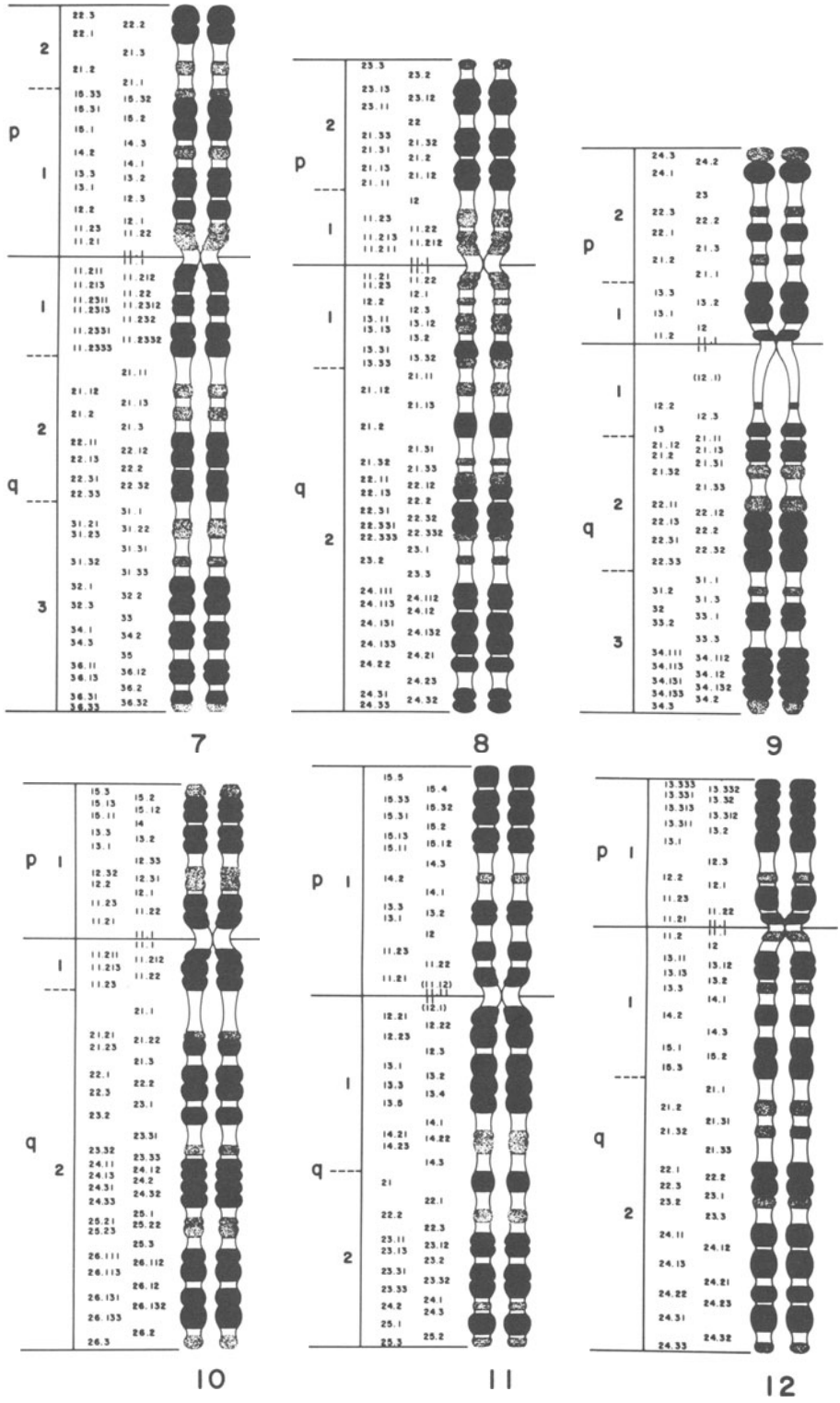

Fig. 8. (*Continued*)

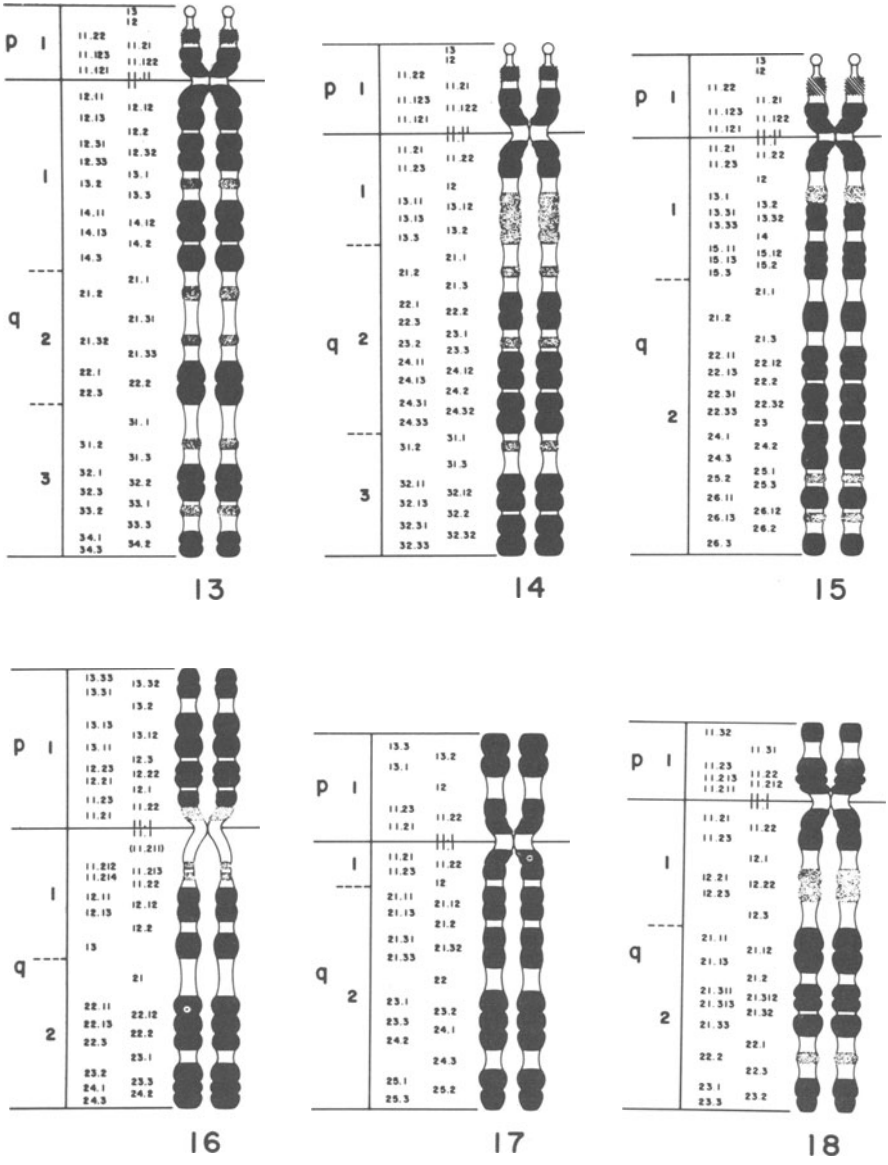

Fig. 8. (*Continued*)

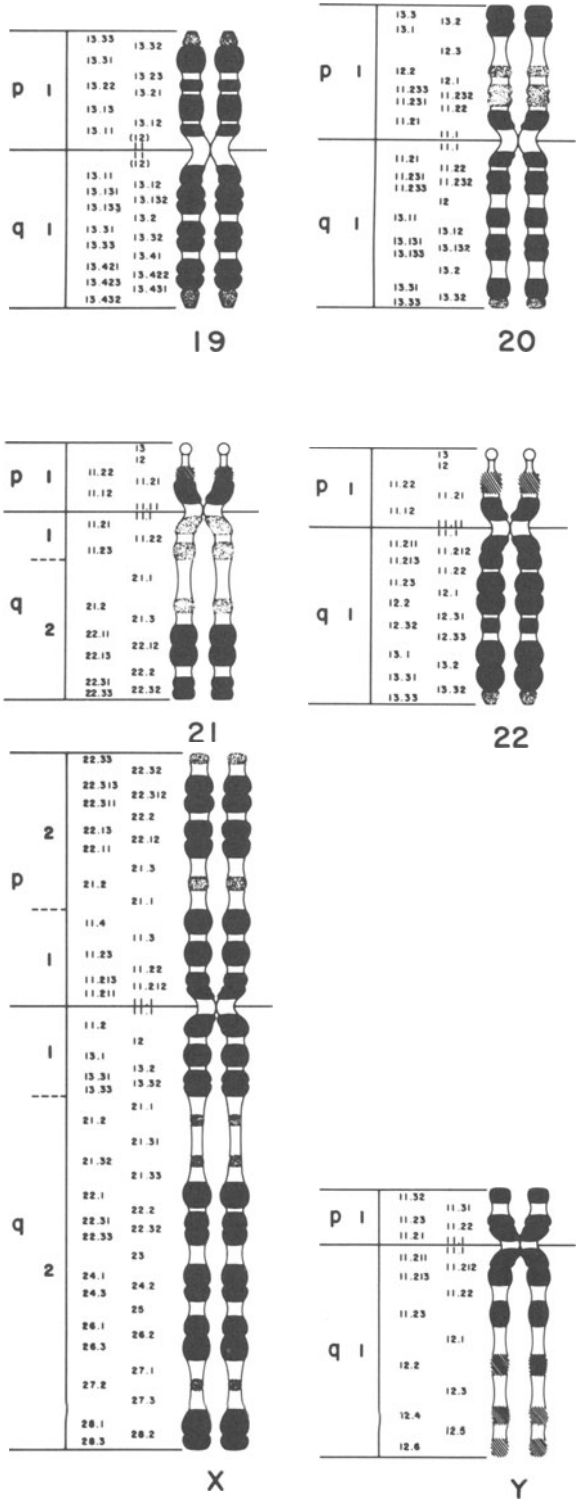

Fig. 8. (*Continued*)

BrdUrd incorporation slows the condensation rate of many substituted bands, so that in early mitoses, delayed bands are wider and less condensed, than they would have been if unsubstituted. GC-rich, early replicating (RBG^+-GBG^-) bands show almost no visible condensation delay; several AT-rich, late replicating (RBG^--GBG^+) bands, such as 11q12.3, 14q24.2, and 17q12, show very little delay; while several other AT-rich, late replicating (RBG^--GBG^+) bands, such as 5p14, 9p21 and 13q31, display a high degree of condensation delay (Figs. 7, 8). The BrdUrd-dependent effect on chromosome condensation is not an inhibition, but a delay, since it is related to the mitotic stage; the delay decreases during the progression of mitosis and is almost fully corrected by late metaphase. Very few bands show evidence of BrdUrd-induced condensation delay in late metaphase chromosomes. Consequently, RHG- and RBG-band patterns are more congruent at low band levels than at high band levels (Drouin *et al.*, 1991a).

The BrdUrd-dependent condensation delay is determined by three factors: (1) the degree of BrdUrd substitution (see above), the condensation delay increases with BrdUrd concentration (Zakharov and Egolina, 1972), (2) the AT content, the greatest delays correlate with AT-rich clusters (Goyanes and Mendez, 1981; Rønne, 1983) which also contain the highest amount of BrdUrd; and (3) the time interval between BrdUrd incorporation in a band during S-phase and mitosis (Zakharov and Egolina, 1972; Zakharov *et al.*, 1974); this means that for a band that replicates late, this time interval is short, and the band displays greater condensation delay than a band replicating earlier during S-phase. Consequently, bands that are the AT-richest and the latest replicating, display the greatest degree of BrdUrd-dependent condensation delay. Indeed, bands displaying the greatest condensation delay (2p12, 4p13, 5p14, 13q21, and 13q31) (Drouin *et al.*, 1991a), generally replicate during the latest intervals (XIV to XVIII) as defined by Dutrillaux *et al.* (1976) and are the brightest when stained with quinacrine (Dutrillaux *et al.*, 1976).

Because late replicating BrdUrd-substituted subbands inside an R-band (a group of $RBG^+{}_{650\text{–}1,250}$ subbands, separated by tiny RBG^- subbands that fuse to form one R-$band_{300}$) display almost no delay, the $RBG^+{}_{650\text{–}1,250}$ bands tend to be grouped in clusters, which are separated by elongated (unstained) regions (these are $RBG^-{}_{650\text{–}1,250}$ bands containing no, or one pale RBG^+ band, which form one $GBG^+{}_{300}$ band, Figs. 7 and 8) (Drouin *et al.*, 1991a). The BrdUrd-dependent condensation delay is more pronounced in the late replicating bands. The thinnest RBG^- bands are elongated by BrdUrd substitution, while the thinnest GBG^- bands are not elongated by BrdUrd substitution, and these barely visible thin unstained bands, which look like "cleavage furrows" in big dark bands (idiograms of Fig. 7), are responsible for the highest level of band resolution. This explains

why RBG banding can be accomplished at a higher band level (1,250 bands/genome) than GBG banding (1,000 bands/genome).

Replication band patterns at high band levels have been reproducibly produced using the TBP culture method (see section 3), not only with human lymphocytes but also with amniotic fluid cells (Qu *et al.*, 1989; Savary *et al.*, 1991), chorionic villus cells (Savary *et al.*, 1991), bone marrow cells (Lemieux *et al.*, 1987; Savary *et al.*, 1992) and tumor cells (Dutrillaux *et al.*, 1986; Muleris *et al.*, 1986, 1987a,b,c; Lemieux and Richer, 1989, 1990; Lemieux *et al.*, 1989). No tissue-specific differences in the replication band patterns were observed or reported at high band levels. Using unsynchronized cell populations, Sheldon and Nichols (1981) are the only investigators to report ill-defined tissue-specific differences in the $band_{200-300}$ patterns of late replication.

Importance of Complementarity to Idiograms

Standard idiograms, diagrams of band patterns, have been based on either GTG banding or RHG banding but never on both, because these two bandings are not quite complementary (Drouin and Richer, 1985; Drouin *et al.*, 1991a). Such idiograms inevitably overemphasize the darkly stained bands, and consequently inadequately represent features of the underlying chromatin pattern. The two replication bandings, GBG and RBG banding, being exactly complementary, together represent a positive staining of the entire genome, providing an accurate basis for making genomic idiogram.

In conclusion, all R-bands are not the same and not the reverse in staining to all G-bands; a variety of different chromatin flavors can be distinguished using the standard morphologic and dynamic bandings (Table VI). The response of a band to RHG banding using hot acidic Earle's balanced salt solution (Dutrillaux and Lejeune, 1971; Richer *et al.*, 1983a; Drouin *et al.*, 1988a), a treatment which presumably selectively denatures low Tm DNA and therefore indicates the base composition of a band (Holmquist *et al.*, 1982; Ambros and Sumner, 1987; Sumner, 1990), is moderately related to replication time; the correspondence being about 80% (Fig. 6). In contrast, the sensitivity of a band to trypsin is, for 95% of all euchromatic bands, correlated with replication time; GTG^+ bands are almost always late replicating and GTG^- bands are almost always early replicating.

Late replication is a phenomenon associated with gene repression (Holmquist, 1987; Goldman, 1988); only tissue specific genes reside in late replicating bands and thus, their resident replicon, but not the entire G-band (Selig *et al.*, 1992), becomes early replicating in tissues where they are expressed. Replication

band patterns are more primitive than morphologic band patterns (Schempp and Schmid, 1981; Holmquist, 1987), and their patterns are more strongly conserved during mammalian evolution (von Kiel *et al.*, 1985). Replication bands or clusters of temporally synchronous replicons are probably present in all chordates, while only vertebrates show GTG banding and only warm blooded vertebrates (birds and mammals) evolved the base composition differences necessary for reasonable quinacrine or RHG differentiation of R-bands (Holmquist, 1987, 1988, 1989; Medrano *et al.*, 1988). Thus, replication bandings reflect the distribution of a function, late replication-repression, and hence, are more important indicators of gene function and genome evolution than are morphologic bandings.

Juxtacentromeric Area

According to the International System for human Cytogenetic Nomenclature (ISCN) (1985) idiogram, a GTG^+-CBG^- band exists between the centromeric CBG^+ band and the most proximal RBG^+ band of chromosome arms 5p, 11p, 11q, and 12q. However, our results indicate that a $CBG^+_{1,250}$ band (RBG^--GBG^+) is always immediately followed by an $RBG^+_{1,250}$-$GBG^-_{1,250}$ band, maintaining the alternation of early and late replicating segments; no G-band was found between a C-band and an R-band (Drouin *et al.*, 1990).

C-band Area

Constitutive heterochromatin differs entirely from euchromatin in that GTG, GBG, RHG and RBG bandings lack the accustomed congruencies and complementarities of euchromatin (Fig. 6). Indeed, the GTG and GBG bandings display low congruency for the C-band regions (the centromeric regions, secondary constrictions of chromosomes 1, 9, and 16, and heterochromatin of the Y chromosome), while the RHG and RBG bandings display a high degree of congruency for these regions. C-band regions are generally GTG^+, GBG^+, RHG^- and RBG^- (Fig. 7), but often are GTG^- and each C-band region can be partly GTG^+ and partly GTG^- (Fig. 7). After GBG banding, the secondary constrictions of chromosomes 1, 9, and 16, often appear to comprise distinct blocks of dark-staining material separated by thin bands of unstained material (Lemieux *et al.*, 1990). On the other hand, after RBG and RHG bandings, one or two small and pale, positive bands can be visualized at high band levels (Richer *et al.*, 1983b; Drouin and Richer, 1989). These pale bands do not appear complementary to the unstained bands observed after GBG banding (Fig. 6). These RHG^+ and RBG^+

bands could represent satellite DNA regions identified immunochemically as GC-rich by Miller *et al.* (1974).

Another interpretation problem is that after GB-AP banding, the C-band regions are not always positively stained (Fig. 5), while after GB-AAu banding (Table 1), the display of gold particles is different than the one seen with euchromatic bands (Drouin *et al.*, 1988b). This type of chromatin most likely has a different structure and the epitope is not as accessible to the BrdUrd antibody.

The short arms of the acrocentrics, bands p11.12 and p11.22, are RBG^+-RBI^+-RHG^+-GBG^--GBI^--GTG^-, whereas p11.21 has the opposite staining (Fig. 5, 7, and 8). Hence, bands p11.12 and p11.22 are early replicating while p11.21 is late replicating. The inconstant, early replicating and probably GC-rich (Okamoto *et al.*, 1981) band, p11.22, sometimes known as "p noir" or "p^+" (Dutrillaux, 1973a), may be totally absent or present in one chromosome per pair, or in both. This band is very useful to quickly determine uniparental disomy with R-banding.

The heterochromatic portion of Yq also shows great interindividual variation in size and replication band patterns. C-banding, in situ hybridization using a satellite DNA repeat sequence probe that hybridizes to Yq (Wall *et al.*, 1988; Wall and Butler, 1989), and $GBG_{550\text{–}1,000}$ banding (Drouin *et al.*, 1990; Lemieux *et al.*, 1990), all show a discontinuous distribution of the heterochromatin into one to four blocks, interspersed with unstained material. Avoidance of prolonged exposure to Colcemid allows these distinct heterochromatin blocks to be revealed after C-banding (Wall and Butler, 1989). After $RBG_{550\text{–}1,250}$ banding without using Colcemid, one to four pale bands can be observed in the distal part of Yq (Schempp and Müller, 1982; Drouin and Richer, 1989); these pale bands are separated by negative bands showing extreme BrdUrd-induced condensation delay. The excellent complementarity of $RBG_{550\text{–}1,250}$- and $GBG_{550\text{–}1,000}$-band patterns for the heterochromatic portions (Fig. 7) (Drouin *et al.*, 1990) shows that these late replicating heterochromatin blocks are separated by early replicating segments. This observation strongly suggests that these fragments could be euchromatic.

Telomeric Area

In this context, we designate as "telomere" or "telomeric region" the most distal $band_{300\text{–}400}$. This band consists of several $subbands_{1,000}$. With replication banding, heterogeneity was found in such telomeric regions. After RBG banding, the 48 different telomeric regions of the human karyotype fall into five distinguishable morphological classes (for description and classification see Drouin *et al.*, 1990). Type I telomeres are illustrated by 5q, 11p, and 14q; type II telomeres are

represented by 6q, 8p, 8q, and 12q; type III telomeres are exemplified by 3p, 4q, and 19q; the short arms of the acrocentrics constitute type IV; and only Yq can be included in type V (Figs. 7, 8). While the complementary band pattern is found in the telomeric area with the dynamic bandings (RBG and RBI complementary to GBG and GBI), several type III telomeric bands are GTG^+ and RHG^+ (Table VI, Fig. 7) (Drouin *et al.*, 1990; Richer and Drouin, 1990).

Telomeric regions of type II and III contain less early replicating DNA and more late replicating DNA than the telomeric regions of type I. Ten Hagen *et al.* (1990) have reported that telomeric repeats of human cells could replicate early or late, but they did not distinguish the replication of individual telomeres. There is no association between a specific type of telomeric region and T-bands, very GC-rich bands or very Alu-rich bands (Holmquist and Drouin, unpublished data). We want to emphasize that this classification is based upon the morphology of the telomeric regions after dynamic banding, and thus reflects the replication time. The biological significance of these telomeric classes remains unknown.

Inactive X-Chromosome

The inactive X-chromosome shows that morphologic band patterns and dynamic band patterns are independent phenomena. The inactive X and active X have identical GTG- and RHG-band patterns even though the inactive X replicates its DNA during late S-phase and has replication band patterns different from the active X (Drouin *et al.*, 1990). The TBP culture method now reveals two additional replication features of the inactive X: the five earliest replicating bands of the inactive X actually replicate before the R/G transition instead of afterwards as previously believed, and, since all inactive X-chromosomes retain similar replication band patterns after the TBP culture method, previously reported differences in cell and tissue specific band replication times are minor because the varying band replication times never transgress the R/G transition.

The inactive X, after the TBP culture method allowing late-BrdUrd incorporation, appears decondensed and filiform with fewer $RBG^+_{450\text{–}1,250}$ bands than its homolog; these positive bands are smaller and paler than their counterparts on the active X (Drouin *et al.*, 1990). After $GBG_{450\text{–}1,000}$ banding, some small unstained (GBG^-) bands are interspersed in an otherwise darkly (GBG^+) stained inactive X (Drouin *et al.*, 1990; Lemieux *et al.*, 1990). Since the $RBG_{450\text{–}1,250}$ and $GBG_{450\text{–}1,000}$ band patterns are complementary, these five small bands are considered to replicate before the R/G transition. Indeed, bands p11.2, p22.31 or p22.13 (undetermined as to precisely which one), p22.33, q13, and q26 in the inactive X replicate at least in part before the R/G transition (Fig. 8; Drouin *et al.*, 1990).

Even in the inactive X, sequential R-band replication followed by G-band replication is conserved (Camargo and Cervenka, 1982; Schmidt *et al.*, 1982; Babu *et al.*, 1986; Reddy *et al.*, 1988; Schwemmle *et al.*, 1989), although several authors firmly believe that R-band replication in the inactive X starts after the R/G transition and coincides with autosomal G-band replication (Camargo and Cervenka, 1980, 1982; Schmidt *et al.*, 1982; Schmidt and Stolzmann, 1984; Reddy *et al.*, 1988; Schwemmle *et al.*, 1989).

The bands of the inactive X-chromosome replicating before the R/G transition and concurrent with euchromatic R-bands reveal chromatin areas that escape inactivation. Indeed, active, early replicating genes have been mapped to these bands (Wiles *et al.*, 1988; Fisher *et al.*, 1990; Brown *et al.*, 1991; Ellison *et al.*, 1992; Wang *et al.*, 1992). There is a congruent replication pattern in the pairing segments of both X and Y chromosomes and band Xp22.3 would correspond to Yp11.3, although the resemblance is not obvious after GTG banding (Müller and Schempp, 1982; Schempp and Meer, 1983). Bands p11.2, p22, and q13 have been considered those which initiate replication of the inactive X (Willard, 1977; Biemont *et al.*, 1978; Schmidt *et al.*, 1982; Schempp and Meer, 1983; Babu *et al.*, 1986).

Studies done at low $band_{300-550}$ levels and with unsynchronized cell populations displayed a striking interindividual and intercellular variability in the replication band patterns of the inactive X chromosome (Latt *et al.*, 1976, 1981; Willard and Latt, 1976; Willard, 1977; Kaluzewski, 1982; Schmidt *et al.*, 1982; Schmidt and Stolzmann, 1984; Tsukahara and Kajii, 1985; Babu *et al.*, 1986; Reddy *et al.*, 1988). The TBP culture method, which showed $bands_{1,250}$ replicating before the R/G transition, cannot be used to address the replication sequence of bands replicating *after* the R/G transition. We believe that variations in replication time of these bands, all of which replicate after the R/G transition, will be irrelevant to the question of replication repression (Holmquist, 1987).

Homolog Discordance

In the euchromatin of a given pair of homologs, slight band pattern differences may exist; this difference is called discordance. Discordance is based on visual differences in band number, band size, and band position; the degree of homolog discordance is the percentage of arm pairs that show differences in any one of these three different band characteristics. The degree of discordance increases with available visual information, that is, band level (Schwartz and Palmer, 1984; Drouin *et al.*, 1988a; Lemieux *et al.*, 1990). Discordance can be ascribed to three causes: (1) replication asynchrony, (2) unequal BrdUrd-

dependent condensation delay, and (3) technical factors. Only the third factor applies equally to both morphologic and replication bandings. The interpretations of previous replication bandings have always been limited by intercellular variability and homolog discordance. The TBP culture method combined with a good banding method (FPG or BAB), serves to dramatically reduce the intercellular variability of the band patterns (see p. 63), and also decreases homolog discordance. Indeed, after dynamic bandings, homolog discordance is not greater than that of morphological bandings (Fig. 9) (Drouin *et al.*, 1988a,b, 1989a; Lemieux *et al.*, 1990). Consequently, technical factors explain the homolog discordance observed after dynamic bandings and morphologic bandings.

When discordance of replication bands is due to replication asynchrony, a given band does not replicate simultaneously with its homologous band. This phenomenon has been widely reported with protocols following treatment of unsynchronized cell populations with BrdUrd and seems to affect predominantly the late replicating bands (Grzeschik *et al.*, 1975; Kim *et al.*, 1975; Latt, 1975; Dutrillaux *et al.*, 1976; Kondra and Ray, 1978). When the cells are released from a

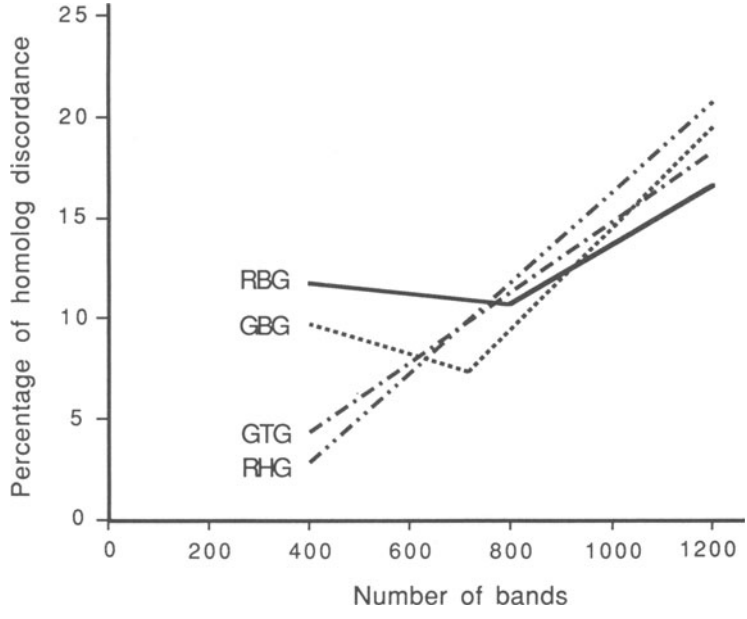

Fig. 9. Relationship between the total number of bands per haploid set and the percentage of homolog discordance for GTG, GBG, RHG, and RBG banding (combination of figures from Drouin *et al.*, 1988a and Lemieux *et al.*, 1990).

G_1/S transition block, replication asynchrony between homologs is a common finding (Schempp and Vogel, 1979; Schempp, 1980). With the TBP culture method, there is complete synchrony between homologs at the R/G transition, including band 15q11.2. This synchrony may be ascribed to the blocking agent, although the R/G transition could be a checkpoint during the cell cycle. In all likelihood, some asynchrony within each half of the S-phase occurs, therefore, when asynchrony is found, the cell probably had not been released from an R/G transition block. Indeed, Izumikawa *et al.* (1991) studied the R-band 15q11.2 in particular, which contains the Prader-Willi syndrome critical region, and found replication asynchrony between homologs in about 40% of the cells. They used a methotrexate block and most of the mitoses studied had not been stopped at the R/G transition. This higher replication asynchrony for 15q11.2 than for other autosomal R-bands is presumably due to an imprinting effect (Izumikawa *et al.*, 1991). Molecular cytogenetic studies have confirmed the replication asynchrony between homologs of the imprinted chromosomal region 15q11–15q13 (Kitsberg *et al.*, 1993; Knoll *et al.*, 1994).

BrdUrd delays condensation of both chromosomes of a pair equally and does not increase the homolog discordance. One may regard the differential condensation delay pattern for a given chromosome as stable and specific. We have never observed the striking discordance found by Schollmayer *et al.* (1981) in the condensation process of the BrdUrd-substituted bands of homologs as reflected by the variability of the arm ratio.

The technical factors, which include hypotonic treatment, fixation, spreading, chromosome overlapping, slide cleanliness, banding technique, and staining, explain why replication banding shows more discordance than morphologic banding at low resolution (<500 bands) (Fig. 9). At low band levels, FPG and BAB techniques are less reliable at revealing fine bands along metaphase chromosomes. Technical factors can also be responsible for very high homolog discordance after dynamic banding (Schwartz and Palmer, 1984; Latos-Bielenska *et al.*, 1987).

Lateral Asymmetry

Lateral asymmetry (Lin *et al.*, 1974) is seen as sister chromatid differentiation (SCD, differentiation of TB-TB chromatids) in C-band regions after BrdUrd incorporation for only one replication cycle (For extensive review, see Richer and Drouin, 1990; Sumner, 1990). In some C-band regions, only one chromatid fluoresces brightly after staining with Hoechst 33258 (Latt *et al.*, 1974; Lin *et al.*, 1974) or DAPI (Lin and Alfi, 1978); one chromatid stains darkly while the other

stains lightly after the FPG technique (Angell and Jacobs, 1975); and one shows green fluorescence while the other shows red fluorescence after acridine orange staining (Dutrillaux *et al.*, 1976). Lateral asymmetry is seen in the long arm of the Y chromosome; the secondary constrictions of 1, 9, and 16; the short arm of chromosome 15 and the centromeric regions of human chromosomes 2, 3, 4, 5, 7, 13, 14, 17, 19, 20, 21, 22; and of all mouse chromosomes (ref. in Richer and Drouin, 1990). It is a heritable heteromorphic feature, not present in every individual but constant within an individual (Angell and Jacobs, 1978; Lin and Alfi, 1978).

Lateral asymmetry is presumably associated with an asymmetric strand distribution of A and T in satellite DNA of C-banded regions (Latt *et al.*, 1974; Lin *et al.*, 1974). One replication cycle with BrdUrd produces asymmetrical BrdUrd incorporation in such a satellite; one daughter chromatid is rich in thymidine (template strand) and poor in BrdUrd (nascent strand) and the other chromatid is poor in thymidine and rich in BrdUrd. A banding technique sensitive to this difference in BrdUrd concentration should differentiate the chromatids in such a satellite region. This explanation probably applies well to the mouse C-bands whose major murine satellite DNA (Pardue and Gall, 1970) contains one strand with 45% thymine while the other strand has only 22% thymine (Flamm *et al.*, 1967). However, in humans there are at least four classes of well-defined satellite DNA (Saunders, 1974) and the strand difference in thymine distribution is only about 10% (32% and 42% in the heavy and light strands respectively) for satellite I DNA, and about 4% (26% to 30%) for satellite II DNA; but it is not known for satellite III and IV DNA (Schildkraut and Maio, 1969; Galloway and Evans, 1975). These smaller differences in thymine content were presumed responsible for the less pronounced asymmetry in fluorescence of human chromosomes than of mouse chromosomes (Latt *et al.*, 1974).

There are contradictions to this explanation for lateral asymmetry in humans:

1. Lateral asymmetry was not observed after $RBG_{550\text{–}1,250}$ banding (Viegas-Péquignot and Dutrillaux, 1978; Pai and Thomas, 1980; Meer *et al.*, 1981; Schollmayer *et al.*, 1981; Drouin *et al.*, 1988a). Lateral asymmetry seems to be a characteristic of low-band-level chromosomes. The lateral differentiation appears to be much less pronounced on chromosomes at high band levels than on chromosomes at low band levels (Schempp and Müller, 1982).
2. Lateral asymmetry has never been reported with the BAB technique.
3. When this sister chromatid differentiation was initially revealed by the FPG technique, the FPG protocol used always favored the second mecha-

nism, i.e., alterations of chromatin properties (see above). The hot saline treatment seems to be an essential step of the FPG technique in order to reveal the lateral asymmetry.

If strand asymmetry is the basis for lateral asymmetry, then it is revealed on chromosomes at low band level through BrdUrd-induced conformational chromatin changes. We believe the very sensitive approaches (high band level, FPG technique optimizing selective photolysis and BAB technique) do not detect small interstrand differences, each chromatid having more than enough BrdUrd incorporated to be stained lightly or darkly depending upon the method used.

R/G TRANSITION AND 3C PAUSE

The R/G transition reflects the transition from early (R-) to late (G- & C-) band DNA replication. This important physiological transition during the S-phase has been referred to as the 3C pause (Holmquist *et al.*, 1982; Holmquist, 1988). While the concept of an R/G transition is well accepted, the concept of the 3C pause is much more controversial. Some reports showed a clear demarcation between early and late S-phase (Schmidt, 1980; Kaluzewski, 1982; Vogel *et al.*, 1985; Vogel and Speit, 1986) and an absence of DNA synthesis occurring in the middle of the S-phase was reported (Klevecz *et al.*, 1975; Schempp and Vogel, 1978, 1979; Holmquist *et al.*, 1982). However, studies of unsynchronized cell populations found no period of complete cessation of DNA synthesis and demonstrated overlapping between R- and G-band replication (Dutrillaux, 1975a; Kim *et al.*, 1975; Cawood and Savage, 1985; Vogel *et al.*, 1989; Aghamohammadi and Savage, 1990). On the other hand, our results showing that a fully-developed R-band pattern is complementary to a fully-developed G- and C-band pattern (Drouin *et al.*, 1989a, 1990; Fetni *et al.*, 1995) indicate that all R-bands terminate their replication before all G- and C-bands initiate their replication. It is possible that the DNA synthesis blocking agents generate an artificial synchrony by allowing chain elongation of the R-band replicon clusters while blocking initiation of G-band replicon clusters. How the R/G transition occurs still remains largely unresolved.

During the four to four-and-a-half hours after release of cells previously blocked at the R/G transition, there occur the synthesis of late replicating DNA, wherein the G- and C-bands replicate, and G_2. The duration of the late S-phase (S_L) was previously believed to be roughly as long as the early S-phase (S_E) (Dutrillaux *et al.*, 1976; Schempp *et al.*, 1978; Schmidt, 1980). However, if G_2 lasts two hours, only two to two-and-a-half hours are available for S_L; thus S_L

would represent 20 to 30% of the S-phase duration, assuming that the duration of the S- and G_2-phases for cultured human lymphocytes varies from eight to ten hours and two to four hours, respectively. Placing the 3C pause at 65 to 75% of the total duration of S-phase would offer a plausible explanation for the short S_L (Figs. 1, 2). In addition to this short release period, other evidence supports this hypothesis. First, during S_L, only 33 to 40% of the DNA replicates. Second, flow cytometry studies of several mammalian cell types showed that S_E constitutes 60 to 70% of the length of the S-phase (Klevecz *et al.*, 1975; Klevecz, personal communications). Third, using very short BrdUrd pulse labeling of unsynchronized lymphocytes, Vogel *et al.* (1989) found that S_L was much shorter than S_E (S_L:25% versus S_E:75%).

Two other factors might explain the short duration of S_L. (1) A temporary inhibition of DNA synthesis by the S-phase synchronizing agent could be followed by an increase in replication origins and result in bursts of DNA synthesis and shortening of the S_L (Carnevali and Mariotti, 1977; Taylor, 1977). (2) Since late replicating DNA is inactive and more repetitive, replication could be faster, since it is known that heterochromatin replicates its DNA more rapidly than euchromatin (Schmid and Leppert, 1969; Comings, 1970; Stubblefield and Gay, 1970; Kimura *et al.*, 1980).

QUANTIFICATION OF R-, G- AND C-BAND CHROMATIN

The relative amount of each type of replication $bands_{1,250}$ is shown in Fig. 10 and Table VII. These calculations were possible because RBG and GBG bandings are exactly complementary patterns of positive information and can be used together to compensate for the halo effect (overrepresentation of positive information). More than half of the DNA is early replicating (Fig. 10) (Drouin *et al.*, 1991a), in accordance with flow cytometry studies showing that about 60% of the DNA is replicated during the early S-phase (Klevecz *et al.*, 1975), with the R/G transition occurring after 60 to 66% of the DNA has been replicated (see p. 92).

$G_{1,250}$-bands within metaphase R_{300}-bands represent less than 10% of the width of R_{300}-bands, while the $R_{1,250}$-bands within metaphase G_{300}-bands represent almost half of G_{300}-bands (Table VII). However, the premitotic condensation of G-band chromatin (Goyanes and Mendez, 1981) could decrease its relative proportion compared with R-band chromatin after cytogenetic evaluation. Furthermore, the DNA concentration might be higher in G-bands because they consist of more condensed DNA than do R-bands. G-band chromatin could contain more DNA than is cytogenetically estimated from band width.

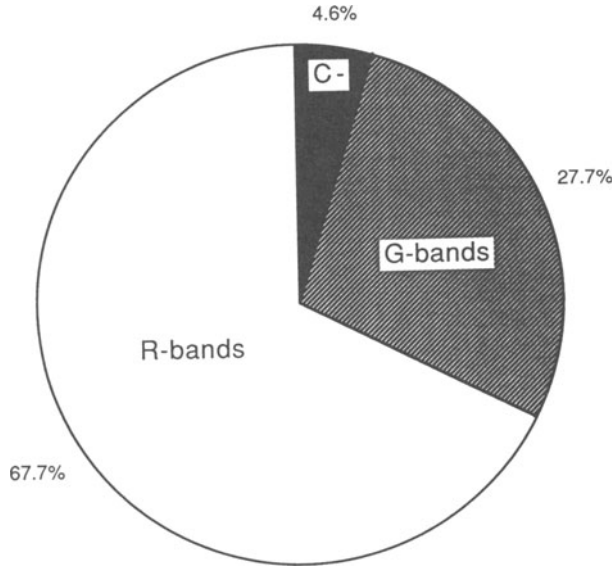

Fig. 10. Relative amounts of the three main types of chromosome bands$_{1,250}$ based on the width of each band.

TABLE VII. Percentage of Prophase Chromosome Length in Different Kinds of Bands

C-bands	4.6%
Prophase $G_{1,250}$-bands	27.7%
In metaphase G_{300}-bands	23.5%
In metaphase R_{300}-bands	4.2%
In mundane R_{300}-bands	1.9%
In $vAlu^+$ vGC^- R_{300}-bands	0.3%
In $vAlu^-$ vGC^+ R_{300}-bands	0.7%
In $vAlu^+$ vGC^+ R_{300}-bands	1.3%
Prophase $R_{1,250}$-bands	67.7%
In metaphase G_{300}-bands	11.8%
In metaphase R_{300}-bands	55.9%
In mundane R_{300}-bands	32.9%
In $vAlu^+$ vGC^- R_{300}-bands	2.9%
In $vAlu^-$ vGC^+ R_{300}-bands	7.3%
In $vAlu^+$ vGC^+ R_{300}-bands	12.8%

The human genome can be separated according to base content into five buoyant density fractions. These correspond to various base-composition isochores, which are large genomic DNA segments (well above 200 kb) of fairly homogeneous base composition (Bernardi *et al.*, 1985). The three heaviest fractions (H1, H2, and H3) are GC-rich and constitute 34% of the genome; it has been suggested that they corresponded to R-band DNA. The two lighter (L1 and L2), GC-poor, fractions constitute 66% of the genome and could correspond to G-band DNA (Cuny *et al.*, 1981; Bernardi *et al.*, 1985; Bernardi, 1989). Our estimates of 60 to 66% R-band DNA represent much more DNA than is in Bernardi's H1-3 isochore fractions, so many R-bands must contain DNA from the AT-rich (GC-poor) isochore fractions. Indeed, the R-bands which are not T-bands, are composed of an almost equal amount of L and H1 isochore families (with a minor contribution of the H2 and H3 families) (Saccone *et al.*, 1993). Saccone *et al.* (1993) also showed that G-bands consist essentially of L isochore families, with a minor contribution of H1 isochores. The relative proportion of light and heavy isochore fractions could represent the molecular basis for the different chromatin flavors of the R-bands (Holmquist, 1990a, 1992), and account for both the incomplete complementarity between RHG and GTG band patterns and the incomplete congruency between RHG and RBG band patterns (see section 5.2). The very GC-rich (vGC^+) (Ambros and Sumner, 1987) and THG^+ (Dutrillaux, 1973b) bands are composed predominantly of GC-rich isochores of the H1 and H2 families and in part of the GC-richest isochores of the H3 family (Saccone *et al.*, 1993). The high content of GC-rich isochores of the T-bands probably represents the banding basis of the THG^+ bands which are more resistant to heat denaturation (Dutrillaux and Covic, 1974).

CONDENSATION AND REPLICATION: TWO INTERRELATED PHENOMENA

Chromosome condensation was evaluated cytogenetically from late prophase, $band_{1,250}$, to late metaphase, $band_{300}$ (Drouin *et al.*, 1991b). This phenomenon is seen as the shortening of chromosome segments and fusion of subbands. During mitotic condensation, many of the 1,250 subbands of prometaphase chromosomes fuse until, at metaphase, only 300 distinguishable bands remain (Fig. 11). Generally, two major (thicker) subbands, flanking one minor (thinner) subband coalesce and fuse together, forming one band with cytological characteristics similar to the original flanking subbands (Fig. 11). The band resulting from fusion always maintains the cytological features of the two major flanking

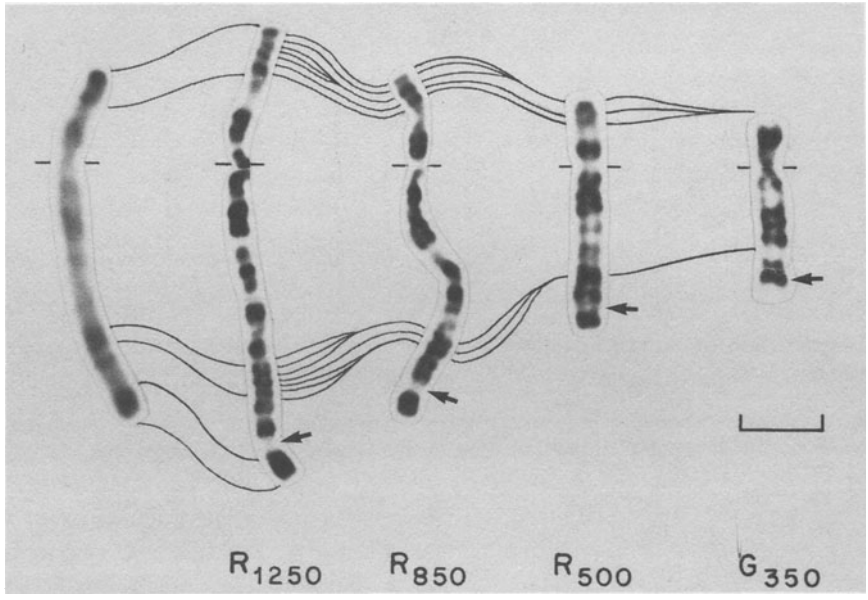

Fig. 11. RBG- and GTG-banded chromosome 5 at various stages of chromosome condensation (modified from Holmquist, 1992). The number of different resolved bands per haploid genome, as indicated by subscripts, decreases as the chromosomes condense (Drouin *et al.*, 1991b). The decrease is due to fusions of many prophase subbands. The lines indicate the fusion of 7 $bands_{1,250}$ (4 RBG^+ and 3 RBG^-). During this fusion, three G-bands are swallowed without affecting the cytological features of the final R-$band_{350}$ (RBG^+ and GBG^-). In some regions of preferential condensation, subbands fuse quite readily. Other regions (arrows) show no fusion. More than one third of the 125 metaphase $GBG^+{}_{300}$ bands do not show any fusion, while less than 4% of the 164 metaphase $RBG^+{}_{300}$ bands fail to fuse (Drouin *et al.*, 1991b). The leftmost chromosome, at 850-band level, was treated by THG-banding. It shows that, at prophase, the heat-resistant T_{850}-subbands are clustered. In shorter chromosomes, these clusters are fused and form a single metaphase T_{300}-band (not shown).

subbands, that is, the minor band and its contribution to the fused band seem to disappear. This is true for replication banding using FPG or BAB detection and for morphologic GTG and RHG bandings. This implies that during condensation, the chromatin structure is reorganized to allow the middle bands to be integrated and take on the cytological features of the flanking bands.

Exactly how subbands fuse remains a mystery. The disappearance during fusion of a minor band from FPG or BAB detection may imply that the FPG and BAB techniques do not simply differentiate BrdUrd-substituted from un-substituted chromatin as suggested above. Immunochemical banding studies in TEM showed that many anti-BrdUrd antibody binding sites become inaccessible

during band fusion (Messier *et al.*, 1989). All staining results concerning band fusion are inconsistent with the tight stacking of subbands as suggested in the coiling models of chromatin structure (Manuelidis and Chen, 1990).

During G_2 and early prophase, late replicating DNA (G-bands) is the first chromatin to condense followed by the early replicating DNA (R-bands) which condenses less rapidly (Kuroiwa, 1971; Goyanes and Mendez, 1981). From late prophase to late metaphase, R-bands condense more rapidly than G-bands, and this trend is present throughout this mitotic period (Drouin *et al.*, 1991b). Fusion of subbands along the chromosomes occurs in a specific chronological order so that all cells of one mitotic stage have the same pattern of fused bands (Drouin *et al.*, 1991b). Fusion of subbands is asynchronous along the chromosome, there being regions of preferential condensation and regions of slight condensation (Fig. 11) (Richer *et al.*, 1983a,b; Drouin and Richer, 1985, 1989; Romagnano *et al.*, 1987; Drouin *et al.*, 1991b). In general, the degree of condensation by band type is T-bands followed by R-bands followed by G-bands (Holmquist, 1992). Since the order of replication during S-phase is T-bands, followed by R-bands followed by G-bands, the replication time of a band and its degree of mitotic condensation seem directly related.

The fusion process, which is highly coordinated like replication, represents as characteristic a feature of chromosome organization as does banding or replication pattern. Metaphase G- and R-bands behave dynamically as independent units of chromatin condensation (Goyannes and Mendez, 1981; Drouin *et al.*, 1991b). Presumably, the regulation of replication and condensation is not only interrelated but is autonomous for each G- and R-band unit. Indeed, after DNA replication, each metaphase band is a unit where the DNA is packaged into a defined and specific structure. Each of these structural units is distinguished from its neighbors by the banding techniques. At any condensation step, the cytological features of a band remain the same; for example, a T-band remains a T-band from the 850- to the 300-band level (Fig. 11) (Holmquist, 1992).

The numbering of prophase subbands in idiograms is based on and requires an exact knowledge of the fusion pathways of each subband (ISCN, 1985). Since the ISCN idiograms have been generated almost entirely from G-banded chromosomes, these idiograms have favored G-bands and do not properly reflect the band fusion pathway. For example, in the ISCN idiograms, the R-band 9q32 is shown undivided while the G-band 9q33 is subdivided in three subbands (Fig. 8 follows ISCN numbering). However, the fusion pathway derived from GTG, GBG, RHG and RBG bandings (Drouin and Richer, unpublished data) shows very clearly that in 9q32 two R-subbands fuse and a middle G-band disappears, while 9q33 never fuses from the 1,250 to the 300 band level (9q32.1, 32.2, 32.3) instead

TABLE VIII. Distinctive Features of R-Bands and G-Bands[a]

Band features	R-bands	G-bands
Cytological features		
Quinacrine	Dull	Bright
Hoechst 33258 fluorescence[b]	Dull	Bright
Acridine orange fluorescence[c]	Yellow-green	Orange-red
Chromomycin A_3 fluorescence[d]	Bright	Dull
Basophilia sensitivity to protein denaturation	Sensitive (GTG^-)	More resistant (GTG^+)
Basophilia sensitivity to heat denaturation	More resistant (RHG^+)	Sensitive (RHG^-)
DNase II and Hae III sensitivity	Sensitive	More resistant
Access to DNAse I-nick translation	Open	Closed
Pachytene DNA	Inter-chromomeres	Chromomeres
Heteropycnosis in prometaphase	Negative	More condensed
Functional features		
Replication time during the S-phase	Early	Late
Condensation rate during mitosis[e]	Fast	Slow
Mitotic chiasmata frequency	High	Low
Meiotic chiasmata frequency	High	Low
X-ray-induced break frequency	High	Low
Synaptic initiation	Yes	No
Synapsis	Homologous	Homology independent
Molecular features		
Base composition	dG+dC rich DNA	dA+dT rich DNA
Third codon bases	dG+dC rich	dA+dT rich
Mapped genes	Most of the genes	Few
Housekeeping vs tissue specific (TS) location	All housekeeping genes many TS genes (>50%)	Only TS genes
CpG islands in housekeeping and TS genes	Yes	No
Promoter sequence	Upstream GGGCGGG	Rare Sp1 binding sequence
Interspersed repetitive sequences	SINE rich	LINE rich
Specific repeats	Alu in humans B1 and B2 in rodents	L1 retroposons
Amplification rate	High	Low
Sequence divergence rate	Slow	Faster molecular clock
Immunocytochemical features		
Affinity of anti-Z-DNA antibodies (Ab)	Strong	Weak
Affinity of tumor antigen Ab	Weak	Bind anti-T-antigen Ab
Affinity of anti-double-stranded DNA Ab[f]	Strong	Weak
Affinity of anti-triplex DNA Ab[g]	Weak	Strong
Affinity of high-mobility group I protein Ab[h]	Weak	Strong
Acetylation of H4 histones[i]	Yes	No

(*Continued*)

TABLE VIII. (*Continued*)

Band features	R-bands	G-bands
Immunocytochemical features (*Cont.*)		
Fucosylation of nonhistone proteins[j]	No	Yes
Other features		
Abortion frequency in trisomic state	Frequent	Less frequent
Virus integration sites	Hepatitis B virus	Mouse mammary tumor virus
	bovine leukemia virus	Epstein-Barr virus

[a]Most of these features were tabulated by Holmquist (1989, 1990b,c) or were presented at the 11th International Chromosome Conference or reported as properties of chromatin flavors (Holmquist, 1992). Several new features were added; see FNs b–j for references.
[b]Raposa and Natarajan, 1974
[c]Couturier *et al.*, 1973
[d]Schweizer, 1977
[e]Drouin *et al.*, 1991b
[f]Magaud *et al.*, 1985 (the Ab showed specificity for dG-dC and the band patterns were obtained after slight trypsin digestion of the methanol-acetic acid-fixed chromosome preparations)
[g]Burkholder *et al.*, 1988
[h]Disney *et al.*, 1989
[i]Jeppesen and Turner, 1992
[j]Myllyharju and Nokkala, 1992

of 9q33.1, 33.2, and 33.3). Chromosome condensation should always be studied with complementary banding techniques.

FEATURES OF R- AND G-BANDS

Based on combinations of extreme Alu richness (vAlu) and GC-richness (vGC), Holmquist (1990a) distinguished four different subsets of R-bands based on their chromatin flavors: $vAlu^{-}$-vGC^{-} (mundane R-bands), $vAlu^{+}$-vGC^{-}, $vAlu^{-}$-vGC^{+} and $vAlu^{+}$-vGC^{+}. Each R-band subset has distinctive features (Holmquist, 1992). Subsets of different kinds of G-bands have not been described. However, we believe that several late replicating G-bands (4q13, 5p14, 5q34, 8q23, 9p21, 9p23, 11p14, 13q21, 13q31, and 14q31) are distinct from other G-bands. They share the following distinguishing features: (1) very late replication (groups XV to XVIII, Dutrillaux *et al.*, 1976), (2) failure to fuse or just one fusion (Drouin *et al.*, 1991b), (3) an extreme BrdUrd-induced condensation delay (Drouin *et al.*, 1991a), and (4) only one gene has been mapped to any of these bands

(Human Gene Mapping 11, 1991). These may represent a subset of G-bands, which are particularly AT-rich and particularly devoid of genes.

So far, two major sets of euchromatic bands have been defined according to their Giemsa stainability after trypsin treatment, G-dark (GTG^+) and G-light (GTG^-) bands. This implies that all bands are G-bands (Sumner, 1990). GTG^- bands are not equivalent to RHG^+ bands and neither are GTG^+ and RHG^-. Sumner's definitions are therefore confusing and incorrect. With the TBP culture method, the genome was segregated into two distinct phases, distinguishable by their replication time according to the R/G transition, which acts much like a cell checkpoint. This precisely defines an early replicating subgenome and a late replicating subgenome. Hence, a euchromatic band should be primarily defined by its replication time, an early replicating band being an R-band and a late replicating band being a G-band ($RBG^+ = GBG^-$ and $RBG^- = GBG^+$). Based on this primary definition, R- and G-bands have many distinctive features (Table VIII).

The highest band resolution ever attained by replication banding, using either the FPG technique (Drouin *et al.*, 1988a, 1990) or an ultrastructural immunohistochemical method (Drouin *et al.*, 1988b, 1989a), was 1,250 bands per genome. Only one early report discerned more bands (GTG-bands) (Yunis, 1981). Even the premature chromosome condensation technique (Hameister and Sperling, 1984) does not provide higher resolution. Thus, we believe 1,250 bands to be the most likely maximum number of attainable replication bands. Each would represent represent approximately 2,500 to 3,000 kb of DNA and contain 10 to 50 replicons of 50 to 330 kb (Hand, 1978). This number of chromosome replication units is in agreement with the number of replication granules found with the interphase nuclei (Nakamura *et al.*, 1986; Nakayasu and Berezney, 1989; Fox *et al.*, 1991; O'Keefe *et al.*, 1992).

CONCLUSION

Replication banding can be reproducibly revealed by blocking DNA synthesis at the R/G transition and incorporating BrdUrd into DNA replicated either before the block or after its release. Banding techniques that reveal very specifically the BrdUrd-substituted DNA are available. The thymidine–BrdUrd permutation (TBP) culture method combined with an appropriate banding technique produces replication R-band patterns exactly complementary to replication G-band patterns and are almost exactly congruent to GTG-band patterns. Since the replication time of a band relative to the R/G transition can be determined, it is important to verify the replication time of bands after chromosome rearrangement. Karube and

Watanabe (1988) found a switch from late to early replication of the chromosome segment at the site of a translocation in a case of acute myeloid leukemia with a chromosome translocation. Furthermore, with the TBP culture method, a DNA fragment can be localized to an R- or G-band by *in situ* hybridization directly on $\text{banded}_{1,250}$ chromosomes (Fetni *et al.*, 1991, 1992; Lemieux *et al.*, 1992); such cytological resolution for gene localization is unprecedented. An idiogram representing both the early and late replicating bands (Fig. 8 represents only RBG^+ bands) would represent band widths proportional to the DNA content of each band and would be very useful for genome mapping.

ACKNOWLEDGMENTS. The authors thank Raouf Fetni for communicating unpublished data and helping with the conception of Figures 1 and 4; Steve Bates, Raouf Fetni, and Patricia Visser for reviewing the manuscript; Brigitte Beugnot, Claire Couillard, Diane Lachance, Louise Laquerre, and Elise Ménard for their technical skill and highly motivated work. The artistic work of Emilienne Lambert and the excellent photographic work of Jean Léveillé are gratefully acknowledged. Special thanks go to the blood donors who made this project possible. This work was supported by La Fondation Magali Ducharme and La Société de Recherche sur le Cancer Inc., Montréal. R.D. holds a Centennial Fellowship from the Medical Research Council of Canada.

REFERENCES

Aghamohammadi, S.Z., and Savage, J.R.K., 1990, BrdU pulse/reverse staining protocols for investigating chromosome replication, *Chromosoma* **99:**76–82.

Alves, P., and Jonasson, J., 1978, New staining method for the detection of sister-chromatid exchanges in BrdU-labelled chromosomes, *J. Cell Sci.* **32:**185–195.

Ambros, P.F., and Sumner, A.T., 1987, Correlation of pachytene chromomeres and metaphase bands of human chromosomes, and distinctive properties of telomeric regions, *Cytogenet. Cell Genet.* **44:**223–228.

Angell, R.R., and Jacobs, P.A., 1975, Lateral asymmetry in human constitutive heterochromatin, *Chromosoma* **51:**301–310.

Angell, R.R., and Jacobs, P.A., 1978, Lateral asymmetry in human constitutive heterochromatin: Frequency and inheritance, *Am. J. Hum. Genet.* **30:**144–152.

Ashman, C.R., and Davidson, R.L., 1981, Bromodeoxyuridine mutagenesis in mammalian cells is related to deoxyribonucleotide pool imbalance, *Mol. Cell. Biol.* **1:**254–260.

Augenlicht, L., Nicolini, C., and Baserga, R., 1974, Circular dichroism and thermal denaturation studies of chromatin and DNA from BrdU-treated mouse fibroblasts, *Biochem. Biophys. Res. Commun.* **59:**920–926.

Babu, A., Chemitiganti, S., and Verma, R.S., 1986, Heterochromatinization of human X-chromosomes: Classification of replication profile, *Clin. Genet.* **30:**108–111.

Bernardi, G., 1989, The isochore organization of the human genome, *Annu. Rev. Genet.* **23:**637–661.

Bernardi, G., Olofsson, B., Filipski, J., Zerial, M., Salinas, J., Cuny, G., Meunier-Rotival, M., and Rodier, F., 1985, The mosaic genome of warm-blooded vertebrates, *Science* **228:**953–958.

Bertino, J.R., 1963, The mechanism of action of the folate antagonists in man, *Cancer Res.* **23:**1286–1306.

Bianchi, N.O., Bianchi, M.S., and Cleaver, J.E., 1984, The action of ultraviolet light on the patterns of banding induced by restriction endonucleases in human chromosomes, *Chromosoma* **90:**133–138.

Bianchi, N.O., Morgan, W.F., and Cleaver, J.E., 1985, Relationship of ultraviolet light-induced DNA-protein cross-linkage to chromatin structure, *Exp. Cell Res.* **156:**405–418.

Biemont, M.C., Laurent, C., Couturier, J., and Dutrillaux, B., 1978, Chronologie de la réplication des bandes des chromosomes sexuels dans les lymphocytes de sujets normaux et anormaux, *Ann. Génét.* **21:**133–141.

Bjursell, G., and Reichard, P., 1973, Effects of thymidine on deoxyribonucleoside triphosphate pools and deoxyribonucleic acid synthesis in chinese hamster ovary cells, *J. Biol. Chem.* **248:**3904–3909.

Bontemps, J., Houssier, C., and Fredericq, E., 1975, Physico-chemical study of the complexes of "33258 Hoechst" with DNA and nucleohistone, *Nucleic Acids Res.* **2:**971–984.

Bootsma, D., Budke, L., and Vos, O., 1964, Studies on synchronous division of tissue culture cells initiated by excess thymidine, *Exp. Cell Res.* **33:**301–309.

Brown, C.J., Lafrenière, R.G., Powers, V.E., Sebastio, G., Ballabio, A., Pettigrew, A.L., Ledbetter, D.H., Levy, E., Craig, I.W., and Willard, H.F., 1991, Localization of the X inactivation centre on the human X chromosome in Xq13, *Nature* **349:**82–84.

Burkholder, G.D., 1978, Reciprocal Giemsa staining of late DNA replicating regions produced by low and high pH sodium phosphate, *Exp. Cell Res.* **111:**489–492.

Burkholder, G.D., 1979, An investigation of the mechanism of the reciprocal differential staining of BUdR-substituted and unsubstituted chromosome regions, *Exp. Cell Res.* **121:**209–219.

Burkholder, G.D., 1982, The mechanisms responsible for reciprocal BrdU-Giemsa staining, *Exp. Cell Res.* **141:**127–137.

Burkholder, G.D., Latimer, L.J.P., and Lee, J.S., 1988, Immunofluorescent staining of mammalian nuclei and chromosomes with a monoclonal antibody to triplex DNA, *Chromosoma* **97:**185–192.

Buys, C.H.C.M., and Osinga, J., 1981, The role of chromosomal proteins in the induction of a differential staining of sister chromatids by light, *Histochem. J.* **13:**735–746.

Buys, C.H.C.M., and Stienstra, S., 1980, Involvement of sulfhydryl groups of chromosomal proteins in sister chromatid differentiation, *Chromosoma* **77:**325–332.

Buys, C.H.C.M., and van der Veen, A.Y., 1982, Different effects of 33258 Hoechst and DAPI in fluorescent staining of sister chromatids differentially substituted with bromodeoxyuridine, *Histochemistry* **75:**169–177.

Buys, C.H.C.M., Osinga, J., and Stienstra, S., 1981, Rapid irradiation procedure for obtaining permanent differential staining of sister chromatids and aspects of its underlying mechanism, *Hum. Genet.* **57:**35–38.

Buys, C.H.C.M., Osinga, J., and van der Veen, A.Y., 1982, Effects on chromosomal proteins in sister chromatid differentiation by incorporation of 5-bromodeoxyuridine into DNA, *Exp. Cell Res.* **137:**452–455.

Buys, C.H.C.M., Mesa, J., van der Veen, A.Y., and Aten, J.A., 1986, A comparison of the effect of 5–bromodeoxyuridine substitution on 33258 Hoechst- and DAPI-fluorescence of isolated chromosomes by bivariate flow karyotyping, *Histochemistry* **84:**462–470.

Camargo, M., and Cervenka, J., 1980, Pattern of chromosomal replication in synchronized lymphocytes I. Evaluation and application of methotrexate block, *Hum. Genet.* **54:**47–53.

Camargo, M., and Cervenka, J., 1982, Patterns of DNA replication of human chromosomes. II. Replication map and replication model, *Am. J. Hum. Genet.* **34:**757–780.

Carnevali, F., and Mariotti, D., 1977, Variations in the length of S-phase related to the time cells are blocked at the G_1-S interface, *Chromosoma* **63:**33–37.

Cave, M.D., 1966a, Reverse patterns of thymidine-H^3 incorporation in human chromosomes, *Hereditas* **54:**338–355.

Cave, M.D, 1966b, Incorporation of tritium-labeled thymidine and lysine into chromosomes of cultured human leukocytes, *J. Cell Biol.* **29:**209–222.

Cawood, A.H., and Savage, J.R.K., 1985, Uninterrupted DNA synthesis during S-phase in untransformed diploid hamster fibroblasts, *Chromosoma* **91:**164–166.

Chen, J.F., and Lin, Y.J., 1985, Improved light sources for induction of sister chromatid differentiation, *Cytobios* **44:**73–87.

Cohen, S.S., Flaks, J.G., Barner, H.D., Loeb, M.R, and Lichtenstein, J., 1958, The mode of action of 5-fluorouracil and its derivatives, *Proc. Natl. Acad. Sci. USA* **44:**1004–1012.

Comings, D.E., 1970, Quantitative autoradiography of heterochromatin replication in Microtus agrestis, *Chromosoma* **29:**434–445.

Comings, D.E., 1975a, Mechanisms of chromosome banding. IV. Optical properties of the Giemsa dyes, *Chromosoma* **50:**89–110.

Comings, D.E., 1975b, Mechanisms of chromosome banding. VIII. Hoechst 33258-DNA interaction. *Chromosoma* **52:**229–243.

Cortés, F., and Andersson, H.C., 1987, Analysis of SCEs in Vicia faba chromosomes by a simple fluorescent plus Giemsa technique, *Hereditas* **107:**7–13.

Couturier, J., Dutrillaux, B., and Lejeune, J., 1973, Etude de fluorescences spécifiques des bandes R et des bandes Q des chromosomes humains, *C.R. Séances Acad. Sci. (Paris) D* **276:**339–342.

Cuny, G., Soriano, P., Macaya, G., and Bernardi, G., 1981, The major components of the mouse and human genomes 1. Preparation, basic properties and compositional heterogeneity, *Eur. J. Biochem.* **115:**227–233.

David, J., Gordon, J.S., and Rutter, W.J., 1974, Increased thermal stability of chromatin containing 5-bromodeoxyuridine-substituted DNA, *Proc. Natl. Acad. Sci. USA* **71:**2808–2812.

Disney, J.E., Johnson, K.R., Magnuson, N.S., Sylvester, S.R., and Reeves, R., 1989, High-mobility group protein HMG-I localizes to G/Q- and C-bands of human and mouse chromosomes, *J. Cell Biol.* **109:**1975–1982.

Dolbeare, F., Gratzner, H., Pallavicini, M.G., and Gray, J.W., 1983, Flow cytometric measurement of total DNA content and incorporated bromodeoxyuridine, *Proc. Natl. Acad. Sci. USA* **80:**5573–5577.

Drouin, R., and Richer, C.-L., 1985, Analysis of high-resolution R-bands, obtained by heat-denaturation and Giemsa staining, on human prophase chromosomes, *Can. J. Genet. Cytol.* **27:**83–91.

Drouin, R., and Richer, C.-L., 1989, High-resolution R-banding at the 1250-band level. II. Schematic representation and nomenclature of human RBG-banded chromosomes, *Genome* **32:**425–439.

Drouin, R., Lemieux, N., and Richer, C.-L., 1988a, High-resolution R-banding at the 1250-band level I. Technical considerations on cell synchronization and R-banding (RHG and RBG), *Cytobios* **56:**107–125.

Drouin, R., Messier, P.-E., and Richer, C.-L., 1988b, Human chromosome banding specific for electron microscopy, *Cytogenet. Cell Genet.* **47:**117–120.

Drouin, R., Messier, P.-E., and Richer, C.-L., 1989a, Dynamic G- and R-banding of human chromosomes for electron microscopy, *Chromosoma* **98:**40–48.

Drouin, R., Messier, P.-E., and Richer, C.-L., 1989b, DNA denaturation for ultrastructural banding and the mechanism underlying the fluorochrome-photolysis-Giemsa technique studied with anti-5-bromodeoxyuridine antibodies, *Chromosoma* **98:**174–180.

Drouin, R., Lemieux, N., and Richer, C.-L., 1990, Analysis of DNA replication during S-phase by means of dynamic chromosome banding at high resolution, *Chromosoma* **99:**273–280.

Drouin, R., Lemieux, N., and Richer, C.-L., 1991a, High-resolution R-banding at the 1250-band level. III. Comparative analysis of morphologic and dynamic R-band patterns (RHG and RBG), *Hereditas* **114:**65–77.

Drouin, R., Lemieux, N., and Richer, C.-L., 1991b, Chromosome condensation from prophase to late metaphase: Relationship to chromosome bands and their replication time, *Cytogenet. Cell Genet.* **57:**91–99.

Dutrillaux, B., 1973a, Chromosomal aspects of human male sterility, in: *Proc. 23rd Nobel Symposium*, Stockholm, (September 25–27, 1972), Nobel Foundation, pp. 205–208, Stockholm and Academic Press, New York.

Dutrillaux, B., 1973b, Nouveau système de marquage chromosomique: Les bandes T, *Chromosoma* **41:**395–402.

Dutrillaux, B., 1975a, Traitements discontinus par le BrdU et coloration par l'acridine orange: obtention de marquages R, Q et intermédiaires, *Chromosoma* **52:**261–273.

Dutrillaux, B., 1975b, Obtention simultanée de plusieurs marquages chromosomiques sur les mêmes préparations, après traitement par le BrdU, *Humangenetik* **30:**297–306.

Dutrillaux, B., 1977, The relationship between DNA replication and chromosome structure, *Hum. Genet.* **35:**247–253.

Dutrillaux, B., and Covic, M., 1974, Etude de facteurs influençant la dénaturation thermique ménagée des chromosomes, *Exp. Cell Res.* **85:**143–153.

Dutrillaux, B., and Fosse, A.-M., 1974, Sur le mécanisme de la segmentation chromosomique induite par le BUDR (5-bromodeoxyuridine), *Ann. Génét.* **17:**207–211.

Dutrillaux, B., and Fosse, A.-M., 1976, Utilisation du BrdU dans l'étude du cycle cellulaire de sujets normaux et anormaux, *Ann. Génét.* **19:**95–102.

Dutrillaux, B., and Lejeune, J., 1971, Sur une nouvelle technique d'analyse du caryotype humain, *C. R. Séances Acad. Sci. (Paris) D* **272:**2638–2640.

Dutrillaux, B., and Viegas-Péquignot, E., 1981, High resolution R- and G-banding on the same preparation, *Hum. Genet.* **57:**93–95.

Dutrillaux, B., Laurent, C., Couturier, J., and Lejeune, J., 1973, Coloration des chromosomes humains par l'acridine orange après traitement par le 5-bromodéoxyuridine, *C. R. Séances Acad. Sci. (Paris) D* **276:**3179–3181.

Dutrillaux, B., Couturier, J., Richer, C.-L., and Viegas-Péquignot, E., 1976, Sequence of DNA replication in 277 R- and Q-bands of human chromosomes using a BrdU treatment, *Chromosoma* **58:**51–61.

Dutrillaux, B., Muleris, M., and Gerbault Seureau, M., 1986, Imbalance of sex chromosomes, with gain of early-replicating X, in human solid tumors, *Int. J. Cancer* **38:**475–479.

Eiberg, H., 1973, G, R and C banding patterns of human chromosomes produced by heat treatment in organic and inorganic salt solutions, *Clin. Genet.* **4:**556–562.

Eidinoff, M.L., and Rich, M.A., 1959, Growth inhibition of a human tumor cell strain by 5-fluoro-2′-deoxyuridine: Time parameters for subsequent reversal by thymidine, *Cancer Res.* **19:**521–524.

Elejalde, B.R., Pleyte, K., and Mercedes de Elejalde, M., 1984, The use of mercaptoethanol to obtain high-resolution RBG-banded chromosomes and a more successful chromosome analysis in humans, *Rev. Brasil. Genet. VII* **4:**767–775.

Ellison, J., Passage, M., Yu, L-C., Yen, P., Mohandas, T.K., and Shapiro, L., 1992, Directed isolation of human genes that escape X inactivation, *Somat. Cell Mol. Genet.* **18:**259–268.

Emanuel, B.S., 1978, Compound lateral asymmetry in human chromosome 6: BrdU-dye studies of 6q12→6q14, *Am. J. Hum. Genet.* **30:**153–159.

Epplen, J.T., and Vogel, W., 1975, DNA replication patterns of human C group chromosomes from fibroblasts and amniotic fluid cells revealed by a Giemsa staining technique, *Humangenetik* **30:**337–339.

Epplen, J.T., Siebers, J.-W., and Vogel, W., 1975, DNA replication patterns of human chromosomes from fibroblasts and amniotic fluid cells revealed by a Giemsa staining technique, *Cytogenet. Cell Genet.* **15:**177–185.

Epplen, J.T., Bauknecht, T., and Vogel, W., 1976, DNA replication patterns of the early S phase from amniotic fluid cells as revealed by a Giemsa staining technique, *Hum. Genet.* **31:**117–119.

Fasy, T.M., Cullen, B.R., Luk, D., and Bick, M.D., 1980, Studies on the enhanced interaction of halodeoxyuridine-substituted DNAs with H1 histones and other polypeptides, *J. Biol. Chem.* **255:**1380–1387.

Fetni, R., Drouin, R., Lemieux, N., Messier, P.-E., and Richer, C.- L., 1991, Simultaneous visualization of chromosome bands and hybridization signal using colloidal-gold labeling in electron microscopy, *Proc. Natl. Acad. Sci. USA* **88:**10916–10920.

Fetni, R., Lemieux, N., Malfoy, B., Dutrillaux, B., Messier, P.-E., and Richer, C.-L., 1992, Detection of small, single-copy genes on protein-G-banded chromosomes by electron microscopy, *Cytogenet. Cell Genet.* **60:**187–189.

Fetni, R., Drouin, R., Richer, C.-L., and Lemieux, N., 1995, Complementary R- and G-band patterns after dynamic banding by blocking the cells at the R-band/G-band transition, *Submitted.*

Fisher, E.M.C., Beer-Romero, P., Brown, L.G., Ridley, A., McNeil, J.A., Bentley Lawrence, J., Willard, H.F., Bieber, F.R., and Page, D.C., 1990, Homologous ribosomal protein genes on the human X and Y chromosomes: Escape from X inactivation and possible implications for Turner syndrome, *Cell* **63:**1205–1218.

Flamm, W.G., McCallum, M., and Walker, P.M.B., 1967, The isolation of complementary strands from a mouse DNA fraction, *Proc. Natl. Acad. Sci. USA* **57:**1729–1734.

Fox, M.H., Arndt-Jovin, D.J., Jovin, T.M., Baumann, P.H., and Robert-Nicoud, M., 1991, Spatial and temporal distribution of DNA replication sites localized by immunofluorescence and confocal microscopy in mouse fibroblasts, *J. Cell Sci.* **99:**247–253.

Gagné, R., 1980, Obtention des bandes "R" par incorporation de BUDR et coloration par le Hoescht 33258 et le Giemsa, *Union Méd. Canada* **109:**552–556.

Galloway, S.M., and Evans, H.J., 1975, Asymmetrical C-bands and satellite DNA in man, *Exp. Cell Res.* **94:**454–459.

Gantt, R., Jones, G.M., Stephens, E.V., Baeck, A.E., and Sanford, K.K., 1979, Visible light-induced DNA crosslinks in cultured mouse and human cells, *Biochim. Biophys. Acta* **565:**231–240.

Gentry, G.A., Morse, P.A., and van Potter, R., 1965, Pyrimidine metabolism in tissue culture cells derived from rat hepatomas. III. Relationship of thymidine to the metabolism of other pyrimidine nucleosides in suspension cultures derived from the Novikoff hepatoma, *Cancer Res.* **25:**517–525.

Ghosh, P.K., Rani, R., and Nand, R., 1979, Lateral asymmetry of constitutive heterochromatin in human chromosomes, *Hum. Genet.* **52:**79–84.

Gibas, Z., and Limon, J., 1978, Isolabeling of the long arm of the human Y chromosome demonstrated by the FPG technique, *Chromosoma* **69:**113–120.

Goldman, M.A., 1988, The chromatin domain as a unit of gene regulation, *BioEssays* **9:**50–55.

González-Gil, G., and Navarrete, M.H., 1982, On the mechanism of differential Giemsa staining of BrdU-substituted chromatids, *Chromosoma* **86:**375–382.

Gordon, J.S., Bell, G.I., Martinson, H.C., and Rutter, W.J., 1976, Selective interaction of 5′-bromodeoxyuridine substituted DNA with different chromosomal proteins, *Biochemistry* **15:**4778–4786.

Goto, K., Akematsu, T., Shimazu, H., and Sugiyama, T., 1975, Simple differential Giemsa staining of sister chromatids after treatment with photosensitive dyes and exposure to light and the mechanism of staining, *Chromosoma* **53:**223–230.

Goto, K., Maeda, S., Kano, Y., and Sugiyama, T., 1978, Factors involved in differential Giemsa-staining of sister chromatids, *Chromosoma* **66:**351–359.

Goyanes, V.J., and Mendez, J., 1981, Karyotyping chromosomes by electron microscopy. Condensation-inhibition of G bands in human and chinese hamster chromosomes by a BrdU-Hoechst 33258 treatment. *Cancer Genet. Cytogenet.* **4:**45–51.

Gratzner, H.G., 1982, Monoclonal antibody to 5-bromo- and 5-iododeoxyuridine: a new reagent for detection of DNA replication, *Science* **218:**474–475.

Grzeschik, K.-H., Kim, M.A., and Johannsmann, R., 1975, Late replicating bands of human chromosomes demonstrated by fluorochrome and Giemsa staining, *Humangenetik* **29:**41–59.

Guo, X.-C., Morgan, W.F., and Cleaver, J.E., 1986, Hoechst 33258 dye generates DNA-protein cross-links during ultraviolet light-induced photolysis of bromodeoxyuridine in replicated and repaired DNA, *Photochem. Photobiol.* **44:**131–136.

Hameister, H., and Sperling, K., 1984, Description of a chromosome replication unit in individual prematurely condensed human S-phase chromosomes, *Chromosoma* **90:**389–393.

Han, A., Korbelik, M., and Ban, J., 1975, DNA-to-protein cross-linking in synchronized HeLa cells exposed to ultra-violet light, *Int. J. Radiat. Biol.* **27:**63–74.

Hancock, J.M., and Sumner, A.T., 1982, The role of proteins in the production of different types of chromosome bands, *Cytobios* **35:**37–46.

Hand, R., 1978, Eucaryotic DNA: Organization of the genome for replication, *Cell* **15:**317–325.

Härd, T., Fan, P., and Kearns, D.R., 1990, A fluorescence study of the binding of Hoechst 33258 and DAPI to halogenated DNAs, *Photochem. Photobiol.* **51:**77–86.

Harshman, K.D., and Dervan, P.B., 1985, Molecular recognition of B-DNA by Hoechst 33258, *Nucleic Acids Res.* **13:**4825–4835.

Hartmann, K.-U., and Heidelberger, C., 1961, Studies on fluorinated pyrimidines XIII. Inhibition of thymidylate synthetase, *J. Biol. Chem.* **236:**3006–3013.

Heidelberger, C., 1975, Fluorinated pyrimidines and their nucleosides, in: *Handbook of Experimental Pharmacology* (A.C. Sartorelli and D.G. Johns, eds.), pp. 193–231, Springer-Verlag, New York.

Holmquist, G.P., 1987, Role of replication time in the control of tissue-specific gene expression, *Am. J. Hum. Genet.* **40:**151–173.

Holmquist, G., 1988, DNA sequences in G-bands and R-bands, in: *Chromosomes and chromatin*, Volume II (K.W. Adolph, ed.), pp. 75–121, CRC Press, Boca Raton, Florida.

Holmquist, G.P., 1989, Evolution of chromosome bands: Molecular ecology of noncoding DNA, *J. Mol. Evol.* **28:**469–486.

Holmquist, G.P., 1990a, Mutational bias, molecular ecology, and chromosome evolution, in: *Advances in Mutagenesis Research*, Volume 2 (G. Obe, ed.), pp. 95–126, Springer-Verlag, New York.

Holmquist, G.P., 1990b, DNA sequences in G- and R-bands: Evolution and Molecular Ecology, in: *Chromosomes Today*, Volume 10 (K. Fredga, B.A. Kihlman, and M.D. Bennett, eds.), pp. 21–32, Unwin Hyman, London.

Holmquist, G.P., 1990*c*, Contents of G- and R-bands defy contemporary paradigms, in: *Trends in Chromosome Research* (T. Sharma, ed.), pp. 39–52, Springer-Verlag, New York.

Holmquist, G.P., 1992, Chromosome bands, their chromatin flavors, and their functional features, *Am. J. Hum. Genet.* **51:**17–37.

Holmquist, G.P., and Motara, M.A., 1987, The magic of cytogenetic technology, in: *Cytogenetics: Basic and Applied Aspects* (G. Obe and A. Basler, eds.), pp. 30–47, Springer-Verlag, New York.

Holmquist, G, Gray, M., Porter, T., and Jordan, J., 1982, Characterization of Giemsa dark- and light-band DNA, *Cell* **31:**121–129.

Hsu, T.C., 1964, Mammalian chromosomes in vitro XVIII. DNA replication sequence in the Chinese hamster, *J. Cell Biol.* **23:**53–62.

Human Gene Mapping 11 (1991), 1991, *Cytogenet. Cell Genet.* **58:**1–2200.

Hutchinson, F., 1973, The lesions produced by ultraviolet light in DNA containing 5-bromouracil, *Quart. Rev. Biophys.* **6:**201–246.

Hutchinson, F., and Köhnlein, W., 1980, The photochemistry of 5-bromouracil and 5-iodouracil in DNA, *Prog. Mol. Subcell. Biol.* **7:**1–42.

Ieshima, A, Yorita, T., and Takeshita, K., 1984, A simple R-banding technique by BrdU-Hoechst

treatment and Giemsa staining following heating and ultraviolet exposure, *Jpn. J. Hum. Genet.* **29:**133–138.

ISCN (1985): An International System for Human Cytogenetic Nomenclature (D.G. Harden and H.P. Klinger, eds.), published in collaboration with *Cytogenet. Cell Genet.* (Karger, Basel, 1985).

Izumikawa, Y., Naritomi, K., and Hirayama, K., 1991, Replication asynchrony between homologs 15q11.2: Cytogenetic evidence for genomic imprinting, *Hum. Genet.* **87:**1–5.

Jack, E.M., Harrison, C.J., White, G.R.M., Ockey, C.H., and Allen, T.D., 1989, Fine-structural aspects of bromodeoxyuridine incorporation in sister chromatid differentiation and replication banding, *J. Cell Sci.* **94:**287–297.

Jan, K.Y., Yang, J.L., and Su, P.F., 1984, DNA lysis is involved in the simplified fluorescence plus Giemsa method for differential staining of sister chromatids, *Chromosoma* **89:**76–78.

Jan, K.Y., Su, P.-F., and Lee, T.-C., 1985, Reverse differential staining of sister chromatids induced by Hoechst plus black light and endonuclease, *Exp. Cell Res.* **157:**307–314.

Jeppesen, P., and Turner, B., 1992, Immunofluorescence of metaphase chromosomes demonstrates underacetylation of histone H4 in the inactive X-chromosome and other non-transcribed regions, *Proceedings of the 11th International Chromosome Conference* (August 1992), Edinburgh, Scotland, p. 16.

Jorgenson, K.F., Varshney, U., and van de Sande, J.H., 1988, Interaction of Hoechst 33258 with repeating synthetic DNA polymers and natural DNA, *J. Biomol. Struct. Dyn.* **5:**1005–1023.

Kaluzewski, B., 1982, BrdU-Hoechst-Giemsa analysis of DNA replication in synchronized lymphocyte cultures. Study of human X and Y chromosomes, *Chromosoma* **85:**553–569.

Karube, T., and Watanabe, S., 1988, Analysis of the chromosomal DNA replication pattern using the bromodeoxyuridine labeling method, *Cancer Res.* **48:**219–222.

Kim, M.A., Johannsmann, R., and Grzeschik, K.-H., 1975, Giemsa staining of the sites replicating DNA early in human lymphocyte chromosomes, *Cytogenet. Cell Genet.* **15:**363–371.

Kimura, S., Yamazaki, K., and Kato, Y., 1980, Kinetics of DNA replication in the indian muntjac chromosomes as studied by quantitative autoradiography, *Chromosoma* **77:**309–323.

Kitsberg, D., Selig, S., Brandeis, M., Simon, I., Keshet, I., Driscoll, D.J., Nicholls, R.D., and Cedar, H., 1993, Allele-specific replication timing of imprinted gene regions, *Nature* **364:** 459–463.

Klevecz, R.R., Keniston, B.A., and Deaven, L.L., 1975, The temporal structure of S phase, *Cell* **5:**195–203.

Knoll, J.H.M., Cheng, S.-D., and Lalande, M., 1994, Allele specificity of DNA replication timing in the Angelman/Prader-Willi syndrome imprinted chromosomal region, *Nature Genet.* **6:**41–46.

Kondra, P.M., and Ray, M., 1978, Analysis of DNA replication patterns of human fibroblast chromosomes. The replication map, *Hum. Genet.* **43:**139–149.

Korenberg, J.R., and Freedlender, E.F., 1974, Giemsa technique for the detection of sister chromatid exchanges, *Chromosoma* **48:**355–360.

Kornhauser, A., 1976, UV induced DNA-protein cross-links in vitro and in vivo, *Photochem. Photobiol.* **23:**457–460.

Krasin, F., and Hutchinson, F., 1978, Double-strand breaks from single photochemical events in DNA containing 5-bromouracil, *Biophys. J.* **24:**645–656.

Kuroiwa, T., 1971, Asynchronous condensation of chromosomes from early prophase to late prophase as revealed by electron microscopic autoradiography, *Exp. Cell Res.* **69:**97–105.

Lapeyre, J.-N., and Bekhor, I., 1974, Effects of 5-bromo-2′-deoxyuridine and dimethyl sulfoxide on properties and structure of chromatin, *J. Mol. Biol.* **89:**137–162.

Latos-Bielenska, A., Hameister, H., and Vogel, W., 1987, Detection of BrdUrd incorporation in mammalian chromosomes by a BrdUrd antibody. III. Demonstration of replication patterns in highly resolved chromosomes, *Hum. Genet.* **76:**293–295.

Latt, S.A., 1973, Microfluorometric detection of deoxyribonucleic acid replication in human metaphase chromosomes, *Proc. Natl. Acad. Sci. USA* **70:**3395–3399.

Latt, S.A., 1974, Microfluorometric analysis of deoxyribonucleic acid replication kinetics and sister chromatid exchanges in human chromosomes, *J. Histochem. Cytochem.* **22:**478–491.

Latt, S.A., 1975, Fluorescence analysis of late DNA replication in human metaphase chromosomes, *Somatic Cell Genet.* **1:**293–321.

Latt, S.A., and Wohlleb, J.C., 1975, Optical studies of the interaction of 33258 Hoechst with DNA, chromatin, and metaphase chromosomes, *Chromosoma* **52:**297–316.

Latt, S.A., Davidson, R.L., Lin, M.S., and Gerald, P.S., 1974, Lateral asymmetry in the fluorescence of human Y chromosomes stained with 33258 Hoechst, *Exp. Cell Res.* **87:**425–429.

Latt, S.A., Willard, H.F., and Gerald, P.S., 1976, BrdU-33258 Hoechst analysis of DNA replication in human lymphocytes with supernumerary or structurally abnormal X chromosomes, *Chromosoma* **57:**135–153.

Latt, S.A., Barell, E.F., Dougherty, C.P., and Lazarus, H., 1981, Patterns of late replication in X chromosomes of human lymphoid cells, *Cancer Genet. Cytogenet.* **3:**171–181.

Lemieux, N., and Richer, C.-L., 1989, Synchronization of cultured retinoblastoma cells for high-resolution chromosomes showing up to 1000 bands, *Cancer Genet. Cytogenet.* **40:**55–63.

Lemieux, N., and Richer, C.-L., 1990, Chromosome evolution and high-resolution analysis of leucocytes, bone marrow, and tumor cells of retinoblastoma patients, *Am. J. Med. Genet.* **36:** 456–462.

Lemieux, N., Richer, C.-L., and Jean, P., 1987, Combined myeloid cell synchronization and chromosome G-banding by bromodeoxyuridine, *Cancer Genet. Cytogenet.* **28:**229–236.

Lemieux, N., Milot, J., Barsoum-Homsy, M., Michaud, J., Leung, T.-K., and Richer, C.-L., 1989, First cytogenetic evidence of homozygosity for the retinoblastoma deletion in chromosomes 13, *Cancer Genet. Cytogenet.* **43:**73–78.

Lemieux, N., Drouin, R., and Richer, C.-L., 1990, High-resolution dynamic and morphological G-bands (GBG and GTG): A comparative study, *Hum. Genet.* **85:**261–266.

Lemieux, N., Dutrillaux, B., and Viegas-Péquignot, E., 1992, A simple method for simultaneous R- or G-banding and fluorescence in situ hybridization of small single-copy genes, *Cytogenet. Cell Genet.* **59:**311–312.

Limoli, C.L., and Ward J.F., 1993, A new method for introducing double-strand breaks into cellular DNA, *Radiation Res.* **134:**160–169.

Lin, M.S., and Alfi, O.S., 1978, Variation in lateral asymmetry of human chromosome 1, *Cytogenet. Cell Genet.* **21:**243–250.

Lin, S., and Riggs, A.D., 1974, Photochemical attachment of lac repressor to bromodeoxyuridine-substituted lac operator by ultraviolet irradiation, *Proc. Natl. Acad. Sci. USA* **71:**947–951.

Lin, M.S., Latt, S.A., and Davidson, R.L., 1974, Microfluorometric detection of asymmetry in the centromeric region of mouse chromosomes, *Exp. Cell Res.* **86:**392–395.

Lin, M.S., Alfi, O.S., and Donnell, G.N., 1976a, Differential fluorescence of sister chromatids with 4′-6-diamidino-2-phenylindole, *Can. J. Genet. Cytol.* **18:**545–547.

Lin, S., Lin, D., and Riggs, A.D., 1976b, Histones bind more tightly to bromodeoxyuridine-substituted DNA than to normal DNA, *Nucleic Acids Res.* **3:**2183–2190.

Lin, C.C., Draper, P.N., and De Braekeleer, M., 1985, High-resolution chromosomal localization of the β-gene of the human β-globin gene complex by in situ hybridization, *Cytogenet. Cell Genet.* **39:**269–274.

Magaud, J.-P., Rimokh, R., Brochier, J., Lafage, M., and Germain, D., 1985, Chromosomal R-banding with a monoclonal antidouble-stranded DNA antibody, *Hum. Genet.* **69:**238–242.

Manuelidis, L., and Chen, T.L., 1990, A unified model of eukaryotic chromosomes, *Cytometry* **11:**8–25.

Martin, R.F., and Holmes, N., 1983, Use of an ^{125}I-labelled DNA ligand to probe DNA structure, *Nature* **302:**452–454.

Martinson, H.G., Shetlar, M.D., and McCarthy, B.J., 1976, Histone-histone interactions within chromatin. Cross-linking studies using ultraviolet light, *Biochemistry* **15:**2002–2007.

Matthes, E., Fenske, H., Eichhorn, I., Langen, P., and Lindigkeit, R., 1977, Altered histone-DNA interactions in rat liver chromatin containing 5-bromodeoxyuridine-substituted DNA, *Cell Differentiation* **6:**241–251.

Medrano, L., Bernardi, G., Couturier, J., Dutrillaux, B., and Bernardi, G., 1988, Chromosome banding and genome compartmentalization in fishes, *Chromosoma* **96:**178–183.

Meer, B., Hameister, H., and Cerrillo, M., 1981, Early and late replication patterns of increased resolution in human lymphocyte chromosomes, *Chromosoma* **82:**315–319.

Messier, P.-E., Drouin, R., and Richer, C.-L., 1989, Electron microscopy of gold-labeled human and equine chromosomes, *J. Histochem. Cytochem.* **37:**1443–1447.

Meuth, M., and Green, H., 1974, Induction of a deoxycytidineless state in cultured mammalian cells by bromodeoxyuridine, *Cell* **2:**109–112.

Mezzanotte, R., Rossino, R., Orru, S., Mameli, M., and Peretti, D., 1989a, Nuclease activity in human metaphase chromosomes substituted with 5′-bromodeoxyuridine, *Chromosoma* **97:**334–338.

Mezzanotte, R., Peretti, D., Orru, S., Rossino, R., Ennas, M.G., and Gosalvez, J., 1989b, DNA alteration induced by ultraviolet light in human metaphase chromosomes substituted with 5′-bromodeoxyuridine: Monitoring by monoclonal antibodies to double-stranded and single-stranded DNA, *Chromosoma* **97:**356–362.

Mikhailov, M.V., Zasedatelev, A.S., Krylov, A.S., and Gurskii, G.V., 1981, Mechanism of the recognition of AT base pairs in DNA by molecules of the dye Hoechst 33258, *Mol. Biol.* (USSR, Engl. trans.) **15:**541–554.

Miller, O.J., Schnedl, W., Allen, J., and Erlanger, B.F., 1974, 5-Methylcytosine localised in mammalian constitutive heterochromatin, *Nature* **251:**636–637.

Miller, M.R., Heyneman, C., Walker, S., and Ulrich, R.G., 1986, Interaction of monoclonal antibodies directed against bromodeoxyuridine with pyrimidine bases, nucleosides, and DNA, *J. Immunol.* **136:**1791–1795.

Moran, R., Darzynkiewicz, Z., Staiano-Coico, L., and Melamed, M.R., 1985, Detection of 5-bromodeoxyuridine (BrdUrd) incorporation by monoclonal antibodies: Role of the DNA denaturation step, *J. Histochem. Cytochem.* **33:**821–827.

Morris, N.R., and Fischer, G.A., 1963, Studies concerning the inhibition of cellular reproduction by deoxyribonucleosides I. Inhibition of the synthesis of deoxycytidine by a phosphorylated derivative of thymidine, *Biochim. Biophys. Acta* **68:**84–92.

Morris, N.R., Reichard, P., and Fischer, G.A., 1963, Studies concerning the inhibition of cellular reproduction by deoxyribonucleosides II. Inhibition of the synthesis of deoxycytidine by thymidine, deoxyadenosine and deoxyguanosine, *Biochim. Biophys. Acta* **68:**93–99.

Morstyn, G., Hsu, S.-M., Kinsella, T., Gratzner, H., Russo, A., and Mitchell, J.B., 1983, Bromodeoxyuridine in tumors and chromosomes detected with a monoclonal antibody, *J. Clin. Invest.* **72:**1844–1850.

Muleris, M., Salmon, R.J., and Dutrillaux, B., 1986, Chromosomal study demonstrating the clonal evolution and metastatic origin of a metachronous colorectal carcinoma, *Int. J. Cancer* **38:** 167–172.

Muleris, M., Dutrillaux, A.-M., Lombard, M., and Dutrillaux, B., 1987a, Noninvolvement of a constitutional heritable fragile site at 10q24.2 in rearranged chromosomes from rectal carcinoma cells, *Cancer Genet. Cytogenet.* **25:**7–13.

Muleris, M., Salmon, R.-J., Dutrillaux, A.-M., Vielh, P., Zafrani, B., Girodet, J., and Dutrillaux, B., 1987b, Characteristic chromosomal imbalances in 18 near-diploid colorectal tumors, *Cancer Genet. Cytogenet.* **29:**289–301.

Muleris, M., Salmon, R.-J., Girodet, J., Zafrani, B., and Dutrillaux, B., 1987*c*, Recurrent deletions of chromosomes 11q and 3p in anal canal carcinoma, *Int. J. Cancer* **39:**595–598.

Müller, W., and Gautier, F., 1975, Interactions of heteroaromatic compounds with nucleic acids. A-T specific non-intercalating DNA ligands, *Eur. J. Biochem.* **54:**385–394.

Müller, U., and Schempp, W., 1982, Homologous early replication patterns of the distal short arms of prometaphasic X and Y chromosomes, *Hum. Genet.* **60:**274–275.

Myllyharju, J., and Nokkala, S., 1992, The role of glycosylated nonhistone proteins in chinese hamster metaphase chromosome structure, *Proceedings of the 11th International Chromosome Conference* (August 1992), Edinburgh, Scotland, p. 17.

Nakagome, Y., 1977, Initiation of DNA replication in human chromosomes, *Exp. Cell Res.* **106:** 457–461.

Nakamura, H., Morita, T., and Sato, C., 1986, Structural organizations of replicon domains during DNA synthetic phase in the mammalian nucleus, *Exp. Cell Res.* **165:**291–297.

Nakayasu, H., and Berezney, R., 1989, Mapping replicational sites in the eucaryotic cell nucleus, *J. Cell Biol.* **108:**1–11.

Natarajan, A.T., Rotteveel, A.H.M., van Pieterson, J., and Schliermann, M.G., 1986, Influence of incorporated 5-bromodeoxyuridine on the frequencies of spontaneous and induced sister-chromatid exchanges, detected by immunological methods, *Mutat. Res.* **163:**51–55.

Ockey, C.H., 1980, Autoradiographic evidence of differential loss of BUdR-substituted DNA after UV exposure in FPG harlequin staining, *Exp. Cell Res.* **125:**511–514.

Okamoto, E., Miller, D.A., Erlanger, B.F., and Miller, O.J., 1981, Polymorphism of 5-methylcytosine-rich DNA in human acrocentric chromosomes, *Hum. Genet.* **58:**255–259.

O'Keefe, R.T., Henderson, S.C., and Spector, D.L., 1992, Dynamic organization of DNA replication in mammalian cell nuclei: Spatially and temporally defined replication of chromosome-specific alpha-satellite DNA sequences, *J. Cell Biol.* **116:**1095–1110.

Pai, G.S., and Thomas, G.H., 1980, A new R-banding technique in clinical cytogenetics, *Hum. Genet.* **54:**41–45.

Painter, R.B., 1982, A replication model for sister chromatid exchange, in: *Sister chromatid exchange, Progress and Topics in cytogenetics*, Volume 2 (A.A. Sandberg, ed.), pp. 115–121, Alan R. Riss, New York.

Pardue, M.L., and Gall, J.G., 1970, Chromosomal localization of mouse satellite DNA, *Science* **168:**1356–1358.

Perry, P., and Wolff, S., 1974, New Giemsa method for the differential staining of sister chromatids, *Nature* **251:**156–158.

Petersen, A.J., 1964, DNA synthesis and chromsomal asynchrony, *J. Cell Biol.* **23:**651–654.

Pinkel, D., Thompson, L.H., Gray, J.W., and Vanderlaan, M., 1985, Measurement of sister chromatid exchanges at very low bromodeoxyuridine substitution levels using a monoclonal antibody in chinese hamster ovary cells, *Cancer Res.* **45:**5795–5798.

Pjura, P.E., Grzeskowiak, K., and Dickerson, R.E., 1987, Binding of Hoechst 33258 to the minor groove of B-DNA, *J. Mol. Biol.* **197:**257–271.

Priest, J.H., Heady, J.E., and Priest, R.E., 1967, Synchronization of human diploid cells by fluorodeoxyuridine. The first ten minutes of synthesis in female cells, *J. Natl. Cancer Inst.* **38:** 61–72.

Prieur, M., Dutrillaux, B., and Lejeune, J., 1973, Planches descriptives des chromosomes humains (Analyse en bandes R et nomenclature selon la Conférence de Paris 1971), *Ann. Génét.* **16:**39–46.

Qu, J.Y., Dallaire, L., Lemieux, N., Drouin, R., and Richer, C.-L., 1989, Synchronization of amniotic fluid cells for high resolution cytogenetics, *Prenat. Diagn.* **9:**49–56.

Rahn, R.O., and Sellin, H.G., 1992, Hoechst 33258 photosensitization of 5-iododeoxyuridine-substituted DNA to 365 nm light: Dependence of dehalogenation on the dye-to-nucleotide ratio, *Photochem. Photobiol.* **55:**309–312.

Raposa, T., and Natarajan, A.T., 1974, Fluorescence banding pattern of human and mouse chromosomes with a benzimidazol derivative (Hoechst 33258), *Humangenetik* **21:**221–226.

Raza, A., Kempski, M., Preisler, H.D., and Block, A.W., 1985, A permanent method of detecting SCE by immunofluorescence using monoclonal anti-BrdU antibodies, *Cancer Genet. Cytogenet.* **15:**187–189.

Reddy, K.S., Savage, J.R.K., and Papworth, D.G., 1988, Replication kinetics of X chromosomes in fibroblasts and lymphocytes, *Hum. Genet.* **79:**44–48.

Reichard, P., 1988, Interactions between deoxyribonucleotide and DNA synthesis, *Annu. Rev. Biochem.* **57:**349–374.

Richer, C.-L., and Drouin, R., 1990, Dynamic banding for high-resolution analysis of chromosomes and assignment of DNA replication times, in: *Advances in Mutagenesis Research*, Volume 2 (G. Obe, ed.), pp. 55–94, Springer-Verlag, New York.

Richer, C.-L., Murer-Orlando, M., and Drouin, R., 1983a, R-banding of human chromosomes by heat denaturation and Giemsa staining after amethopterin-synchronization, *Can. J. Genet. Cytol.* **25:**261–269.

Richer, C.-L., Drouin, R., Murer-Orlando, M., and Jean, P. 1983b, High-resolution idiogram of Giemsa R-banded human prophase chromosomes, *Can. J. Genet. Cytol.* **25:**642–650.

Richer, C.-L., Senécal-Quevillon, M., and Duquette, P., 1987, Analysis of low concentrations of 5-bromo-2-deoxyuridine on sister chromatid exchanges in human lymphocytes, *Genome* **29:** 165–168.

Romagnano, A., Drouin, R., and Richer, C.-L., 1987, Idiograms of horse chromosomes at prometaphase, early metaphase, and midmetaphase after R-banding by BrdU incorporation followed by the fluorochrome-photolysis-Giemsa technique, *Genome* **29:**674–679.

Rønne, M., 1983, Simultaneous R-banding and localization of dA-dT clusters in human chromosomes, *Hereditas* **98:**241–248.

Rønne, M., 1984a, Fluorouracil synchronization of human lymphocyte cultures. Induction of high resolution R-banding by simultaneous in vitro exposure to 5-bromodeoxyuridine/Hoechst 33258, *Hereditas* **101:**205–208.

Rønne, M., 1984b, Fluorouracil synchronization of human bone marrow cultures. In vitro induction of high resolution R-banding by simultaneous exposure to 5-bromodeoxyuridine/Hoechst 33258, *Anticancer Res.* **4:**279–281.

Rønne, M., 1985, Double synchronization of human lymphocyte cultures: Selection for high-resolution banded metaphases in the first and second division, *Cytogenet. Cell Genet.* **39:** 292–295.

Rønne, M., 1992, Synchronization, banding and in situ hybridization. A short laboratory manual, *In vivo* **6:**49–57.

Rosenstein, B.S., Setlow, R.B., and Ahmed, F.E., 1980, Use of the dye Hoechst 33258 in a modification of the bromodeoxyuridine photolysis technique for the analysis of DNA repair, *Photochem. Photobiol.* **31:**215–222.

Rueckert, R.R., and Mueller, G.C., 1960, Studies on unbalanced growth in tissue culture. I. Induction and consequences of thymidine deficiency, *Cancer Res.* **20:**1584–1591.

Saccone, S., De Sario, A., Wiegant, J., Raap, A.K., Della Valle, G., and Bernardi, G., 1993, Correlations between isochores and chromosomal bands in the human genome, *Proc. Natl. Acad. Sci. USA* **90:**11929–11933.

Safronov, V.V., Ivanova, Z.I., and Makarov, V.B., 1981, Autoradiographical analysis of the molecular mechanism of differential staining of sister chromatids, *Tsitologiia* **23:**94–98.

Sakanishi, S., and Takayama, S., 1977, A simple Giemsa method for the differential staining of sister chromatids with a note on the presumptive mechanism involved, *Proc. Japan Acad.* **53:**143–146.

Sakanishi, S., and Takayama, S., 1978, Reverse differential staining of sister chromatids after substitution with BUdR and incubation in sodium phosphate solution, *Exp. Cell Res.* **115:** 448–451.

Saunders, G.F., 1974, Human repetitious DNA, *Adv. Biol. Med. Phys.* **15:**19–46.

Savage, J.R.K., 1990, Bromodeoxyuridine and chromosome "banding", *Clin. Cytogenet. Bull.* **4**:63–67.

Savage, J.R.K., and Prasad, R., 1988, Generalized blocking in S phase by methotrexate, *Mutat. Res.* **201**:195–201.

Savary, J.B., Vasseur, F., Lai, J.L., Daudignon, A., and Deminatti, M., 1991, Routine cytogenetic prenatal diagnosis using dynamic banding (RBG-GBG): A highly reproducible method for amniocytes, fetal cord blood, and chorionic villus investigations, *Prenat. Diagn.* **11**:883–891.

Savary, J.B., Daudignon, A., Vasseur, F., and Deminatti, M.M., 1992, BrdU related direct revelation of typical dynamic R- and G-banding with the use of monoclonal anti-BrdU antibody, *Ann. Génét.* **35**:27–32.

Scheid, W., 1976, Mechanism of differential staining of BUdR-substituted Vicia faba chromosomes, *Exp. Cell Res.* **101**:55–58.

Schempp, W., 1980, Asynchrony in late replication between homologous autosomes in primary cultures of chinese hamster fibroblasts, *Chromosoma* **79**:199–206.

Schempp, W., and Meer, B., 1983, Cytologic evidence for three human X-chromosomal segments escaping inactivation, *Hum. Genet.* **63**:171–174.

Schempp, W., and Müller, U., 1982, High resolution replication patterns of the human Y chromosome. Intra- and interindividual variation, *Chromosoma* **86**:229–237.

Schempp, W., and Schmid, M., 1981, Chromosome banding in Amphibia VI. BrdU-replication patterns in Anura and demonstration of XX/XY sex chromosomes in *Rana esculenta*, *Chromosoma* **83**:697–710.

Schempp, W., and Vogel, W., 1978, Decrease of DNA synthesis in amniotic fluid cells during the middle part of S-phase revealed by differential chromosome staining after incorporation of BrdU, *Chromosoma* **67**:193–199.

Schempp, W., and Vogel, W., 1979, Difference between diploid and aneuploid chinese hamster cells in replication at mid-S-phase, *Chromosoma* **73**:109–115.

Schempp, W., Sigwarth, I., and Vogel, W., 1978, Demonstration of replication patterns corresponding to G- and R-type banding of chromosomes after partial synchronization of cell cultures with BrdU or dT surplus, *Hum. Genet.* **45**:199–202.

Scheres, J.M.J.C., Merkx, G.F.M., and Hustinx, T.W.J., 1982, Prometaphase banding of human chromosomes with basic fuchsin, *Hum. Genet.* **61**:8–11.

Schiaffonati, L., Tsutsui, Y., Chang, S.-D., and Baserga, R., 1978, Effect of 5-bromodeoxyuridine on deoxyribonucleic acid-protein adducts induced by ultraviolet light on chromatin cells, *Lab. Invest.* **38**:58–66.

Schildkraut, C.L., and Maio, J.J., 1969, Fractions of HeLa DNA differing in their content of guanine and cytosine, *J. Mol. Biol.* **46**:305–312.

Schmid, W., and Leppert, M.F., 1969, Rates of DNA synthesis in heterochromatic and euchromatic segments of the chromosome complements of two rodents, *Cytogenet.* **8**:125–135.

Schmidt, M., 1980, Two phases of DNA replication in human cells, *Chromosoma* **76**:101–110.

Schmidt, M., and Stolzmann, W.M., 1984, Replication variants of the human inactive X chromosome. II. Frequency and replication rate relative to the other chromosomes of the complement, *Chromosoma* **89**:68–75.

Schmidt, M., Stolzmann, W.M., and Baranovskaya, L.I., 1982, Replication variants of the human inactive X chromosome. I. Variability within lymphocytes of single individuals, *Chromosoma* **85**:405–412.

Schollmayer, E., Schäfer, D., Frisch, B., and Schleiermacher, E., 1981, High resolution analysis and differential condensation in RBA-banded human chromosomes, *Hum. Genet.* **59**:187–193.

Schreck, R.R., Erlanger, B.F., and Miller, O.J., 1974, The use of antinucleoside antibodies to probe the organization of chromosomes denatured by ultraviolet irradiation, *Exp. Cell Res.* **88**:31–39.

Schwartz, S.A., 1977, Rat embryo nonhistone chromosomal proteins: Interaction in vitro with normal and bromodeoxyuridine-substituted DNA, *Biochemistry* **16**:4101–4108.

Schwartz, S.A., and Kirsten, W.H., 1974, Distribution of 5-bromodeoxyuridine in the DNA of rat embryo cells, *Proc. Natl. Acad. Sci. USA* **71:**3570–3574.

Schwartz, S., and Palmer, C.G., 1984, High-resolution chromosome analysis: 1. Applications and limitations, *Am. J. Med. Genet.* **19:**291–299.

Schweizer, D., 1977, R-banding produced by DNase I digestion of chromomycin-stained chromosomes, *Chromosoma* **64:**117–124.

Schwemmle, S., Mehnert, K., and Vogel, W., 1989, How does inactivation change timing of replication in the human X chromosome? *Hum. Genet.* **83:**26–32.

Selig, S., Okumura, K., Ward, D.C., and Cedar, H., 1992, Delineation of DNA replication time zones by fluorescence in situ hybridization, *EMBO J.* **11:**1217–1225.

Severin, E., and Ohnemus, B., 1982, UV dose-dependent increase in the Hoechst fluorescence intensity of both normal and BrdU-DNA, *Histochemistry* **74:**279–291.

Shafer, D.A., Selles, W.D., and Brenner, J.F., 1982, Computer image analysis of variance between human chromosome replication sequences and G-bands, *Am. J. Hum. Genet.* **34:**307–321.

Sheldon, S., and Nichols, W.W., 1981, Comparison of the patterns of chromosomal late replication I. Human renal epithelium and lung fibroblasts in vitro, *Cytogenet. Cell Genet.* **29:**40–50.

Shiraishi, Y., and Ohtsuki, Y., 1987, SCE levels in Bloom-syndrome cells at very low bromodeoxyuridine (BrdU) concentrations: Monoclonal anti-BrdU antibody, *Mutat. Res.* **176:**157–164.

Simpson, R.T., and Seale, R.L., 1974, Characterization of chromatin extensively substituted with 5-bromodeoxyuridine, *Biochemistry* **13:**4609–4616.

Speit, G., 1984, Considerations on the mechanism of differential Giemsa staining of BrdU-substituted chromosomes, *Hum. Genet.* **67:**264–269.

Speit, G., and Haupter, S., 1985, On the mechanism of differential Giemsa staining of bromodeoxyuridine-substituted chromosomes. II. Differences between the demonstration of sister chromatid differentiation and replication patterns, *Hum. Genet.* **70:**126–129.

Speit, G., and Vogel, W., 1986, Detection of bromodeoxyuridine incorporation in mammalian chromosomes by a bromodeoxyuridine antibody. II. Demonstration of sister chromatid exchanges, *Chromosoma* **94:**103–106.

Stampe Villadsen, I., and Zeuthen, E., 1970, Synchronization of DNA-synthesis in *Tetrahymena* populations by temporary limitation of access to thymidine compounds, *Exp. Cell Res.* **61:** 302–310.

Steffen, J.A., and Stolzmann, W.M., 1969, Studies on in vitro lymphocyte proliferation in cultures synchronized by the inhibition of DNA synthesis I. Variability of S plus G_2 periods of first generation cells, *Exp. Cell Res.* **56:**453–460.

Stetten, G., Latt, S.A., and Davidson, R.L., 1976, 33258 Hoechst enhancement of the photosensitivity of bromodeoxyuridine- substituted cells, *Somat. Cell Genet.* **2:**285–290.

Stokke, T., and Steen, H.B., 1985, Multiple binding modes for Hoechst 33258 to DNA, *J. Histochem. Cytochem.* **33:**333–338.

Stokke, T., and Steen, H.B., 1986, Binding of Hoechst 33258 to chromatin in situ, *Cytometry* **7:** 227–234.

Stubblefield, E., and Gay, M., 1970, Quantitative tritium autoradiography of mammalian chromosomes II. The kinetics of DNA synthesis in individual chromosomes of chinese hamster fibroblasts, *Chromosoma* **31:**79–90.

Sugiyama, T., Goto, K., and Kano, Y., 1976, Mechanism of differential Giemsa method for sister chromatids, *Nature* **259:**59–60.

Sumner, A.T., 1990, *Chromosome Banding*, 1st ed., Unwin Hyman, London.

Takagi, N., and Sandberg, A.A., 1968, Chronology and pattern of human chromosome replication VIII. Behavior of the X and Y in early S-phase, *Cytogenet.* **7:**135–143.

Takayama, S., and Sakanishi, S., 1977, Differential Giemsa staining of sister chromatids after extraction with acids, *Chromosoma* **64:**109–115.

Takayama, S., and Sakanishi, S., 1978, Differential staining of sister chromatid in BrdU-substituted chromosomes after incubation in alkalified NaCl solution, *Proc. Japan Acad.* **54:**628–633.

Takayama, S., and Sakanishi, S., 1979, Sister chromatid differential staining by direct staining in Na_2HPO_4-Giemsa solution and the mechanism involved, *Chromosoma* **75:**37–44.

Takayama, S., and Tachibana, K., 1980, Two opposite types of sister chromatid differential staining in BUdR-substituted chromosomes using tetrasodium salt of EDTA, *Exp. Cell Res.* **126:**498–501.

Takayama, S., and Taniguchi, T., 1986, Light and scanning electron microscopic observations on the two contrasting types of sister chromatid differential staining after ultraviolet light irradiation, *Chromosoma* **93:**404–408.

Taylor, J.H., 1977, Increase in DNA replication sites in cells held at the beginning of S phase, *Chromosoma* **62:**291–300.

Teng, M., Usman, N., Frederick, C.A., and Wang, A.H.-J., 1988, The molecular structure of the complex of Hoechst 33258 and the DNA dodecamer d(CGCGAATTCGCG), *Nucleic Acids Res.* **16:**2671–2690.

Ten Hagen, K.G., Gilbert, D.M., Willard, H.F., and Cohen, S.N., 1990, Replication timing of DNA sequences associated with human centromeres and telomeres, *Mol. Cell. Biol.* **10:**6348–6355.

Tsukahara, M., and Kajii, T., 1985, Replication of X chromosomes in complete moles, *Hum. Genet.* **71:**7–10.

Tucker, J.D., Christensen, M.L., Strout, C.L., and Carrano, A.V., 1986, Determination of the baseline sister chromatid exchange frequency in human and mouse peripheral lymphocytes using monoclonal antibodies and very low doses of bromodeoxyuridine, *Cytogenet. Cell Genet.* **43:**38–42.

van Duijn, P., van Prooijen-Knegt, A.C., and van der Ploeg, M., 1985, The involvement of nucleosomes in Giemsa staining of chromosomes. A new hypothesis on the banding mechanism, *Histochemistry* **82:**363–376.

Vanderlaan, M., Watkins, B., Thomas, C., Dolbeare, F., and Stanker, L., 1986, Improved high-affinity monoclonal antibody to iododeoxyuridine, *Cytometry* **7:**499–507.

Viegas-Péquignot, E., and Dutrillaux, B., 1978, Une méthode simple pour obtenir des prophases et des prométaphases, *Ann. Génét.* **21:**122–125.

Vogel, W., and Speit, G., 1986, Cytogenetic replication studies with short thymidine pulses in bromodeoxyuridine-substituted chromosomes of different mouse cell lines, *Hum. Genet.* **72:** 63–67.

Vogel, W., Schempp, W., and Sigwarth, I., 1978, Comparison of thymidine, fluorodeoxyuridine, hydroxyurea, and methotrexate blocking at the G_1/S phase transition of the cell cycle, studied by replication patterns, *Hum. Genet.* **45:**193–198.

Vogel, W., Boldin, S., Reisacher, A., and Speit, G., 1985, Characterization of chromosome replication during S-phase with bromodeoxyuridine labelling in chinese hamster ovary and HeLa cells, *Chromosoma* **92:**363–368.

Vogel, W., Autenrieth, M., and Speit, G., 1986, Detection of bromodeoxyuridine-incorporation in mammalian chromosomes by a bromodeoxyuridine-antibody. I. Demonstration of replication patterns, *Hum. Genet.* **72:**129–132.

Vogel, W., Autenrieth, M., and Mehnert, K., 1989, Analysis of chromosome replication by a BrdU antibody technique, *Chromosoma* **98:**335–341.

Vogel, W., Mehnert, K., and Pentz, S., 1990, Demonstration of chromosome replication by BrdU antibody technique and electron microscopy, *Hum. Genet.* **84:**237–240.

von Kiel, K., Hameister, H., Somssich, I.E., and Adolph, S., 1985, Early replication banding reveals a strongly conserved functional pattern in mammalian chromosomes, *Chromosoma* **93:**69–76.

Wall, W.J., and Butler, L.J., 1989, Classification of Y chromosome polymorphisms by DNA content and C-banding, *Chromosoma* **97:**296–300.

Wall, W.J., Clark, M.S., and Coates, P., 1988, Structural complexity of Y chromosome heterochromatin, *Cytobios* **56:**17–22.

Wang, J.C., Passage, M.B., Ellison, J., Becker, M.A., Yen, P.H., Shapiro, L.J., and Mohandas, T.K., 1992, Physical mapping of loci in the distal half of the short arm of the human X chromosome: Implications for the spreading of X-chromosome inactivation, *Somat. Cell Mol. Genet.* **18:** 195–200.

Webber, L.M., and Garson, O.M., 1983, Fluorodeoxyuridine synchronization of bone marrow cultures, *Cancer Genet. Cytogenet.* **8:**123–132.

Webber, L.M., Brasch, J.M., and Smyth, D.R., 1981, DNA extraction during Giemsa differentiation of chromatids singly and doubly substituted with BrdU, *Chromosoma* **81:**691–700.

Weintraub, H., 1973, The assembly of newly replicated DNA into chromatin, *Cold Spring Harbor Symp. Quant. Biol.* **38:**247–256.

Werkheiser, W.C., 1963, The biochemical, cellular, and pharmacological action and effects of the folic acid antagonists, *Cancer Res.* **23:**1277–1285.

Wiles, M.V., Alexander, C.M., and Goodfellow, P.N., 1988, Isolation of an abundantly expressed sequence from the human X chromosome by differential screening, *Somat. Cell Mol. Genet.* **14:**31–39.

Wilkinson, Y.A., and McKenna, P.G., 1989, The effects of thymidine on deoxyribonucleotide pool levels, cytotoxicity and mutation induction in friend mouse erythroleukaemia cells, *Leukemia Res.* **13:**615–620.

Willard, H.F., 1977, Tissue-specific heterogeneity in DNA replication patterns of human X chromosomes, *Chromosoma* **61:**61–73.

Willard, H.F., and Latt, S.A., 1976, Analysis of deoxyribonucleic acid replication in human X chromosomes by fluorescence microscopy, *Am. J. Hum. Genet.* **28:**213–227.

Wolff, S., and Bodycote, J., 1977, The production of harlequin chromosomes by chemical and physical agents that disrupt protein structure, in: *Molecular human cytogenetics*, ICN-UCLA Symposia on Molecular and Cellular Biology, Volume 7 (R.S. Sparkes, D.E. Comings, and C.F. Fox, eds.), pp. 335–340, Academic Press, New York.

Xeros, N., 1962, Deoxyriboside control and synchronization of mitosis, *Nature* **194:**682–683.

Yunis, J.J., 1976, High resolution of human chromosomes, *Science* **191:**1268–1270.

Yunis, J.J., 1981, Mid-prophase human chromosomes. The attainment of 2000 bands, *Hum. Genet.* **56:**293–298.

Yunis, J.J., and Chandler, M.E., 1978, High-resolution chromosome analysis in clinical medicine, *Prog. Clin. Pathol.* **7:**267–288.

Zakharov, A.F., and Egolina, N.A., 1972, Differential spiralization along mammalian mitotic chromosomes I. BUdR-revealed differentiation in chinese hamster chromosomes, *Chromosoma* **38:** 341–365.

Zakharov, A.F., Baranovskaya, L.I., Ibraimov, A.I., Benjusch, V.A., Demintseva, V.S., and Oblapenko, N.G., 1974, Differential spiralization along mammalian mitotic chromosomes II. 5-bromodeoxyuridine and 5-bromodeoxycytidine-revealed differentiation in human chromosomes, *Chromosoma* **44:**343–359.

Zeuthen, E., 1968, Thymine starvation by inhibition of uptake and synthesis of thymine compounds in *Tetrahymena*, *Exp. Cell. Res.* **50:**37–46.

Chapter 3

Molecular Genetics of Charcot-Marie-Tooth Neuropathy

Benjamin B. Roa

Department of Molecular and Human Genetics
Baylor College of Medicine
Houston, Texas 77030

James R. Lupski

Departments of Molecular and Human Genetics, Pediatrics, and Human Genome Center
Baylor College of Medicine
Houston, Texas, and
Texas Children's Hospital
Houston, Texas 77030

INTRODUCTION

The disease described by Charcot and Marie involves a slowly progressive distal muscular atrophy with initial involvement of the feet and legs, followed by variable progressive weakness of the hands (Charcot and Marie, 1886). Independently, Tooth had reported on a peroneal type of progressive muscular atrophy with essentially the same clinical findings (Tooth, 1886). While the inherited nature of the disease was noted in both studies, Tooth had correctly postulated that the disorder is due to an underlying neuropathy, instead of a myelopathy as Charcot and Marie had proposed.

Charcot-Marie-Tooth disease (CMT) represents the most common inherited disorder of the peripheral nervous system, with an estimated population frequency

Advances in Human Genetics, Volume 22, edited by Henry Harris and Kurt Hirschhorn. Plenum Press, New York, 1994.

of 1:2500 (Skre, 1974). CMT is a type of hereditary motor and sensory neuropathy (Dyck *et al.*, 1993) which exhibits both clinical and genetic heterogeneity (Lupski *et al.*, 1991a). Linkage analyses have revealed at least six genetic loci corresponding to subtypes of CMT (Vance *et al.*, 1989; Bird *et al.*, 1982; Chance *et al.*, 1990; Gal *et al.*, 1985; Ben Othmane *et al.*, 1993a; Ben Othmane *et al.*, 1993b). Furthermore, a combination of positional cloning and candidate gene strategies has identified three genes associated with CMT (Valentijn *et al.*, 1992a; Roa *et al.*, 1993c; Kulkens *et al.*, 1993; Hayasaka *et al.*, 1993a; Bergoffen *et al.*, 1993a). Molecular studies have demonstrated that alternative mutational mechanisms of DNA duplication and point mutation are responsible for this disease. These findings serve to elucidate the molecular bases of CMT as well as other inherited primary peripheral neuropathies, and provide key insights into the basic biology of the peripheral nerve.

PATHOLOGICAL FEATURES

Charcot-Marie-Tooth Disease

Charcot-Marie-Tooth polyneuropathy syndrome is characterized by an insidious onset and slowly progressive weakness of the distal muscles (Lupski *et al.*, 1991a). Clinical features include initial weakness of the intrinsic foot muscles and distal leg muscles, including peroneal muscular atrophy, leading to foot deformities and gait abnormalities, respectively. Atrophy of the distal leg muscles can be prominent in some patients, and variable weakness of the intrinsic hand muscles may occur later in the course of the disease. Sensory involvement is rare, although decreased pain to pricking in a stocking distribution is seen in some patients (Lupski *et al.*, 1991a; Lupski, 1992). Clinical symptoms usually manifest within the first two decades of life (Bird and Kraft, 1978), and considerable variation of clinical severity is observed among unrelated CMT patients (Lupski *et al.*, 1991a), in affected individuals within the same family (Kaku *et al.*, 1993a), and even between identical twins (Garcia *et al.*, 1992).

Two major forms are differentiated by electrophysiological studies. CMT type 1 (CMT1), which is also known as hereditary motor and sensory neuropathy type I (HMSNI) (Dyck *et al.*, 1993), is a myelin-defective neuropathy that exhibits moderately to severely reduced motor nerve conduction velocity (NCV) (Lupski *et al.*, 1991a; Kaku *et al.*, 1993b). The conduction deficit in CMT1 is bilaterally symmetric, from nerve to nerve, and between nerve segments, suggesting an intrinsic Schwann cell defect (Kaku *et al.*, 1993b). The electrophysiological

finding of symmetrically reduced motor NCV is a fully penetrant phenotype usually evident by two years of age, before the onset of clinical symptoms (Nicholson, 1991; Kaku *et al.*, 1993b; Kaku *et al.*, 1993a). In contrast to the myelin deficit in CMT1, an axonal lesion underlies CMT type 2 (CMT2). CMT2, which is also known as hereditary motor and sensory neuropathy type II (HMSNII), exhibits normal or only mildly reduced motor NCV with decreased amplitudes (Dyck *et al.*, 1993; Lupski *et al.*, 1991a).

Peripheral nerve biopsies on CMT1 patients reveal a marked decrease in the degree and number of myelinated fibers, and hypertrophic changes due to onion bulb formations (Lupski and Garcia, 1992). These formations consist of concentric membranes derived from Schwann cells around myelinated and demyelinated internodes. In contrast, onion bulb formations are only occasionally seen in peripheral nerves of CMT2 patients (Lupski *et al.*, 1991a; Dyck *et al.*, 1993; Lupski and Garcia, 1992).

Inherited Primary Peripheral Neuropathies Related to CMT

Hereditary neuropathy with liability to pressure palsies (HNPP), also called tomaculous neuropathy, was first described in a family with three generations of affected members who experienced recurrent peroneal neuropathy after digging potatoes in a kneeling position (De Jong, 1947). Symptoms of this autosomal dominant neuropathy include periodic episodes of numbness, muscular weakness, and atrophy following relatively minor compression or trauma to the peripheral nerves (Windebank, 1992). Mild reductions in NCV may be observed by electrophysiology, with evidence of conduction blocks (Dyck *et al.*, 1981). Segmental demyelination and remyelination of the peripheral nerves with tomaculous or sausage-like focal thickenings of the myelin sheath are characteristic features of HNPP (Windebank, 1992).

Dejerine-Sottas syndrome (DSS) is a relatively rare, dysmyelinating hypertrophic neuropathy that was first described in a pair of siblings who were affected in infancy and at 14 years of age (Dejerine and Sottas, 1893). Dejerine-Sottas syndrome or hereditary motor and sensory neuropathy type III (HMSNIII) shares considerable overlap with the clinical, electrophysiological and histopathological findings of CMT, although the symptoms of DSS have an earlier onset and are more severe (Dyck *et al.*, 1993). Motor nerve conduction velocities are greatly reduced (Dyck *et al.*, 1971), and peripheral nerve biopsies reveal dysmyelination and onion bulb formation (Dejerine and Sottas, 1893). Autosomal dominant and autosomal recessive cases of Dejerine-Sottas syndrome have been reported

(McKusick, 1992). The inherited primary peripheral neuropathies HNPP, DSS, and Charcot-Marie-Tooth disease type I all appear to involve a Schwann cell-autonomous defect (Chance *et al.*, 1993; Roa *et al.*, 1993c; Lupski and Garcia, 1992; Roa *et al.*, 1993a; Kaku *et al.*, 1993b). The genetic lesions underlying these related disorders will be discussed in the succeeding sections.

GENETIC HETEROGENEITY OF CHARCOT-MARIE-TOOTH DISEASE

The most common inherited peripheral neuropathy, CMT, exhibits all forms of Mendelian inheritance. The more common dysmyelinating form, CMT1, can be inherited as an autosomal dominant, autosomal recessive, or X-linked trait; sporadic cases of CMT1 have been reported (McKusick, 1992). The axonal or neuronal form of the disease, CMT type 2, is an autosomal dominant disorder that has been genetically differentiated from CMT1 by linkage analysis (Hentati *et al.*, 1992; Loprest *et al.*, 1992) and by mutation analysis (Wise *et al.*, 1993). However, patients with apparent homozygous expression of a CMT2 mutation were reported to exhibit a severe clinical and electrophysiological phenotype similar to HMSNIII or Dejerine-Sottas syndrome (Sghirlanzoni *et al.*, 1992).

Most cases of dysmyelinating CMT1 exhibit autosomal dominant inheritance, and three subtypes have been defined by genetic linkage analysis. The most common subtype is CMT1A, in which the disease locus demonstrates linkage to DNA markers in 17p11.2p12 (Vance *et al.*, 1989). The locus for CMT1B is linked to markers in the 1q21.2q23 region (Bird *et al.*, 1982). A third subtype, CMT1C, appears to be associated with a third autosomal dominant locus, which maps outside of the 1q and 17p regions (Chance *et al.*, 1990; Chance *et al.*, 1992b). The locus for CMTX maps to proximal Xq (Gal *et al.*, 1985; Bergoffen *et al.*, 1993b). In the case of the axonal form of the disease, CMT type 2, an autosomal dominant locus (CMT2A) has been mapped to chromosome 1p; in addition, genetic heterogeneity is apparent in CMT2 (Ben Othmane *et al.*, 1993b).

Autosomal recessive cases of dysmeylinating CMT1 are relatively rare and represent a heterogeneous group, for which the designation of CMT type 4 was recently proposed (Ben Othmane *et al.*, 1993a). A locus was mapped on 8q13q21.1 for a genetic subtype of the disease, CMT4A (Ben Othmane *et al.*, 1993a). In comparison to autosomal dominant cases, the clinical and electrophysiological findings in autosomal recessive cases of dysmyelinating CMT were found to be more severe (Allan, 1939; Harding and Thomas, 1980). The loci corresponding to other forms of autosomal recessive CMT1 remain to be mapped.

GENE DOSAGE AS A NOVEL MECHANISM FOR CMT TYPE 1A

DNA Duplication as the Major Cause of CMT1A

Charcot-Marie-Tooth disease type 1A comprises the majority of CMT cases (Lupski *et al.*, 1991a). CMT1A is usually associated with a stable tandem DNA duplication of a 1.5-Mb region on 17p11.2p12 (Lupski *et al.*, 1991b; Raeymaekers *et al.*, 1991; Lupski *et al.*, 1993b; Pentao *et al.*, 1992; Lupski, 1992). The cytogenetically undetectable CMT1A duplication was identified by a number of molecular methods, including (1) detection of three alleles of a polymorphic $(GT)_n$ repeat mapping within the duplication (*D17S122*) in fully informative patients, (2) demonstration of dosage differences of two-allele RFLPs in heterozygous patients, (3) fluorescence *in situ* hybridization (FISH) analysis using probes within the duplicated region, and (4) the identification of a 500-kb *Sac*II junction fragment specific to the CMT1A duplication by pulsed-field gel electrophoresis (Lupski *et al.*, 1991b).

The DNA duplication is completely linked and associated with the neuropathological phenotype of CMT1A as demonstrated by the original studies conducted on U.S. French-Acadian and Ashkenazi-Jewish families (Lupski *et al.*, 1991b), and independently in twelve European kindreds (Raeymaekers *et al.*, 1991). Electrophysiological analyses in families segregating the CMT1A duplication showed a clear bimodal distribution between reduced motor NCVs in patients carrying the duplication (<42 meters/second), versus normal NCVs in individuals without the duplication (Kaku *et al.*, 1993a). The causative role of the CMT1A duplication was further substantiated by multiple reports of *de novo* duplication concordant with onset of the disease phenotype (Raeymaekers *et al.*, 1991; Hoogendijk *et al.*, 1992; Wise *et al.*, 1993). The presence of the CMT1A duplication was confirmed in different CMT1A patient populations including American (Chance *et al.*, 1992b), Australian (Nicholson *et al.*, 1992), British (Hallam *et al.*, 1992), Belgian and Dutch (Raeymaekers *et al.*, 1992), French (Brice *et al.*, 1992), Italian (Bellone *et al.*, 1992), and Welsh (MacMillan *et al.*, 1992) cohorts.

The frequency of the CMT1A duplication among unrelated CMT1 patients was estimated at approximately 70%–85%, according to three large independent studies (Wise *et al.* 1993; Ionasescu *et al.*, 1993a) (Van Broeckhoven, European Neuromuscular Disorders CMT Consortium Group, written communication, September 13, 1993). Furthermore, two studies that dealt with CMT1 patients with no family history have indicated that *de novo* CMT1A duplication could account for

approximately 90% of sporadic CMT1 cases (Hoogendijk *et al.*, 1992) (Van Broeckhoven, European Neuromuscular Disorders CMT Consortium Group, written communication, September 13, 1993).

Analysis of patient DNA by pulsed-field gel electrophoresis had demonstrated that the same *Sac*II duplication junction fragment of approximately 500 kb was present in the original U.S. French-Acadian and Ashkenazi-Jewish families (Lupski *et al.*, 1991b), in European CMT1A families (Raeymaekers *et al.*, 1991; Raeymaekers *et al.*, 1992), and subsequently in 43 unrelated CMT1A patients of different ethnic backgrounds (Wise *et al.*, 1993). In a separate study, 74 unrelated patients were identified carrying the 1.5–Mb CMT1A duplication; this study also identified a CMT1A patient with an alternatively sized DNA duplication of 460 kb (Valentijn *et al.*, 1993). In addition, two other CMT1A families were reported to segregate DNA duplications smaller than 1.5–Mb, although the exact sizes were unknown (Ionasescu *et al.*, 1993b; Palau *et al.*, 1993). In all three of these cases, the *PMP22* gene was encompassed by the alternative DNA duplications (Valentijn *et al.*, 1993; Ionasescu *et al.*, 1993b; Palau *et al.*, 1993). However, these cases are rare in comparison to the vast majority of CMT1A patients with DNA duplication of 1.5 Mb at 17p11.2p12.

The Region Duplicated in CMT1A Is Flanked by Large Regions of Homology

The finding that a consistently-sized DNA duplication had occurred repeatedly at the 17p11.2p12 region strongly suggests the presence of intrinsic structural features of the genome that predispose the region to discrete DNA rearrangements. Physical mapping of the 17p11.2p12 region in normal and affected individuals determined that the CMT1A duplication is a 3.0–Mb DNA duplication of a 1.5–Mb monomer unit that is flanked by complex CMT1A-REP repeats of approximately 35 kb (Pentao *et al.*, 1992; Chance *et al.*, 1994). The tandem arrangement of the monomer units in the CMT1A duplication was determined by physical mapping (Pentao *et al.*, 1992) and FISH analysis (Valentijn *et al.*, 1992b). Fig. 1 shows the wild-type physical map of the 1.5–Mb region (Pentao *et al.*, 1992), which contains the peripheral nerve myelin gene *PMP22* (Patel *et al.*, 1992; Valentijn *et al.*, 1992b; Timmerman *et al.*, 1992; Matsunami *et al.*, 1992). The corresponding structure of the 3.0–Mb CMT1A duplication is also shown in Fig. 1.

In contrast to the CMT1A duplication, the apparent reciprocal deletion at the 17p11.2p12 region is associated with HNPP (Chance *et al.*, 1993). The HNPP deletion is 1.5–Mb in size, as determined by PFGE detection of *Sac*II junction

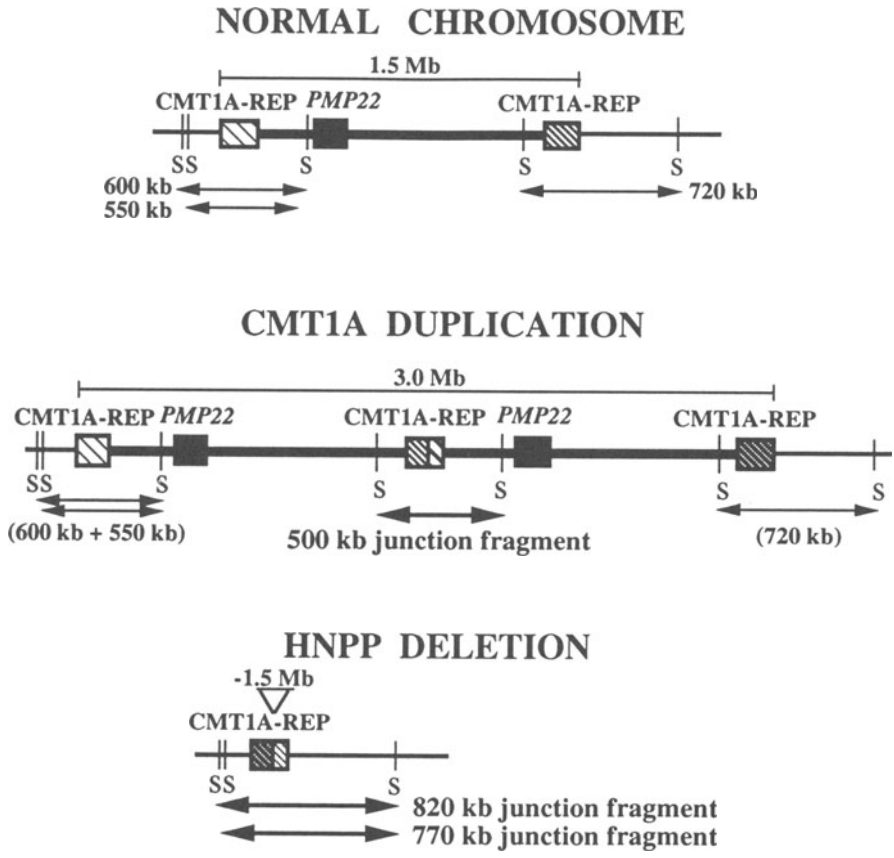

Fig. 1. DNA structure of the 17p11.2p12 region. The 1.5–Mb monomer unit of DNA in the normal chromosome is represented by the thick region. The stippled boxes represent the proximal (light) and distal (heavy) CMT1A-REP repeats of approximately 35 kb, and the solid box represents the *PMP22* gene. The *Sac*II restriction sites (S) are shown with the indicated 550-kb, 600-kb, and 720-kb PFGE fragments detected by a probe to CMT1A-REP. The CMT1A duplication chromosome structure and the 500-kb SacII duplication junction fragment are shown in the middle of the figure. The HNPP deletion chromosome structure, and the dual 770-kb and 820-kb *Sac*II deletion junction fragments, are shown at the bottom.

fragments specific to the deletion (Fig. 1) (Chance *et al.*, 1993; Roa *et al.*, 1993b). Furthermore, the duplication and deletion boundaries appear to lie at CMT1A–REP (Pentao *et al.*, 1992; Chance *et al.*, 1994). The flanking CMT1A–REP is present in three copies in the interstitially duplicated CMT1A chromosome (Pentao *et al.*, 1992), and in a single copy on the deleted HNPP chromosome (Chance *et al.*, 1994) as shown in Fig. 1. A model of unequal crossing over mediated by repeat regions (Bridges, 1936) was applied to the generation of the CMT1A duplication and the HNPP deletion, where reciprocal rearrangements presumably occur via unequal crossing over at misaligned CMT1A–REP repeats during meiosis (Raeymaekers *et al.*, 1991; Pentao *et al.*, 1992; Chance *et al.*, 1994). The proposed recombination model for the CMT1A duplication and the reciprocal HNPP deletion is depicted in Fig. 2.

Evidence Supporting the Gene Dosage Model for CMT1A

The DNA duplication underlying CMT1A could theoretically elicit the disease phenotype by a number of proposed mechanisms (Lupski *et al.*, 1991b). However, the cumulative evidence strongly supports a gene dosage model, in which an extra copy and increased expression of a critical gene within the duplicated region causes the CMT1A disease phenotype (Lupski *et al.*, 1992; Roa *et al.*, 1993*d*). Consistent with this mechanism, homozygous expression of the CMT1A duplication was seen to result in a more severe clinical phenotype compared with heterozygous duplication patients (Fig. 3, pedigrees HOU42 and HOU218) (Killian and Kloepfer, 1979; Lupski *et al.*, 1991b). Furthermore, a total of four rare dup17p partial trisomy patients were identified with larger duplications and different boundaries relative to the CMT1A duplication (e.g., pedigree HOU137 shown in Fig. 3). These patients exhibited the CMT1 electrophysiological phenotype of uniformly decreased NCV as part of their complex phenotype, which argued strongly against a model of gene interruption at the CMT1A duplication boundary (Lupski *et al.*, 1992; Chance *et al.*, 1992a; Upadhyaya *et al.*, 1993; Roa *et al.*, 1993*d*). Finally, a candidate gene was identified in the form of *PMP22*, a gene encoding a 160–amino acid peripheral nerve myelin protein (Patel *et al.*, 1992; Valentijn *et al.*, 1992b; Timmerman *et al.*, 1992; Matsunami *et al.*, 1992). *PMP22* maps within the 1.5–Mb region that is duplicated in CMT1A and is not disrupted at the duplication boundary (Patel *et al.*, 1992; Pentao *et al.*, 1992). Moreover, the *PMP22* gene remained duplicated in a rare CMT1A patient with a 460-kb alternative duplication (Valentijn *et al.*, 1993). *PMP22* was also duplicated in two other CMT1A patients reported to carry smaller DNA duplications of undetermined size (Ionasescu *et al.*, 1993b; Palau *et al.*, 1993).

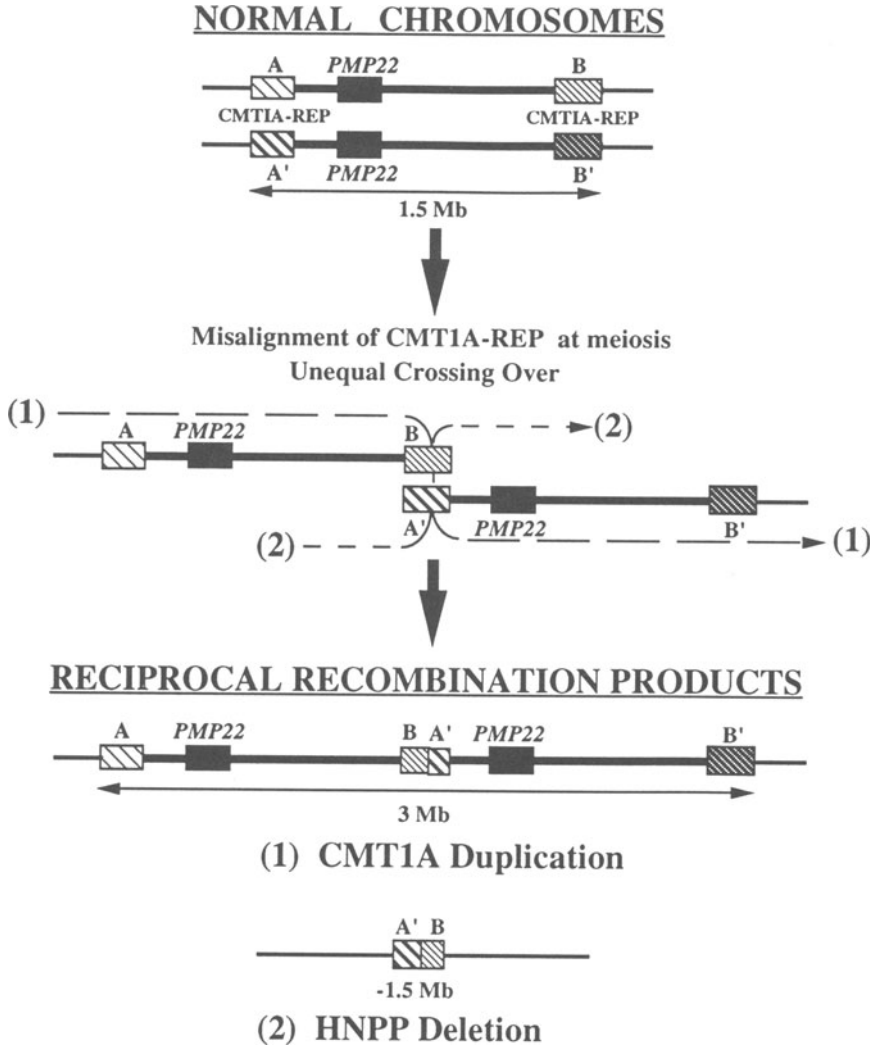

Fig. 2. Proposed recombination model of unequal crossing over leading to the CMT1A duplication and the HNPP deletion. Normal chromosomes are illustrated at the top, where filled boxes represent *PMP22* and the stippled boxes represent the CMT1A-REP repeats flanking the 1.5–Mb region, as in Fig. 1. The boxes are stippled differently to designate the proximal (A and A′) and distal (B and B′) CMT1A-REP repeats on two different chromosomes. Misalignment at meiosis between the distal (B) and proximal (A′) CMT1A-REP regions of two chromosomes is depicted in the middle of the figure. Unequal crossing over leads to a nonsister chromatid exchange, resulting in either of two reciprocal recombination products. Recombination pathway 1 (long dashes) leads to the CMT1A tandem duplication of 3.0-Mb, and recombination pathway 2 (short dashes) results in the HNPP deletion of 1.5–Mb.

HOU218
771
770
669
de novo CMT1A duplication
HOU42
331
332
333
Homozygous
CMT1A duplication
HOU137
529
528
527
partial 17p trisomy
[dup(17)(p11.2p12)]

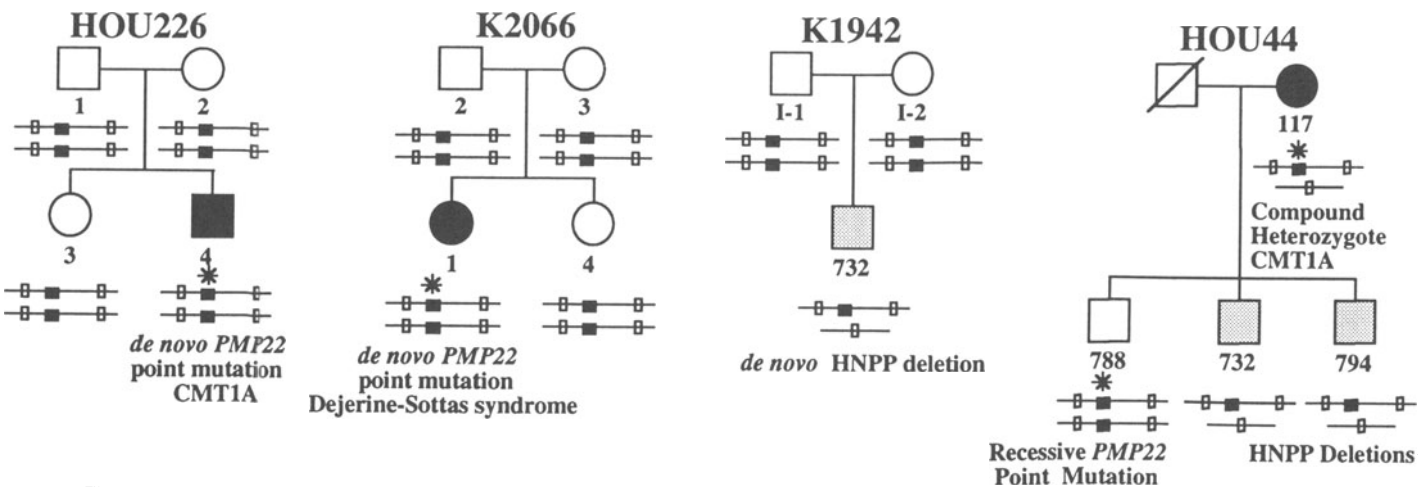

Fig. 3. Representative pedigrees for disease mechanisms leading to inherited primary peripheral neuropathy. In each pedigree, the affected status of each family member is indicated by a filled symbol (CMT1, Dejerine-Sottas syndrome) or a shaded symbol (HNPP). The corresponding genotypes of the 17p11.2p12 region are depicted for each individual (filled rectangle = the *PMP22* gene; open rectangles = CMT1A-REP). Pedigree HOU218 illustrates a case of *de novo* CMT1A duplication (Wise *et al.*, 1993). Pedigree HOU42 represents a CMT1A family with a child who is homozygous for the CMT1A duplication (Lupski *et al.*, 1991b). Pedigree HOU137 illustrates a case of 17p partial trisomy, where the duplication on 17p extends beyond the CMT1A duplication and the complex phenotype includes uniformly slowed nerve conduction velocity (Lupski *et al.*, 1992). Pedigree HOU226 demonstrates a *de novo PMP22* point mutation associated with CMT1A (Roa *et al.*, 1993c). Dejerine-Sottas syndrome pedigree K2066 demonstrates a *de novo* point mutation in *PMP22* (Roa *et al.*, 1993a), and pedigree K1942 demonstrates a *de novo* HNPP deletion (Chance *et al.*, 1993; Chance *et al.*, 1994). Pedigree HOU44 includes a compound heterozygote CMT1A patient who carries an apparent recessive *PMP22* point mutation associated with CMT1A, and the 1.5–Mb deletion associated with HNPP. The segregation pattern is shown in this unusual family (Roa *et al.*, 1993b).

THE *PMP22* GENE IN CHARCOT-MARIE-TOOTH DISEASE AND INHERITED PRIMARY PERIPHERAL NEUROPATHY

PMP22 and Charcot-Marie-Tooth Disease Type 1A

The *PMP22* gene associated with CMT1A was identified through a combination of positional cloning and candidate gene strategies. Two proposed animal models for CMT1, the *Trembler* (Suter *et al.*, 1992b) and *Trembler*^{J} (Suter *et al.*, 1992a) mice were found to carry allelic point mutations in the *Pmp-22* gene (for *P*eripheral nerve *M*yelin *P*rotein, *22*–kDa M_r). This gene encodes a glycosylated membrane-associated myelin protein (Manfioletti *et al.*, 1990). The mouse *Pmp-22* gene was identified based on homology to the rat gene, which was isolated by cDNA subtractive hybridization as a down-regulated gene following peripheral nerve injury (Suter *et al.*, 1992b; Welcher *et al.*, 1991). The *Pmp-22* gene of peripheral myelin turns out to have been previously identified as SR13 (Welcher *et al.*, 1991), CD25 (Spreyer *et al.*, 1991), *gas3* (Schneider *et al.*, 1988; Manfioletti *et al.*, 1990), and PASII (Kitamura *et al.*, 1976). The human homolog of the *PMP22* gene is highly expressed in peripheral nerve (Patel *et al.*, 1992) and maps within the 1.5–Mb region in 17p11.2p12 that is duplicated in CMT1A patients (Patel *et al.*, 1992; Valentijn *et al.*, 1992b; Timmerman *et al.*, 1992; Matsunami *et al.*, 1992). Point mutations in *PMP22* were identified in non-duplication CMT1A patients, confirming the direct role of the *PMP22* gene in the CMT1A disease process. One mutation predicts a Leu16Pro substitution identical to that of *Trembler*^{J} mouse (Valentijn *et al.*, 1992a), and a *de novo* mutation was identified that leads to a Ser79Cys substitution in *PMP22* (Roa *et al.*, 1993c) (Table I) (Fig. 3, pedigree HOU226). These autosomal dominant mutations affect putative transmembrane domains and probably constitute gain of function alleles in *PMP22* (Roa *et al.*, 1993c).

An apparent recessive *PMP22* mutation associated with CMT1A was identified in a family with individuals affected for CMT1A and HNPP (Table I and Fig. 3, pedigree HOU44) (Roa *et al.*, 1993b). A compound heterozygote patient exhibiting the CMT1 phenotype carried a *PMP22* point mutation on one chromosome (predicting a Thr118Met substitution, Table I), in combination with a deletion of *PMP22* and the surrounding 1.5–Mb region on the homologous chromosome (Roa *et al.*, 1993b). This CMT1 patient had one heterozygous son who carried the *PMP22* point mutation in combination with a wild-type *PMP22* allele and exhibited no clinical phenotype. Two other sons were heterozygous for the 1.5–Mb DNA deletion and displayed the distinct clinical phenotype of HNPP. The disease mechanisms in this unusual family are diagramed in Fig. 3, pedigree

HOU44 (Roa *et al.*, 1993b). Thus, the CMT1A disease phenotype can be caused by autosomal dominant and apparent autosomal recessive point mutation alleles in *PMP22*. Fig. 3 also diagrams the different mutational mechanisms involving the 17p11.2p12 region in representative kindreds with inherited primary peripheral neuropathies, CMT1A, Dejerine-Sottas syndrome and HNPP.

PMP22 and Dejerine-Sottas Syndrome

Dejerine-Sottas syndrome (DSS) is a related dysmyelinating disorder whose clinical symptoms overlap with CMT1. Mutational analysis of the *PMP22* gene in patients with DSS identified point mutations associated with the disorder. A *de novo* mutation was identified in a DSS patient that predicts a Met69Lys substitution, and a second mutation in an unrelated patient led to a Ser72Leu substitution in *PMP22* (Table 1) (Roa *et al.*, 1993a). Although the lack of affected parents in most DSS pedigrees is consistent with autosomal recessive transmission, the heterozygous state of these *PMP22* point mutations suggests the action of autosomal dominant alleles (Roa *et al.*, 1993a). Dejerine-Sottas syndrome is an example that demonstrates that autosomal dominant new mutation, instead of presumed autosomal recessive inheritance, can be responsible for the disease. A well characterized precedent is the case of osteogenesis imperfecta type II, where the disease which appeared to show a recessive pattern of inheritance was caused largely by new dominant mutations in the *COLA1* and *COLA2* genes of type I collagen (Byers, 1989). The molecular data on CMT disease and DSS further indicate that instead of being completely distinct entities, these two disorders represent a spectrum of related clinical phenotypes that can arise from allelic missense point mutations in the *PMP22* gene (Roa *et al.*, 1993a).

PMP22 and Hereditary Neuropathy with Liability to Pressure Palsies

The autosomal dominant dysmyelinating disorder HNPP is associated with the apparent reciprocal deletion of 1.5–Mb at 17p11.2p12, which implicates decreased dosage and expression of the *PMP22* gene as a possible cause of HNPP (Chance *et al.*, 1993). This was confirmed by the identification of an apparent loss of function *PMP22* mutation in an HNPP patient who was not deleted for the 1.5–Mb CMT1A/HNPP region (Table I). The 2 bp deletion frameshift mutation in this HNPP patient introduces a premature stop codon early in the reading frame of *PMP22* (Nicholson *et al.*, 1994). This is in contrast to allelic missense *PMP22* point mutations associated with CMT1A and DSS (Table I).

TABLE I. Gene Mutations Associated with Primary Inherited Peripheral Neuropathy

Gene	Disease	Mutation	Change	Reference
PMP22	CMT1A*	TCT-TGT (tv)	Ser (79) Cys	Roa *et al.*, 1993c
		CTG-CCG (ts)	Leu (16) Pro	Valentijn *et al.*, 1992a
		GCA-GTA (ts)	Thr (118) Met	Roa *et al.*, 1993b
	DSS	ATG-AAG (tv)	Met (69) Lys	Roa *et al.*, 1993a
		TCG-TTG* (ts)	Ser (72) Leu	Roa *et al.*, 1993a
	HNPP	GAGT-GT (fs) (2bp deletion)	Ser (7) Tyr to Thr (36) stop	Nicholson *et al.*, 1994
MPZ	CMT1B	AAA-GAA (ts)	Lys (96) Glu	Hayasaka *et al.*, 1993a
		GAC-GAA (tv)	Asp (90) Glu	Hayasaka *et al.*, 1993a
		TCTCCTT-TCTT (3bp deletion)	Ser (63) deletion	Kulkens *et al.*, 1993
		CGC-CAC* (ts)	Arg (98) His	Hayasaka *et al.*, 1993d
		TAT-TGT (ts)	Tyr (82) Cys	Himoro *et al.*, 1993
		ATC-ATG* (tv)	Ile (30) Met	Hayasaka *et al.*, 1993e
	DSS	GGG-CGG* (tv)	Gly (167) Arg	Hayasaka *et al.*, 1993b
		TCC-TGC (tv)	Ser (63) Cys	Hayasaka *et al.*, 1993b
Cx32	CMTX	GGC-AGC (ts)	Gly (12) Ser	Bergoffen *et al.*, 1993
		GTG-ATG* (ts)	Val (139) Met	Bergoffen *et al.*, 1993
		CGG-TGG* (ts)	Arg (142) Trp	Bergoffen *et al.*, 1993
				Ionasescu *et al.*, 1994
		CTC-CGC (tv)	Leu (156) Arg	Bergoffen *et al.*, 1993
		CCC-TCC (ts)	Pro (172) Ser	Bergoffen *et al.*, 1993
		AAC-AAAC (fs) (1bp insertion)	Asn (175) Lys to Glu (242) stop	Bergoffen *et al.*, 1993

GAG-AAG* (ts)	Glu (186) Lys	Bergoffen *et al.*, 1993
CGG-CAG* (ts)	Arg (15) Gln	Fairweather *et al.*, 1994
TGC-TTC (tv)	Cys (60) Phe	Fairweather *et al.*, 1994
GTT-ATT* (ts)	Val (63) Ile	Fairweather *et al.*, 1994
TCCCA-TCCA (fs) (1bp deletion)	His (73) Met to Leu (83) stop	Fairweather *et al.*, 1994
CTGTTGTT-CTGTT (3bp deletion)	Leu (143) deletion	Fairweather *et al.*, 1994
GAG-AAG* (ts)	Glu (208) Lys	Fairweather *et al.*, 1994
CGG-TGG* (ts)	Arg (215) Trp	Fairweather *et al.*, 1994
CGA-TGA* (ts)	Arg (220) stop	Fairweather *et al.*, 1994
GAG-GGG (ts)	Glu (102) Gly	Ionasescu *et al.*, 1994
CGA-TGA* (ts)	Arg (22) stop	Ionasescu *et al.*, 1994
GAG-TAG* (tv)	Glu (186) stop	Ionasescu *et al.*, 1994
TGT-TGA (tv)	Cys (217) stop	Ionasescu *et al.*, 1994

*Inherited primary peripheral neuropathies are abbreviated: CMT1A = Charcot-Marie-Tooth disease type 1A; DSS = Dejerine-Sottas syndrome; HNPP = hereditary neuropathy with liability to pressure palsies; CMTX = X-linked CMT. The identity and nature of 33 mutations are listed; ts = transition (18 mutations), tv = transversion (10), fs = frameshift (3). Two mutations are 3bp in-frame codon deletions. Asterisks indicate point mutations at CpG dinucleotides. The occurrence of 11 transition mutations at CpG dinucleotides (36% of single-base substitutions listed) is consistent with methylation-mediated deamination at CpG hotspots being a major mechanism for point mutations in human genetic disease (Cooper and Krawczak, 1990), as has been previously observed in bacteria (Coulondre *et al.*, 1978; Duncan and Miller, 1980). Change stands for amino acid substitutions. For each frameshift mutation, change is indicated from the first amino acid residue altered by the mutation to the resulting premature stop codon. All missense point mutations listed predict substitutions between structurally nonequivalent amino acid residues that are more likely to disrupt the native protein structure and function (Bordo and Argos, 1991), except for three: (1) the CMT1B mutation in *MPZ* leading to an equivalent Asp(90)Glu substitution (Hayasaka *et al.*, 1993a; Bordo and Argos, 1991), (2) the CMTX mutation in *Cx32* leading to a Gly(12)Ser substitution (Bergoffen *et al.*, 1993a), and (3) the CMTX mutation in *Cx32* leading to a Val(63)Ile substitution (Fairweather *et al.*, 1994).

The results from *PMP22* mutational studies illustrate that *PMP22* is the principal dosage-sensitive gene within the 1.5–Mb CMT1A/HNPP region at 17p11.2p12 responsible for peripheral neuropathy. Underexpression of the *PMP22* gene leads to HNPP, which is either associated with deletion of the 1.5–Mb region containing *PMP22* (Chance *et al.*, 1993), or with a nonsense mutation in the *PMP22* gene (Nicholson *et al.*, 1994). In contrast, increased dosage of the region containing *PMP22* appears to be responsible for the majority of CMT1A cases. While the CMT1A duplication is almost always 1.5–Mb in length, rare CMT1A patients with smaller-sized DNA duplications that encompass the *PMP22* gene have been identified (Valentijn *et al.*, 1993; Ionasescu *et al.*, 1993b; Palau *et al.*, 1993). Alternatively, CMT1A can be caused by *PMP22* point mutations that presumably lead to an altered function of the protein (Roa *et al.*, 1993c; Valentijn *et al.*, 1992a). It is notable that all the *PMP22* missense point mutations identified to date (Table I) predict substitutions between nonequivalent amino acids that are most likely to perturb the structure and function of the native protein (Bordo and Argos, 1991). A complete understanding of the mutational mechanisms awaits the determination of the exact role of *PMP22* in peripheral nerve physiology.

GENES ASSOCIATED WITH OTHER FORMS OF CMT

The Myelin Protein Zero (MPZ) Gene and CMT1B

The *MPZ* gene encoding myelin protein zero (P_0) maps to the 1q22–q23 region where the CMT1B locus was previously assigned (Hayasaka *et al.*, 1993c). The P_0 protein is the most abundant structural protein of peripheral nerve myelin (Lemke, 1993). The first exon of *MPZ* contains the signal sequence, and exons 2 and 3 encode the extracellular immunoglobulin-like (Ig) domain that is important to P_0 function as a homophilic adhesion molecule in myelin compaction (Lemke *et al.*, 1988; Filbin *et al.*, 1990; D'Urso *et al.*, 1990). Exon 4 of *MPZ* encodes a transmembrane segment, and exons 5 and 6 code for the cytoplasmic domain (Lemke *et al.*, 1988). Multiple autosomal dominant mutations in the *MPZ* gene were identified in CMT1B patients (Table I), where the mutations either result in single amino acid substitutions (Hayasaka *et al.*, 1993a; Hayasaka *et al.*, 1993e; Himoro *et al.*, 1993; Hayasaka *et al.*, 1993d), or an in-frame codon deletion in the extracellular domain of P_0 (Kulkens *et al.*, 1993). Except for one CMT1B–associated mutation, which predicts the Asp(90)Glu substitution (Hayasaka *et al.*, 1993a), all the missense point mutations identified in *MPZ* lead to substitutions between structurally nonequivalent amino acids (Table I) (Bordo and Argos, 1991).

MPZ and Dejerine-Sottas Syndrome

Allelic mutations in the *MPZ* gene were similarly identified in sporadic patients with DSS. Individual amino acid substitutions predicted by these *de novo* mutations reside in the extracellular and in the transmembrane domains of P_0 (Hayasaka *et al.*, 1993b). A list of *MPZ* mutations associated with CMT1B and DSS is shown in Table I. In each case, the amino acid residues are numbered from the translation start site, and not the mature P_0 protein. Interestingly, deletion of serine codon 63 (corresponding to deletion of serine codon 34 of the mature P_0 protein) is associated with CMT1B (Kulkens *et al.*, 1993), while a serine-to-cysteine substitution at the same residue (Ser63Cys) is associated with DSS (Hayasaka *et al.*, 1993b; Patel and Lupski, 1994). These findings on *MPZ* mutations are consistent with those of *PMP22*, indicating that CMT type 1 and DSS constitute a spectrum of peripheral neuropathy phenotypes with common genetic bases.

The Cx32 Gene and X-linked CMT

The X-linked form of CMT (CMTX) is associated with mutations in the gene encoding connexin-32 (*Cx32* or *GJB1*), which maps to Xq13.1 (Bergoffen *et al.*, 1993a). The *Cx32* mutations identified in CMTX patients lead to single amino acid substitutions, a codon deletion, or frameshifts, as listed in Table I (Bergoffen *et al.*, 1993a; Fairweather *et al.*, 1994; Ionasescu *et al.*, 1994). All but two of the predicted single amino acid substitutions in connexin-32 (the Gly(12)Ser substitution [Bergoffen *et al.*, 1993a] and the Val(63)Ile substitution [Fairweather *et al.*, 1994]) occur between structurally nonequivalent amino acid residues (Bordo and Argos, 1991). Connexin subunit proteins assemble to form membrane-spanning half-channels called connexons; these interact with connexons in adjacent cells to form complete intercellular channels for transport of ions and small molecules. The localization of gap junction proteins to peripheral nerve myelin was unprecedented (Bergoffen *et al.*, 1993a).

IMPLICATIONS OF CMT STUDIES ON PERIPHERAL NERVE BIOLOGY

The genetics and physiology of myelin are comprehensively discussed in a number of recent reviews (Lemke, 1988; Hudson, 1990; Lemke, 1993). Compact myelin sheaths surrounding the axons facilitate the saltatory conduction of nerve

impulses in both the central nervous system (CNS) and the peripheral nervous system (PNS). Myelin in the CNS is derived from oligodendrocytes while Schwann cells give rise to PNS myelin, with differences in some of their respective protein components. However, the basic structure of compact myelin is the same in the two systems. A composite illustration of myelin organization in the CNS and in the PNS is shown in Fig. 4, which is adapted from several sources (Lemke, 1988; Lemke, 1993; Bergoffen *et al.*, 1993a).

The characterization of the *PMP22*, *MPZ*, and *Cx32* genes has provided additional insights into the function of peripheral nerve myelin components. The *PMP22* gene encodes a membrane-associated 17 kDa protein whose apparent molecular weight is increased to approximately 22 kDa by glycosylation (Manfioletti *et al.*, 1990). *PMP22* expression occurs at high levels in fully differentiated Schwann cells, but is rapidly downregulated by loss of axon-Schwann cell contact resulting from nerve injury (Spreyer *et al.*, 1991; Welcher *et al.*, 1991). The integral membrane protein *PMP22* was located in the compact portion of myelinated fibers in the PNS, but not in the CNS (Snipes *et al.*, 1992). Structural modeling predicted four putative transmembrane domains in *PMP22* (Suter *et al.*, 1992a), which bears striking similarity to proteolipid protein (PLP) of CNS myelin (Fig. 4). The location and membrane-spanning nature of PMP22 have suggested a role in peripheral nerve myelin compaction (Lupski, 1994). Mutations within the *PMP22* gene, as well as increased dosage of the 1.5–Mb region containing *PMP22*, independently give rise to the CMT1A phenotype of uniformly decreased nerve conduction associated with abnormal myelin compaction. Although all this is known, the exact function of PMP22 remains to be determined (Suter *et al.*, 1993).

The P_0 protein is the major glycosylated structural protein that comprises approximately 50% of mammalian peripheral nerve myelin (Lemke, 1988; Hudson, 1990; Lemke, 1993). P_0 is produced by myelinating Schwann cells and is located at the compact myelin layers of the PNS as depicted in Fig. 4. The mature P_0 protein contains a glycosylated extracellular domain highly homologous to those of the immunoglobulin gene superfamily (Lemke and Axel, 1985). Based on structural considerations, the extracellular domain was postulated to mediate adhesion between the extracellular faces of the myelin membrane to form the intraperiod line (Lemke and Axel, 1985). Homophilic adhesion properties of the P_0 extracellular domain have been demonstrated in mammalian cells transfected with P_0 cDNA (Filbin *et al.*, 1990; D'Urso *et al.*, 1990). The complex carbohydrate moieties on the mature P_0 extracellular domain were shown to be important in conferring adhesiveness (Filbin and Tennekoon, 1991). The majority of *MPZ* mutations identified in CMT1B and Dejerine-Sottas patients were found to reside

in the extracellular domain (Table I). Moreover, the inability of transgenic mice homozgyous for P_0 insertion mutations to form intraperiod lines in myelin provides convincing evidence for the adhesion role of the extracellular P_0 domain (Giese *et al.*, 1992). In addition to the role of the extracellular domain, the highly basic P_0 intracellular domain was postulated to participate in the formation of the major dense line of compact myelin. The basic cytoplasmic domain of P_0 is thought to interact with acidic phospholipids on the intracellular surface of the myelin membrane to bring about compaction in a manner analogous to that of myelin basic protein (MBP) in CNS myelin (Lemke and Axel, 1985; Lemke, 1988; Hudson, 1990). Notably, the lack of MBP in the *shiverer* mouse disrupts major dense line formation in CNS myelin but not in PNS myelin (Kirschner and Ganser, 1980). This suggests that major dense line formation in PNS myelin could be carried out by another protein such as P_0 by virtue of its basic intracellular domain (Lemke, 1988). Further mutational analysis of the *MPZ* gene in CMT1B patients may yet uncover mutations residing at the highly basic intracellular domain, which would support a different role in myelin compaction for the carboxy terminal domain of P_0.

The *Cx32* gene is highly expressed in peripheral nerve, and the connexin–32 gap junction proteins are localized adjacent to the nodes of Ranvier and the Schmidt-Lanterman incisures, as shown in Fig. 4 (Bergoffen *et al.*, 1993a). The distribution and apparent function of connexin–32 suggests a role in the formation of intercellular gap junctions to connect the folds of Schwann cell cytoplasm in peripheral nerve myelin. Connexin–32 gap junctions were proposed to mediate transport to the innermost layers of compact myelin, and perhaps indirectly to the axon as well. This proposed function could be consistent with the findings of combined myelin disruption and axonal degeneration in X–linked CMT (Bergoffen *et al.*, 1993a).

GENETIC DIAGNOSIS FOR CMT AND ASSOCIATED NEUROPATHIES

Detection of the CMT1A Duplication

The CMT1A duplication constitutes the most common cause of the disease, having been detected in >70% of patients diagnosed with CMT1 on the basis of electrophysiology (Wise *et al.*, 1993; Ionasescu *et al.*, 1993a) (Van Broeckhoven, European Neuromuscular Disorders CMT Consortium Group, written communication, September 13, 1993). Thus, molecular detection of the CMT1A duplication

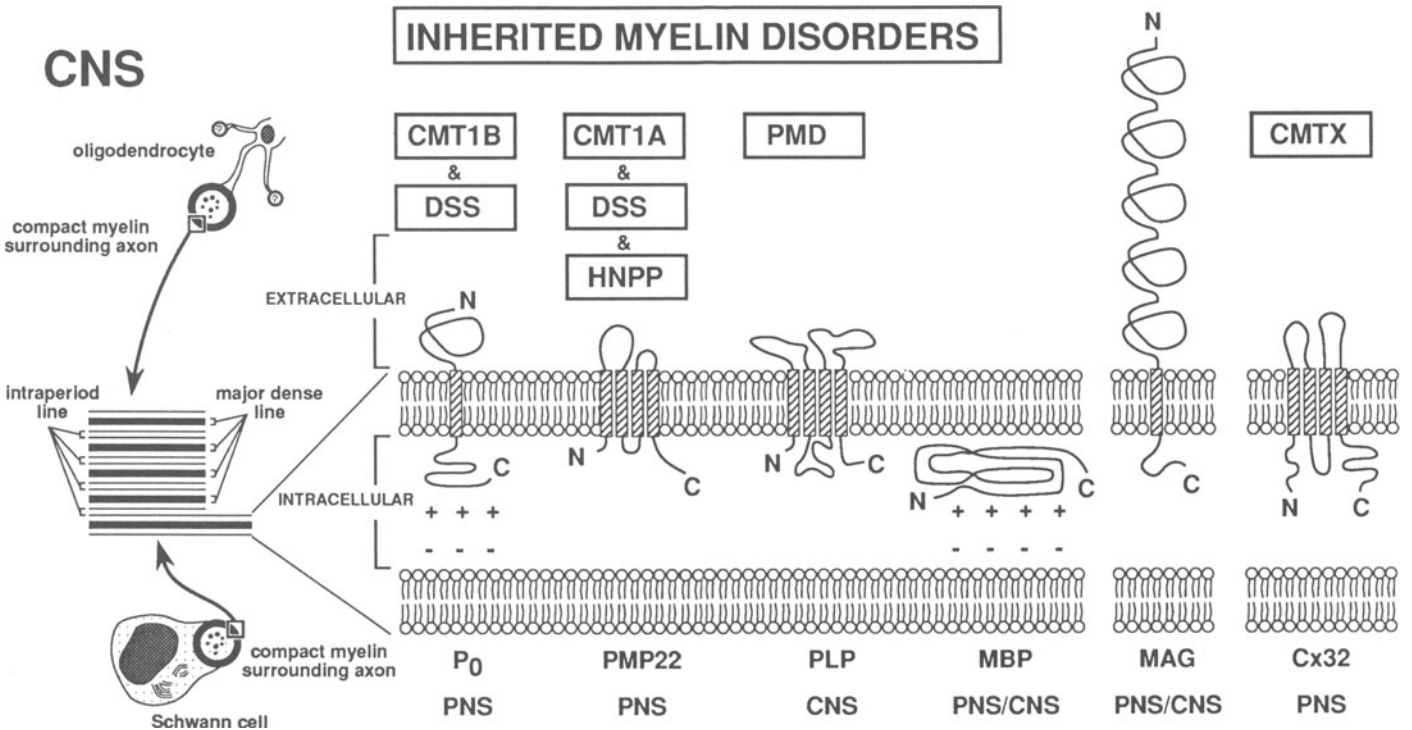
INHERITED MYELIN DISORDERS
CNS
oligodendrocyte
compact myelin surrounding axon
intraperiod line
major dense line
Schwann cell
compact myelin surrounding axon
EXTRACELLULAR
INTRACELLULAR
CMT1B & DSS
CMT1A & DSS & HNPP
PMD
CMTX
N
C
+ + +
- - -
P_0
PMP22
PLP
MBP
MAG
Cx32
PNS
PNS
CNS
PNS/CNS
PNS/CNS
PNS

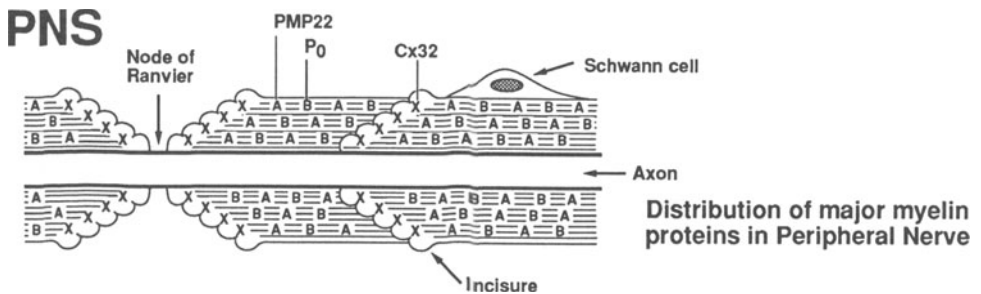

Fig. 4. Myelin organization in the central (CNS) and peripheral nervous system (PNS). Fig. 4 is adapted from Lemke *et al.*, 1988, and Bergoffen *et al.*, 1993, and shows origins of CNS and PNS compact myelin. Note that a single oligodendrocyte can myelinate multiple axons in the CNS, whereas one Schwann cell myelinates a single axon in the PNS. A cross-section illustrates compact myelin organization indicating the major dense line and the intraperiod line, which are formed by apposed intracellular and extracellular membrane surfaces, respectively. The proposed structures of the major CNS and PNS myelin proteins are shown. PMP22 = peripheral nerve myelin protein 22-kDa M_r; P_0 = myelin protein zero; PLP = proteolipid protein; MBP = myelin basic protein; MAG = myelin-associated glycoprotein; Cx32 = connexin 32. The boxes indicate the inherited myelin disorders associated with mutations in each myelin protein. CMT1A = Charcot-Marie-Tooth disease type 1A; CMT1B = Charcot-Marie-Tooth disease type 1B; DSS = Dejerine-Sottas syndrome; PMD = Pelizaeus-Merzbacher disease; CMTX = X-linked CMT. In addition, IgM antibodies against MAG can result in autoimmune peripheral neuropathy (Latov *et al.*, 1988). The gaps in the membrane indicate the different locations of the MAG and Cx32 proteins. The bottom part of the figure depicts the distribution as determined by immunostaining of the major PNS myelin proteins PMP22 (A), P_0 (B), and Cx32 (X) in the peripheral nerve (Bergoffen *et al.*, 1993a).

is a useful DNA diagnostic test for patients with inherited as well as sporadic peripheral neuropathies.

Detection of the CMT1A duplication can be accomplished through various methods (Lupski *et al.*, 1991b), with advantages and limitations inherent to each technique (Wise *et al.*, 1993; Lupski *et al.*, 1993a). Methods requiring the analysis of polymorphic alleles to detect the presence of an extra allele within the duplicated region depend on the informativeness of the markers used. Alternatively, careful quantitation of the signal intensities of duplicated homozygous markers relative to a nonduplicated marker (internal control) has also been used to detect the CMT1A duplication (Hensels *et al.*, 1993; Hoogendijk *et al.*, 1992). In analyzing dosage differences of duplicated alleles, however, it should be noted that artifacts such as partial restriction enzyme digestions, degradation of genomic DNA, or gel overloading could render the results uninterpretable (Hensels *et al.*, 1993; Lupski *et al.*, 1993a; Wise *et al.*, 1993). PCR-based methods such as $(GT)_n$ repeat analysis could be limited by the number of distinguishable alleles and by the reduced quantitative nature of PCR. Analysis by two-color FISH of interphase nuclei can graphically visualize the cytogenetically invisible 1.5–Mb CMT1A duplication. The case of CMT1A was the first application of FISH to the molecular diagnosis of an autosomal dominant disorder due to a cytogenetically undetectable DNA rearrangement (Lupski *et al.*, 1991b). Perhaps the most informative method at present is pulsed-field gel electrophoresis followed by Southern hybridization to detect the junction fragment specific to the CMT1A duplication. This relatively labor-intensive method has the potential of simultaneously detecting and sizing the DNA duplication in CMT1A, whether it be the 1.5–Mb duplication seen in the overwhelming majority of patients (Lupski *et al.*, 1991b; Wise *et al.*, 1993), or rare alternatively sized duplications (Valentijn *et al.*, 1993; Ionasescu *et al.*, 1993b; Palau *et al.*, 1993). An additional advantage of PFGE would be the unambiguous detection of the reciprocal HNPP deletion through identification of the junction fragments specific to the 1.5–Mb HNPP deletion (Chance *et al.*, 1994; Roa *et al.*, 1993b).

Mutation Analysis of Genes Associated with CMT

CMT1 and Dejerine-Sottas patients negative for the CMT1A duplication can be directly screened for mutations in genes associated with CMT: *PMP22*, *MPZ*, and, if X-linked segregation can not be ruled out, *Cx32*. Mutational screening through heteroduplex analysis (Roa *et al.*, 1993c.; Roa *et al.*, 1993b; Roa *et al.*, 1993a) and single-strand conformation polymorphism (Kulkens *et al.*, 1993; Nicholson *et al.*, 1994) have proven to be effective methods for screening

significant numbers of patient samples. Direct sequencing based on PCR amplification of cDNA or genomic DNA has been a powerful tool for detecting and identifying mutations within CMT-associated genes. The recent identification of the *PMP22*, *MPZ*, and *Cx32* genes now provides for the direct analyses for coding sequence alterations in genes associated with CMT. This may be carried out in the absence of linkage information, which is typically the case in most families and in sporadic cases of peripheral neuropathy. The mutational analysis of specific genes would best be applied to CMT1 patients known not to carry the CMT1A duplication, which is the single mutation responsible for the majority of CMT cases.

MOLECULAR INSIGHTS RELATED TO THE CMT1A DUPLICATION

CMT1A Duplication and HNPP Deletion at the 17p11.2p12 Region

The identification of the CMT1A duplication on 17p11.2p12 had profound effects on the genetic and physical mapping of the CMT1A locus. For genetic mapping, it was shown that failure to consider DNA duplication at this region could distort the positioning of the CMT1A locus by conventional linkage analysis (Lupski *et al.*, 1991b; Lupski, 1992). When dosage differences occurring in a two-allele RFLP system were not recognized, the deduced parental origin of alleles was subject to misinterpretation. These errors appear as increased recombination frequency and reduced LOD scores between marker and disease locus. The inclusion of these errors in multipoint linkage analysis have been demonstrated to result in incorrect mapping of the CMT1A locus when the CMT1A duplication is not taken into consideration (Lupski *et al.*, 1991b; Nicholson *et al.*, 1992). In contrast, the effect of the reciprocal deletion in HNPP results in nontransmission of deleted alleles to the affected offspring. This lack of transmission could be erroneously interpreted as nonpaternity or nonmaternity (Chance *et al.*, 1993). Moreover, the identification and physical mapping of the 1.5–Mb duplication/deletion in 17p11.2p12 defined a critical region for the rapid evaluation of candidate genes, which facilitated the characterization of the *PMP22* gene.

The CMT1A duplication/HNPP deletion involving 1.5–Mb of DNA at the 17p11.2p12 region represent stably inherited, repeatedly occurring DNA rearrangements that result in autosomal dominant disease phenotypes. The presence of large regions of homology flanking the 1.5–Mb duplication/deletion region suggests a mechanism of unequal crossing over at misaligned CMT1A–REP elements during

meiosis. The model in Fig. 2 depicts the proposed unequal exchange occurring between nonsister chromatids (Raeymaekers *et al.*, 1991; Pentao *et al.*, 1992). Furthermore, analysis of eleven *de novo* CMT1A duplications indicated an exclusively paternal origin with apparent unequal, nonsister chromatid exchange taking place during spermatogenesis (Palau *et al.*, 1993; Wise *et al.*, 1993).

DNA duplications have been observed in various genomes and can vary in extent, from a portion of a gene as in the haptoglobin Hp^2 allele duplication (Smithies *et al.*, 1962), to large spans that include multiple genes and intergenic DNA. An example of the latter is the *Bar* locus duplication of *Drosophila melanogaster* for which the unequal crossing over model was originally proposed (Bridges, 1936). In the case of the CMT1A/HNPP "locus," with its apparent ancestral duplication of flanking CMT1A-REP regions, determination of the recombination mechanisms would require extensive sequence comparisons of the proximal and distal CMT1A-REP repeats and a better understanding of recombination pathways in humans. At this point, it would be helpful to consider information derived from other model systems for insights into the recombination events leading to the CMT1A and HNPP peripheral neuropathies.

Homologous Recombination in Model Systems

Prokaryotic genomes contain various low-copy number repeated sequences such as insertion elements, rRNA operons, tRNA genes, and short interspersed repeats such as REP and ERIC sequences (Lupski and Weinstock, 1992). The major large repeat units of *E. coli* and *S. typhimurium* chromosomes are the seven *rrn* ribosomal RNA operons of approximately 5 kb each (Petes and Hill, 1988). A relatively frequent class of DNA duplications and deletions involving ribosomal RNA operons involve recombination between the *E. coli rrnB* and *rrnE* operons, which lie in direct orientation with 39.5 kb of intervening DNA (Hill *et al.*, 1977). Similarly, the analysis of duplications along the *S. typhimurium* chromosome showed that tandem duplications involving the *ilv*, *metF*, *leu* or *thr* genes very often had duplication endpoints mapping to *rrn* operons that flank the duplicated region in a direct orientation (Anderson and Roth, 1978).

The substrate homology requirements of *E. coli* recombination *in vivo* were analyzed using lambda phage and plasmid vectors to correlate the rate of recombination with the length and degree of the homologous regions (Shen and Huang, 1986). The results indicated that a minimum length of uninterrupted homology was required for efficient recombination, and that the length of the minimal efficient processing segments (MEPS) in *E. coli* was 23–27 bp for the RecBC pathway and 44–90 bp for the RecF pathway (Shen and Huang, 1986). Similar

analyses of homology requirements in mammalian recombination were carried out using a simian virus 40–pBR322 hybrid substrate in cultured monkey cells, indicating a minimum homology requirement (MEPS) above 200 bp for the major pathway of extrachromosomal recombination in mammalian cells (Rubnitz and Subramani, 1984). Furthermore, the extrachromosomal recombination frequency increased linearly with length of substrate homology over a range of 0.25–5 kb (Rubnitz and Subramani, 1984). A related study of intrachromosomal recombination in mouse cells showed that a minimum stretch between 134 and 232 bp of perfect sequence homology was required for efficient recombination (Waldman and Liskay, 1988). It was also shown that single base-pair mismatches interrupting continuous stretches of homology had a more detrimental effect on intrachromosomal recombination rather than on extrachromosomal recombination, denoting differences in the two mechanisms (Waldman and Liskay, 1987). Furthermore, gene targeting experiments in mouse embryonic stem cells showed that the gene targeting frequency increases approximately 200–fold as homology is increased from 1.3 to 6.8 kb in replacement and insertion vectors (Hasty *et al.*, 1991).

The preceding experiments mostly involved recombination substrates separated by a few kilobases of DNA, while the CMT1A duplication/HNPP deletion at 17p11.2p12 involves large CMT1A-REP repeat sequences that are separated by 1.5–Mb of DNA. These distant CMT1A-REP sequences could perhaps be brought into close proximity by higher order chromatin structures. Chromatin loops contain an average of 50–100 kb of DNA in human metaphase chromosomes, and the scaffolding organization appears to be mediated by the interaction of "scaffold associated regions" (SAR) with DNA-binding proteins such as topoisomerase II and histone H1 (Gasser *et al.*, 1986; Laemmli *et al.*, 1992). The recombination at misaligned CMT1A-REP repeats may require a considerably larger MEPS unit of uninterrupted sequence identity to facilitate unequal crossing over at meiosis. Nucleotide sequence analysis of the proximal and distal CMT1A-REP repeats, and the fusion CMT1A-REP sequences will be required to delimit the crossover regions for the CMT1A duplication and the HNPP deletion. This sequence information could enable the design of PCR primers flanking the crossover points that could lead to the development of a rapid and efficient PCR assay for the CMT1A duplication and the HNPP deletion.

DNA Rearrangements Associated with Disease Phenotypes

The CMT1A/HNPP region flanked by CMT1A-REP and the globin gene clusters of tandemly duplicated genes represent comparable systems where un-

equal homologous recombination apparently occurs at flanking homologous regions in direct orientation. DNA rearrangements associated with thalassemia are well-characterized, in which thalassemia may result from a reduction in α or β globin gene dosage by deletion events at tandemly repeated globin gene clusters (Maniatis, 1980; Weatherall and Clegg, 1982). The α globin gene cluster on chromosome 16p, which spans approximately 30kb, includes a single embryonic globin gene, three pseudogenes, and the functional adult α_1 and α_2 genes (5′-ζ_2-$\psi\zeta_1$-$\psi\alpha_2$-$\psi\alpha_1$-α_2-α_1-θ-3′) (Lauer *et al.*, 1980). The different classes of α-globin gene rearrangements include short α–thal-2 deletions that eliminate one α globin gene as an apparent result of unequal crossing over between the α_1 and α_2 genes (Maniatis, 1980; Weatherall and Clegg, 1982). Individuals were identified with the apparent reciprocal recombinant chromosome containing three copies of α instead of the normal two copies (Goosens *et al.*, 1980; Zimmer *et al.*, 1980; Shimizu *et al.*, 1986). The β globin gene cluster on chromosome 11 has a similar structure of tandemly arrayed genes (5′-ε-$^{G}\gamma$-$^{A}\gamma$-$\psi\beta$-δ-β-3′), which includes a functional embryonic ε globin gene, two fetal γ genes, and one pseudogene, and two functional adult δ and β globin genes (Slightom *et al.*, 1980; Shen *et al.*, 1981). The identification of the Hb Lepore type encoding a β–type fusion protein (N′δ, C′β) in β-thalassemia provided the classic evidence for deletion resulting from unequal crossing over between highly homologous linked genes (Baglioni, 1962). Different Hb Lepore types were further differentiated on the basis of their respective deletion crossover regions (Metzenberg *et al.*, 1991). In addition, gamma thalassemia has been associated with fetal γ gene deletion, wherein unequal crossing over between the $^{G}\gamma$ and $^{A}\gamma$ genes apparently results in a fusion $^{G}\gamma^{A}\gamma$ gene (Sukumaran *et al.*, 1983). The apparent reciprocal duplication chromosome carrying three copies of γ was similarly identified in multiple individuals from different ethnic groups (Trent *et al.*, 1981; Liu *et al.*, 1988).

While some parallels may be drawn between CMT1A/HNPP and the thalassemias, it must be noted that the disease phenotypes are elicited by dosage effects of different regions relative to the endpoints of the duplication/deletion. CMT1A and HNPP apparently depend on the dosage of the *PMP22* gene that lies *between* the flanking CMT1A-REP sequences where recombination occurs. On the other hand, thalassemias are associated with reduced dosage of tandem globin genes, which also appear to be the endpoints of the DNA rearrangements in most cases (Maniatis, 1980; Weatherall and Clegg, 1982).

CMT1A and HNPP may be thought of as examples of a "genomic disease," whose mutational mechanism is a function of intrinsic structural features located at the 17p11.2p12 region of the human genome. The CMT1A duplication is not strictly an ancient inherited mutation, but one that has arisen repeatedly in *de novo*

cases. Other examples of "genomic diseases" would include thalassemias resulting from DNA rearrangements at tandemly duplicated α-like and β-like genes on chromosome 16 and 11, respectively. A more recently characterized example is the X-linked severe hemophilia A, which can be caused by inversions that disrupt the factor VIII gene. These inversions apparently result from intrachromosomal crossover between an A gene located within the factor VIII gene, and either of two A genes lying outside the factor VIII gene in an inverse orientation (Lakich *et al.*, 1993). It remains to be seen whether other genetic diseases such as contiguous gene deletion syndromes are generated by a similar mechanism of homologous recombination at flanking repeat sequences.

CONCLUSIONS

The molecular analysis of Charcot-Marie-Tooth disease has been highly informative in elucidating the underlying causes of this genetically heterogeneous nerve disorder. The cytogenetically undetectable CMT1A duplication of 3.0 Mb, which includes the *PMP22* gene was found to be the major cause of demyelinating CMT type 1. This presents a novel mechanism whereby increased gene dosage due to a submicroscopic DNA duplication results in an autosomal dominantly inherited disorder. Alternatively, CMT1A can be caused by point mutation of the *PMP22* gene in the absence of DNA duplication. Thus far, three genes have been identified for subtypes of demyelinating CMT type 1: the *PMP22* gene of CMT1A, the *MPZ* gene of CMT1B, and the *Cx32* gene of CMTX. The proteins respectively encoded by these genes are illustrated in Fig. 4. The identification of multiple mutations, particularly in the case of the *MPZ* gene, has enabled structure-function correlations that are important to elucidating the CMT disease process and the basic biology of the peripheral nerve.

The *PMP22* gene has been particularly interesting due to its involvement in alternative mutational mechanisms, and in different primary inherited peripheral neuropathies. Increased dosage of *PMP22* through duplication (three copies of *PMP22* versus two normal copies) is apparently the major cause of CMT1A. It appears that other Mendelian disorders apart from CMT can also be secondary to gene dosage effects. The dysmyelinating neuropathy Pelizaeus-Merzbacher disease is associated with duplication of the *PLP* gene, which encodes the proteolipid protein of central nervous system myelin (Cremers *et al.*, 1987; Ellis *et al.*, 1993). Interestingly, PLP bears some structural similarity to PMP22 as illustrated in Fig. 4. Autosomal dominant retinitis pigmentosa provides another example, where transgenic mice expressing increased levels of the normal human rhodopsin gene

were shown to develop photoreceptor degeneration characteristic of the disease (Olsson *et al.*, 1992).

On the other hand, underexpression of *PMP22*, mainly through the reciprocal deletion, is associated with the distinct demyelinating disorder HNPP. CMT1A and HNPP provide a key example in which human Mendelian disorders arise by means of reciprocal duplication/deletion events generated by unequal crossing over (Chance *et al.*, 1993; Chance *et al.*, 1994). Although multiple genes may lie in the 1.5–Mb CMT1A duplication/HNPP deletion region, the collective evidence strongly points to *PMP22* as the key dosage-sensitive gene. The *PMP22* gene is contained within the reduced critical region of 460-kb defined by an alternative CMT1A duplication (Valentijn *et al.*, 1993). Also, an apparent loss of function mutation in *PMP22* results in the HNPP phenotype (Nicholson *et al.*, 1994). This demonstrates that underexpression of PMP22 alone, out of all the potential genes in the 1.5–Mb deletion region, is sufficient to cause HNPP. The CMT1A and HNPP disease states associated with *PMP22* copy number differences due to reciprocal DNA duplication/deletion provide a novel example in humans wherein a full range of dosage of a particular gene results in distinct phenotypic consequences (Chance *et al.*, 1993). Moreover, these findings serve to blur the artificial boundaries between two major classes of genetic diseases: single gene disorders that segregate in a Mendelian pattern, and chromosome aberration syndromes resulting from either altered chromosome number (aneuploidies) or altered chromosome structure (microduplication or microdeletion syndromes).

In the absence of gene dosage effects due to duplication, CMT1A can be caused by autosomal dominant and apparent autosomal recessive point mutation alleles of the *PMP22* gene. Dominant point mutation alleles of *PMP22* that predict single amino acid substitutions can also give rise to Dejerine-Sottas syndrome. A similar case is seen with the *MPZ* gene, where allelic mutations in *MPZ* are associated with CMT1B and with Dejerine-Sottas syndrome. These findings indicate that CMT type 1 and Dejerine-Sottas syndrome represent a spectrum of overlapping clinical phenotypes sharing common genetic bases. Furthermore, the identification of heterozygous *de novo* point mutations in *PMP22* and *MPZ* demonstrates that Dejerine-Sottas syndrome, which was largely considered to be an autosomal recessive disorder, could actually arise from autosomal dominant new mutations in myelin genes.

The molecular studies on CMT have significantly advanced our understanding of the disease processes involved, and ongoing investigations continue to yield additional information. A fundamental understanding of the underlying disease mechanisms could provide a foundation for the eventual development of therapeutic regimens for CMT. Gene replacement strategies have been successful in

disorders such as adenosine deaminase deficiency, where the defect can be compensated by supplying the functional gene (Anderson, 1992). This approach may be of limited efficacy for CMT1 however, since the majority of cases are caused by DNA duplication apparently leading to increased dosage of a normal *PMP22* gene. Gene replacement could potentially apply to cases of inherited primary peripheral neuropathy, where loss of gene function is the underlying defect. For the majority of cases involving the CMT1A duplication, down-regulation of gene expression by using antisense nucleic acid constructs could theoretically be considered (Wickstrom, 1991). It should be kept in mind, however, that the *PMP22* gene is extremely dosage sensitive, and that reduced expression of *PMP22* below a certain threshold apparently leads to the different, although relatively less severe neurological phenotype of HNPP. Apart from gene therapy, conventional drug design could lead to a viable therapeutic regimen. Nevertheless, a comprehensive understanding of the molecular mechanisms responsible for CMT is required for the development of any effective therapeutic intervention for the most common inherited primary peripheral neuropathy. The studies on Charcot-Marie-Tooth disease have already generated a considerable amount of exciting information, which have provided insights extending to the molecular bases of human inherited disease at large.

ACKNOWLEDGMENTS We are grateful to the CMT patients and their families for their cooperation and collaboration, and we thank the members of the Lupski laboratory for their hard work. This research was made possible by the generous support of the Muscular Dystrophy Association; the National Institute of Neurological Disorders and Stroke, National Institutes of Health; the Texas Higher Education Advanced Technology Program; the Baylor Human Genome Center; the Baylor Mental Retardation Research Center; and the Texas Children's Hospital General Clinical Research Center. Benjamin B. Roa is a postdoctoral fellow of the Muscular Dystrophy Association. James R. Lupski acknowledges the support of the Pew Scholars Program in Biomedical Sciences.

REFERENCES

Allan, W., 1939, Relation of hereditary pattern to clinical severity as illustrated by peroneal atrophy, *Arch. Intern. Med.* **63:**1123–1131.

Anderson, R.P., and Roth, J.R., 1978, Gene duplication in bacteria: alteration of gene dosage by sister-chromatid exchanges, *Cold Spring Harbor Symp. Quant. Biol.* **43:**1083–1087.

Anderson, W.F., 1992, Human gene therapy, *Science* **256:**808–813.

Baglioni, C., 1962, The fusion of two polypeptide chains in hemoglobin Lepore and its interpretation as a genetic deletion, *Proc. Natl. Acad. Sci. USA* **48:**1880–1885.

Bellone, E., Mandich, P., Mancardi, G.L., Schenone, A., Uccelli, A., Abbruzzese, M., Sghirlanzoni, A., Pareyson, D., and Ajmar, F. 1992, Charcot-Marie-Tooth (CMT) c1a duplication in 17p11.2 in Italian families, *J. Med. Genet.* **29:**492–493.

Ben Othmane, K., Hentati, F., Lennon, F., Ben Hamida, C., Blel, S., Roses, A.D., Pericak-Vance, M.A., Ben Hamida, M., and Vance, J.M., 1993a, Linkage of a locus (CMT4A) for autosomal recessive Charcot-Marie-Tooth disease to chromosome 8q, *Hum. Mol. Genet.* **2:**1625–1628.

Ben Othmane, K., Middleton, L.T., Loprest, L.J., Wilkinson, K.M., Lennon, F., Rozear, M.P., Stajich, J.M., Gaskell, P.C., Roses, A.D., Pericak-Vance, M.A., and Vance, J.M., 1993b, Localization of a gene (CMT2A) for autosomal dominant Charcot-Marie-Tooth disease type 2 to chromosome 1p and evidence of genetic heterogeneity, *Genomics* **17:**370–375.

Bergoffen, J., Scherer, S.S., Wang, S., Oronzi Scott, M., Bone, L.J., Paul, D.L., Chen, K., Lensch, M.W., Chance, P.F., and Fischbeck, K.H., 1993a, Connexin mutations in X-linked Charcot-Marie-Tooth disease, *Science* **262:**2039–2042.

Bergoffen, J., Trofatter, J., Pericak-Vance, M., Haines, J.L., Chance, P.F., and Fischbeck, K.H., 1993b, Linkage localization of X-linked Charcot-Marie-Tooth disease, *Am. J. Hum. Genet.* **52:**312–318.

Bird, T.D., Ott, J., and Gilblett, E.R., 1982, Evidence for linkage of Charcot-Marie-Tooth disease neuropathy to the Duffy locus on chromosome number 1, *Am. J. Hum. Genet.* **34:**388–394.

Bird, T.D., and Kraft, G.H., 1978, Charcot-Marie-Tooth disease: data for genetic counseling relating age to risk, *Clin. Genet.* **14:**43–49.

Bordo, D., and Argos, P., 1991, Suggestions for "safe" residue substitutions in site-directed mutagenesis, *J. Mol. Biol.* **217:**721–729.

Brice, A., Ravise, N., Stevanin, G., Gugenheim, M., Bouche, P., Penet, C., Agid, Y., and the French CMT Research Group, 1992, Duplication within chromosome 17p11.2 in 12 families of French ancestry with Charcot-Marie-Tooth disease type 1a, *J. Med. Genet.* **29:**807–812.

Bridges, C.B., 1936, The Bar "gene" a duplication, *Science* **83:**210–211.

Byers, P.H., 1989, Disorders of collagen biosynthesis and structure, in: *The Metabolic Basis of Inherited Disease* (C.R. Scriver, A.L. Beaudet, W.S. Sly, and D. Valle, eds.), pp. 2805–2842, McGraw-Hill, Inc., New York.

Chance, P.F., Bird, T.D., O'Connell, P., Lipe, H., Lalouel, J.-M., and Leppert, M., 1990, Genetic linkage and heterogeneity in type I Charcot-Marie-Tooth disease (hereditary motor and sensory neuropathy type I), *Am. J. Hum. Genet.* **47:**915–925.

Chance, P.F., Bird, T.D., Matsunami, N., Lensch, M., Brothman, A.R., and Feldman, G.M., 1992a, Trisomy 17p associated with Charcot-Marie-Tooth neuropathy type 1A phenotype: evidence for gene dosage as a mechanism in CMT1A, *Neurology* **42:**2295–2299.

Chance, P.F., Matsunami, N., Lensch, W., Smith, B., and Bird, T.D., 1992b, Analysis of the DNA duplication 17p11.2 in Charcot-Marie-Tooth neuropathy type 1 pedigrees: additional evidence for a third autosomal CMT1 locus, *Neurology* **42:**2037–2041.

Chance, P.F., Alderson, M.K., Leppig, K.A., Lensch, M.W., Matsunami, N., Smith, B., Swanson, P.D., Odelberg, S.J., Disteche, C.M., and Bird, T.D., 1993, DNA deletion associated with hereditary neuropathy with liability to pressure palsies, *Cell* **72:**143–151.

Chance, P.F., Abbas, N., Lensch, M.W., Pentao, L., Roa, B.B., Patel, P.I., and Lupski, J.R., 1994, Two autosomal dominant neuropathies result from reciprocal DNA duplication/deletion of a region on chromosome 17, *Hum. Mol. Genet.* **3:**223–228.

Charcot, J.-M., and Marie, P., 1886, Sur une forme particuliere d'atrophie musculaire progressive, souvent familiale, debutant par les pieds et les jambes et atteignant plus tard les mains, *Rev. Med.* **6:**97–138.

Cooper, D.N., and Krawczak, M., 1990, The mutational spectrum of single base-pair substitutions, causing human genetic disease: patterns and predictions, *Hum. Genet.* **85:**55–74.

Coulondre, C., Miller, J.H., Farabaugh, P.J., and Gilbert, W., 1978, Molecular basis of base substitution hotspots in *Escherichia coli*, *Nature* **274:**775–780.

Cremers, F.P.M., Pfeiffer, R.A., van de Pol, T.J.R., Hofker, M.H., Kruse, T.A., Wieringa, B., and Ropers, H.H., 1987, An interstitial duplication of the X chromosome in a male allows fine physical mapping of probes from the Xq13-q22 region, *Hum. Genet.* **77:**23–27.

D'Urso, D., Brophy, P.J., Staugaitis, S.M., Gilespie, C.S., Frey, A.B., Stempak, J.G., and Colman, D.R., 1990, Protein zero of peripheral nerve myelin: biosynthesis, membrane insertion, and evidence for homotypic interaction, *Neuron* **2:**449–460.

De Jong, J.G.Y., 1947, Over families met hereditaire dispositie tot het optreden van neuritiden gecorreleered met migraine, *Psychiatr. Neurol. Bull.* **50:**60–76.

Dejerine, J., and Sottas, J., 1893, Sur la nevrite interstitielle, hypertrophique et progressive de l'enfance, *Comptes Rendus de la Societe de Biologie Paris* **45:**63–96.

Duncan, B.K., and Miller, J.H., 1980, Mutagenic deamination of cytosine residues in DNA, *Nature* **287:**560–561.

Dyck, P.J., Lambert, E.H., Sanders, K., and O'Brien, P.C., 1971, Severe hypomyelination and marked abnormality of conduction in Dejerine-Sottas hypertrophic neuropathy: Myelin thickness and compound action potentials of sural nerve in vitro, *Mayo Clin. Proc.* **46:**432–435.

Dyck, P.J., Oviatt, K.F., and Lambert, E.H., 1981, Intensive evaluation of referred unclassified neuropathies yields improved diagnosis, *Ann. Neurol.* **10:**222–226.

Dyck, P.J., Chance, P., Lebo, R., and Carney, J.A., 1993, Hereditary motor and sensory neuropathies, in: *Peripheral Neuropathy* (P.J. Dyck, P.K. Thomas, J.W. Griffin, P.A. Low, and J.F. Poduslo, eds.), pp. 1094–1136, W.B. Saunders Company, Philadelphia.

Ellis, D., Strautnieks, S., and Malcolm, S., 1993, Pelizaeus-Merzbacher disease caused by a splice mutation of the proteolipid protein gene and a rearrangement leading to duplication, *Am. J. Hum. Genet.* **53** Suppl:1155.

Fairweather, N., Bell, C., Cochrane, S., Chelly, J., Wang, S., Mostacciuolo, M.L., Monaco, A.P., and Haites, N.E., 1994, Mutations in the connexin 32 gene in X-linked dominant Charcot-Marie-Tooth disease (CMTX1), *Hum. Mol. Genet.* **3:**29–34.

Filbin, M.T., Walsh, F.S., Trapp, B.D., Pizzey, J.A., and Tennekoon, G.I., 1990, Role of myelin P_0 protein as a homophilic adhesion molecule, *Nature* **344:**871–872.

Filbin, M.T., and Tennekoon, G.I., 1991, The role of complex carbohydrates in adhesion of the myelin protein, P_0, *Neuron* **7:**845–855.

Gal, A., Mucke, J., Theile, H., Wieacker, P.F., Ropers, H.H., and Wienker, T.F., 1985, X-linked dominant Charcot-Marie-Tooth disease: Suggestion of linkage with a cloned DNA sequence from the proximal Xq, *Hum. Genet.* **70:**38–42.

Garcia, C.A., Malamut, R., Parry, G., Lupski, J.R., and Patel, P.I., 1992, Clinical heterogeneity of HMSN-I in two pairs of identical twins, *Neurology* **40**(suppl):301.

Gasser, S.M., Laroche, T., Falquet, J., de la Tour, E.B., and Laemmli, U.K., 1986, Metaphase chromosome structure involvement of topoisomerase II, *J. Mol. Biol.* **188:**613–629.

Giese, K.P., Martini, R., Lemke, G., Soriano, P., and Schachner, M., 1992, Mouse P_0 gene disruption leads to hypomyelination, abnormal expression of recognition molecules, and degeneration of myelin and axons, *Cell* **71:**565–576.

Goosens, M., Dozy, A.M., Embury, S.H., Zacharides, Z., Hadjiminas, M., Stamatoyannopoulos, G., and Kan, Y.W., 1980, Triplicated α-globin loci in humans, *Proc. Natl. Acad. Sci. USA* **77:** 518–521.

Hallam, P.J., Harding, A.E., Berciano, J., Barker, D.F., and Malcolm, S., 1992, Duplication of part of chromosome 17 is commonly associated with hereditary motor and sensory neuropathy type 1 (Charcot-Marie-Tooth disease type 1), *Ann. Neurol.* **31:**570–572.

Harding, A.E., and Thomas, P.K., 1980, Autosomal recessive forms of hereditary motor and sensory neuropathy, *J. Neurol. Neurosurg. Psych.* **43:**669–678.

Hasty, P., Rivera-Perez, J., and Bradley, A., 1991, The length of homology required for gene targeting in embryonic stem cells, *Mol. Cell. Biol.* **11**:5586–5591.

Hayasaka, K., Himoro, M., Sato, W., Takada, G., Uyemura, K., Shimizu, N., Bird, T.D., Conneally, P.M., and Chance, P.F., 1993a, Charcot-Marie-Tooth neuropathy type 1B is associated with mutations of the myelin P_0 gene, *Nature Genetics* **5**:31–34.

Hayasaka, K., Himoro, M., Sawaishi, Y., Nanao, K., Takahashi, T., Takada, G., Nicholson, G.A., Ouvrier, R.A., and Tachi, N., 1993b, *De novo* mutation of the myelin P_0 gene in Dejerine-Sottas disease (hereditary motor and sensory neuropathy type III), *Nature Genetics* **5**:266–268.

Hayasaka, K., Himoro, M., Wang, Y., Takata, M., Minoshima, S., Shimizu, N., Miura, M., Uyemura, K., and Takada, G., 1993c, Structure and chromosomal localization of the gene encoding the human myelin protein zero (MPZ), *Genomics* **17**:755–758.

Hayasaka, K., Ohnishi, A., Takada, G., Fukushima, Y., and Murai, Y., 1993d, Mutation of the myelin Po gene in Charcot-Marie-Tooth neuropathy type 1, *Biochem. Biophys. Res. Comm.* **194**:1317–1322.

Hayasaka, K., Takada, G., and Ionasescu, V.V., 1993e, Mutation of the myelin Po gene in Charcot-Marie-Tooth neuropathy type 1B, *Hum. Mol. Genet.* **2**:1369–1372.

Hensels, G.W., Janssen, E.A.M., Hoogendijk, J.E., Valentijn, L.J., Baas, F., and Bolhius, P.A., 1993, Quantitative measurement of duplicated DNA as a diagnostic test for Charcot-Marie-Tooth disease type 1a, *Clin. Chem.* **39**:1845–1849.

Hentati, A., Lamy, C., Melki, J., Zuber, M., Munnich, A., and de Recondo, J., 1992, Clinical and genetic heterogeneity of Charcot-Marie-Tooth disease, *Genomics* **12**:155–157.

Hill, C.W., Grafstrom, R.H., Harnish, B.W., and Hillman, B.S., 1977, Tandem duplications resulting from recombination between ribosomal RNA genes in *Escherichia coli*, *J. Mol. Biol.* **116**: 407–428.

Himoro, M., Yoshikawa, H., Matsui, T., Mitsui, Y., Takahashi, M., Kaido, M., Nishimura, T., Sawaishi, Y., Takada, G., and Hayasaka, K., 1993, New mutation of the myelin P_0 gene in a pedigree of Charcot-Marie-Tooth neuropathy type 1, *Biochem. Mol. Biol. Int.* **31**:169–173.

Hoogendijk, J.E., Hensels, G.W., Gabreels-Festen, A.A.W.M., Gabreels, F.J.M., Janssen, E.A.M., De Jonghe, P., Martin, J.-J., van Broeckhoven, C., Valentijn, L.J., Baas, F., de Visser, M., and Bolhius, P.A., 1992, *de novo* mutation in hereditary motor and sensory neuropathy type 1, *Lancet* **339**:1081–1082.

Hudson, L.D., 1990, Molecular biology of myelin proteins in the central and peripheral nervous systems, *Sem. Neurosci.* **2**:483–496.

Ionasescu, V.V., Ionasescu, R., and Searby, C., 1993a, Screening of dominantly inherited Charcot-Marie-Tooth neuropathies, *Muscle and Nerve* **16**:1232–1238.

Ionasescu, V.V. Ionasescu, R., Searby, C., and Barker, D.F., 1993b, Charcot-Marie-Tooth neuropathy type 1A with both duplication and non-duplication, *Hum. Mol. Genet.* **2**:405–410.

Ionasescu, V., Searby, C., and Ionasescu, R., 1994, Point mutations of the connexin32 (GJB1) gene in X-linked dominant Charcot-Marie-Tooth neuropathy, *Hum. Mol. Genet.* **3**:355–358.

Kaku, D.A., Parry, G.J., Malamut, R., Lupski, J.R., and Garcia, C.A., 1993a, Nerve conduction studies in Charcot-Marie-Tooth polyneuropathy associated with a segmental duplication of chromosome 17, *Neurology* **43**:1806–1808.

Kaku, D.A., Parry, G.J., Malamut, R., Lupski, J.R., and Garcia, C.A., 1993b, Uniform slowing of conduction velocities in Charcot-Marie-Tooth polyneuropathy type 1, *Neurology* **43**:2664–2667.

Killian, J.M., and Kloepfer, H.W., 1979, Homozygous expression of a dominant gene for Charcot-Marie-Tooth neuropathy, *Ann. Neurol.* **5**:515–522.

Kirschner, D.A., and Ganser, A.L., 1980, Compact myelin exists in the absence of basic protein in the shiverer mutant mouse, *Nature* **283**:207–210.

Kitamura, K., Suzuki, M., and Uyemura, K., 1976, Purification and partial characterization of two glycoproteins in bovine peripheral nerve myelin membrane, *Biochemica Biophysica Acta* **455**: 806–816.

Kulkens, T., Bolhius, P.A., Wolterman, R.A., Kemp, S., te Nijenhuis, S., Valentijn, L.J., Hensels, G.W., Jennekens, F.G.I., de Visser, M., Hoogendijk, J.E., and Baas, F., 1993, Deletion of the serine 34 codon from the major peripheral myelin protein P_0 gene in Charcot-Marie-Tooth disease type 1B, *Nature Genetics* **5**:35–39.

Laemmli, U.K., Kas, E., Poljak, L., and Adachi, Y., 1992, Scaffold-associated regions: *cis*-acting determinants of chromatin structural loops and functional domains, *Curr. Opin. Genet. Dev.* **2**: 275–285.

Lakich, D., Kazazian, H.H., Antonarakis, S.E., and Gitschier, J., 1993, Inversions disrupting the factor VIII gene are a common cause of severe haemophilia A, *Nature Genetics* **5**:236–241.

Latov, N., Hays, A.P., and Sherman, W.H., 1988, Peripheral neuropathy and anti-MAG antibodies, *CRC Crit. Rev. Neurobiol.* **3**:301–332.

Lauer, J., Shen, C.-K.J., and Maniatis, T., 1980, The chromosomal arrangement of human α-like globin genes: sequence homology and α-globin gene deletions, *Cell* **20**:119–130.

Lemke, G., 1988, Unwrapping the genes of myelin, *Neuron* **1**:535–543.

Lemke, G., Lamar, E., and Patterson, J., 1988, Isolation and analysis of the gene encoding peripheral myelin protein zero, *Neuron* **1**:73–83.

Lemke, G., 1993, The molecular genetics of myelination: An update, *GLIA* **7**:263–271.

Lemke, G., and Axel, R., 1985, Isolation and sequence of a cDNA encoding the major structural protein of peripheral myelin, *Cell* **40**:501–508.

Liu, J.Z., Gilman, J.G., Cao, Q., Bakioglu, I., and Huisman, T.H.J., 1988, Four categories of γ-globin gene triplications: DNA sequence comparison of low γ-G and high γ-A triplications, *Blood* **72**:480–484.

Loprest, L.J., Pericak-Vance, M.A., Stajich, J., Gaskell, P.C., Lucas, A.M., Lennon, F., Yamaoka, L.H., Roses, A.D., and Vance, J.M., 1992, Linkage studies in Charcot-Marie-Tooth disease type 2: evidence that CMT types 1 and 2 are distinct genetic entities, *Neurology* **42**:597–601.

Lupski, J.R., Garcia, C.A., Parry, G.J., and Patel, P.I., 1991a, Charcot-Marie-Tooth Polyneuropathy Syndrome: Clinical Electrophysiologic and Genetic Aspects, in: *Current Neurology* (S. Appel, ed.), pp. 1–25, Mosby-Yearbook, Chicago.

Lupski, J.R., Montes de Oca-Luna, R., Slaugenhaupt, S., Pentao, L., Guzzetta, V., Trask, B.J., Saucedo-Cardenas, O., Barker, D.F., Killian, J.M., Garcia, C.A., Chakravarti, A., and Patel, P.I., 1991b, DNA duplication associated with Charcot-Marie-Tooth disease type 1A, *Cell* **66**:219–232.

Lupski, J.R., 1992, An inherited DNA rearrangement and gene dosage effect are responsible for the most common autosomal dominant peripheral neuropathy: Charcot-Marie-Tooth disease type 1A, *Clinical Research* **40**:645–652.

Lupski, J.R., Wise, C.A., Kuwano, A., Pentao, L., Parke, J.T., Glaze, D.G., Ledbetter, D.H., Greenberg, F., and Patel, P.I., 1992, Gene dosage is a mechanism for Charcot-Marie-Tooth disease type 1A, *Nature Genetics* **1**:29–33.

Lupski, J.R., Chance, P.F., and Garcia, C.A., 1993a, Inherited primary peripheral neuropathies molecular genetics and clinical implications of CMT1A and HNPP, *JAMA* **270**:2326–2330.

Lupski, J.R., Pentao, L., Williams, L.L., and Patel, P.I. 1993b, Stable inheritance of the CMT1A DNA duplication in two patients with CMT1 and NF1, *Am. J. Med. Genet.* **45**:92–96.

Lupski, J.R., Molecular genetics of Charcot-Marie-Tooth disorders: DNA duplication and gene dosage as a novel mechanism for a common autosomal dominant trait, *Jikken Igaku* **12**:109–120.

Lupski, J.R., and Garcia, C.A., 1992, Molecular genetics and neuropathology of Charcot-Marie-Tooth disease type 1A, *Brain Pathology* **2**:337–349.

Lupski, J.R., and Weinstock, G.M., 1992, Short, interspersed repetitive DNA sequences in prokaryotic genomes. *J. Bacteriol.* **174**:4525–4529.

MacMillan, J.C., Upadhyaya, M., and Harper, P.S., 1992, Charcot-Marie-Tooth disease 1a (CMT1a): evidence for trisomy of the region p11.2 of chromosome 17 in South Wales families, *J. Med. Genet.* **29**:12–13.

Manfioletti, G., Ruaro, M.E., Del Sal, G., Philipson, L., and Schneider, C., 1990, A growth arrest-specific (*gas*) gene codes for a membrane protein, *Mol. Cell. Biol.* **10:**2924–2930.

Maniatis, T., Fritsch, E.F., Lauer, J., and Lawn, R.M., 1980, The molecular genetics of human hemoglobins, *Ann. Rev. Genet.* **14:**145–178.

Matsunami, N., Smith, B., Ballard, L., Lensch, M.W., Robertson, M., Albertsen, H., Hanemann, C.O., Muller, H.W., Bird, T.D., White, R., and Chance, P.F., 1992, Peripheral myelin protein-22 gene maps in the duplication in chromosome 17p11.2 associated with Charcot-Marie-Tooth 1A, *Nature Genetics* **1:**176–179.

McKusick, V.A., 1992, *Mendelian Inheritance in Man*, The Johns Hopkins University Press, Baltimore.

Metzenberg, A.B., Wurzer, G., Huisman, T.H.J., and Smithies, O., 1991, Homology requirements for unequal crossing over in humans, *Genetics* **128:**143–161.

Nicholson, G.A., 1991, Penetrance of the hereditary motor and sensory neuropathy Ia mutation: Assessment by nerve conduction studies, *Neurology* **41:**547–552.

Nicholson, G.A., Kennerson, M.L., Keats, B.J.B., Mesterovik, N., Churcher, W., Barker, D., and Ross, D.A., 1992, Charcot-Marie-Tooth neuropathy type 1A mutation: Apparent crossovers with D17S122 are due to a duplication, *Am. J. Med. Genet.* **44:**455–460.

Nicholson, G.A., Valentijn, L.J., Cherryson, A.K., Kennerson, M.L., Bragg, T.L., De Kroon, R.M., Ross, D.A., Pollard, J.D., McLeod, J.G., Bolhuis, P.A., and Baas, F., 1994, A frame shift mutation in the *PMP22* gene in hereditary neuropathy with liability to pressure palsies, *Nature Genetics* **6:**263–266.

Olsson, J.E., Gordon, J.W., Pawlyk, B.S., Roof, D., Hayes, A., Molday, R.S., Mukai, S., Cowley, G.S., Berson, E.L., and Dryja, T.P., 1992, Transgenic mice with a rhodopsin mutation (Pro23His): A mouse model of autosomal dominant retinitis pigmentosa, *Neuron* **9:**815–830.

Palau, F., Lofgren, A., De Jonghe, P., Bort, S., Nelis, E., Sevilla, T., Martin, J.J., Vilchez, J., Prieto, F., Van Broeckhoven, C., 1993, Origin of the *de novo* duplication in Charcot-Marie-Tooth disease type 1A: unequal nonsister chromatid exchange during spermatogenesis, *Hum. Mol. Genet.* **2:**2031–2035.

Patel, P.I., Roa, B.B., Welcher, A.A., Schoener-Scott, R., Trask, B.J., Pentao, L., Snipes, G.J., Garcia, C.A., Francke, U., Shooter, E.M., Lupski, J.R., Suter, U., 1992, The gene for the peripheral myelin protein *PMP-22* is a candidate for Charcot-Marie-Tooth disease type 1A, *Nature Genetics* **1:**159–165.

Patel, P.I., and Lupski, J.R., 1994, Charcot-Marie-Tooth disease: a new paradigm for the mechanism of inherited disease, *Trends in Genetics* **10:**128–133.

Pentao, L., Wise, C.A., Chinault, A.C., Patel, P.I., and Lupski, J.R., 1992, Charcot-Marie-Tooth type 1A duplication appears to arise from recombination at repeat sequences flanking the 1.5 Mb monomer unit, *Nature Genetics* **2:**292–300.

Petes, T.D., and Hill, C.W., 1988, Recombination between repeated genes in microorganisms, *Ann. Rev. Genet.* **22:**147–168.

Raeymaekers, P., Timmerman, V., Nelis, E., De Jonghe, P., Hoogendijk, J.E., Baas, F., Barker, D.F., Martin, J.J., De Visser M., Bolhuis, P.A., Van Broeckhoven, C., and the HMSN Collaborative Research Group, 1991, Duplication in chromosome 17p11.2 in Charcot-Marie-Tooth neuropathy type 1a (CMT1a), *Neuromuscular Disorders* **1:**93–97.

Raeymaekers, P., Timmerman, V., Nelis, E., Van Hul, W., De Jonghe, P., Martin, J.J., Van Broeckhoven, C., and the HMSN Collaborative Research Group, 1992, Estimation of the size of the chromosome 17p11.2 duplication Charcot-Marie-Tooth neuropathy type 1a (CMT1a), *J. Med. Genet.* **29:**5–11.

Roa, B.B., Dyck, P.J., Marks, H.G., Chance, P.F., and Lupski, J.R., 1993a, Dejerine-Sottas syndrome associated with point mutation in the peripheral myelin protein 22 (*PMP22*) gene, *Nature Genetics* **5:**269–273.

Roa, B.B., Garcia, C.A., Pentao, L., Killian, J.M., Trask, B.J., Suter, U., Snipes, G.J., Ortiz-Lopez, R., Shooter, E.M., Patel, P.I., and Lupski, J.R., 1993b, Evidence for a recessive *PMP22* point mutation in Charcot-Marie-Tooth disease type 1A, *Nature Genetics* **5:**189–194.

Roa, B.B., Garcia, C.A., Suter, U., Kulpa, D.A., Wise, C.A., Mueller, J., Welcher, A.A., Snipes, G.J., Shooter, E.M., Patel, P.I., and Lupski, J.R., 1993c, Charcot-Marie-Tooth disease type 1A: association with a spontaneous point mutation in the *PMP22* gene, *N. Engl. J. Med.* **329:**96–101.

Roa, B.B., Garcia, C.A., Wise, C.A., Anderson, K., Greenberg, F., Patel, P.I., and Lupski, J.R., 1993d, Gene dosage as a mechanism for a common autosomal dominant peripheral neuropathy: Charcot-Marie-Tooth disease type 1A, in: *Phenotypic Mapping of Down Syndrome and Other Aneuploid Conditions* (C.J. Epstein, ed.), Wiley-Liss, Inc., New York.

Rubnitz, J., and Subramani, S., 1984, The minimum amount of homology required for homologous recombination in mammalian cells, *Mol. Cell. Biol.* **4:**2253–2258.

Schneider, C., King, R.M., and Philipson, L., 1988, Genes specifically expressed at growth arrest of mammalian cells, *Cell* **54:**787–793.

Sghirlanzoni, A., Pareyson, D., Balestrini, M.R., Bellone, E., Berta, E., Ciano, C., Mandich, P., and Marazzi, R., 1992, HMSNIII phenotype due to homozygous expression of a dominant HMSNII gene, *Neurology* **42:**2201–2204.

Shen, P., and Huang, H.V., 1986, Homologous recombination in *Escherichia coli*: Dependence on substrate length and homology, *Genetics* **112:**441–457.

Shen, S., Slightom, J.L., and Smithies, O., 1981, A history of the human fetal globin gene duplication, *Cell* **26:**191–203.

Shimizu, K., Harano, T., Harano, K., Miwa, S., Amenomori, Y., Ohba, Y., Kutlar, F., and Huisman, T.H.J., 1986, Abnormal arrangements in the α- and γ-globin gene clusters in a relatively large group of Japanese newborns, *Am. J. Hum. Genet.* **38:**45–58.

Skre, H., 1974, Genetic and clinical aspects of Charcot-Marie-Tooth's disease, *Clin. Genet.* **6:**98–118.

Slightom, J.L., Blechl, A.E., and Smithies, O., 1980, Human fetal $^{G}\gamma$- and $^{A}\gamma$-globin genes: complete nucleotide sequences suggest that DNA can be exchanged between these duplicated genes, *Cell* **21:**627–638.

Smithies, O., Connell, G.E., and Dixon, G.H., 1962, Chromosomal rearrangements and the evolution of haptoglobin genes, *Nature* **196:**232–236.

Snipes, G.J., Suter, U., Welcher, A.A., and Shooter, E.M., 1992, Characterization of a novel peripheral nervous system myelin protein (PMP-22/SR13), *J. Cell. Biol.* **117:**225–238.

Spreyer, P., Kuhn, G., Hanemann, C.O., Gillen, C., Schaal, H., Kuhn, R., Lemke, G., and Muller, H.W., 1991, Axon-regulated expression of a Schwann cell transcript that is homologous to a 'growth arrest-specific' gene, *EMBO J.* **10:**3661–3668.

Sukumaran, P.K., Nakatsuji, T., Gardiner, M.B., Reese, A.L., Gilman, J.G., and Huisman, T.H.J., 1983, Gamma thalassemia resulting from the deletion of a γ-globin gene, *Nuc. Acids Res.* **11:** 4635–4643.

Suter, U., Moskow, J.J., Welcher, A.A., Snipes, G.J., Kosaras, B., Sidman, R.L., Buchberg, A.M., and Shooter, E.M., 1992a, A leucine-to-proline mutation in the putative first transmembrane domain of the 22-kDa peripheral myelin protein in the trembler-J mouse, *Proc. Natl. Acad. Sci. USA* **89:**4382–4386.

Suter, U., Welcher, A.A., Ozcelik T., Snipes, G.J., Kosaras, B., Francke, U., Billings-Gagliardi, S., Sidman, R.L., and Shooter, E.M., 1992b, *Trembler* mouse carries a point mutation in a myelin gene, *Nature* **356:**241–244.

Suter, U., Welcher, A.A., and Snipes, G.J., 1993, Progress in the molecular understanding of hereditary peripheral neuropathies reveals new insights into the biology of the peripheral nervous system, *Trends Neurosci.* **16:**50–56.

Timmerman, V., Nelis, E., Van Hul, W., Nieuwenhuijsen, B.W., Chen, K.L., Wang, S., Ben Othman, K., Cullen, B., Leach, R.J., Hanemann, C.O., De Jonghe, P., Raeymaekers, P., van Ommen,

G.-J.B., Martin, J.-J., Muller, H.W., Vance, J.M., Fischbeck, K.H., and Van Broeckhoven, C., 1992, The peripheral myelin protein gene *PMP-22* is contained within the Charcot-Marie-Tooth disease type 1A duplication, *Nature Genetics* **1**:171–175.

Tooth, H.H., 1886, *The Peroneal Type of Progressive Muscular Atrophy*, H.K. Lewis, London.

Trent, R.J., Bowden, D.K., Old, J.M., Wainscoat, J.S., Clegg, J.B., and Weatherall, D.J., 1981, A novel rearrangement of the human β-like globin gene cluster, *Nuc. Acids Res.* **9**:6723–6733.

Upadhyaya, M., Roberts, S.H., Farnham, J., MacMillan, J.C., Clarke, A., Heath, J.P., Hodges, I.C.G., and Harper, P.S., 1993, Charcot-Marie-Tooth disease 1A (CMT1A) associated with a maternal duplication of chromosome 17p11.2-12, *Hum. Genet.* **91**:392–394.

Valentijn, L.J., Baas, F., Wolterman, R.A., Hoogendijk, J.E., van den Bosch, N.H.A., Zorn, I., Gabreels-Festen, A.A.W.M., de Visser, M., and Bolhuis, P.A., 1992a, Identical point mutations of *PMP-22* in *Trembler*-J mouse and Charcot-Marie-Tooth disease type 1A, *Nature Genetics* **2**:288–291.

Valentijn, L.J., Bolhuis, P.A., Zorn, I., Hoogendijk, J.E., van den Bosch, N., Hensels, G.W., Stanton, V.P., Housman, D.E., Fischbeck, K.H., Ross, D.A., Nicholson, G.A., Meershoek, E. J., Dauwerse, H.G., van Ommen, G.J.B., and Baas, F., 1992b, The peripheral myelin gene *PMP-22/GAS-3* is duplicated in Charcot-Marie-Tooth disease type 1A, *Nature Genetics* **1**:166–170.

Valentijn, L.J., Baas, F., Zorn, I., Hensels, G.W., De Visser M., and Bolhius, P.A., 1993, Alternatively sized duplication in Charcot-Marie-Tooth disease type 1A, *Hum. Mol. Genet.* **2**:2143–2146.

Vance, J.M., Nicholson, G.A., Yamaoka, L.H., Stajich, J., Stewart, C.S., Speer, M.C., Hung, W.-Y., Roses, A.D., Barker, D.F., and Pericak-Vance, M.A., 1989, Linkage of Charcot-Marie-Tooth neuropathy type 1a to chromosome 17, *Exp. Neurol.* **104**:186–189.

Waldman, A.S., and Liskay, R.M., 1987, Differential effects of base-pair mismatch on intrachromosomal versus extrachromosomal recombination in mouse cells, *Proc. Natl. Acad. Sci. USA* **84**: 5340–5344.

Waldman, A.S., and Liskay, R.M., 1988, Dependence of intrachromosomal recombination in mammalian cells on uninterrupted homology, *Mol. Cell. Biol.* **8**:5350–5357.

Weatherall, D.J., and Clegg, J.B., 1982, Thalassemia revisited, *Cell* **29**:7–9.

Welcher, A.A., Suter, U., De Leon, M., Snipes, G.J., and Shooter, E.M., 1991, A myelin protein is encoded by the homologue of a growth arrest-specific gene, *Proc. Natl. Acad. Sci. USA* **88**:7195–7199.

Wickstrom, E., (ed.) 1991, *Prospects for Antisense Nucleic Acid Therapy of Cancer and AIDS*, Wiley-Liss, New York.

Windebank, A. J., 1993, Inherited recurrent focal neuropathies, in: *Peripheral Neuropathy* (P.J. Dyck, P.K. Thomas, J.W. Griffin, P.A. Low, and J.F., Poduslo, eds.), pp. 1137–1148, W.B. Saunders, Philadelphia.

Wise, C.A., Garcia, C.A., Davis, S.N., Heju, Z., Pentao, L., Patel, P.I., and Lupski, J.R., 1993, Molecular analyses of unrelated Charcot-Marie-Tooth (CMT) disease patients suggest a high frequency of the CMT1A duplication, *Am. J. Hum. Genet.* **53**:853–863.

Zimmer, E.A., Martin, S.L., Beverly, S.M., Kan, Y.W., and Wilson, A.C., 1980, Rapid duplication and loss of genes coding for the α chains of hemoglobin, *Proc. Natl. Acad. Sci. USA* **77**:2158–2162.

Chapter 4

Marfan's Syndrome and Other Microfibrillar Diseases

Harry C. Dietz

Departments of Pediatrics, Medicine, and Molecular Biology and Genetics
Johns Hopkins University School of Medicine
Baltimore, Maryland

Francesco Ramirez

Brookdale Center for Molecular Biology
Mount Sinai School of Medicine
New York, New York

Lynn Y. Sakai

Shriners Hospital for Crippled Children
and Department of Biochemistry and Molecular Biology
Oregon Health Sciences University
Portland, Oregon

INTRODUCTION

During the past twenty years, the molecular causes of several heritable disorders of connective tissue have been firmly established. These advances have been facilitated by the development of new means of experimental analysis, and by the identification of new extracellular matrix (ECM) components. Most of the progress has increased our understanding of collagenopathies and the contribution of the fibrillar collagens to the structural integrity of bone, cartilage, skin, ligaments and internal organs (Lee *et al.*, 1991a). We have also discovered causal associations between mutations in nonfibrillar collagens and the clinical manifestations of

Advances in Human Genetics, Volume 22, edited by Henry Harris and Kurt Hirschhorn. Plenum Press, New York, 1994.

epidermolysis bullosa, Alport's syndrome, and the Schmid form of metaphyseal chondrodysplasia (Uitto and Christiano, 1992; Hudson *et al.*, 1993; Jacenko *et al.*, 1994).

Progress has also occurred in the study of noncollagenous connective tissue disorders. Advances in elastic fiber biology have led to the recent linkage between the phenotype of Marfan's syndrome (MFS) and mutations in fibrillin, a component of the elastic fiber (Ramirez *et al.*, 1993). MFS is a systemic disorder with autosomal dominant mode of inheritance and cardinal manifestations in the ocular, skeletal, and cardiovascular systems. The first evidence for a possible involvement of fibrillin in the pathogenesis of MFS came with the immunolocalization of this protein to the many tissues altered in the disease phenotype (Sakai *et al.*, 1986). Subsequently it was observed that immunofluorescence with antifibrillin antibodies was substantially less in MFS samples than control samples (Hollister *et al.*, 1990). This was later supported by a biosynthetic study showing abnormal fibrillin in cultured fibroblasts from individuals with MFS (McGookey-Milewicz *et al.*, 1992). The cloning work of Lee *et al.* (1991b) and Maslen *et al.* (1991) derived part of the fibrillin structure, and mapped the gene (FBN1) to the same region of chromosome 15 where the MFS locus had been previously located (Kainulainen *et al.*, 1990). Finally, the first FNB1 mutation was identified in two sporadic cases of MFS (Dietz *et al.*, 1991). The FBN1 gene was also associated with dominantly inherited ectopia lentis (EL) (Tsipouras *et al.*, 1992). In addition, the cloning work identified a second fibrillin transcript from a gene (FBN2) located on chromosome 5 and genetically linked to the congenital contractural arachnodactyly (CCA) phenotype (Lee *et al.*, 1991b). This rare connective tissue disorder has significant clinical overlap with MFS, including all typical skeletal features but no ocular or aortic involvement (Beals and Hecht, 1971).

Altogether, these findings raised the possibility that abnormalities related to microfibrils might form the basis for a variety of diseases with features similar to those found in MFS. In addition, they implied that mutations in microfibrillar components other than fibrillin may also lead to phenotypes that could ultimately be classified as microfibrillar diseases. In this chapter, we will discuss with recent advances in microfibril biology with particular reference to our current understanding of MFS pathogenesis.

ELASTIC FIBERS AND MICROFIBRILS

Elastic fibers, the supramolecular aggregates ubiquitously distributed in the ECM of elastic tissues (Cleary and Gibson, 1983), consist of two morphologically

distinct components: a core of elastin and a sheath of microfibrils (Fig. 1). Microfibrils can also be found without association with elastin in both elastic and nonelastic tissues.

Using conventional electron microscopic techniques, microfibrils can easily be distinguished from banded collagen fibers. Individual microfibrils have a uniform diameter of about 10–12 nm and display no periodic banding pattern, unlike collagen fibers, which have variable diameters and a clear banding pattern. Microfibrils are organized into fiber bundles rather than into webs or nets of individual strands. In longitudinal sections, microfibrils display characteristic light and dark staining patterns, giving the microfibril a beaded appearance (Fig. 2); in cross sections, microfibrils can appear to be hollow. In elastic fibers, microfibrils form a peripheral mantle and are also thought to be embedded within the amorphous elastin core (Fig. 1).

Organization and Distribution

The gross organization of elastic fibers and microfibrils varies in the different connective tissues. In skin, a network of elastic fibers containing differing ratios of elastin and microfibrils has been described. At the dermal–epidermal junction, bundles of microfibrils that have little to no association with elastin extend perpendicularly toward the dermal–epidermal junction. These microfibrils have been called "oxytalan" fibers. Deeper in the dermis, and coursing in a more parallel direction to the dermal–epidermal junction, are thicker elastic fibers with large amorphous elastin cores. Connecting the bundles of microfibrils at the dermal–epidermal junction with the deep dermal elastic fibers are "elaunin fibers" or bundles of microfibrils with small, varying amounts of amorphous elastin (Cotta-Pereira *et al.*, 1976). Oxytalan and elaunin fibers have been thought to be "immature" forms of elastic fiber. The light microscopic pattern of the elastic fiber network in skin is easily distinguished (Dahlback *et al.*, 1990) (Fig. 3*a*).

Elastic fibers are abundant in blood vessel walls. In this connective tissue, elastic fibers form concentric rings around the lumen of the vessel (Fig. 3*b*). Several layers of elastic lamellae are connected with one another by finer elastic fibers. Smooth muscle in other tissues, such as stomach and uterus, is also well-endowed with elastic fibers. Ligaments and tendons are also rich in elastic fibers. In these tissues, the fibers are characteristically long with parallel orientation, following the basic tissue organization. Elastic fibers are a predominant structural feature of the developing cartilage, where they form a large circumference. In perichondrium and periosteum, elastic fibers are long and they appear to intercon-

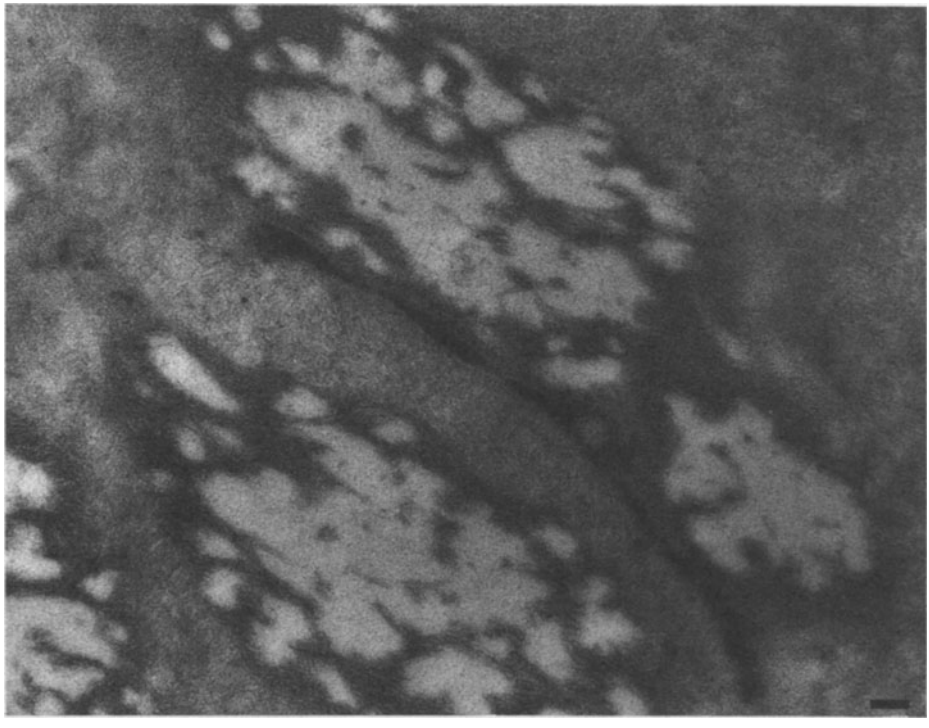

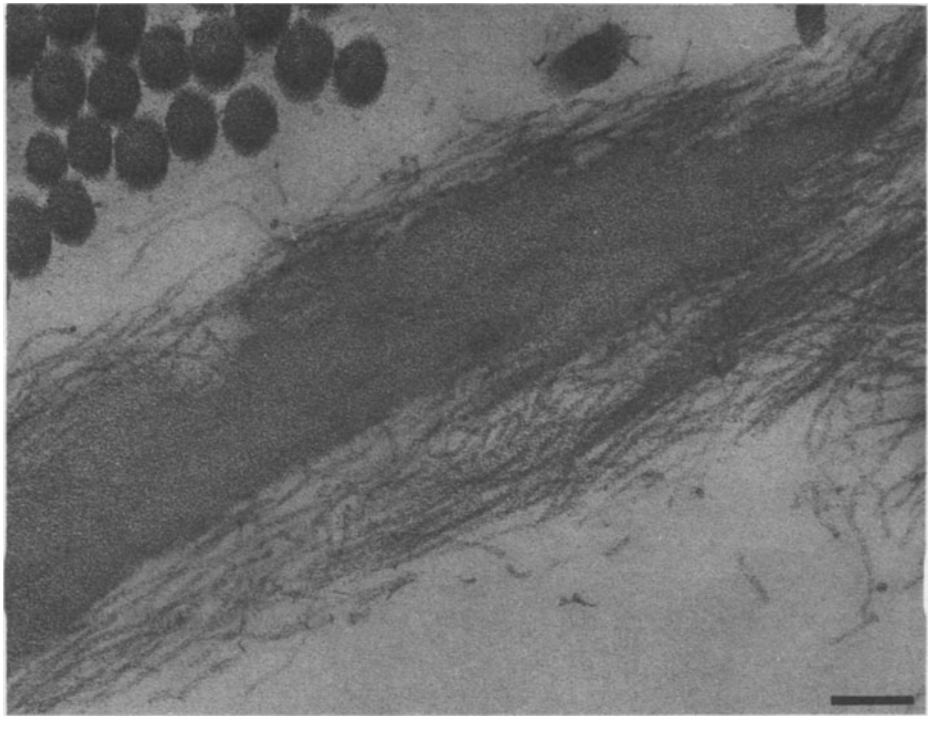

nect with merging elastic fibers from tendons and with finer fibers within the cartilage matrix. In cartilage, the finer fibers appear to be organized in a honeycomb configuration. In elastic cartilage, they contain both elastin and fibrillin; in hyaline cartilage, they are solely made of fibrillin. Microfibrils and elastic fibers are present in many other connective tissues, like the dural sheaths, the thin sheaths around muscles and nerves (Fig. 3*c*), and in areas close to basement membranes (e.g., lung alveolar connective tissue and kidney glomerulus). However, in tissues which have only small amounts of matrix, the histological significance of microfibrils and elastin fibers is unclear.

As mentioned, some tissues contain microfibrils without elastin: the corneal stroma, where microfibrillar fiber bundles are highly organized (Burns *et al.*, 1987); and the ciliary zonule (Raviola, 1971), the suspensory ligament that connects the muscles at the wall of the eye directly to the surface of the lens (Fig. 4). Zonular microfibrils travel across the surface of the lens until they appear to merge directly into the basement membrane of the lens capsule. The ciliary zonule appears to be composed solely of microfibrils, with no other structural elements (Fig. 4).

Composition

Cross-linked elastin constitutes the amorphous core of the elastic fibers. Elastin is a hydrophobic protein initially synthesized in a precursor form, tropoelastin, with a molecular weight of about 72,000. Elastin is relatively rich in glycine and proline and, to a lesser extent, lysine. Unlike those of collagen, the proline residues of elastin are not subjected to posttranslational modifications. The tropoelastin structure consists of an alternating series of several hydrophilic and hydrophobic segments. Within the highly basic carboxy-terminus is a conserved 14 amino acid sequence containing two cysteines (Rosenbloom *et al.*, 1993).

The polyfunctional cross-links of elastin involve the posttranslational modification of most of the 40 lysyl residues by the enzyme lysyl oxidase. A pair of lysines is usually located in the intercalating hydrophilic segments of the tropoelastin molecule. The composition and organization of these cross-linking sites

←

Fig. 1. Elastic fibers in skin visualized by transmission electron microscopy with high pressure cryopreservation techniques (top), and with conventional fixation techniques (bottom). Conventional fixation and embedding techniques lead to the loss of some ECM components, which are better preserved by the high pressure freezing technique. The ECM around microfibrils and in the "spaces" between collagen fibers and elastic fibers is actually densely occupied, suggesting noncovalent interactions between the structural components of the fibrous elements (which remain after conventional fixation) and other ECM components. Bars = 150 μm.

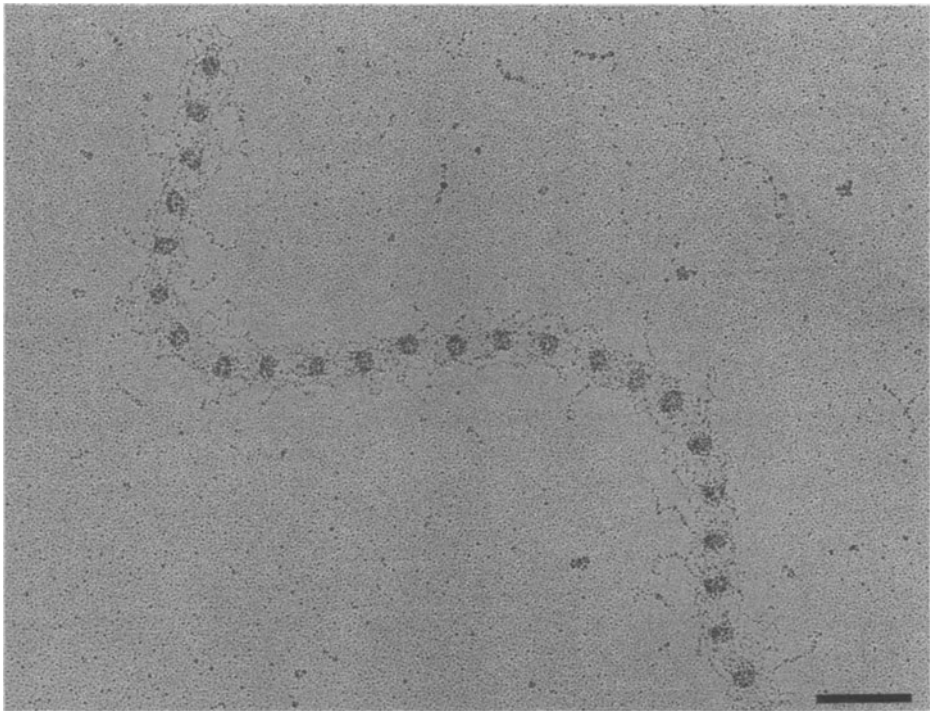

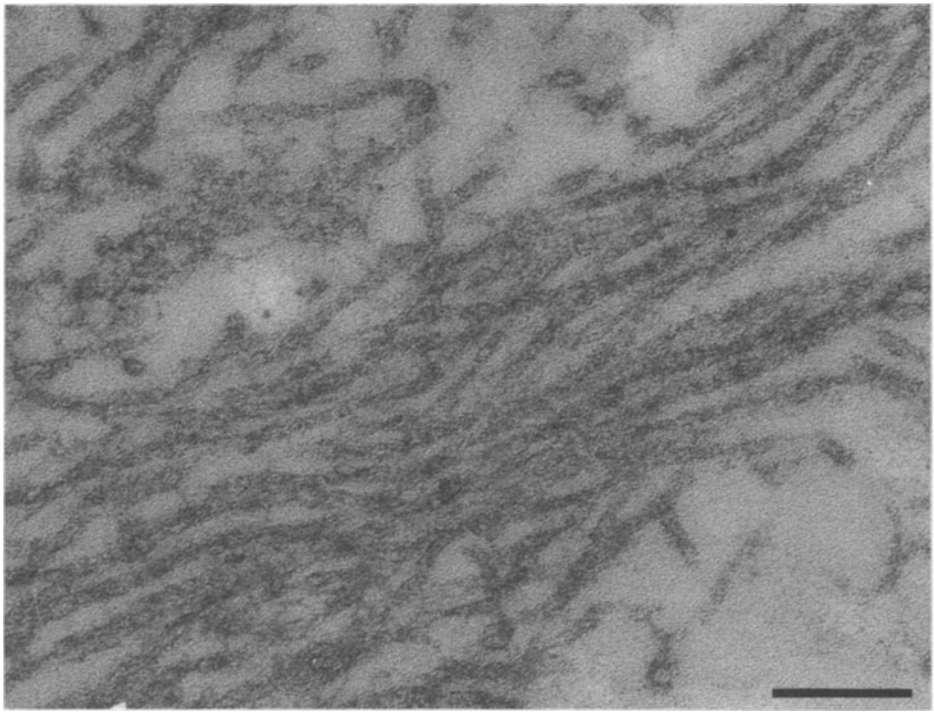

across the taxa are strictly maintained (Rosenbloom *et al.*, 1993). Mature elastin protein has several isoforms, but their functional significance is still the subject of speculation (Raju and Anwar, 1987; Indik *et al.*, 1987). Rosenbloom *et al.* (1993) postulate that the elastin isoforms may produce tighter or looser networks by changing the relative distance between two adjacent cross-linking sites. Another structural property of the elastin molecule, notably its ability of adopting various random-coil configurations, has also been used to explain the rubberlike behavior of the elastic fiber. Synchronous changes in the random-coil conformation of cross-linked elastin molecules are believed to be responsible for the expansion and contraction of the entire network as a single unit. It has also been hypothesized that the microfibrillar mantle may prevent excessive stretching of the fibers, and thus tearing of the elastic tissue. In this respect, the two cysteines of the highly basic carboxy-terminus of elastin are thought to mediate the postulated interactions with the acidic components of the microfibrils.

Microfibrils, the other morphologically distinct component of the elastic fiber, have proven to be extremely difficult to analyze because they are so highly insoluble. Since microfibrillar components have not been easily identified, it is still unclear whether or not microfibrils are compositionally identical. Currently, the fibrillins, microfibril associated glycoprotein (MAGP) and associated microfibril protein (AMP) are believed to contribute to microfibrils (Gibson *et al.*, 1991; Horrigan *et al.*, 1992). Although initially thought to be a single gene product, fibrillin is now recognized to represent a small family of structurally related proteins. They include the products of the FBN1 and FBN2 genes, as well as FLP, a putative fibrillin-like protein recently identified by cloning experiments (Ramirez *et al.*, 1993; Rosenbloom *et al.*, 1993). Other proteins, such as emilin, lysyl oxidase, and elastin, reside in elastic fibers without contributing to microfibril structure (Bressan *et al.*, 1993; Kagan *et al.*, 1986). There may also be microfibril-associated proteins interacting with some microfibrils but not others. Examples of these include vitronectin, amyloid P component, and the 36,000 molecular weight MAP (microfibril associated protein) found in aorta (Dahlback *et al.*, 1989; Breathnach *et al.*, 1991; Kobayashi *et al.*, 1983). Proteoglycans have also been suggested to be associated with microfibrils, and versican has been specifically localized in skin to microfibrils (Baccarani-Contri *et al.*, 1990; Zimmerman *et al.*, 1994).

In developing elastic tissues, microfibrils are the first component to appear in

←

Fig. 2. Rotary shadowed beaded fibril showing periodically spaced globules connected by many linear arms (top). Conventional transmission electron microscopy of microfibrils (bottom). If beaded fibrils are pelleted, fixed and stained as for tissue samples, they take on the appearance of microfibrils. Bars = 100 μm.

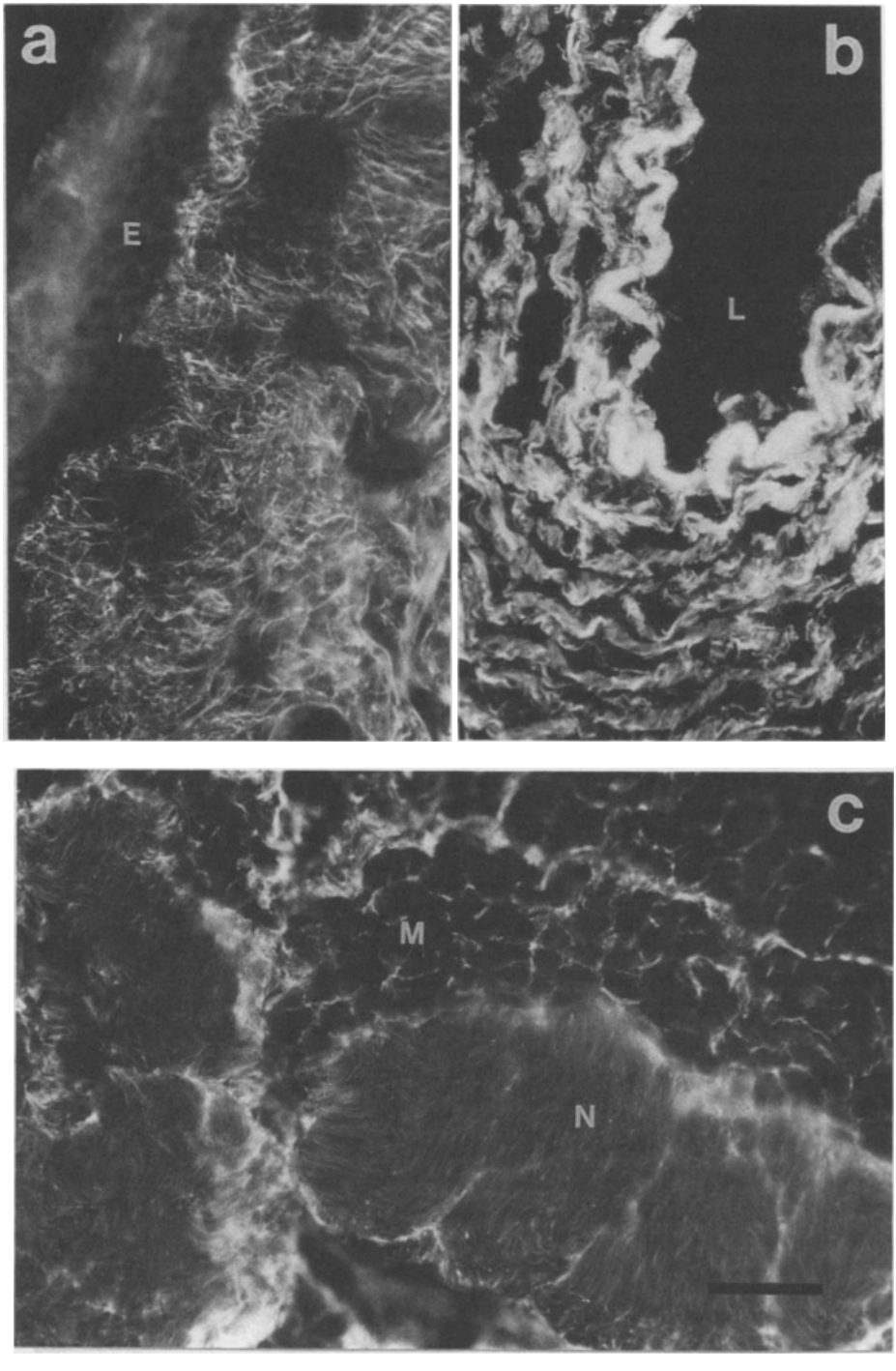
a
E
b
L
c
M
N

the ECM; subsequently, elastin is found deposited on the microfibrils (Greenlee *et al.*, 1966). Elastin deposition and the formation of the mature elastic fibers continues throughout embryogenesis up to early childhood. Thereafter, elastogenesis ceases almost completely, unless stimulated by local injury. Thus, the organization and composition of the mature elastic fibers are determined during the relatively early stages of organ growth, and there is very little turnover of elastic fiber components during the great majority of an individual's life.

FIBRILLINS

Fibrillin was first identified with the aid of monoclonal antibody technology (Sakai *et al.*, 1986). Subsequently, it was described as pepsin-resistant fragments obtained from extracts of human amnion and as intact native molecules obtained from cell culture medium (Maddox *et al.*, 1989; Sakai *et al.*, 1991). Initial investigations demonstrated that fibrillin is large (mass 350 kiloDaltons), cysteine-rich, and likely to contain significant intrachain disulfide bonds. Fibrillin was given its name because of the hypothesized structural role in uniting a ubiquitous class of morphologically similar microfibrils (Sakai *et al.*, 1986). Fibrillin has now been designated fibrillin 1 in order to distinguish it from a structurally related protein, fibrillin 2 (FBN2), more recently identified through cloning experiments (Zhang *et al.*, 1994).

The molecular structure of the fibrillin proteins has been derived in its entirety through the cloning and sequencing of overlapping cDNAs (Lee *et al.*, 1991b; Maslen *et al.*, 1991; Corson *et al.*, 1993; Pereira *et al.*, 1993; Zhang *et al.*, 1994). The size and overall modular nature of the fibrillins are strikingly similar; accordingly, their common structural features will be discussed together.

Protein Structure

The fibrillin protein consists of five structurally distinct regions (A–E in Fig. 5) preceded by a short signal peptide. Two of these regions (B and D, Fig. 5) are exclusively made of cysteine-rich sequences, the majority of which adhere to the epidermal growth factor (EGF) peptide motif. This sequence is characterized by the presence of six cysteinyl residues, which form three intramolecular

Fig. 3. Immunofluorescence of elastic fiber organization in (a) skin, (b) artery, and (c) nerve and muscle as demonstrated by anti-fibrillin antibodies. E, epidermis; L, lumen; M, muscle; N, nerve. Bar = 50 μm.

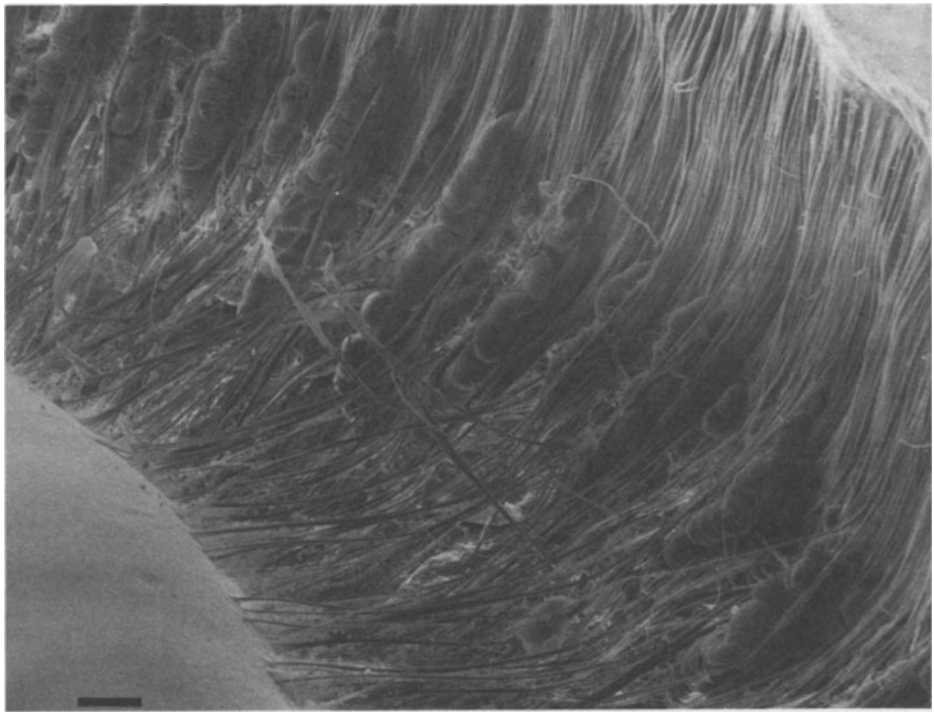

disulfide bonds (C1–C3; C2–C4; C5–C6) in an antiparallel β-pleated sheet conformation (Fig. 6) (Savage *et al.*, 1973; Cooke *et al.*, 1987). In fibrillin, the invariant distance between the last cysteine of one EGF-like repeat and the first of the next one suggests that an additional β-sheet might form between each of these sequences (Pereira *et al.*, 1993). This, in turn, may allow a series of EGF-like repeats to act as a functional unit. It is predicted that a replacement of one cysteine would have an obligate effect on the conformation of an individual repeat and on the function of a tandem array.

Both the carboxy and amino termini of fibrillin (Fig. 5, A and E) are sequences of unique composition. The latter is highly basic, while the former is somewhat enriched in lysines and contains an invariant peptide with two cysteines (Fig. 5). The fibrillins contain putative glycosylation sites and cell-attachment signals at comparable locations (Fig. 5). Finally, the most striking difference between the two fibrillin proteins is the substitution of the proline-rich region C of fibrillin 1 for the glycine-rich region of fibrillin 2 (Fig. 5).

There are 47 EGF-like repeats in fibrillin; four of them are of the generic type. Three are positioned directly adjacent to the amino terminal sequence, and the fourth one is adjacent to region C (Fig. 5). The remaining 43 EGF-like repeats form a special subtype, the calcium-binding type of EGF-like repeat (cbEGF-like repeat) (Handford *et al.*, 1990). In fibrillin, the cbEGF-like repeats have the consensus sequence shown in Fig. 5. As discussed more extensively later, the cbEGF-like repeat contains a consensus sequence associated with calcium binding in other proteins and engineered domains.

Fibrillin molecules bind calcium, but only when intrachain disulfide bonds are intact (Corson *et al.*, 1993). Although this supports the notion that the cbEGF-like repeat might be involved in this function, it does not exclude that other sequences may also be responsible for calcium binding by fibrillin. Moreover, it is not known whether all or only some of the 43 potential calcium binding sequences are utilized.

By analogy to other proteins, such as protein S and Drosophila Notch, which also contain cbEGF-like repeats, calcium binding may stabilize protein conformation and mediate protein–protein interactions (Dahlback *et al.*, 1990; Fehon *et al.*, 1990). For fibrillin, conformational stability is likely to be important for proper assembly of microfibrils, and for the long-term stability of microfibrils against proteases. Because microfibrils are complex structures that may perform a variety

Fig. 4. Scanning electron microscopic visualization of ciliary zonule (top) and transmission electron micrograph of a zonular fiber (bottom), apparently composed only of microfibrils. Bars = 200 μm.

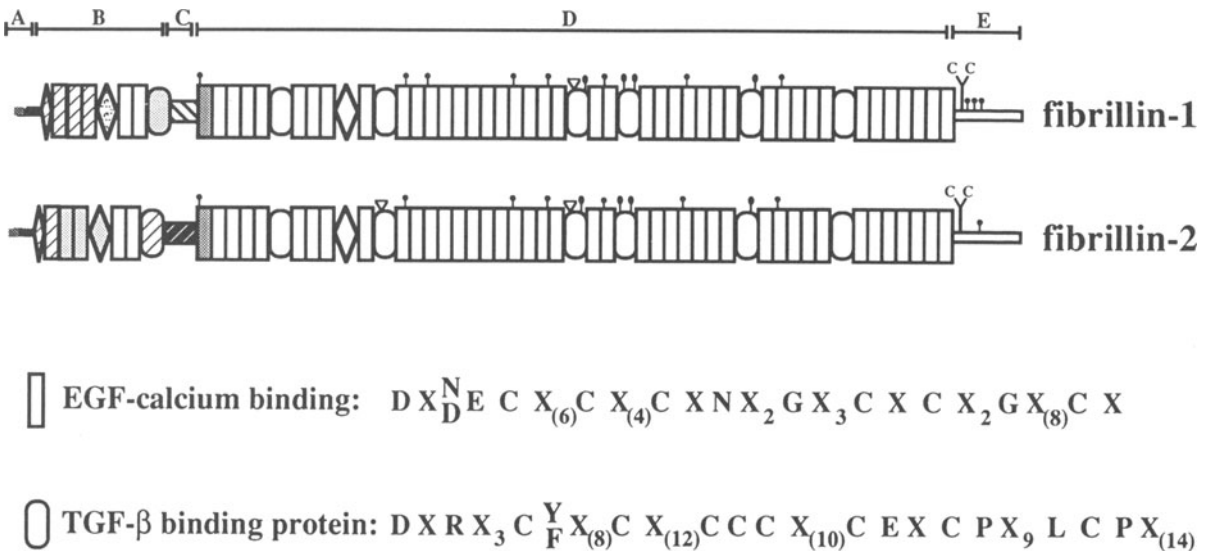

Fig. 5. Schematic representation of the fibrillin chains. The boundaries of the five structurally distinct regions (A to E) are highlighted at the top. White rectangles and ovals indicate the sequences homologous to the EGF-calcium binding and TGF-β binding protein motifs, whose consensus sequences are shown below. The other rectangles signify generic EGF-like sequences, while additional symbols indicate the fibrillin motifs. The letter C signifies the cysteinyl residues of region E, while the pin-head and the triangle symbolize putative glycosylation and cell attachment sites, respectively.

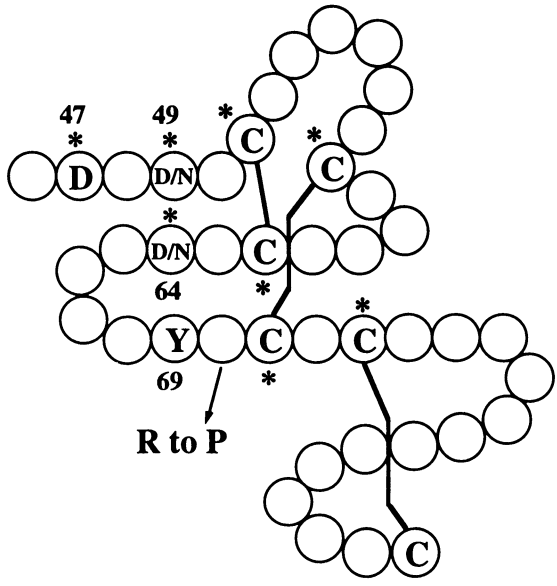

Fig. 6. Structure of fibrillin cbEGF-like domain as modeled after the solution structure of native EGF. Disulfide linkages (bold lines) between the six predictably spaced cysteine (C) residues create an antiparallel β-pleated sheet conformation. The positions of the aspartic acid (D), asparagine (N), and aromatic (tyrosine (Y)) residues that are believed critical for calcium binding are indicated. Numbers indicate the corresponding positions in the first cbEGF-like domain of coagulation factor IX. The sites of naturally occurring mutations are indicated by asterisks. The position of the only mutation that does not substitute a highly conserved residue (arginine (R) to proline (P)) is shown by the arrow.

functions in various regions of the connective tissue space, important calcium–mediated protein–protein interactions can be hypothesized.

In addition to the EGF-like repeats, fibrillin contains seven cysteine-rich motifs characterized by the presence of eight cysteine residues with the consensus sequence shown in Fig. 5. It is not yet known whether the cysteine residues in these repeats are free or involved in intrachain disulfide bonds. However, the cluster of three consecutive cysteines in the center of the motif may implicate free cysteines here. So far, these eight-cysteine repeats have been found in only one other gene, namely, the one coding for the TGF-β1 binding protein (Kanzaki *et al.*, 1990). Incidentally, the potential cell-attachment sequences of the fibrillins are both within these eight-cysteine sequences (Fig. 5).

One other cysteine-rich motif is repeated twice in fibrillin. It has been called the hybrid motif, because it is similar to the consensus sequence of the eight-cysteine repeat at its amino terminal end and more similar to the EGF-like

sequence at the carboxyl end. A similar hybrid motif is also found in TGF-β1 binding protein.

Gene Structure

The modular arrangement of the fibrillin protein is replicated in the multicassette organization of the genes, which contain 65 exons and span more than 100 kilobase-pairs of DNA (Pereira *et al.*, 1993). Fifty of the 57 cysteine-rich motifs are encoded by single exons. Sixty of the exons begin and end with in-phase split codons. Because of this configuration, most of the mutations removing one or more exons are expected to give rise to in-frame shortened proteins. Another interesting feature of the fibrillin gene organization is the presence of "mosaic" exons coding for the sequences of transition between the major structural regions of the protein.

Based on the genomic organization, it has been suggested that most of the ancestral fibrillin gene arose by multiple duplications of a cbEGF-like coding exon (Pereira *et al.*, 1993). Following the inclusion of the eight-cysteine coding exon, rearrangements between this and the cbEGF-like coding exon produced the units for the other cysteine-rich motifs in fibrillin. Once established, the ancestral gene duplicated and transposed on different chromosomes to give rise to FBN1 (chromosome 15q15–21) and FBN2 (chromosome 5q23–31).

Microfibrillar Assembly

Using rotary shadowing electron microscopic techniques to visualize fibers present in the vitreous, Wright and Mayne (1988) first suggested that an unusual "beaded fibril" might represent the microfibril present in the ciliary zonule. Subsequently, Keene *et al.* (1991) demonstrated that similar beaded fibrils from amnion and skin contain fibrillin and that, when fixed and stained, the beaded fibrils have the same appearance as microfibrils in tissues. Rotary shadowed images of beaded fibrils (Fig. 4) depict periodically spaced globular domains separated by many (six-to-eight) linear arms.

Since rotary shadowed images of fibrillin monomers isolated from cell culture medium revealed flexible linear molecules, fibrillin molecules may conceivably form the arms and contribute to the globular domain of the beaded fibril as well (Sakai *et al.*, 1991). Immunolocalization of a monoclonal antibody specific for fibrillin demonstrated periodic labeling just to one side of each globule, suggesting one fibrillin monomer per globular period (Keene *et al.* 1991). In

tissues, immunolocalization of multiple different fibrillin antibodies yielded a single periodicity (Sakai *et al.*, 1991). These data, together with double immunolocalization of fibrillin antibodies, suggested that fibrillin molecules are arranged in a head-to-tail fashion in the microfibril.

How do fibrillin molecules assemble into microfibrils? Fibrillin, with its high content of cysteine residues, is likely to be stabilized by extensive intrachain disulfide bonds (Ross and Bornstein, 1966). Treatment of tissues with a disulfide bond reducing agent results in the disappearance of microfibrils. Reduction of beaded fibrils also leads to loss of morphology, while nonreducible cross-links maintain the aggregate. Moreover, only small amounts of fibrillin monomers can be solubilized by reducing agents from fetal tissues, suggesting that only newly synthesized fibrillin is released by reduction and that fibrillin is normally further cross-linked by nonreducible bonds (Sakai, 1990). Fibrillin is secreted as a monomer and is then very rapidly assembled into disulfide bonded aggregates. In addition, purified fibrillin monomers will form intermolecular disulfide bonded species *in vitro* under physiological conditions (Sakai, unpublished observations).

Which domains in fibrillin are used for intermolecular disulfide cross-linking? Candidate domains include the amino and carboxyl terminal ends, which contain regions of sequence identity around the conserved cysteine residues of both chains. The proline-rich domain in fibrillin 1 and the glycine-rich domain in fibrillin 2 have been proposed to function as a bend or hinge, facilitating interactions required for assembly (Pereira *et al.*, 1993; Zhang *et al.*, 1994). Aside from intermolecular disulfide bond formation, calcium binding may also be important to the assembly of fibrillin. Calcium has been shown to promote the deposition of fibrillin into the ECM of fibroblasts in culture (Aoyama *et al.*, 1993). Moreover, removal of calcium with a chelating agent has been shown to alter the conformation of beaded fibrils (Kielty and Shuttleworth, 1993).

An important question is whether microfibrils are heteropolymers composed of fibrillins 1 and 2 or of two distinct homopolymeric species. In this regard, the tissue distribution of fibrillins 1 and 2 should be considered (Zhang *et al.*, 1994). In many tissues, there appears to be a similar codistribution of fibrillins 1 and 2. However, fibrillin 1 but not fibrillin 2 seems to be present in hyaline cartilage, and fibrillin 2 but not fibrillin 1 is apparent in elastic cartilage. In the aortic wall, fibrillin 2 seems to be restricted to the elastic media, while fibrillin 1 is present throughout the wall. This differential pattern of expression was also noted during mouse embryogenesis, with fibrillin 2 being produced transiently and earlier than fibrillin 1 (Ramirez, unpublished observations). These differences, together with the distinct pathologies linked to the fibrillin genes, suggest distinct contributions of the two glycoproteins to the assembly and maintenance of microfibrils.

MARFAN'S SYNDROME

Commencing in the 1950s, a series of large-scale prospective studies helped to delineate the inheritance pattern, clinical spectrum, and natural history of this disorder. The knowledge accumulated during this phase of investigation has provided a critical foundation for the development of diagnostic criteria, for the formulation and implementation of therapeutic strategies, and for the investigation of the etiology and pathogenesis of MFS. Accordingly, MFS is now recognized as a heritable disorder of connective tissue, which affects approximately 1 in 10,000 individuals, without an ethnic bias (Pyeritz and McKusick, 1978). It is estimated that between 15 and 25% of cases manifest new mutations, presumably due to parental germ line defects. There are no documented examples of skipped generations (high penetrance), but marked clinical variability in the distribution and severity of manifestations can be seen within and between families. The lack of a reliable detection test for the disorder, compounded by a high rate of sporadic mutations and the marked clinical variability, may have perpetuated an underestimation of disease prevalence.

Clinical Features

The cardinal manifestations in MFS are evident in the ocular, skeletal, and cardiovascular systems (Pyeritz and McKusick, 1979). The ocular pathology is characterized by early (preadolescent) and severe myopia and dislocation of the lens (Maumenee, 1981). The ciliary zonules, comprising the suspensory apparatus of the ocular lens, are thinned and stretched. Predisposition of the inferomedial ligaments leads to the characteristic superior dislocation of the lens in up to 80% of patients (Fig. 7). Any resultant visual deficit can generally be compensated with corrective lenses; surgical removal of the lens is reserved for situations when the displaced lens directly obstructs the path of light. While high myopia is often seen in isolation, ectopia lentis can predispose to refractive defects, glaucoma, and retinal detachment.

The skeletal system is best characterized by overgrowth of the long bones (Fig. 8) (Magid *et al.*, 1990). While the mechanism remains unclear, it has been proposed that the periosteum may normally provide a physical limit to the rate and extent of bone growth. An abnormally lax periosteum might, therefore, release this structural inhibition. Manifestations include tall stature (mainly due to excessive leg length), arachnodactyly, anterior chest deformity, scoliosis, highly arched and narrow palate with tooth crowding, and variable forms of foot and leg

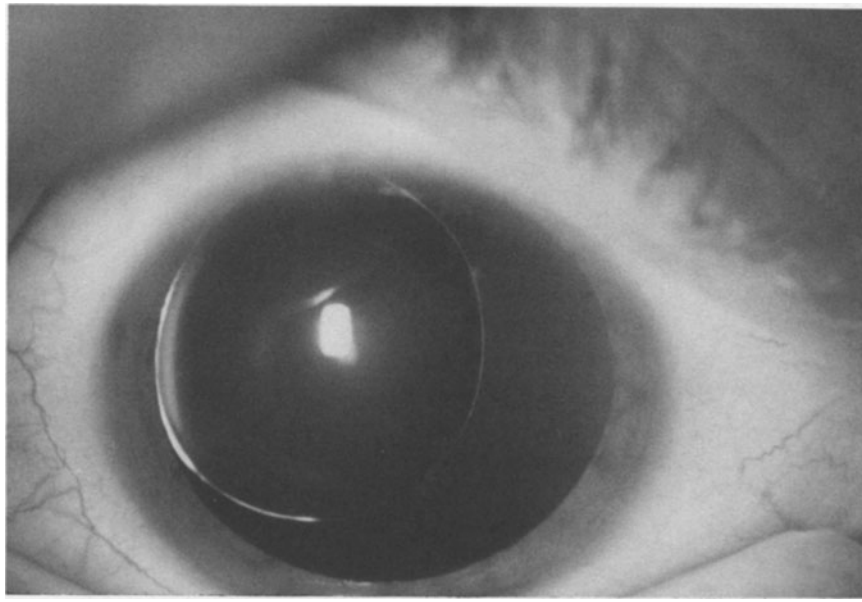

Fig. 7. Examination of the eye in a patient with MFS revealing the characteristic upward dislocation of the ocular lens.

deformity. Joint laxity is also common. Sequelae of musculoskeletal abnormalities can include joint dislocation, chronic pain, difficulty with ambulation, and cardiopulmonary impairment.

Because of a clear association with early morbidity and mortality, the cardiovascular manifestations of MFS have received considerable attention. Retrospective study in the early 1970s demonstrated that the majority of patients with MFS died by the third decade of life due to cardiovascular complications (Murdoch *et al.*, 1972). An early age of onset of heart disease was clearly correlated with a less favorable outcome.

The majority of children and nearly 80% of adults with MFS show dilatation of the aorta (Roberts and Honig, 1982). Classically, aortic disease begins at the sinuses of Valsalva and extends to the proximal ascending arch (Fig. 9), but it can be seen anywhere along the course of the vessel. Aortic regurgitation is a secondary event and is manifested in the stretching of the commissures at the sinotubular junction. Dissection of the adult aortic root rarely occurs before the maximal dimension at the sinuses reaches 55-to-60 mm. In childhood, such a correlation of aortic size and the risk for dissection has not been clearly established. Factors such as the aortic root dimension in relation to body surface area,

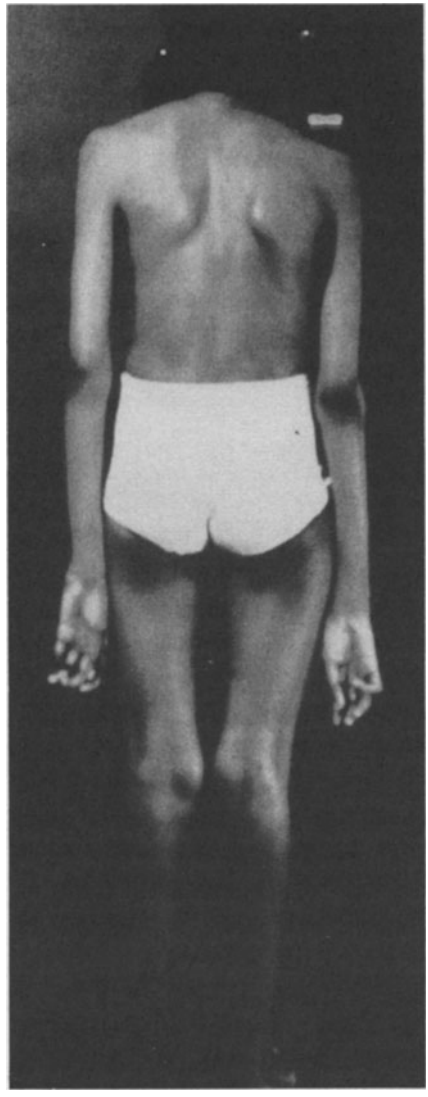

Fig. 8. Skeletal features in the MFS manifest long bone overgrowth. Features seen here include arachnodactyly, disproportionate tall stature due to excessive length of the limbs, scoliosis, and genu recurvatum.

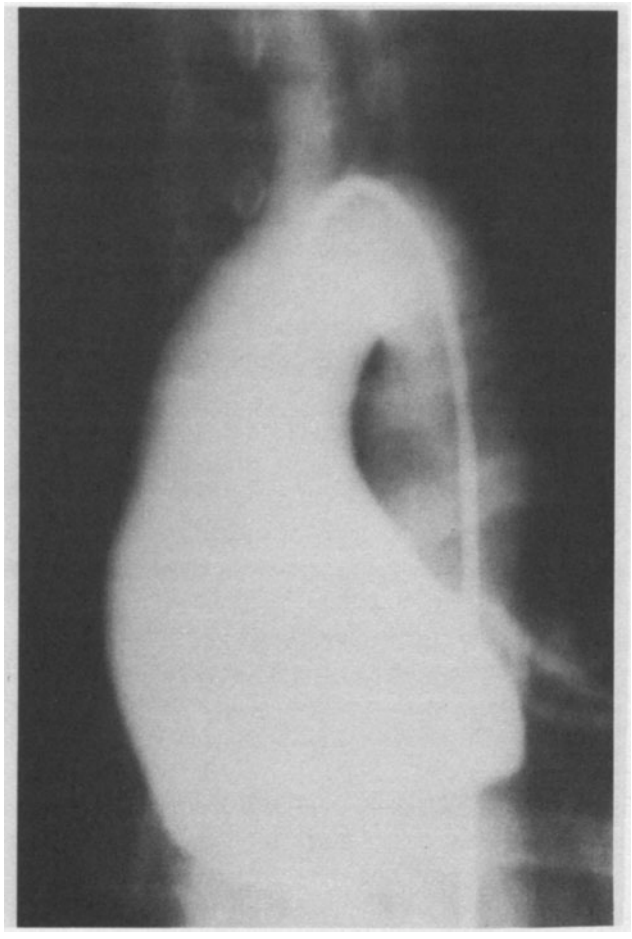

Fig. 9. Aortogram in the anterior-posterior projection showing marked dilatation of the aortic root at the level of the sinuses of Valsalva in an MFS patient.

family history of early dissection, and the rate of dilatation over time must be considered. Aortic regurgitation can lead to myocardial dysfunction and can accelerate aortic dilatation, by increasing stroke volume, and hence, wall stress. Dysplasia and prolapse of the mitral valve, with or without regurgitation, are as commonly seen in the MFS as aortic dilatation, occurring in approximately 75% of patients. Sequelae include myocardial dysfunction, dysrhythmia, thrombo-embolic events, and bacterial endocarditis. Less common cardiovascular features

include tricuspid valve prolapse, pulmonary artery dilatation and dissection, descending thoracic or abdominal aortic aneurysm, and primary cardiomyopathy.

Other less common manifestations in the MFS include spontaneous pneumothorax, striae distensae, dural ectasia (with rare nerve impingement), protrusio acetabulae, and mild learning disability with or without hyperactivity. These associated features can be quite useful for clinical diagnosis when classic features in other organ systems are mild or lacking. In the absence of a family history, current diagnostic guidelines require involvement of the skeleton and at least two other organ systems, with at least one "major" manifestation (aortic dilatation, ectopia lentis, or dural ectasia) (Beighton *et al.*, 1988). In the presence of an unequivocally affected first degree relative, features must only involve two organ systems; a "major" manifestation is preferred but not required.

Clinical Management

Effective management of the cardiovascular manifestations of MFS relies upon frequent clinical and echocardiographic assessment, institution of medical therapy to slow the rate of aortic dilatation, and prophylactic surgical intervention to replace the diseased aorta prior to dissection. Current recommendations call for yearly examination for adults with aortic root dimensions less than 50 mm or for children with slowly progressive disease. Individuals with more advanced or aggressive disease should be followed at more frequent intervals. Prophylactic surgery is indicated once the aortic root exceeds 55 mm in adults; precise guidelines have not been established for children, but rapid progression, measurements that exceed twice the expected size for body size, or ventricular dysfunction should precipitate early intervention (Morse *et al.*, 1980). Heart failure due to advanced mitral valve pathology is the most common indication for surgery in preadolescent years. Surgery for aortic disease generally involves replacement of the aortic root with a valved synthetic conduit, frequently substituted by homografts in childhood (Bentall and DeBono, 1987; Gott *et al.*, 1991). In most instances it is possible to repair a redundant mitral valve using a rigid or flexible prosthetic ring.

In 1971 the use of β–adrenergic blockade was first proposed for use in MFS patients to slow the rate of aortic dilatation and delay the need for surgery. Decades later, it has been demonstrated that this strategy has the desired effect in at least a subpopulation of patients (Shores *et al.*, 1994). Another mainstay of medical management is the prescription of antibiotic prophylaxis for dental work or any other procedure expected to contaminate the bloodstream with bacteria. Although often reserved for patients with valvular regurgitation or prosthetic implants, it

must be considered that MFS patients have an abnormal connective tissue substrate that appears predisposed to bacterial infection in the cardiovascular system. It is preferable, therefore, to institute antibiotic prophylaxis in all patients at the time of diagnosis.

Fibrillin Mutations

As discussed, the first FBN1 mutation was identified in two sporadic cases of MFS (Dietz *et al.*, 1991). A G-to-C transversion was identified in one allele from a patient with neonatal presentation of severe and rapidly progressive disease, and in an unrelated individual with severe disease that presented at birth. The mutation causes the substitution of proline for arginine in one of the cbEGF–like repeats of FBN1. It was predicted that introduction of a proline residue would alter the secondary structure of the domain, perhaps resulting in abnormal folding of a larger portion of the monomer. Alternatively, these changes could lead to an alteration in conformation that might impair calcium binding. Recent determination of the nuclear magnetic resonance structure (NMR) of this FBN1 cbEGF-like domain, in both its wild type and mutant forms, demonstrated both altered structure and calcium-binding properties when proline is substituted for arginine (J. Berg, personal communication).

The more than 30 MFS mutations hitherto identified are beginning to reveal some interesting patterns. First, with the exception of the first mutation, all others have been specific to single families. This observation probably reflects a relatively high rate of new mutation, and impaired reproductive fitness in the MFS due to early morbidity and mortality. Second, mutations have been identified with approximately equal frequency along the length of the gene. Thus, there is no definitive correlation between the position of a mutation and the severity of the resultant phenotype. One possible exception is the recent report of fibrillin 1 mutations associated with neonatal presentation of severe disease that are clustered in the central portion of region D (Kainulainen *et al.*, 1994; Milewicz and Duvic, 1994). Because of the relatively small number of cases and the non-neonatal presentation of other mutations at this site, this correlation would still have to be confirmed.

An early and continuing observation is that the majority of identified mutations causing MFS substitute cysteine residues in cbEGF–like domains (Dietz *et al.*, 1992; Tynan *et al.*, 1993; Kainulainen *et al.*, 1994). As previously mentioned, such mutations would cause an obligate disruption of the conformation and perhaps the calcium-binding property of a repeat. The structural features of EGF-like domains that have been shown to bind calcium are illustrated in Fig. 6.

These features include: an antiparallel β-sheet conformation, six predictably spaced cysteine residues, aspartic acid (D) and aspartic acid or asparagine (N) residues at the positions corresponding to residues 47 and 49 of the first cbEGF–like domain of human coagulation factor IX, respectively, D or N at the position corresponding to residue 64, and an aromatic residue at position 69 (Handford *et al.*, 1991; Mayhew *et al.*, 1992). The D/N at position 64 is typically found within the consensus sequence that promotes the β-hydroxylation of these residues. Recently, the ligand requirements for calcium binding to EGF-like domains were determined through analysis of the first cbEGF–like domain in human coagulation factor IX (Mayhew *et al.*, 1992). The wild type and various mutant sequences were chemically synthesized and studied by H–NMR spectroscopy, in the presence and absence of calcium. Residues 47 and 64 directly contributed ligands to the calcium ion. Four naturally occurring mutations causing MFS do not substitute cysteine residues in cbEGF–like domains; all substitute residues in fibrillin 1 correspond to positions 47 and 64 in factor IX (Dietz *et al.*, 1993a; Hewett *et al.*, 1993; Kainulainen *et al.*, 1994). A fifth mutation substitutes a highly conserved glutamic acid (E) with a lysine (K) residue at a position corresponding to residue 50 in factor IX (Kainulainen *et al.*, 1994). While this residue has not been shown to be essential to calcium binding, the presence of E at this position can partially compensate for the lack of N at position 64 in factor IX. Since N is present in the fibrillin 1 domain where E is substituted, the relevance, if any, of this mutation for calcium binding may conceivably reside in the nature of the substituting K residue.

While these and previously discussed data suggest that calcium binding may be critical to the normal function of fibrillin, and that a majority of missense mutations causing MFS may act by perturbation of this process, the precise role of disrupted domain conformation and altered calcium binding in the pathogenesis of this disorder remains unclear. Recent quantitative pulse–chase studies, examining fibrillin metabolism in cell lines with known mutant genotypes, has begun to shed light on this matter (Aoyama *et al.*, 1993). While the cell lines showed normal levels of fibrillin synthesis (relative to control lines), nearly all lines carrying mutations that substitute cysteine residues in cbEGF-like repeats showed a dramatic delay in the secretion of fibrillin, and reduced fibrillin deposition into the ECM. Addition of a reducing agent to the culture media of control cells reproduced this cysteine-substitution phenotype. Delayed secretion could manifest failure of folding or the formation of abnormal protein-protein complexes. Thus, proper folding of individual cbEGF-like repeats and of a given cluster of repeats seems to be critical to normal intracellular trafficking of fibrillin. In contrast, mutations predicted to have an isolated effect on calcium binding impair extra-

cellular incorporation. This cellular phenotype was reproducible when control lines were deprived of calcium. Both abnormal conformation or altered calcium binding leads to a failure of incorporation of fibrillin into the ECM. The mechanism remains unclear. Possibilities include impaired intermolecular interactions or increased susceptibility of abnormal monomers or multimers to the activity of proteases.

A broad second class of mutations are predicted to result in the formation of shortened fibrillin monomers. Defects belonging to this class include splice-site mutations leading to single exon skipping and the loss of an internal repeat, genomic deletions causing the loss of multiple repeats, and frameshift or nonsense mutations that lead to the production of monomers with carboxy-terminal truncations. All types of defects can be associated with classic MFS (Kainulainen *et al.*, 1992; Dietz *et al.*, 1993a,b; Godfrey *et al.*, 1993; Tynan *et al.*, 1993; Kainulainen *et al.*, 1994). Because microfibrillogenesis is believed to involve an orderly aggregation of fibrillin monomers, perhaps in association with other proteins, it could be postulated that the presence of shortened fibrillin polypeptides could interfere with intermolecular interactions and with the phasing of polymerizing fibrillin multimers. The abnormal structure of these aggregates could directly impair their functional integrity, or they could be predisposed to untimely degradation. In one circumstance, a genomic deletion causes the in-frame removal of three cbEGF-like repeats (Kainulainen *et al.*, 1992). A stable truncated peptide, in an amount apparently equal to that expressed from the wild type allele, could be immunoprecipitated from a fibroblast cell line carrying this mutation. While immunofluorescent assay of cultured cells showed a dramatic decrease in the extracellular deposition of fibrillin, the precise mechanism underlying this cellular phenotype remains to be determined.

An insight into the pathogenesis of MFS has come from the study of mutant alleles that encode premature termination codons (PTC). Work by Urlaub *et al.* (1989) and Cheng *et al.* (1990) has clearly shown that the presence of a PTC prior to the penultimate exon of a gene is generally associated with a severe reduction in the level of mutant transcript. Two models have been proposed to account for this phenomenon. First, the nuclear scanning model suggests that a yet uncharacterized nuclear factor has the ability to read the frame of mature mRNA. If a PTC is encountered, the mRNA is degraded. The translational translocation model proposes that extrusion of mRNA through the nuclear pore is physically coupled to, and partially dependent upon, the cytoplasmic translation machinery. If a PTC is encountered, the transcript will fail to be trafficked to the cytoplasm and will ultimately be degraded.

The first such mutation identified in FBN1 involved a four base-pair insertion

(Dietz *et al.*, 1993a). This frameshift leads to the formation of a PTC and is associated with a mutant transcript level that is only 6% of that observed from the wild type allele. Unlike all patients with missense mutations and normal transcript levels, this patient had an extremely mild phenotype that failed to meet the established diagnostic criteria for MFS. This data suggested a dominant negative pathogenesis of the MFS. This model presumes that the presence of an abnormal protein that impairs processing of the wild type product, rather than a relative deficiency of normal peptide, is central to expression of the disease phenotype (Herskowitz, 1987). The mild phenotype observed in this patient can be reconciled in either of two ways (Dietz *et al.*, 1993a). First, the predicted truncated peptide from the mutant allele may be so different from the normal monomer, that it fails to participate in multimer formation. Alternatively, the severely reduced mutant transcript level predicts very low amounts of mutant peptide and leads to a preponderance of normal multimer and an abbreviated disease phenotype (Fig. 10).

Additional information stems from the study of two other reduced-transcript mutants and from a quantitative biosynthetic study of cell lines carrying these mutant alleles (Dietz *et al.*, 1993a,b). In one patient, a nonsense mutation in exon 51 led to a complex exon skipping phenotype and a mutant transcript level of 25%. In the other patient, a splice-site mutation caused the skipping of exon 2, leading to a frameshift in exon 3 and a PTC in exon 4. The mutant transcript level was 16% of that observed from the wild type allele. Interestingly, both of these patients had a classic and severe form of MFS. These data suggest that a relatively small amount of mutant peptide can cause disease. Specifically, a critical threshold, between 6 and 16% of wild type levels, may be necessary to cause sufficient disruption of microfibrillar assembly to produce the classic phenotype.

The apparent correlation between the amount of abnormal protein and disease severity is analogous to what has been observed with collagen gene defects, another multimeric protein system (Lee *et al.*, 1991a). Quantitative pulse–chase analysis of these cell lines has provided data consistent with the dominant negative hypothesis (T. Aoyama, personal communication). All three cell lines synthesize approximately half of the amount of fibrillin made by control lines. The mutant line with 6% mutant transcript, associated with a mild phenotype, deposits all synthesized fibrillin into the matrix. The two cell lines carrying the reduced-transcript mutants associated with a classic phenotype deposit only a fraction of synthesized wild type fibrillin, identical to the situation observed with missense mutations.

Preliminary data support the antimorphic behavior of this group of FBN1

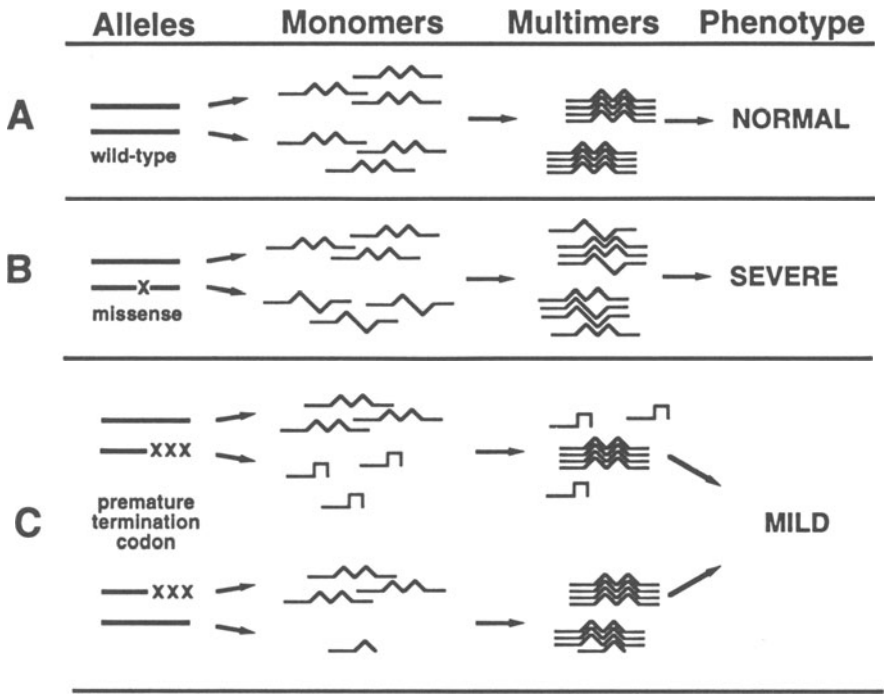

Fig. 10. A dominant negative model for MFS. (A) Two normal copies of the fibrillin gene lead to homogeneous populations of normal monomer and multimer, and hence a normal phenotype. (B) Missense mutations that substitute one amino acid for another lead to equal populations of normal and mutant monomer, a homogeneous population of abnormal multimer, and hence severe disease. (C) The mild phenotype observed in the patient with a premature termination codon and only 6% of the expected amount of mutant RNA can be reconciled in two ways. The truncated protein could be so dissimilar to the wild-type product that the two can no longer interact. Alternatively, the reduced RNA level predicts a very low amount of mutant monomer. Either situation predicts a preponderance of normal multimer and hence mild disease.

mutations. Stable expression of the exon-2–skipping allele in cultured control fibroblasts was sufficient to cause a marked decrease in the amount of ECM fibrillin and disorganized and fragmented microfibrillar bundles (H.C.D., unpublished data). The isolated expression of the extreme amino terminus of fibrillin 1 upon a normal genetic background can recreate an MFS-like cellular phenotype. These data suggest that the amino-terminal end of the molecule plays a critical role in the polymerization of fibrillin aggregates, in keeping with the previously mentioned head-to-tail model of microfibrillar assembly (Sakai *et al.*, 1991).

Intrafamilial Variability

A firm understanding of the etiology of MFS led to the investigation of several unresolved clinical issues, including the molecular basis for marked intrafamilial clinical variability. The identification of a cysteine substitution in a cbEGF-like repeat has recently shed some light on this phenomenon. The mutation segregates with disease in a large kindred with classic MFS; however, the phenotype observed in family members varied widely with respect to age of onset, tissue distribution, and severity of manifestations (Dietz *et al.*, 1992). The only two individuals who shared the identical phenotype were monozygotic twins. These data suggest the presence of genetic modifiers influencing the clinical expression of an FBN1 gene defect. Such modifiers would vary with genetic background, explaining divergent phenotypes in and between families.

Recent experience with haplotype segregation analysis in selected families offers a second molecular explanation for intrafamilial clinical variability (Pereira *et al.*, 1994). A panel of four intragenic FBN1 microsatellite polymorphisms was identified and typed in families in whom selected individuals had classic MFS, while others had a milder but related phenotype that included typical skeletal abnormality, mitral valve prolapse, early myopia, joint laxity, and/or striae distensae but no "major" manifestations. In the presence of an unequivocally affected first degree relative, all mildly affected individuals satisfied the MFS diagnostic criteria (Beighton *et al.*, 1988); all individuals were counseled and managed accordingly.

In Fig. 11, family A, the proband (II-6) with classic MFS passed the same FBN1 allele to each of her affected daughters. This allele was not carried by family members with the milder phenotype; rather they all shared a distinct FBN1 allele. These data suggest that the proband carries a *de novo* mutation causing MFS that she passed to her affected daughters. This occurred upon the genetic background for a milder, albeit related, connective tissue phenotype not associated with aortic disease or ectopia lentis. The data are consistent with, but no conclusive for, the possibility that the milder phenotype is also caused by a FBN1 gene defect. In family B, members with a milder phenotype also share a common FBN1 allele that is not carried by the proband (III-1), who has a distinctly more severe phenotype involving the aorta. A *de novo* mutation in FBN1 was identified in III-2 that is not carried by any other family members (Dietz *et al.*, 1993a).

The results demonstrate that genetic and/or allelic heterogeneity can be the basis for the observation of phenotypic variability in selected families. The analysis should allow for stratification of cardiovascular risk within families. Implications include the need for individualized counseling and management and

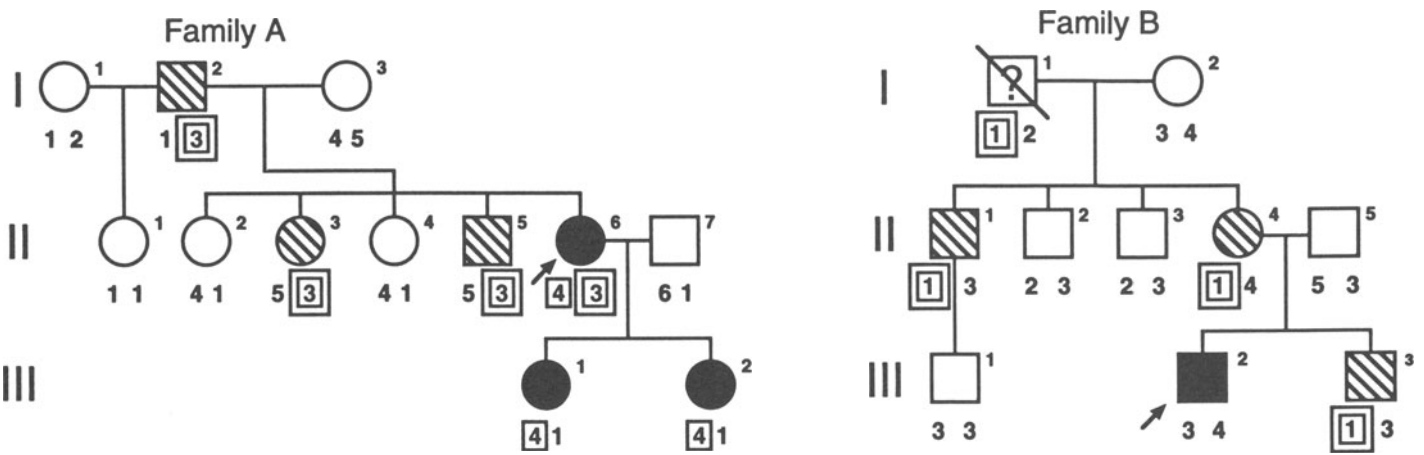

Fig. 11. Haplotype segregation analysis in two families segregating both MFS (blackened symbols) and a related but milder connective tissue phenotype (hatched symbols). In family A, MFS is inherited on the number 4 allele (boxed), while the milder disorder cosegregates with the number 3 allele (double box). Because multiple unaffected individuals carry the number 4 allele, it appears that a new mutation has occurred on this copy of the fibrillin gene in the proband (arrow). In family B, a mild connective tissue disorder cosegregates with the number 1 allele (double box), a copy of the fibrillin gene that is not carried by the proband with more severe disease involving the aorta. Additional analyses allowed the detection of a new mutation in III-2. This figure was adapted from Dietz *et al.* (1994).

for judicious caution when interpreting linkage, natural history, or therapeutic outcome studies. For example, these data could explain why a large French kindred with incomplete, atypical, mild, and variable manifestations of MFS, in which abnormal members were considered affected with the same disorder, failed to demonstrate linkage to the fibrillin gene (Boileau *et al.*, 1993). It appears that the diagnostic criteria for MFS should be modified to require a "major" manifestation despite the presence of an unequivocal family history.

MARFAN-LIKE CONDITIONS

The medical significance of fibrillin 1 may not be limited to its role in the pathogenesis of MFS. In fact, the FBN1 gene has been genetically linked to the isolated ectopia lentis phenotype with no recombination (Tsipouras *et al.*, 1992). Consistent with this finding, a fibrillin 1 mutation has recently been reported in a patient with eye involvement out of proportion to the involvement of other tissues (Kainulainen *et al.*, 1994). A fibrillin 1 mutation has also been characterized in a patient with the mitral-aortic-skin-skeletal (MASS) phenotype, which includes mitral valve prolapse and borderline aortic dilatation without progression to dissection (Dietz *et al.*, 1993a). It is reasonable to speculate that fibrillin gene defects may play an etiologic role in patients with other isolated or atypical features of the MFS phenotype, such as mitral valve prolapse syndrome, idiopathic scoliosis, or annuloaortic ectasia.

The causal association between FBN2 and congenital contractural arachnodactyly (CCA) (Lee *et al.*, 1991) is yet to be rigorously supported by the finding of a fibrillin 2 mutation in this disorder. With this limitation, one can speculate the significance of this linkage, in relation to the one established between MFS and FBN1, and in view of the differences in the pattern of expression of the two fibrillins (Zhang *et al.*, 1994). Accordingly, two distinct scenarios could be envisioned. In the first, the aforementioned differences imply that different microfibrils have different composition, and thus diverse functions in distinct tissues or at different developmental stages. For example, it is conceivable that fibrillin 2, which is expressed earlier than fibrillin 1, may serve as the first nucleation center directing the subsequent deposition of fibrillin 1. The substantially lower incidence of CCA cases compared with MFS reflects the low viability of fibrillin 2 mutations and implies that fibrillin 2 plays a more critical role than fibrillin 1 during the early stages of morphorganogenesis. Alternatively, one could argue that the fibrillins may form homo- or heteropolymers of differing ratios, depending upon the specific genetic program of the cell type. In some tissues, one

fibrillin may be more abundant than the other, while in other tissues they may be more equally expressed. In tissues where the fibrillins are more equally expressed, a defect in one fibrillin may be compensated for by the other fibrillin. In tissues where one fibrillin is exclusively or more prevalently expressed than the other, such a compensatory process may not occur because of its more critical structural role.

CONCLUSIONS AND FUTURE PROSPECTIVES

To date, molecular studies of the MFS and the FBN1 gene have resulted in a firm understanding of the molecular origins of the disorder, have begun to shed some light on the origins of pleiotropy and clinical variability, and have contributed to a greater understanding of pathobiology and pathogenesis. Direct clinical application has ensued, with successful efforts at presymptomatic and prenatal diagnosis. Despite this early success in clinical application of molecular data, the greatest challenges and rewards await attempts at a full understanding of pathogenesis, and efforts to relieve the clinical burden of this disorder using novel therapeutic strategies. While correlation of mutant genotype to phenotype in patients has provided some insight, this approach is limited by a number of factors including the low number of patients carrying the same mutation, the great diversity in genetic background (and of potential genetic modifiers) in and between affected families, the inability to study protein expression and interactions at different stages of early fetal development, the limitation of following the natural history of MFS serially using invasive diagnostic techniques, and the hardships associated with execution and interpretation of experimental therapeutic trials in a limited number of human subjects. In this light, the creation of a transgenic animal model of MFS should prove invaluable to future studies.

In order to gain greater knowledge of the biology of normal and mutant fibrillin 1, the protein and its interactions will need to be studied *in vivo*. The application of transgenic technology will provide insight into the biochemical and developmental significance of the normal protein and the consequence of expressing an altered gene in a system that mimics the physiologic complexity of the human system. For example and by analogy to the human mutations, introduction of a mutant allele producing a truncated peptide into fertilized mouse pronuclei should be sufficient to recreate the clinical phenotype in the animals. The use of techniques of homologous recombination in embryonic stem cells should elucidate whether there are phenotypic differences in qualitative versus quantitative mutations of fibrillin 1. Finally, the transgenic techniques will also allow investigators

to compare and contrast the consequences of identical mutations in the two fibrillin chains.

The development of murine and nonmurine models for MFS should provide a means to evaluate conventional medical therapies. They include the optimal preparation, time of initiation, dosage, or route of administration of pharmacologic agents that slow the rate of aortic root dilatation. Animal research will also be necessary to test novel gene therapy strategies. For example, if the dominant negative hypothesis is confirmed, selective inhibition of expression from the mutant allele should help to alleviate the clinical burden carried by MFS patients. The emergence of antisense strategies for such purposes, coupled with innovative methods for direct gene delivery to the cardiovascular system, may ultimately allow the correction of defective FBN1 gene expression by somatic gene therapy.

ACKNOWLEDGMENTS. The authors wish to thank Dr. Douglass Keene for the generous gift of the micrographs shown in this review, and Ms. Liana Apelis for the preparation and typing of the manuscript. They also acknowledge the support of the Smilow Family Foundation, the Dr. Amy and James Elster Research Fund, the Shriners Hospital for Crippled Children, and the National Marfan Foundation. This is article 167 from the Brookdale Center for Molecular Biology at the Mt. Sinai School of Medicine in New York City.

REFERENCES

Aoyama, T., Tynan, K., Dietz, H.C., Francke, U., and Furthmayer, H., 1993, Missense mutations impair intracellular processing of fibrillin and microfibril assembly in Marfan syndrome, *Hum. Mol. Genet.* **2**:2135–2140.

Baccarani-Contri, M., Vincenzi, D., Cicchetti, F., Mori, G., and Pasquali-Ronchetti, I., 1990, Immunocytochemical localization of proteoglycans within normal elastin fibers, *Eur. J. Cell Biol.* **53**:305–312.

Beals, R.K., and Hecht, F., 1971, Congenital contractural arachnodactyly; a heritable disorder of connective tissue, *J. Bone Joint Surg.* **53**-A:887–903.

Bentall, H.H., and DeBono, A.A., 1987, A technique for complete replacement of the ascending aorta, *Thorax* **23**:338–339.

Beighton, P., De Paepe, A., Danks, D., Finidori, G., Gedde-Dahl, T., Goodman, R., Hall, J., Hollister, D.W., Horton, W., McKusick, V.A., Opitz, J.M., Pope, J.M., Pyeritz, R.E., Rimoin, D.L., Sillence, D., Spranger, J.W., Thompson, E., Tsipouras, P., Viljoen, D., Winship, I., and Young, I., 1986, International nosology of heritable disorders of connective tissue, Berlin 1986, *Am. J. Med. Genet.* **29**:581–594.

Boileau, C., Jondeau, G., Babron, M.-C., Coulon, M., Alexandre, J.A., Sakai, L., Melki, J., Delorme, G., Dubourg, O., Bonaiti-Pellie, C., Bouradarias, J.P., and Junien, C., 1993, Autosomal dominant Marfan-like connective tissue disorder with aortic dilatation and skeletal anomalies not linked to the fibrillin genes, *Am. J. Hum. Genet.* **53**:46–54.

Breathnach, S.M., Melrose, S.M., Bhogal, B., deBeer, F.C., Dyck, R.F., Black, M.M., Tennent, G., and Pepys, M.B., 1991, Amyloid P component is located on elastic fibre microfibrils in normal human tissue, *Nature* **293:**652–654.

Bressan, G.M., Daga-Gordini, D., Colombatti, A., Castellani, I., Marigo, V., and Volpin, D., 1993, Emilin, a component of elastic fibers preferentially located at the elastic-microfibrils interface, *J. Cell Biol.* **121:**201–212.

Bruns, R.R., Press, W., and Ross, J., 1987, A large-scale, orthogonal network of microfibril bundles in the corneal stroma, *J. Invest. Dermatol.* **28:**1939–1946.

Cheng, J., Fogel-Petrovic, M., and Maquat, L.E., 1990, Translation to near the distal end of the penultimate exon is required for normal levels of spliced triosephosphate isomerase mRNA, *Mol. Cell. Biol.* **10:**5215–5225.

Cleary, E.G., and Gibson, M.A., 1983, Elastin-associated microfibrils and microfibrillar proteins, *Int. Rev. Connect. Tissue Res.* **10:**197–209.

Cooke, R.M., Wilkinson, A.J., Baron, M., Pastore, A., Tappin, M.J., Campbell, I.D., Gregory, H., and Sheard, B., 1987, The solution structure of human epidermal growth factor, *Nature* **327:** 339–341.

Corson, G.M., Chalberg, S.C., Dietz, H.C., Charbonneau, N.L., and Sakai, L.Y., 1993, Fibrillin binds calcium and is coded by cDNAs that reveal a multidomain structure and alternatively spliced exons at the 5′end, *Genomics* **17:**476–484.

Cotta-Pereira, G., Guerra Rodrigo, F., and Bittencourt-Sampaio, S., 1976, Oxytalan, elaunin, and elastic fibers in the human skin, *J. Invest. Dermatol.* **66:**143–148.

Dahlback, B., Hildebrant, B., and Linse, S., 1990, Novel type of very high affinity calcium-binding sites in β-hydroxyasparagine-containing epidermal growth factor-like domains in vitamin K-dependent protein S, *Cell* 18481–18489.

Dahlback, K., Lofberg, H.H., Alumes, J., and Dahlback, B., 1989, Immunochistochemical demonstration of age-related deposition of vitronectin (S-protein of complement) and terminal complement complex on dermal elastic fibers, *Invest. Dermatol.* **93:**727–733.

Dahlback, K., Ljungquist, A., Lafberg, H., Dahlback, B., Engvall, E., and Sakai, L.Y., 1990, Fibrillin immunoreactive fibers constitute a unique network in the human dermis: Immunohistochemical comparison of the distribution of fibrillin, vitronectin, amyloid P component, and orcein stainable structures in normal skin and elastosis, *J. Invest. Dermatol.* **94:**284–291.

Dietz, H.C., Cutting, G.R., Pyeritz, R.E., Maslen, C.L., Sakai, L.Y., Corson, G.M., Puffenberger, E.G., Hamosh, A., Nanthakumar, E.J., Curristin, S.M., Stetten, G., Meyers, D.A., and Francomano, C.A., 1991, Marfan syndrome caused by a recurrent *de novo* missense mutation in the fibrillin gene, *Nature* **352:**337–339.

Dietz, H.C., Pyeritz, R.E., Puffenberger, E.G., Kendzior, R.J., Corson, G.M., Maslen, C.J., Sakai, L.Y., Francomano, C.A., and Cutting, G.R., 1992, Marfan phenotype variability in a family segregating a missense mutation in the EGF-like motif of the fibrillin gene, *J. Clin. Invest.* **89:**1674–1680.

Dietz, H.C., McIntosh, I., Sakai, L.Y., Corson, G.M., Chalberg, S.C., Pyeritz, R.E., and Francomano, C.A., 1993a, Four novel FBN1 mutations: Significance for mutant transcript level and EGF-like domain calcium binding in the pathogenesis of Marfan syndrome, *Genomics* **17:**468–475.

Dietz, H.C., Valle, D., Francomano, C.A., Kendzior, F.J., Pieritz, R.E., and Cutting, G.R., 1993b, The skipping of constitutive exons in vivo induced by nonsense mutations, *Science* **254:**680–683.

Fehon, R.G., Kooh, P.J., Rebay, I., Regan, C.L., xu, T., Muskavich, M.A.T., and Artavanis-Tsakonas, S., 1990, Molecular interactions between the protein products of the neurogenic loci notch and delta, two EGF-homologus genes in *Drosophila*, *Cell* **61:**523–534.

Gibson, M.A., Sandburg, L.B., Grosso, L.E., and Cleary, E.G., 1991, Complementary DNA cloning establishes microfibril-associated glycoprotein (MAGP) to be a discrete component of the elastin-associated microfibrils, *J. Biol. Chem.* **266:**7596–7601.

Godfrey, M., Vandemark, N., Wang, M., Velinov, M., Wargowski, D., Tsipouras, P., Haw, J., Becker, J., Robertson, W., Droste, S., and Rao, V.H., 1993, Prenatal diagnosis and a donor splice mutation in fibrillin in a family with Marfan syndrome, *Am. J. Hum. Genet.* **53:**472–480.

Gott, V.L., Pyeritz, R.E., Cameron, D.E., Green, P.S., and McKusick, V.A., 1991, Composite graft repair of Marfan aneurysm of the ascending aorta: results in 100 patients, *Ann. Thorac. Surg.* **52:**38–45.

Greenlee, Jr., T.K., Ross, R., and Hartman, J.L., 1966, The fine structure of elastic fibers, *J. Cell Biol.* **30:**59–71.

Handford, P.A., Baron, M., Mayhew, M., Willis, A., Beesley, T., Brownlee, G.G., and Campbell, I.D., 1990, The first EGF-like domain from human factor IX contains a high affinity calcium binding site, *EMBO J.* **9:**475–480.

Handford, P.A., Mayhew, M., Baron, M., Winship, P.R., Campbell, I.D., and Brownlee, G.G., 1991, Key residues involved in calcium-binding motifs in EGF-like domains, *Nature* **351:**164–167.

Herskowitz, I., 1993, Functional inactivation of genes by dominant negative mutations, *Nature* **329:**219–222.

Hewett, D.R., Lynch, J.R., Smith, R., and Sykes, B., 1993, Fibrillin mutation in the Marfan syndrome may disrupt calcium binding of the epidermal growth factor module, *Hum. Mol. Genet.* **2:** 475–477.

Hollister, D.W., Godfrey, M., Sakai, L.Y., and Pyeritz, R.E., 1990, Marfan syndrome: immunohistologic abnormalities of the elastin-associated microfibrillar fiber system, *N. Engl. J. Med.* **323:**152–159.

Horrigan, S.K., Rich, C.B., Streeten, B.W., Li, Z.Y., and Foster, J.A., 1992, Characterization of an associated microfibril protein through recombinant DNA techniques, *J. Biol. Chem.* **267:**10087–10095.

Hudson, B.G., Reeders, S.T., and Tryggvason, K., 1993, Type IV collagen: structure, gene organization, and role in human diseases, *J. Biol. Chem.* **268:**26033–26036.

Indik, A., Yah, H., Ornstein-Goldstein, N., Sheppard, P., Anderson, N., Rosenbloom, J.C., Peltonen, L., and Rosenbloom, J., 1987, Alternative splicing of human elastic mRNA indicated by sequence analysis of cloned genomic and complimentary DNA, *Proc. Natl. Acad. Sci. USA* **84:**5680–5684.

Jacenko, O., Olsen, B.R., and Warman, M.L., 1994, Of mice and men: heritable skeletal disorders, *Am. J. Hum. Genet.* **54:**163–168.

Kagan, H.M., Vaccaro, C.A., Bronxon, R.E., Tang, S.S., and Brody, J.S., 1986, Ultrastructural immunolocalization of lysyl oxidase in vascular connective tissue, *J. Cell Bio.* **103:**1121–1128.

Kainulainen, K., Pulkkinen, L., Savolainen, A., Kaitila, I., and Peltonen, L., 1990, Location of chromosome 15 of the gene defect causing Marfan syndrome, *N. Engl. J. Med.* **323:**935–939.

Kainulainen, K., Sakai, L.Y., Child, A., Pope, M.F., Puhakka, L., Ryhanen, L., Palotie, A., Kaitila, I., and Peltonen, L., 1992, Two unique mutations in Marfan syndrome resulting in truncated polypeptide chains of fibrillin, *Proc. Natl. Acad. Sci. USA* **88:**5917–5921.

Kainulainen, K., Karttunen, L., Puhakka, L., Sakai, L.Y., and Peltonen, L., 1994, Mutations in the fibrillin gene responsible for dominant ectopia lentis and neonatal Marfan syndrome, *Nature Genet.* **6:**64–69.

Kanzaki, T., Olofsson, A., Moren, A., Wernstedt, C., Hellman, U., Miyazono, K., Claesson-Welsh, L., and Heldin, C-H., 1990, TGF-β1 binding protein: a component of the large latent complex of TGF-β1 with multiple repeat sequences, *Cell* **61:**1051–1061.

Keene, D.R., Maddox, K.B., Kuo, H.S., Sakai, L.Y., and Glanville, R.W., 1991, Extraction of extendable beaded structures and their identification as fibrillin-containing extracellular matrix microfibrils, *J. Histochem. Cytochem.* **39:**441–449.

Kielty, C.M., and Shuttleworth, C.A., 1993, The role of calcium in the organization of fibrillin microfibrils, *FEBS Lett.* **336:**323–326.

Kobayashi, R., Tashima, Y., Masuda, H., Shozawa, S., Numata, Y., Miyauchi, K., and Hayakawa, T.,

1989, Isolation and characterization of a new 36-kDA microfibril-associated glycoprotein from porcine aorta, *J. Biol. Chem.* **264:**17437–17444.

Lee, B., D'Alessio, M., and Ramirez, F., 1991a, Modifications in the organization and expression of collagen genes associated with skeletal disorders, *Crit. Rev. Euk. Gene. Exp.* **1:**173–187.

Lee, B., Godfrey, M., Vitale, E., Hori, H., Mattei, M.G., Sarfarazi, M., Tsipouras, P., Ramirez, F., and Hollister, D.W., 1991b, Linkage of Marfan syndrome and a phenotypically related disorder to two fibrillin genes, *Nature* **352:**330–334.

Maddox, B.K., Sakai, L.Y., Keene, D.R., and Glanville, R.W., 1989, Connective tissue microfibrils; isolation and characterization of three large pepsin-resistant domains of fibrillin, *J. Biol. Chem.* **264:**21381–21385.

Magid, D., Pyeritz, R.E., and Fishman, E.K., 1990, Musculoskeletal manifestations of the Marfan syndrome: radiologic features, *Am. J. Roentgenol.* **155:**99–104.

Maslen, C.L., Corson, G.M., Maddox, B.K., Glanville, R.W., and Sakai, L.Y., 1991, Partial sequence of a candidate gene for the Marfan syndrome, *Nature* **352:**334–337.

Maumenee, I.H., 1981, The eye in the Marfan syndrome, *Trans. Am. Ophthal. Soc.* **79:**684–733.

Mayhew, M., Handford, P.A., Baron, M., Tse, A.G.D., Campbell, I.D., and Brownlee, G.G., 1992, Ligand requirements for calcium binding to EGF-like domains, *Prot. Engineering* **15:**489–494.

McGookey-Milewicz, D., Pyeritz, R.E., Crawford, E.S., and Byers, P.H., 1992, Marfan syndrome: defective synthesis, secretion and extracellular matrix formation of fibrillin by cultured dermal fibroblasts, *J. Clin. Invest.* **89:**79–86.

Milewicz, D.M., and Duvic, M., 1994, Severe neonatal Marfan syndrome resulting from a *de novo* 3-bp inser ion into the fibrillin gene on chromosome 15, *Am. J. Hum. Genet.* **54:**447–453.

Morse, R.P., Rockenmacher, S., Pyeritz, R.E., Sanders, S.P., Bieber, F.R., Lin, A., MacLeod, P., Hall, B., and Graham, Jr., J.M., 1990, Diagnosis and management of infantile Marfan syndrome, *Pediatrics* **86:**888–895.

Murdoch, J.L., Walker, B.A., Halpern, B.I., Kuzma, J.W., and McKusick, V.A., 1972, Life expectancy and causes of death in the Marfan syndrome, *N. Engl. J. Med.* **286:**804–808.

Pereira, L., D'Alessio, M., Ramirez, F., Lynch, J.R., Sykes, B., Pangilinan, T., and Bonadio, J., 1993, Genomic organization of the sequence coding for fibrillin, the defective gene product in Marfan syndrome, *Hum. Mol. Genet.* **2:**961–968.

Pereira, L., Levran, O., Ramirez, F., Lynch, J.R., Sykes, B., Pyeritz, R.E., and Dietz, H.C., 1994, Diagnosis of Marfan syndrome: a molecular approach for stratification of cardiovascular risk within families, *N. Engl. J. Med.* (in press).

Pyeritz, R.E., and McKusick, V.A., 1979, The Marfan syndrome: diagnosis and management, *N. Engl. J. Med.* **300:**772–777.

Ramirez, F., Pereira, L., Zhang, H., and Lee, B., 1993, The fibrillin-Marfan syndrome connection, *BioEssays* **15:**589–594.

Raju, K., and Anwar, R.A., 1987, Primary structures of bovine elastin a,b, and c deduced from sequences of cDNA clones, *J. Biol. Chem.* **262:**5755–5762.

Raviola, G., 1971, The fine structure of the ciliary zonule and ciliary epithelium, *J. Invest. Opthal.* **10:**851–869.

Roberts, W.C., and Honig, H.S., 1982, The spectrum of cardiovascular disease in the Marfan syndrome: A clinico-morphologic study of 18 necropsy patients and comparison to 151 previously reported necropsy patients, *Am. Heart J.* **104:**115–135.

Rosenbloom, J., Abrams, W.R., and Mecham, R., 1993, Extracellular matrix 4: the elastic fiber, *FASEB J.* **7:**1208–1218.

Ross, R., and Bornstein, P., 1966, The elastic fiber, *J. Cell Biol.* **40:**336–381.

Sakai, L.Y., 1990, Disulfide bonds crosslink molecules of fibrillin in the connective tissue space, in *Elastin: Chemical and Biological Aspects* (A. Tamburro and J.M. Davidson, eds.), pp. 213–227, Congedo Editore, Galatina, Italy.

Sakai, L.Y., Keene, D.R., and Engvall, E., 1986, Fibrillin, a new 350-kD glycoprotein, is a component of extracellular microfibrils, *J. Cell Biol.* **103:**2499–2509.

Sakai, L.Y., Keene, D.R., Glanville, R.W., and Bachinger, H.P., 1991, Purification and partial characterization of fibrillin, a cysteine-rich structural component of connective tissue microfibrils, *J. Biol. Chem.* **266:**14763–16770.

Savage, Jr., R.C., Wilkinson, A.J., Baron, B., Pastore, A., Tappin, M.J., Campbell, I.D., Gregory, G., and Sheard, B., 1987, The solution structure of human epidermal growth factor, *Nature* **327:** 339–341.

Shores, J., Berger, K.R., Murphy, E.A., and Pyeritz, R.E., 1994, Progression of aortic dilatation and the benefit of long-term β-adrenergic blockade in the Marfan syndrome, *N. Engl. J. Med.* (in press).

Tsipouras, P., Del Mastro, R., Sarfarazi, M., Lee, B., Vitale, E., Child, A., Godfrey, M., Devereux, R., Hewett, D., Steinmann, B., Viljoen, D., Sykes, B.C., Kilkpatrick, M., and Ramirez, F., 1992, Linkage of Marfan syndrome, dominant ectopia lentis and congenital contractural arachnodactyly to the fibrillin genes on chromosomes 15 and 5, *N. Engl. J. Med.* **326:**905–909.

Tynan, K., Comeau, K., Pearson, M., Wilgenbus, P., Levitt, D., Gasner, C., Berg, M.A., Miller, D.C., and Francke, U., 1993, Mutation screening of complete fibrillin-1 coding sequence: Report of five new mutations, including two in 8-cysteine domains, *Hum. Mol. Genet.* **2:**1813–1821.

Uitto, J., and Christiano, A.M., 1992, Molecular genetics of the cutaneous basement membrane zone, *J. Clin. Invest.* **90:**687–692.

Urlaub, G., Mitchell, P.J., Ciudad, C.J., and Chasin, L.A., 1989, Nonsense mutations in the dihydrofolate reductase gene affect RNA processing, *Mol. Cell. Biol.* 1989; **9:**2868–2880.

Wright. D.W., and Mayne, R., 1988, Vitreous humor of chicken contains two fibrillar systems: an analysis of their structure, *J. Ultrastruct. Mol. Res.* **100:**234–244.

Zhang, H., Apfelroth, S.D., Hu, W., Davis, E.C., Sanguineti, C., Bonadio, J., Mecham, R.P., and Ramirez, F., 1994, Structure and expression of fibrillin-2, a novel microfibrillar component preferentially located in elastic matrices, *J. Cell Biol.* **124:**855–863.

Zimmermann, D.R., Dours-Zimmermann, M.T., Schubert, M., and Bruchner-Tuderman, L., 1994, Versican is expressed in the proliferating zone in the epidermis and in association with the elastic network of the dermis, *J. Cell Biol.* **124:**817–825.

Chapter 5

Nonisotopic *in Situ* Hybridization
Clinical Cytogenetics and Gene Mapping Applications

Matteo Adinolfi*

Division of Medical & Molecular Genetics
United Medical and Dental Schools
Guy's and St. Thomas's Hospitals
London Bridge, London, England SE1 9RT

John Crolla

Wessex Regional Genetics Laboratory
Salisbury District Hospital
Salisbury, Wiltshire, England SP2 8BJ

INTRODUCTION

The detection of DNA or RNA sequences in cells in interphase or metaphase can readily be achieved by *in situ* hybridization procedures based on the specific annealing of sequences (probes), previously labeled with appropriate reporter molecules, to their corresponding genomic DNA or RNA regions. Under special conditions, stable complexes are formed that can be visualized.

In early studies, radiolabeled DNA or RNA probes were employed, and the hybridization complexes were detected as "silver grains" on photographic films or emulsion (Buongiorno-Nardelli and Amaldi, 1969; Gall and Pardue, 1969; John *et al.*, 1969).

Present address: The Galton Laboratory, University College London, Wolfson House, 4 Stephenson Way, London, England NW1 2HE

Advances in Human Genetics, Volume 22, edited by Henry Harris and Kurt Hirschhorn. Plenum Press, New York, 1994.

A nonisotopic *in situ* hybridization (NISH) method was first introduced in 1975 by Manning *et al.*; using electron microscopy, the nucleic acid sequences were labeled with biotin and the hybridization complexes were detected by avidin-coated microspheres. Subsequently, a variety of procedures had been developed to improve the visualization of the hybridization complexes, ranging from the use of different reporter molecules to label the probes (Langer *et al.*, 1981; Tchen *et al.*, 1984; Landegent *et al.*, 1984; Hopman *et al.*, 1986a,b,c; Khalfan *et al.*, 1986) to the exploitation of various fluorochromes, enzymatic reactions, and antibodies to amplify the signals* (Pinkel *et al.*, 1986; Landegent *et al.*, 1987; Cremer *et al.*, 1986; Kozma and Adinolfi, 1987; Singer *et al.*, 1987; Hopman *et al.*, 1988; Nederlof *et al.*, 1989; Herrington and McGee, 1990; Nederlof *et al.*, 1990; Trask, 1991).

The advent of new molecular technologies has also improved the availability and preparation of probes that are free of contaminants. Whereas in early studies only repetitive sequences could be visualized, the introduction of competitive hybridization techniques and digital imaging microscopy meant that probes between one and two kb can now be employed (Lawrence, 1990; Ried *et al.*, 1992; Adinolfi and Davies, 1994). With fluorescence *in situ* hybridization (FISH) assays, by a careful selection of appropriate fluorochromes, several probes, previously labeled with different reporter molecules or mixtures (ratios) of such molecules, can be used simultaneously and visualized in cells in interphase or metaphase (Landegent *et al.*, 1984; Pinkel *et al.*, 1986; Hopman *et al.*, 1986a,b,c, 1988; Singer *et al.*, 1987; Emmerich *et al.*, 1989).

The simultaneous visualization of several sequences is one of the many advantages that FISH has over the radioactive method (Nederlof *et al.*, 1990; Lichter and Ward, 1990; Wiegant *et al.*, 1993). The use of enzymes to stain hybridization complexes provides the opportunity to obtain permanent preparations that can be counterstained and to identify specific chromosomal regions. Another advantage of NISH over the radioactive method is that the former allows greater spatial resolution of specific sequences. The signals of the isotopically labeled probes, visualized on films or photographic emulsions, are often located outside their specific genomic targets. The radioisotopic technique requires several days before results can be analyzed, while most NISH procedures can be performed in a relatively short period of time. In addition, once the probes are labeled with reporter molecules, they can be stored for several years.

Among the factors that have tilted the balance toward the nonisotopic

*When fluorochromes are employed, the short term FISH is used to indicate the specific method. In this study, we will use NISH as a general term, and FISH when fluorescent dyes are employed in the quoted papers.

methods is the possibility of successfully using the polymerase chain reaction (PCR), either to amplify and label single DNA sequences that are then hybridized to the target DNA, or to amplify DNA extracted from previously sorted chromosomes. An alternative is to amplify directly DNA sequences in cells in interphase or metaphase that have been spread on glass slides (Baldini and Ward, 1991; Gosden *et al.*, 1991; Koch *et al.*, 1989, 1991, 1992; Telenius *et al.*, 1992; Vooijs *et al.*, 1993). This last procedure, termed PRINS (from primed *in situ*), is being applied with increasing frequency because it is simple and rapid.

The final choice, when selecting one of the many NISH methods, depends on the specific requirements and the availability of appropriate equipment. Enzymatic staining has the advantage over FISH methods that slides can be stored for a long period of time; however, the combination of fluorescence microscopy with computerized digital image enhancement and memory storage technology allows results to be stored and recalled for further analysis.

Digital imaging techniques have also significantly increased the range of fluorochrome combinations that can be used in varying "ratio" combinations, which in expert hands can lead to multiple color (and hence probe) analyses (Cremer *et al.*, 1991). Colored chromosome staining patterns, termed chromosomal "bar codes" (CBCs), have been produced in human chromosomes by FISH with pools of Alu-PCR probes derived from yeast artificial chromosome (YAC) clones containing human DNA inserts ranging from 100 kilobase-pairs (kb) to 1 million base-pairs (Mb). Individual colors and relative signal intensity of each "bar" could readily be modified depending on probe selection and labeling procedures (Lengauer *et al.*, 1993).

During the past few years, NISH has become an indispensable procedure in many areas of research and clinical cytogenetics, including: the analysis of chromosomal abnormalities not readily detected or unequivocally resolved by conventional cytogenetic methods; the possibility of performing rapid prenatal identification of major chromosomal defects in cells in interphase; the localization of genes on specific chromosomes using cells in interphase or metaphase; and the detection of duplications or deletions associated with some diseases.

We will discuss selected clinical applications of NISH methods for the detection of DNA sequences. The specific techniques will not be described in detail: they are available in several publications (Buckle and Craig, 1986; Polak and McGee, 1990; Adinolfi and Davies, 1994; Leitch *et al.*, 1994).

NISH has become a widely used tool, and the number of studies based on or supported by this method is increasing exponentially. Though our presentation will be incomplete and important papers omitted, we hope our selection will be representative of many areas of research and clinical diagnosis in which NISH can be applied.

THE PROBES

The majority of NISH techniques in routine use conforms to a simple protocol in which a nonisotopically labeled single-stranded (or denatured genomic) nucleic acid probe is hybridized to a denatured complimentary target preparation (e.g., tissue section, metaphase chromosomes, or interphase nuclei), rendering the target nucleic acid molecules available for complimentary hybridization and visualization using enzymatic or fluorometric detection methods (Fig. 1).

Probes propagated in plasmids, cosmids, YAC vectors, and oligonucleotides are suitable for NISH. Centromeric repetitive DNA sequences are particularly useful for identifying specific chromosomes and are employed extensively. The centromeric regions of human chromosomes vary in length from a few hundred kb to several Mb and are composed of several families of satellite DNA (Willard and Waye, 1987; Willard, 1985, 1990, 1992).

The fundamental unit of human α-satellite DNA is a monomer of about 171 bp long (Manuelidis and Wu, 1978); available data suggest that the majority of α-satellite tandem repeats can stretch for several Mb.

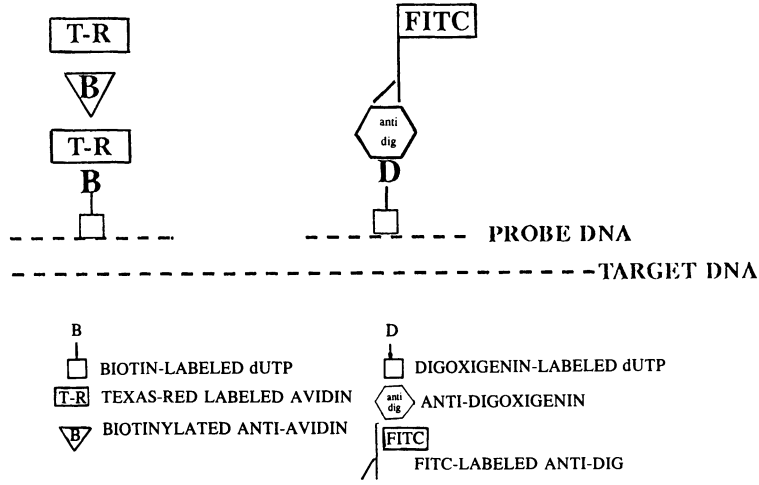

Fig. 1. Schematic representation of the basic principle for the simultaneous detection of two probes with reporter molecules marked with different fluorochromes. The digoxigenin-labeled probe will be seen as a green (FITC) fluorescent signal, while the biotin-labeled probe will appear as a red (Texas Red) signal.

Since 1985, it has been demonstrated that centromeric α-satellite sequences are organized in a highly specific fashion in each chromosome (Willard, 1985; Mitchell *et al.*, 1985; Jorgensen *et al.*, 1987; Choo *et al.*, 1989); the individual subsets are usually known by their cognate chromosome (e.g., α X subset, α 1 subset). Centromeric α-satellites have been identified, on chromosomes 13, 18, and 21 (Devilee *et al.*, 1986); 22 (McDermid *et al.*, 1986); 13, 14, and 21 (Choo *et al.*, 1988); 15 (Choo *et al.*, 1990); and 12 (Baldini *et al.*, 1990; Looijenga *et al.*, 1990). A survey of the genomic distribution of α-satellite DNA in all human chromosomes and their sequences has been published by Choo *et al.* (1991).

An intriguing observation derived from the analysis of the organization of α-satellites is their polymorphism. The coexistence of several distinct high-order repeat forms with a single alphoid array has been demonstrated for several chromosomes. These forms differ from each other in the overall length of the multicopy units (e.g., 13 to 16) and/or primary nucleotide sequences.

In a few instances the molecular basis for α-satellite polymorphisms has been determined: for the chromosome 17 α-satellite, evidence has been obtained from primary sequence data to support a mechanism of unequal recombination (inter- or intrachromatid) between misaligned repeats (Willard and Waye, 1987). The polymorphism of some α-satellites can also be detected by FISH as varying intensities of fluorescent staining (Verma and Luke, 1992).

A new family of centromeric repetitive probes has been identified from an investigation into the origin of the chromosomal abnormality in a female infant whose peripheral blood lymphocytes contained two copies of a marker chromosome, in addition to a uniform tetraploid karyotype. This new group of satellites (sn5) seems to be primate-specific and shows a distribution in the human chromosomes similar to that of the α-satellite family 2 because it is distributed at the pericentromeric regions of chromosomes 13, 14, 15, 21, and 22, but not of chromosomes 5 and 7 (Johnson *et al.*, 1992).

Beside the centromeric repetitive probes, other repetitive sequences have been used for NISH analysis: the proximal Yp and distal Yq heterochromatin regions (Cooke *et al.*, 1982; Müller *et al.*, 1986a,b); the satellite II and III probes derived from the heterochromatic regions of 1qh, 9qh, and 16qh (Cook and Hindley, 1987; Moyzis, 1987); and the 15 short arm satellite III heterochromatin (Higgins *et al.*, 1985).

In contrast, the use and detection of probes cloned from unique genomic sequences located at specific regions of each chromosome were later developments of NISH technology, and came about with the introduction of a competitive hybridization methodology known as chromosome *in situ* suppression hybridization (CISS). CISS made it possible to "compete out" the repetitive sequences that

are ubiquitously interspersed between the unique sequences within each probe (Pinkel *et al.*, 1988; Cremer *et al.*, 1988; Kievits *et al.*, 1990). This modification of NISH technology has revolutionized and dramatically expanded the applications of the technique, and, for the first time, has allowed the use of probes derived from cosmids or pools of overlapping cosmids (contigs), and of "chromosome forward and reverse paint" procedures (Fig. 2).

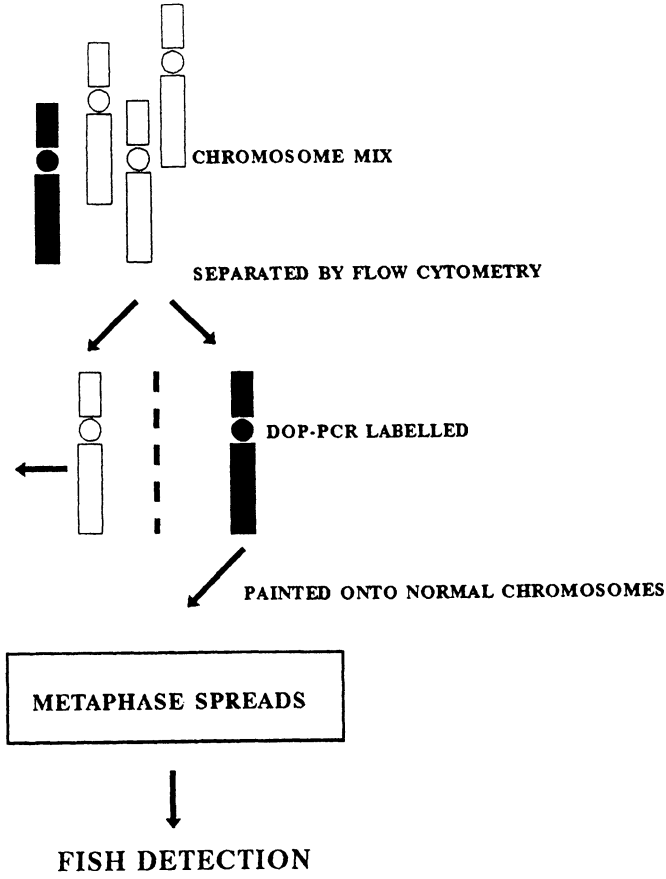

Fig. 2. Schematic representation of the preparation of chromosome-specific libraries using dual laser flow cytometry. An individual chromosome (black) is identified by its size, shape, and differential fluorescence and "sorted" into a tube by the flow cytometer. DOP-PCR (see text) is then used to amplify the sorted chromosomal DNA and label with either biotin, digoxigenin or FITC. These sorted and labeled probes can then be applied, following a competitive-hybridization pretreatment as a chromosome-specific probe, which is "painted" onto metaphase chromosome preparations.

The use of CISS also made possible the expansion of *in situ* methodologies to utilize probes derived from vectors containing large regions of cloned genomic DNA, for example sequences cloned in YACs. Such probes can be used either after purification by pulsed field electrophoresis, aimed at removing contaminating endogenous yeast DNA, or following extraction from the entire DNA present in the YACs (Schwartz and Cantor, 1984; Montanaro *et al.*, 1991; Selleri *et al.*, 1991a; Baldini *et al.*, 1992; Lengauer *et al.*, 1993; Adinolfi and Davies, 1994).

Cosmid and YAC probes allow precise localization of DNA sequences on individual chromosomes, and are often employed with other methods during the process of gene mapping.

DNA that has been prepared from a single chromosome (previously isolated by flow cytometry from a preparation containing normal chromosomes in metaphase or from a somatic cell hybrid) can be used to identify the corresponding chromosome in metaphase spreads after labeling with a degenerate primed-PCR reaction (DOP-PCR). This method, "forward chromosome painting" (Telenius *et al.*, 1992) has many practical applications, particularly in the field of translocations and aberrations found in cancer cells (Cremer *et al.*, 1988; Lichter *et al.*, 1988), and in the resolution of some classes of constitutional chromosome abnormalities (Hulten *et al.*, 1991; Carter *et al.*, 1992). These approaches may prove unsatisfactory in some subtle forms of structural rearrangements such as very small duplications (Gould *et al.*, 1992). An alternative method can be employed: the abnormal chromosome can be isolated by flow cytometry and used to form DOP-PCR "reverse" paint, which, when hybridized back onto normal metaphase spreads, may reveal the chromosomal origin and extent of the abnormality being investigated (Carter *et al.*, 1992; Joos *et al.*, 1993). This approach has also been extended to the study of constitutional and acquired types of marker chromosomes, and, in some examples, has revealed hidden chromosome structures of considerable complexity (Blennow *et al.*, 1992).

Chromosome microdissection is another powerful and frequently employed approach for generating region-specific probes (Kao, 1987; Kao and Yu, 1991; Lüdecke *et al.*, 1989; Senger *et al.*, 1990; Meltzer *et al.*, 1993). DNA sequences, from a few fragments collected by microdissection, are amplified by PCR and then utilized for NISH (Deng *et al.*, 1992).

Most microdissection techniques are based on the time-consuming and labor-intensive collection of up to 40 fragments from the target region to obtain enough DNA template for PCR amplification. The addition of each fragment to the pool increases the probability of contamination. Guan *et al.* (1993) have described a protocol that reduces the number of copies of dissected target DNA. It is based on the pretreatment of the dissected chromatin with topoisomerase I (Topo I), before

PCR. A single microdissected fragment is sufficient to construct a region-specific probe for FISH.

Chromosome-specific probes obtained by microdissection have proved to be useful in identifying a chromosome marker when DNA was collected from the chromosome fragment by microdissection, and the sequences amplified and labeled. The probes were then hybridized by FISH to metaphase spreads prepared from a normal subject, revealing the chromosomal origin of the marker (Ohta *et al.*, 1993). This technique has also been successfully applied for the identification of the mechanism that leads to the generation of deleted chromosomes and their stabilization in cancer cells. Meltzer and colleagues (1993) have generated probes by microdissection from apparent terminal deficiencies of chromosome 6 prepared from patients with malignant melanoma. The terminal portion of the long arm of a der(6) chromosome was collected by microdissection, amplified by PCR, and biotinylated for FISH analysis. While the isolated sequences hybridized to the dissected region of der(6), thus documenting the authenticity of the prepared probe, a strong signal was observed on the terminal portion of chromosome 20q on hybridization to normal lymphocyte chromosomes. These results demonstrated that the apparent terminal deficiency of chromosome 6 was actually a cryptic translocation involving chromosome 20 (Meltzer *et al.*, 1993).

A variant microdissection technique has also been described by Hozier *et al.* (1994); the probe can be either the insert fraction of a cDNA library or a cDNA primer ligated to an adapter designed for subsequent PCR. The amplified, unlabeled products are hybridized to metaphase spreads. After hybridization, the chromosomes are stained to produce the characteristic banding pattern that allows their identification. The chromosome of interest is then microdissected, the collected material, containing the hybridized DNA, is amplified *in vitro* using PCR and cloned into a suitable vector for analysis. According to Hozier *et al.* (1994), this preparative *in situ* hybridization (pre-ISH) method has useful applications for studying gene expression and genomic organization.

DETECTION BY NISH OF CHROMOSOMAL DISORDERS IN METAPHASE SPREADS

Many published reports document the diagnostic value of using NISH to detect chromosomal disorders that cannot readily be analyzed by conventional cytogenetic methods, including the identification of translocations, small deletions, duplications, and chromosome markers. In most instances, the origin and

nature of the abnormalities can best be established using metaphase spreads, but interphase analysis by NISH can also provide useful diagnostic information about major chromosomal defects. This is particularly true when this approach is exploited as a prenatal test on amniotic or chorionic cells (Kuo *et al.*, 1991; Zheng *et al.*, 1992; Klinger *et al.*, 1992; Ward *et al.*, 1992; Davies *et al.*, 1994a,b). We will describe first the applications of NISH on metaphase spreads for the detection of translocations, isochromosomes, chromosome markers, deletions, and duplications; and then the use of NISH on cells in interphase.

Translocations and Isochromosomes

The great majority of these chromosomal disorders can readily be detected by conventional cytogenetics. In some cases, NISH has been employed mainly to confirm the diagnosis or to clarify the nature and characteristics of the abnormality.

We will illustrate a few situations where NISH has been instrumental in documenting small translocations or isochromosomes, such as those involving the Y chromosome. Interest in this type of disorder probably derives from the knowledge that the differentiation of the primordial gonad into testis depends on the presence of a gene on the short arm of the Y chromosome (Yp). The testicular differentiation gene (TDY) that maps on Yp has recently been cloned (Sinclair *et al.*, 1990). Termed the sex-related Y gene (SRY), this sequence is present in normal males (46,XY), and the great majority of phenotypic males with two X chromosomes (46,XX) or other Yp translocations. It is absent in normal females (46,XX) and in phenotypic females who have a 46,XY chromosome complement and deletion of the SRY gene (Goodfellow and Lovell-Badge, 1993). SRY is expressed at particular stages of gonadal differentiation in male embryos and can induce male development in chromosomally female mice transgenic for this sequence (Koopman *et al.*, 1990, 1991).

While the presence or absence of the SRY gene can be readily determined by PCR amplification, the site of translocation can only be established by NISH, using the SRY sequence or other closely linked Yp probes; for example, the Y190 and Y431 pericentric probes have been successfully employed to investigate patients with Y chromosome abnormalities (Kozma and Adinolfi, 1988).

Fig. 3 shows a Y;10 translocation that was initially detected in a 45,X patient and later confirmed by molecular studies that also documented the presence of an inversion within the translocated Y fragment (Müller *et al.*, 1989). Another interesting case has been described by von Hemel *et al.* (1992). The boy, who had a 45,X karyotype, had dysmorphic features, hypoglycemia, and pancytopenia.

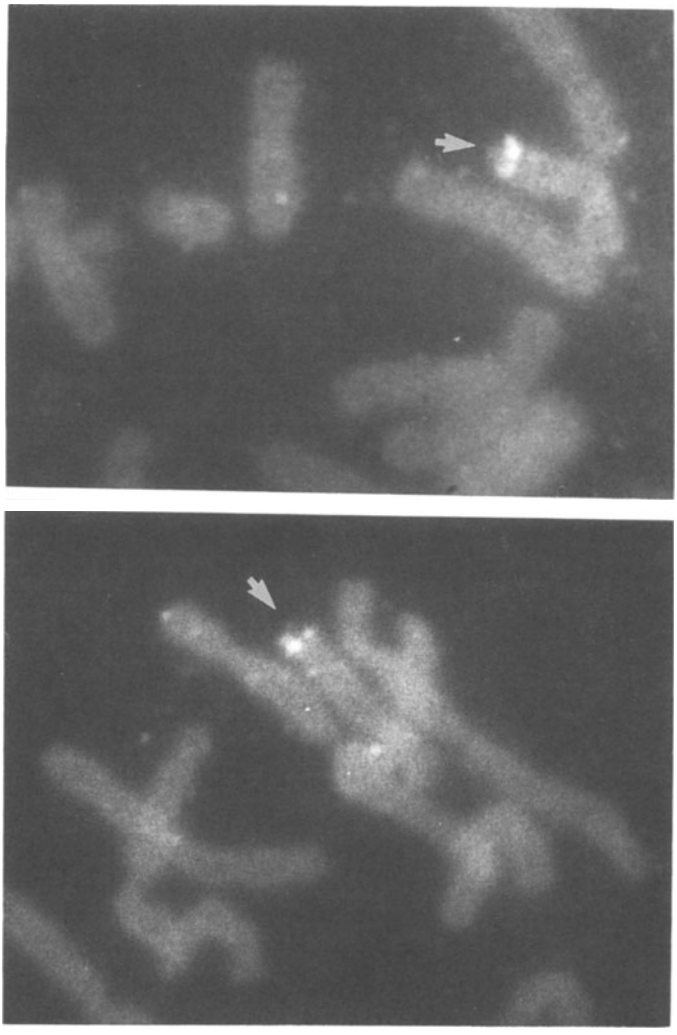

Fig. 3. Detection by FISH and Y190 probe of a translocation of the short arm of the Y chromosome to chromosome 10 in a 45,X male patient (partial metaphase).

Jacobsen syndrome was suggested by the presence of trigonocephaly, ptosis, deep-set short nose, and a carp-shaped mouth. Using a Yp-derived probe and FISH, a Y;11 translocation was detected, associated with an 11q24→qter deletion. According to von Hemel *et al.* (1992), some of the Jacobsen symptoms observed in this patient could be attributed to a deletion affecting the long arm of chromosome 11. A list of Y translocations investigated by FISH is reported in Adinolfi and Davies (1994).

Another example of the diagnostic value of FISH is illustrated in Fig. 4. Conventional cytogenetic analysis of metaphase spreads obtained from a six-year-old girl with short stature, webbed neck, and suspected behavioral disorders documented the presence of two normal chromosomes 21, one normal chromosome X, and a partially deleted X with a possible translocation of a small fragment of chromosome 21 (Barber and Crichter, 1994). When tested by FISH with an X-centromeric probe (pSV2X5) and a 21-derived probe mapping to the 21q22.2 region, two normal chromosomes 21, and a normal X chromosome could be detected in each metaphase spread. The other X chromosome showed a bright hybridization signal on the tip of the long arm with the 21 probe. This patient was, therefore, trisomic for the 21q22.2 region but did not show clinical symptoms of Down syndrome and had normal dermatoglyphics. Further studies showed that the X chromosome containing the translocation was inactivated, as was the translocated 21-derived fragment. The only overt clinical symptoms associated with the abnormalities were the short stature and webbed neck, typical of patients with Turner syndrome.

In some patients, NISH tests can provide useful information about the structural arrangements of isochromosomes. Sharp *et al.* (1990) have investigated three patients with long arm X isochromosomes and an isodicentric X chromosome, using FISH and an X-centromeric probe. The results showed that in each patient, the chromosomal abnormality was due to different, unique pericentromeric structures. The isodicentric X (isodic X) showed two distinct α-satellite hybridization signals and duplication of the short arm material. Two isochromosomes X showed a longer than normal, bifid α-satellite signal and had different duplications of the Xp region. The third X isochromosome had an α-satellite signal similar in size to that present on the normal X.

FISH has also been successfully applied to characterize *de novo* chromosomal duplications. In six of eight patients investigated by Leana-Cox *et al.* (1993), the clinical phenotype and/or conventional cytogenetics had already suggested the likely origin of the duplicated material. The other two cases necessitated multiple hybridization to determine the chromosomal origin of the duplication. In one infant, the abnormality, suspected to involve chromosome 1,

was instead shown to result from a duplication of a fragment from chromosome 17. In the third case, a suspected duplication involving chromosome 13 demonstrated that the extra fragment was derived from chromosome 3q.

Reverse chromosome painting has also been successfully applied to the resolution of a number of subtle structural constitutional chromosome abnormalities (Carter *et al.*, 1992). This approach requires flow sorting of the abnormal derivative chromosomes, labeling of the resultant DNA using degenerate primed PCR (DOP–PCR: Telenius *et al.*, 1992), and the use of the biotinylated DOP–PCR products as a paint onto normal metaphase spreads. Using this approach, Carter *et al.* (1992) were able to resolve the origin and composition of a number of structural abnormalities (e.g., a duplication of 8p and a 13q33 insertion into 1p36); significantly they proved that this method not only determines the origin of some rearrangements, but also gives precise information on the regional location of the origin of the chromosomal material being investigated. Using a similar technique, Rack *et al.* (1993) resolved the structure of three *de novo* derivative chromosomes 16.

Marker Chromosomes

Marker chromosomes are found in karyotypes of constitutional and acquired chromosome abnormalities, and provide unique problems for accurate cytogenetic identification and classification. In this review, our discussion is restricted to the application of NISH methodology to the study of constitutional supernumerary marker chromosomes (SMCs), such as small additional chromosomes whose origin or composition cannot be identified by conventional cytogenetic staining techniques. Excluded by this definition are isochromosomes for the short arms of chromosomes 12, 18, and X, which, in normal circumstances, can be diagnosed by a variety of standard methods and are associated with relatively well characterized syndromes (Schinzel, 1984).

SMCs are seen with a frequency of approximately 0.24/1000 in phenotypically normal individuals but 13 times more frequently (3.27/1000) among mentally retarded populations (Buckton *et al.*, 1985). Approximately 16% are familial, and, if found in a phenotypically normal parent, are generally transmitted without detrimental effects. The remaining 84% arise *de novo*, and the prediction of phenotypic risks in this latter group is problematic due mostly to the paucity of long-term follow-up data from such cases. The published estimates are, therefore, given with large margins of error (Hsu, 1986; Warburton, 1991). Based on a large survey of over 33,000 consecutive amniocentesis samples karyotyped in the USA and Canada, Warburton (1991) estimated that the overall risk for physical

and/or mental retardation associated with the prenatal ascertainment of a *de novo* SMC is approximately 13%.

Conventional cytogenetic studies have shown that the majority of SMCs (~86%) are derived from the short arm and pericentromeric regions of acrocentric chromosomes (Buckton *et al.*, 1985; Friedrich and Jensen, 1983; Maraschio *et al.*, 1988), of which approximately half are distamycin/DAPI (DA/DAPI) stained (Schweizer *et al.*, 1978), and therefore, involve the short arm region of chromosome 15. Seventy percent of the DA/DAPI positive markers are conventionally described as inverted duplications (inv dup) involving the pericentromeric region of chromosome 15 (Maraschio *et al.*, 1988). This class of SMC provides an interesting model for a study of phenotypic effects associated with marker chromosomes as patients have been reported with varying size and shapes of inv dup(15) markers and phenotypes ranging from the physically and intellectually normal to the severely mentally retarded; in rare cases, these SMCs have been detected in patients with either Prader-Willi (PWS) or Angelman's syndromes (AS) (Maraschio *et al.*, 1988; Robinson *et al.*, 1993a). Molecular genetics and, more recently, FISH methods have been used to formally demonstrate that duplications of the imprinted proximal 15q region within some types of inv dup (15)s are, as expected, correlated with adverse phenotypic outcomes (Robinson *et al.*, 1993a; Crolla *et al.*, 1994).

With the exception of mar(15) chromosomes, conventional cytogenetic techniques can provide only general information on the origin of SMCs. More specific information can only be obtained using a combination of NISH and molecular genetic techniques. The most frequent NISH strategy used to identify the chromosomal origin of SMCs is based on the systematic use of a series of centromere-specific probes on metaphase spreads either singly or in multi-colored combinations. Metaphases containing the marker are analyzed after *in situ* hybridization, and the marker's centromeric composition is deduced when both the SMC and the internal normal homologous centromeres show hybridization signals (Fig. 5). If the marker is suspected to contain additional euchromatic material, further molecular strategies may be required to deduce the exact nature and chromosomal composition of the marker chromosome (Fig. 6).

A systematic NISH approach to the molecular characterization of SMCs was first applied to patients with sex chromosome mosaicism and a cell line containing a small marker or ring chromosome thought to be derived from either the X or Y chromosome (Kushnick *et al.*, 1987; Crolla and Llerena, 1988; Kozma *et al.*, 1988; Crolla *et al.*, 1989; Jacobs *et al.*, 1990; Koch *et al.*, 1990). The cloning of alphoid repeats from all human centromeres meant that by using this approach, autosomally derived SMCs could be identified systematically (Callen *et al.*, 1990,

1991, 1992; Crolla *et al.*, 1992; Rauch *et al.*, 1992; Plattner *et al.*, 1993a,b). In addition to these systematic studies on relatively large series of patients with SMCs, smaller groups of patients have been reported so that, to date, the chromosomal origins of over 120 cases of autosomally derived SMCs have been identified (Fig. 7), including 58 patients with SMCs studied at the Wessex Regional Genetics Laboratory (Crolla *et al.*, 1992, 1994, and unpublished data).

Approximately half of SMCs identified with NISH methods (in contrast to the 86% tentatively identified with conventional techniques) have been found to be derived from acrocentric chromosomes (Fig. 7). However, there is an inevitable ascertainment bias in most of the NISH studies on marker chromosomes published to date because phenotypically abnormal probands are overrepresented. SMCs of chromosome 15 and either chromosome 14 or 22 origins were found with the same frequencies, that is, approximately 44% of all the acrocentric-derived SMCs, with the remainder containing the centromeric heterochromatin of either chromosome

Fig. 4. FISH analysis of metaphase spread from a patient known by conventional cytogenetic analysis to have a karyotype with two normal chromosomes 21, one normal X chromosome, and a partially deleted X chromosome, with a possible translocation of a small fragment of chromosome 21. FISH tests using an X-derived centromeric probe (pSV2X5) and a 21q22.3 probe documented the 21;X translocation (arrow) and therefore trisomy 21. However, the patient had no clinical symptoms of Down's syndrome due to nonrandom inactivation of the partially deleted X chromosome together with the translocated 21.

Fig. 5. A patient with a karyotype containing a supernumerary marker chromosome of chromosome 3 origin. Hybridization with the chromosome 3 centromere-specific probe (pα3.8;D3Z1, kindly supplied by Dr. H. Willard) shows signals from the two #3 centromeres and from the marker 3 (arrowed). Forward chromosome painting with a flow sorted chromosome 3 library showed that the unlabeled (red) portion of the ring was composed entirely of chromosome 3 material.

Fig. 6. **A**. A patient with a small supernumerary marker 15 chromosome showing positive signals from the two normal 15 homologues and the mar(15). The marker in this patient is a small ring and the probe is D15Z1, specific for the satellite III repetitive sequence on the short arm of chromosome 15. This patient was ascertained because of severe mental retardation. **B**. The same patient as shown in **A** following hybridization with the GABRB3 cosmid from proximal 15q. Signal can be seen from the marker 15 (arrow) showing that it contains the GABRB3 region of the Prader-Willi/Angelman syndrome.

Fig. 8. A patient with DiGeorge syndrome and a submicroscopic deletion in 22q11 identified by the cosmid EO (kindly provided by Dr. Peter Scambler, Institute of Child Health, London). The normal 22 (arrowhead) shows signals at both 22q11 and 22qter (the latter being a cohybridized cosmid pH17, supplied by Dr. Marcia Budarf, Philadelphia). The deleted 22 (arrow) shows only a signal from the distal 22q cosmid.

Fig. 11. Transcervical cells collected at nine weeks of gestation tested by FISH with two probes simultaneously, one specific for the X chromosome (red signal) and one for the Y (green signal). This sample was obtained by aspiration from the endocervical canal of a mother with a male fetus.

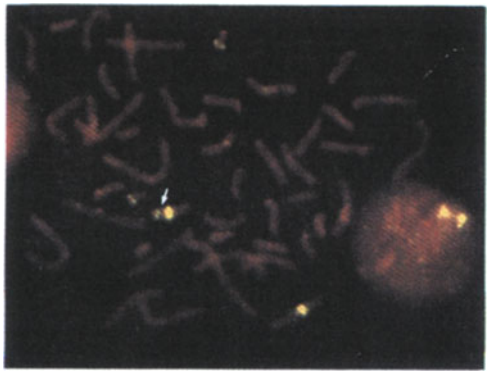

Figure 4

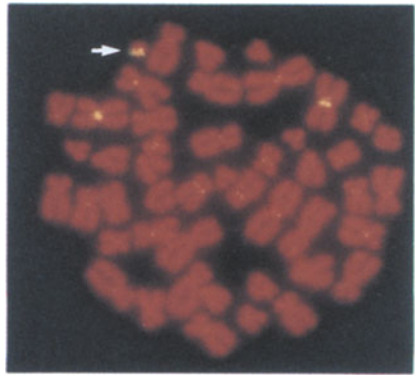

Figure 5

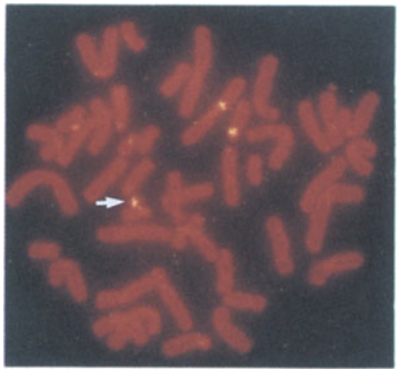

Figure 6a

Figure 6b

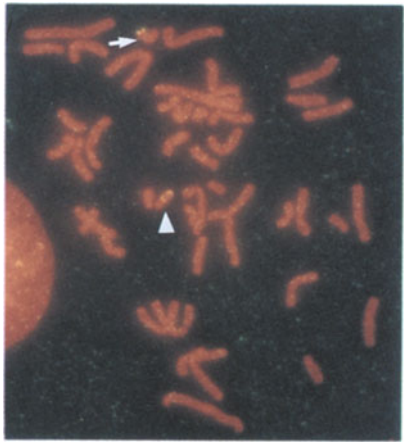

Figure 8

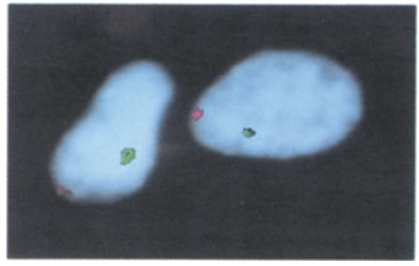

Figure 11

Figure 12

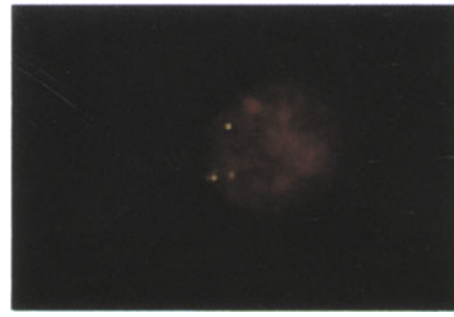

Figure 13

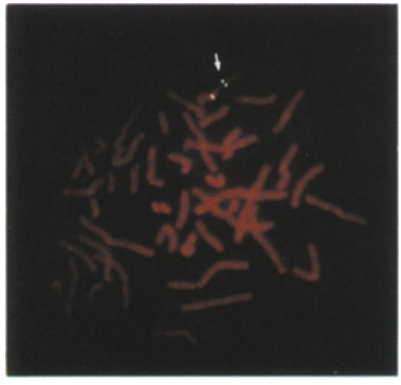

Figure 14

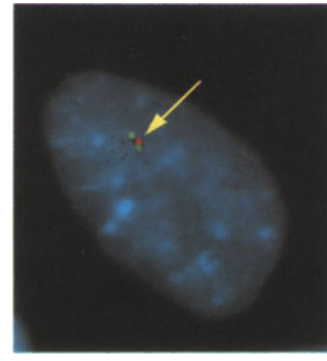

Figure 15

Figure 16

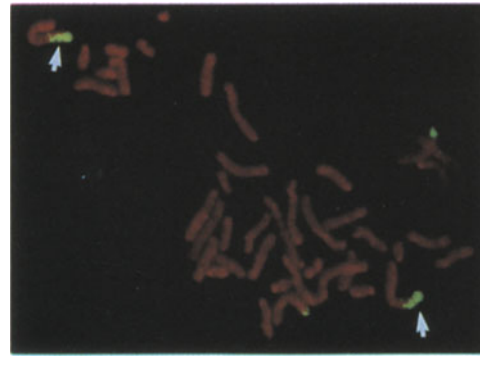

Figure 17

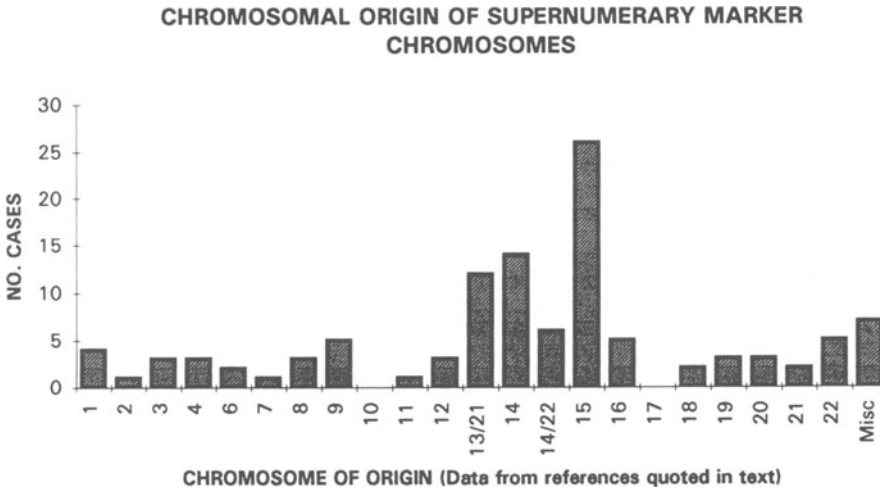

Fig. 7. Distribution of the origin of supernumerary marker chromosomes identified by FISH.

←

Fig. 12. FISH detection of trisomy 21 using two differentially labeled cosmid contigs, 242c and cCMP21a. Three double signals, one red (TRUTC) and one green (FITC) can be seen in the nucleus of an amniotic cell from a fetus with Down's syndrome.

Fig. 13. Trisomy 21 detected by FISH in a transcervical cell in interphase collected at 10 weeks of gestation. The diagnosis was confirmed by testing placental cells.

Fig. 14. Mapping of the XLA gene by FISH (arrow) using an X-derived probe (pSV2X5) to identify the X chromosomes.

Fig. 15. FISH mapping in interphase. Three probes (two cosmids and a YAC) were hybridized to G1 interphase cells and the distances between signals were measured in twenty cases using image analysis software. These distances (in microns) were converted to genomic distance in Kb by comparison with a calibration curve that had been constructed using cosmid probes from the same region. The average distance between the two green signals was determined to be $>$ 500 Kb; the distance between the consistently larger green signal (presumably the YAC) and the red signal was 300 Kb and between the red signal and the smaller green signal, approximately 150 Kb.

Fig. 16. DNA from isolated human chromosome 4 was labeled and hybridized to marmoset chromosomes in metaphase. The entire long arm of chromosome 7 shows bright fluorescent signals (photograph supplied by Jon Sherlock).

Fig. 17. Marmoset chromosomes painted with DNA from human chromosome 13. Cross reactivity with short arm of marmoset chromosome 1 (arrow) and telomeric region of chromosome 3 (photograph supplied by Jon Sherlock).

13 or 21 (16%). It is not surprising that such a relatively high proportion of acrocentric SMCs originates from chromosome 13, 14, or 22, as these may represent the reciprocal products of Robertsonian translocations, which in humans involve chromosomes 13 and 14 more frequently than other acrocentrics (Jacobs *et al.*, 1974).

The distribution of the origin of SMCs derived from the nonacrocentric chromosomes shows that the centromeres of all chromosomes except 10 and 17 are represented (Fig. 7). Two of the markers in this figure: case 14 (Crolla *et al.*, 1992), and case 20 (Callen *et al.*, 1992) did not show a hybridization signal with any of the alphoid repeat probes used. These exceptional cases suggest that the origin and composition of some SMCs may involve either complex rearrangements of centromeric heterochromatin that makes them unamenable to hybridization with alphoid repeat probes, or that in exceptional circumstances, the presence of alphoid sequences may not be a prerequisite for functional kinetochore activity. Alternatively, some markers may comprise structurally different forms of repetitive DNA, such as the sn5 satellite DNA described by Johnson *et al.* (1992). Although the majority of cases reported to date have karyotypes containing a single SMC, some were observed with two or more markers of different chromosomal origins (Callen *et al.*, 1991, case 3).

Other NISH methods have been utilized successfully to determine the chromosomal origin of SMCs. For example, Blennow *et al.* (1992) were able to flow sort a SMC approximately the size of an F-group chromosome; when the DNA from the marker was used as a reverse paint on normal metaphases, it was found to hybridize and thus to be composed of material from chromosomes X, 5, and 7. This structural complexity may help to explain why in some cases a wide spectrum of phenotypic effects is associated with this group of nonacrocentric SMCs. Chromosome microdissection has also been successfully applied to isolate DNA from one SMC; after labeling, the DNA was used to identify the marker as of chromosome 20 origin. Sequence data also revealed that it contained an unidentified family of centromere repetitive DNA which the authors termed sn5 (Johnson *et al.*, 1992).

As mentioned before, conventional cytogenetic studies have previously shown that some types of marker 15 chromosomes (inverted duplications) are associated with significant phenotypic effects, most notably mental retardation. Molecular genetic and FISH studies (Robinson *et al.*, 1993*b*; Crolla *et al.*, 1994) had recently been applied to patients presenting with mental retardation and karyotypes containing either a classical *de novo* inv dup(15) chromosome or a small r(15). In five patients studied by Robinson *et al.* (1993b) using PCR and Southern blotting techniques, and six cases reported by Crolla *et al.* (1994) using a combined FISH and molecular approach, all 11 *de novo* markers were shown to be

maternally derived and in addition contained duplications of the PWS/AS critical regions. Eleven more patients with mar(15) chromosomes were also examined by Crolla *et al.* (1994), and in contrast, none of these mar(15) chromosomes contained sequences from the PWS/AS regions. Ten of these 12 patients were intellectually and physically normal, but two were ascertained because of mental retardation, thus making problematical a straightforward correlation between the presence or absence from within a mar(15) of the proximal 15q imprinted genes and mental retardation. Either the presence of the mar(15)s in these two mentally impaired individuals was coincidental (due to ascertainment bias), or, in some way, was implicated in the aetiology of the phenotype.

A secondary effect of marker chromosomes was postulated by Robinson *et al.* (1993a) who found that in a PWS and AS patient—each with a small inv dup(15) marker chromosome—the phenotypes were caused by uniparental disomy for the paternal and maternal copies of chromosome 15, respectively. Robinson *et al.* (1993a) postulated that either the presence of the mar(15) had in some way caused nondisjunction of the normal 15 bivalent in the meiosis preceeding fertilization, resulting in a trisomy 15 zygote that was "rescued" by the loss of either the single paternal or maternal 15; or that the "rescue" involved a somatic recombination in a trisomy 15 zygote, with the mar(15) being the remaining product of this event. If such an intrachromosomal effect is possible for mar(15) chromosomes, then an interchromosomal effect might explain some of the phenotypic variability observed in other patients with *de novo* autosomally derived marker chromosomes.

In this context, from the NISH data published so far, it is clear that different phenotypes observed in patients with SMCs have apparently the same, or very similar chromosomal compositions at least at the level of sensitivity of the tests employed. For example, three cases with small mosaic *de novo* chromosome 12 markers have been reported, two with detailed clinical follow-up information. The first patient, case 5 (Callen *et al.*, 1991) had dysmorphic facial features, developmental delay, and mental retardation. The second *de novo* marker, case 3 (Crolla *et al.*, 1992) was ascertained prenatally in a fetus which went to term, and was developing normally at six months.

An interesting range of phenotypic/karyotypic associations have also been observed in patients with markers derived from chromosome 22. Nonmosaic bisatellited marker 22 chromosomes are frequently associated with patients with the Cat-Eye syndrome (CES) (Schinzel *et al.*, 1981). Isotopic *in situ* hybridization and Southern blotting densitometric studies have shown that the dicentric mar(22) chromosome in some CES patients contains two copies of D22S9, a probe mapped to 22q11 (McDermid *et al.*, 1986), thus making these patients tetrasomic for a portion of proximal 22q. However, Urioste *et al.* (1994) reported a pedigree in

which the proband, her sister, and their mother all exhibited some features of CES but the severity of the phenotype correlated with the proportion of cells containing a mar(22) chromosome that showed signal when hybridized with NISH using the single copy probe D22S9. Furthermore, the mar(22) was apparently unstable and was observed in five distinct forms in all the family members, and therefore exhibited what the authors termed "dynamic mosaicism."

A similar relationship between the frequency with which a mosaic population of a bisatellited mar(22) chromosome is observed and the severity of phenotype was reported by Cullen *et al.* (1993). The proband in this family presented with a spectrum of congenital abnormalities including left renal agenesis, absent uterus, bilateral sensorineural deafness, bilateral preauricular skin tags and sinus, and Duane anomaly. Duane anomaly is a form of congenital strabismus characterized by a retraction of the eye and an inability to abduct the eye (Duane, 1905). NISH studies showed that the marker segregating in this family was an inv dup(22), but the proband's father—who had 8% of cells with the mar(22)—only showed preauricular skin tags, while her brother, with 50% of cells with the mar(22), exhibited a phenotype only slightly milder than his sister's, but he also had the Duane's anomaly. From these data, the authors postulated that a gene for Duane's anomaly is present in a region of 22q11, and that the absence of overlap of the phenotypes with CES reflected the extent of the region of proximal 22q present in the marker segregating in this family.

In the context of this argument, Crolla *et al.* (1992) reported two patients (12 and 13), who were both phenotypically normal, with nonmosaic bisatellited, dicentric mar(22) chromosomes. In one of these cases, FISH with a cosmid from the 22q11 region did not show signal from the mar(22), thus showing that the region most commonly deleted in DiGeorge Syndrome was not present in this marker. Whether absence of a duplication of this region alone within a mar(22) is sufficient to classify such markers as harmless clearly remains to be proven; the evidence from the small number of cases reviewed here strongly suggests that detailed molecular and clinical evaluations in many more cases are required before clear karyotypic and phenotypic correlations can be made in patients with *de novo* supernumerary marker chromosomes.

Deletions and Duplications

Deletions in Patients with Autosomal Inherited Diseases

Waardenburg syndrome (WS) is an autosomal dominant disorder with incomplete penetrance and a population frequency of approximately 1 in 37,000. It is

characterized by dystopia canthorum, abnormalities of pigmentation, and sensorineural deafness. The syndrome is subdivided into two types, WS1 and WS2, according to the presence or absence of lateral displacement of the inner canthi (dystopia canthorum). The deafness is due to defects of the organ of Corti, with atrophic changes of the spiral ganglia and nerves. Deafness is a feature in 25% of patients with WS1, and 50% with WS2 (Waardenburg, 1951; Partington, 1964; Arias, 1971; McKusick, 1992).

Several investigations have suggested that the WS locus maps at human chromosomes 2q32–37, since a *de novo* paracentric inversion involving this region has been observed in a child with classical symptoms of the disorder (Ishikiryama *et al.*, 1989), while Kirkpatrick *et al.* (1992) have described a WS patient with a deletion of 2q35–36.2. In 1990, Foy *et al.* documented a close linkage of the WS1 locus in five families to the placental alkaline phosphatase gene (ALPP), previously mapped to 2q37 (Martin *et al.*, 1987). In another family, a linkage between WS1, ALPP, and the fibronectin (FN1) loci was also observed by Colombi *et al.* (1988).

In 1990, Asher and Friedman, and Foy *et al.* proposed that the WS1 gene is the equivalent of the murine splotch gene, close to the Pax-3 gene (Goulding *et al.*, 1991). Finally, Epstein *et al.* (1991) confirmed that the splotch phenotype is caused by mutation of the Pax-3 gene, and Baldwin *et al.* (1992) and Tassabehji *et al.* (1992) produced evidence that mutation of the human PAX-3 gene can cause WS1.

Support for PAX-3 gene involvement in the pathogenesis of the disease has now been obtained by testing metaphase chromosomes from a WS1 patient with FISH, using probes for PAX-3, FN1, ALPP, and ALPI (intestinal alkaline phosphatase). The result of this analysis showed that both ALPI and FN1 were retained on chromosome 2, while PAX-3, which maps to 2q35, was deleted (Lu-Kuo *et al.*, 1993).

Deletions and cryptic translocations have also been successfully detected by NISH in patients with the Miller-Dieker syndrome (MDS), a rare disease due to an arrest of neuronal migration during embryogenesis. It is characterized by lissencephaly (smooth brain) and malformation of the facies (Dobyns *et al.*, 1991). A microdeletion of the short arm of chromosome 17 (17p33) can be detected by high resolution cytogenetics in about half of MDS patients (Dobyns *et al.*, 1991). In the remaining patients, only an analysis by restriction fragment length polymorphism (RFLP) of selected anonymous DNA markers revealed deletions that were not visible by conventional cytogenetic methods (Schwartz *et al.*, 1988).

NISH approaches can detect deletions in MDS patients, as shown by Kuwano *et al.* (1991) in three subjects with the disease tested with two cosmids (41A and P13). While normal relatives showed hybridization signals on the short arms of

both chromosomes 17, microdeletions were clearly visible in the three patients, since only one chromosome 17 in each metaphase was found to be labeled.

In the same investigation, two other patients with cryptic translocations were tested. One subject, with a der(17p+) karyotype and a microdeletion that could be detected by RFLP analysis, showed hybridization signals on only one chromosome 17 in each metaphase spread, when tested by FISH and the two cosmids. Her mother, who also had a der(17p+) karyotype, showed a specific hybridization signal on one chromosome 17, but a second signal could be seen on chromosome 3, indicating the presence of a 3q:17p balanced translocation. In the patient, a chromosome 17 deletion could only be detected by RFLP analysis. FISH tests showed that in metaphase spreads, probes labeled only one chromosome 17. The patient's father and brother had an 8q:17p translocation.

A variety of mutations, including deletions, unbalanced translocations, and monosomies is responsible for inducing the clinical symptoms that typify DiGeorge syndrome (DGS), a disorder characterized by the absence or severe hypoplasia of the thymus and the parathyroid, together with cardiac malformations and dysmorphic facial features (DiGeorge *et al.*, 1960). Usually the disease is sporadic, but it may be inherited as an autosomal dominant condition (Scambler *et al.*, 1991; Halford *et al.*, 1993; Lindsay *et al.*, 1993).

In a large kindred, four patients were observed by de la Chapelle *et al.* (1981) with unbalanced translocations involving chromosomes 20 and 22, resulting in monosomy 22 and trisomy for the short arm of chromosome 20. Further investigation in patients with interstitial deletions suggested that the gene responsible for the disease mapped to the 22q11 region (Greenberg *et al.*, 1988; Scambler *et al.*, 1991; Driscoll *et al.*, 1992; Carey *et al.*, 1992; Scambler, 1993).

The small size of some deletions has often hindered the cytogenetic analysis of the mutation, but molecular tests and more recently FISH studies (Fig. 8) have greatly facilitated and improved the diagnosis of DGS (Scambler *et al.*, 1991; Halford *et al.*, 1993; Lindsay *et al.*, 1993).

Using nine cosmids and three YAC clones previously shown to map in the 22q11 region, Lindsay *et al.* (1993) ordered them on chromosome 22 relative to the breakpoints in two subjects with balanced translocations: one patient with DGS and the unaffected father of another patient. The results of FISH tests have narrowed down the region to which the DGS gene(s) are expected to map and provided evidence for the existence of low copy repeats in the area. The repeats are organized in blocks, one centromeric and one telomeric to the translocation breakpoints, possibly causing instability and thus predisposing to deletions (Lindsay *et al.*, 1993).

A submicroscopic deletion in 7q11.2 has recently been shown to be associ-

ated with familial and sporadic Williams syndrome, a developmental disorder affecting connective tissue and the central nervous system (Ewart *et al.*, 1993b). Patients may present with a combination of features including congenital heart disease, dysmorphic facial features, premature aging of the skin, infantile hypercalcaemia, a gregarious personality, and mental retardation. A common feature also seen in Williams syndrome patients is supravalvular aortic stenosis (SVAS). The relationship between these two syndromes was unclear until linkage between SVAS and the elastin gene was demonstrated in two families (Ewart *et al.*, 1993a), and in a third family cosegregating with a chromosome translocation disrupting the elastin gene on 7q (Curran *et al.*, 1993).

Using a combination of PCR, Southern blotting, and NISH, Ewart *et al.* (1993b) have demonstrated hemizygosity at the elastin locus in four familial and five sporadic cases of WS. Using 114 kb elastin cosmids cELN-272 and cELN-11D, they showed in both the familial and sporadic forms of WS that hybridization signals with these cosmids were visible on only one of the two chromosomes 7. The linkage and physical mapping data presented by Ewart *et al.* (1993b) suggest that WS is caused by deletions which extend beyond the elastin gene, in contrast to SVAS, which to date has only been found in association with deletions at the 3′ end of the gene.

From these data, however, it is clear that significant deletions involving the elastin and, possibly, adjacent genes will be the most common mechanism for the aetiology of Williams syndrome, and that NISH, using the elastin cosmids, will be an important diagnostic tool for the confirmation of diagnoses and predicting outcomes in familial cases.

Rubenstein-Taybi syndrome (RTS) patients present with a well characterized complex of congenital malformations including facial anomalies, broad thumbs, big toes, and mental retardation. A link between this syndrome and a locus at the distal end of the short arm of chromosome 16 was first postulated by Imaizumi and Kuroki (1991), who described a patient with RTS and a *de novo* reciprocal translocation between chromosomes 2 and 16 (t(2;16) (p13.1; p13.3); two further patients with *de novo* translocations involving 16p13.3 have since been described (Lacombe *et al.*, 1992; Tommerup *et al.*, 1992). Other cytogenetically detectable structural abnormalities such as deletions, duplications, or inversions have not been described in these patients (Imaizumi *et al.*, 1993).

Using FISH and a panel of cosmids from distal 16p, Breuning *et al.* (1993) have analyzed metaphases prepared from patients with RTS and reciprocal translocations. Two cosmids, N2 and RT1, were found to be proximal and distal to the breakpoint, respectively. By using dual color FISH on a number of RTS (nontranslocation) patients, Breuning *et al.* (1993) showed that only signals from

the N2 cosmid could be seen in only some cases, suggesting that the sequence contained in the RT1 cosmid was deleted.

Microdeletions have been detected by FISH in some patients with sporadic aniridia, using probes from the WAGR locus (Wilms' tumor, aniridia, genitourinary abnormalities, and mental retardation).

Aniridia is a rare familial or sporadic congenital abnormality of the eye which occurs with a frequency of one in 50,000 to 100,000, and is characterized by absence of all or part of the iris. Several candidate genes for the aniridia locus (AN2) have been defined by breakpoint analysis either in patients with translocations associated with familial aniridia or by analysis of Wilms' tumor-associated deletions, with and without aniridia. The Wilms' tumor gene (WT1) has been cloned and extensively studied (van Heyningen and Hastie, 1992), and sequencing of the human aniridia locus (AN2) revealed it to be PAX-6 (Ton *et al.*, 1991), the homologue of the mouse Pax-6 gene (Hill *et al.*, 1991).

Cosmid clones derived from the PAX-6 and flanking regions of the WAGR complex (including the WT1 locus) have recently been used by Fantes *et al.* (1992), in a FISH study of patients with both sporadic and familial aniridia. In three patients with deletions within this region, FISH with the cosmids FAT5 (aniridia) and B2.1 (Wilms' tumor) showed signals in the p13 region of only one of the two chromosomes 11, demonstrating that this approach is an efficient way of detecting submicroscopic deletions. It has been known for a long time that sporadic aniridia is sometimes associated with genomic deletions. These frequently include the WT1 gene and when this is the case, the patient is at a considerably increased risk (~60%) of developing Wilms' tumor (Miller *et al.*, 1964). Screening sporadic aniridia patients with these cosmids offers a rapid prognostic test for the development of Wilms' tumor in a proportion of sporadic aniridia cases.

In addition to the syndromes and conditions mentioned above, there are FISH approaches currently in use for the detection of submicroscopic chromosomal deletions such as the use of FISH for the detection of deletions in the 15q11–13 region in patients with Prader-Willi or Angelman syndromes (PWS or AS). Approximately 60% of PWS and AS patients have deletions of this imprinted region of chromosome 15, respectively, on the paternally or maternally inherited chromosome. Cytogenetic analysis of proximal 15q is often hampered by the presence of heterochromatic polymorphisms, which can make the visualization of a small deletion very difficult. Good quality banding (>500 bands) is required for the diagnosis.

Cosmids from the PWS and AS critical regions have been isolated (Kuwano *et al.*, 1992; Ozcelik *et al.*, 1992) and are used in the detection of both visible and

submicroscopic deletions within the proximal 15q region. If only one of the two cosmids hybridizes to the target region, the diagnosis can be confidently made. However, an obvious limitation of this approach is that it cannot differentiate between biparentally (potentially deleted) and uniparentally (not deleted) derived chromosomes 15. In order to make this differential diagnosis, molecular techniques are required using either a Southern blotting approach with a methylation sensitive probe (PW71: Dittrich *et al.*, 1992), or a multiplex PCR method using a combination of primers for CA repeats from within the PWS and AS critical regions (Mutirangura *et al.*, 1993).

The molecular approach to the diagnosis of PWS and AS provides an excellent example of how an integrated use of molecular genetics, molecular cytogenetics and conventional cytogenetics can provide the optimal conditions not only for the definitive and rapid diagnosis of a number of complex conditions, but also for unraveling the molecular mechanisms responsible for their etiology.

In all the cases detailed above, deletions or duplications were first established by conventional cytogenetics and gene mapping studies as the cause of the syndromes. Other examples of this approach are the Wolf-Hirschhorn syndrome (chromosome 4) (Gandelman *et al.*, 1992), and preliminary studies also suggest that a cosmid based FISH analysis of the Langer-Giedion (8q24) and Smith-Magenis syndromes (17p11.2) may soon be possible. Other conditions will soon be added that can benefit from the diagnostic value of NISH.

Carrier Detection of X-Linked Deletions

The diagnosis of the carrier status of female relatives of patients with X-linked diseases is hampered by technical difficulties, when the mutation is due to a deletion. Gene dosage of DNA sequences by Southern blotting analysis has been claimed to produce useful information about the carrier status of female relatives of patients with Duchenne or Becker muscular dystrophy (DMD/BMD) (Mao and Cremer, 1989). This approach is not always informative and an alternative approach has been developed, based on the estimation of the products of reverse transcription and PCR amplification (RT–PCR) of dystrophin exons most commonly deleted in DMD/BMD patients (Roberts *et al.*, 1990a; Prior *et al.*, 1990). Deletions of the dystrophin gene in female relatives of DMD/BMD patients can also be detected directly by NISH analysis of metaphase spreads (Fig. 9) (Ried *et al.*, 1990; Adinolfi *et al.*, 1992; Bunyan *et al.*, 1994a).

The dystrophin gene contains 79 exons distributed over 2.3 Mb, and maps on the short arm of the X chromosome (Xp21) (Love and Davies, 1989). The corresponding proteins appear to be absent in muscle biopsies of DMD patients

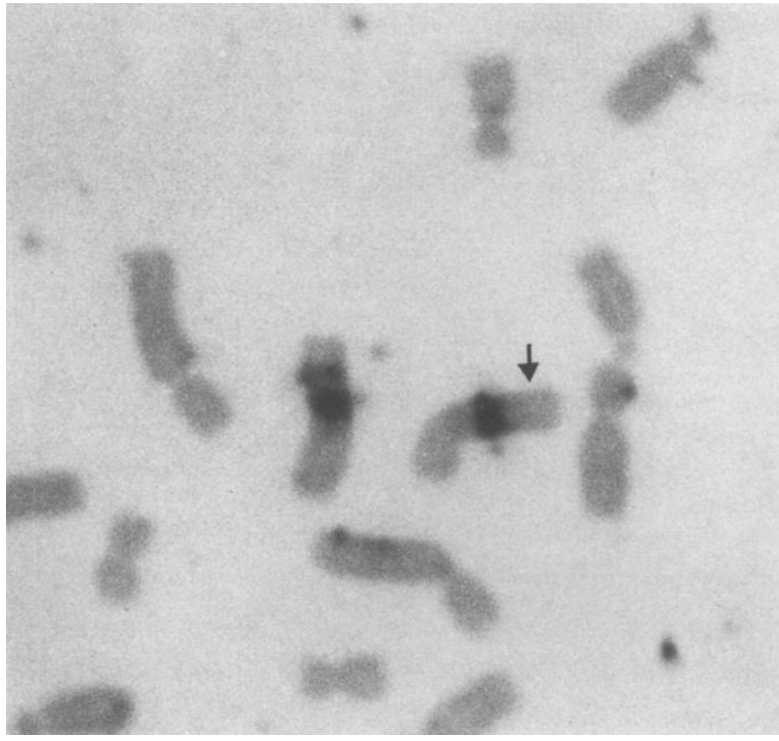

Fig. 9. Metaphase spread prepared from the mother of a patient with Duchenne muscular dystrophy (DMD) and tested using a centromeric X-derived probe and three cosmids specific for the P20 region of the dystrophin gene. NISH analysis (peroxidase staining) showed the deletion of the dystrophin gene in one X chromosome (arrow).

tested with specific antibodies and immunohistochemical staining, while an altered form of dystrophin is detectable in BMD subjects (Hoffman *et al.*, 1987; Bonilla *et al.*, 1988; Arahata *et al.*, 1989).

In about 60% of DMD patients part of the dystrophin gene is deleted, and in about two-thirds of this group, the deletion involves the P20 region, which includes exon 45 (Wapenaar *et al.*, 1988; Den Dunnen *et al.*, 1989; Koenig *et al.*, 1989).

Rapid, accurate analysis of the specific deletion responsible for DMD/BMD disorders can be achieved using multiplex PCR amplification and analysis of its products (Chamberlain *et al.*, 1989; Beggs *et al.*, 1990).

In about 30% of DMD patients, the disease results from a new mutation that

has occurred in the germ cells of the mother, while in the remaining patients, the mutation originates in a previous generation (Love and Davies, 1989). In the latter cases, the mother and other female relatives of the patients are or may be carriers of the abnormal gene, and require genetic counseling. Carrier status for deletions can be unequivocally established by NISH using selected cosmid clones (Ried *et al.*, 1990; Adinolfi *et al.*, 1992). In the study of Ried and colleagues (1990), four nonrelated families were tested with three cosmids (CPT1, CAL24, and CPT4) mapping to the P20 region. Deletions were detected in five female relatives when their metaphase spreads were tested by NISH using the cosmids, either singly or as a pool of three. In another study (Adinolfi *et al.*, 1992), female relatives of DMD patients known to have deletions were tested by NISH using an X-centromeric probe (pSV2X5) and cosmids derived from the P20 region. Metaphase spreads from normal males showed a centromeric signal on the X chromosome and a single hybridization complex on each chromatid of the short arm. Cells in interphase also showed a strong hybridization signal (X-centromeric) and a weak one that detected the dystrophin gene.

While normal females showed signals on the short arm of both X chromosomes, in three mothers of DMD patients, the dystrophin probes hybridized with only one X chromosome, within the Xp region. This pattern was observed with single probes (cPT1, cAL24 or cPT4) or a pool of the three.

Another series of 16 females from DMD/BMD pedigrees has been investigated. These patients had already been studied using RT–PCR and/or intragenic polymorphic markers and shown to be either deletion carriers, noncarriers, or suspected germ-line mosaics; one was a known mosaic (Bunyan *et al.*, 1994a). FISH was used with a panel of cosmids cloned from DMD exons 45, 46 + 47, 48, 49 + 50, 51, and 52. The results were informative for the deletions examined. In five known carriers, signals showed at Xp21 on only one of the two X chromosomes; the seven nondeletion cases all showed an Xp21 hybridization signal on both X chromosomes. An interesting finding of this study was that two of the four either suspected or known germ-line mosaics for the deletions were also shown, using this FISH approach, to be somatic mosaics, with one female showing a deleted X in 77% of metaphases, and the other in 43%, with the remainder of the metaphases producing normal hybridization signals in both X chromosomes. By comparison, two suspected germline mosaics were found to have a normal Xp21 signal distribution on both of their X chromosomes. These results show that FISH can be used to detect somatic mosaics in females with apparent *de novo* DMD/BMD deletions. Furthermore, they indicate that a proportion of *de novo* dystrophin gene deletions occur as mitotic errors during development rather than as meiotic errors during gametogenesis (Bunyan *et al.*, 1994b).

The same NISH approach has been used to detect deletions in female relatives of patients with Hunter syndrome (Stone and Adinolfi, 1992). This X-linked metabolic disorder (mucopolysaccharidosis II, MPSII) is caused by the absence of the lysosomal enzyme α-iduronate sulphate sulphatase (α-ISS, IDS; EC3.1.6.13), and results in the accumulation of glycosaminoglycans in various tissues (McKusick and Neufeld, 1983; Spranger, 1984; Benson and Fensom, 1985).

Cytogenetic tests of a female patient with Hunter syndrome suggested the localization of the lysosomal gene in the distal region of the long arm of the X chromosome (Mossman *et al.*, 1983), and analysis of families with affected patients has successfully confirmed that the Hunter gene maps to the tip of the Xq region (Xq27–28) (Chase *et al.*, 1986; Upadhyaya *et al.*, 1986).

Different types of mutations have been shown to be responsible for the deficiency of the α-ISS enzyme and the manifestation of the disease symptoms. In about 128 Hunter patients investigated, deletions of the gene were detected in 12 subjects. All other patients had missense or nonsense mutations, or partial loss of an exon (Adinolfi, 1993).

For many years, technical difficulties have hampered the genetic counseling of female relatives of Hunter patients, particularly since the estimation of the enzyme in extracts from white cells or fibroblasts could not provide evidence for the carrier condition. Clearcut results could only be obtained by measuring the levels of α-ISS in hair root cells (Chase *et al.*, 1986). However, this procedure cannot reveal the type of mutation responsible for the disease.

Unequivocal diagnosis of the carrier status of female relatives of Hunter patients with deletions can be readily obtained with NISH, using probes containing the α-ISS gene (Fig. 10). In one family, whose members had previously been tested by hair root analysis (Chase *et al.*, 1986), female relatives were investigated by NISH with a YAC clone containing the entire Hunter gene (Flomen *et al.*, 1992) and an X-derived centromeric probe (pSV2X5). In two women (the mother and a cousin of the affected boy) both X chromosomes in each metaphase spread were labeled by the centromeric probe, but only one X chromosome in each cell showed hybridization signals on the Xq distal region. This pattern was observed in almost 90% of the metaphases examined.

Deletions causing X-linked lymphoproliferative (XLP) disease can also be monitored by FISH. This is a rare inherited disorder that manifests itself in boys who are generally healthy until infected by the Epstein–Barr virus (Sullivan *et al.*, 1983; Grierson and Purtilo, 1987). Following infection, the majority of patients develop immunodeficiency and often succumb to infectious mononucleosis. The XLP gene maps to the long arm of the X chromosome (Skare *et al.*, 1989a,b), and deletions in the Xq25 region have been detected in patients (Wyandt *et al.*, 1989;

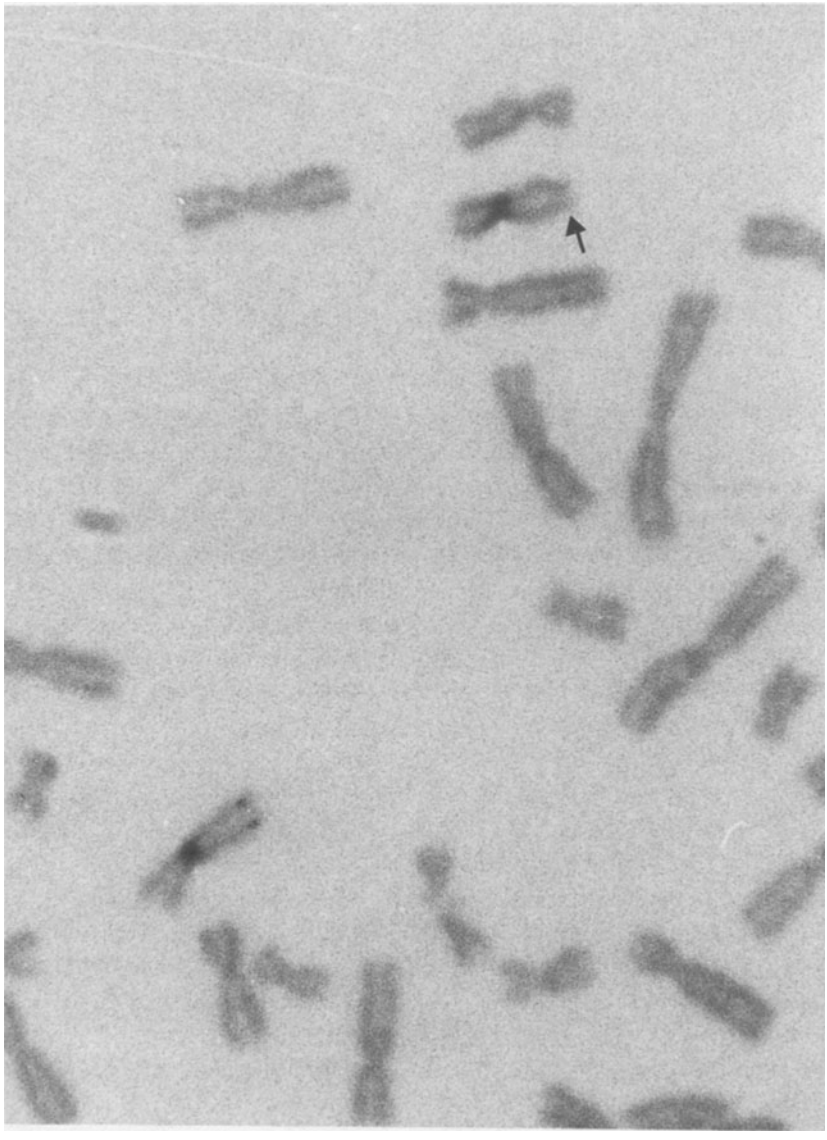

Fig. 10. Detection of a deletion of the Hunter gene in a mother of a patient with the Hunter syndrome. Partial chromosome metaphase analyzed by NISH using an X-derived probe (pSV2X5) and a YAC probe (Mo105I) containing the Hunter gene. Site of deletions marked with arrow.

Sanger *et al.*, 1990). Further molecular studies indicated that the deletions involve several regions of Xq25, including the loci DXS6, SXS739, and DXS100 (Skare *et al.*, 1993), DXS575 and DXS982 (Wu *et al.*, 1993). The smallest deletion removes about one-third of Xq25. FISH analysis has confirmed that the deletion can vary between 2 and 4 Mb and that the candidate gene should be located in the region between DXS6 and DXS100 (Wu *et al.*, 1993).

Duplications Detectable by NISH

The NISH method has been successfully employed to detect duplications in patients with the Charcot-Marie-Tooth (CMT) syndrome, which is one of the most common inherited peripheral neuropathies (incidence: 1 in 2,500), involving motor and sensory nerves (Lovelace and Shapiro, 1990).

CMT, characterized by a progressive muscular atrophy that primarily affects distal muscles, is inherited as an autosomal dominant, recessive, or occasionally X-linked condition (Skre, 1974; McKusick, 1992; Patel, 1993). The autosomal dominant form is the most frequent and it is classified into at least two major subtypes. CMT1, associated with a decreased nerve conduction velocity (NCV), and CMT2, with normal or near normal NCV (Dyck and Lambert, 1968a,b; Dyck, 1993). Since patients have a normal lifespan, it has been possible to collect large pedigrees and to perform accurate linkage studies. This has documented the existence of at least three autosomal dominant loci for CMT1. The CMT1A gene maps to the short arm of chromosome 17 (17p11.2–12 (Vance *et al.*, 1989); the CMT1B to chromosome 1 (1q23–25) (Bird *et al.*, 1982); while the third locus, CMT1C, has not yet been mapped (Patel, 1993).

Considerable insight has so far been gained into the types of mutation responsible for the CMT1A syndrome, including the presence of a submicroscopic DNA duplication (Patel, 1993). The duplication was recognized by the detection of three distinct polymorphic alleles, instead of the expected two, at the Gt^n–containing locus (marker DM 11-GT at D17S122). As expected, all affected individuals demonstrated dosage differences between alleles. In rare instances, three distinct alleles were seen; this unique mutation for an inherited disorder prompted Lebo and collaborators (1992) to investigate patients with CMT1A syndrome using a multicolor FISH method. Three red signals for the CMT1A site hybridized to probe VAW4097, and two green signals for the control site could be seen in the majority of nuclei in interphase obtained from heterozygous patients; cells from homozygotes showed four red and two green signals.

Lebo *et al.* (1991) have also documented a duplication of the gene responsible for the clinical manifestations of the CMT1B syndrome, using FISH and a probe for the FcγRII receptor that consegregates with the CMT1B locus.

Recent studies have shown that "hereditary neuropathy with liability to pressure palsy" (HNPP), a less frequently diagnosed autosomal dominant syndrome, is associated with a deletion in the 17p11.2–12 region (Chance *et al.*, 1993, 1994). This supports the hypothesis that a meiotic unequal crossover is the mechanism responsible for the generation of the duplication in CTM1A patients and the deletion in HNPP subjects. The deletions in HNPP patients should be readily detectable using FISH methods.

DETECTION BY NISH OF CHROMOSOMAL ABNORMALITIES IN CELLS IN INTERPHASE

Several attempts have been made in recent years at improving the application of NISH methods to the detection of major chromosomal disorders in nuclei of resting cells. The main advantages of this approach are that the cells can be analyzed without the risk of selection generated by the *in vitro* cultures employed to prepare metaphase spreads, and that samples containing a small proportion of cells with chromosomal abnormalities may be investigated in detail. The most fruitful areas of application of this approach are in prenatal diagnosis using amniotic cells, chorionic cellular elements or fetal cells partially isolated from maternal blood or endocervical samples. The technique also provides useful information for detecting mosaicism or chromosome abnormalities following radiation therapy, for investigating patients with leukemia or who have received bone marrow transplants, and for mapping genes.

Prenatal Tests on Cells in Interphase by NISH

Sex Detection

One of the first studies on the detection by NISH of Y-derived sequences in cells in interphase was published by Burns *et al.* in 1985. A repetitive probe, pHY2.1, that labels the distal part of the Y long arm, was used to establish the presence of the Y chromosome in freshly collected, PHA-stimulated peripheral blood lymphocytes, amniotic cells, chorionic cellular elements, spermatozoa, and buccal cells; human tissues were also collected during surgical procedures, frozen, and stored in liquid nitrogen (Fig. 11).

The pHY2.1 probe gave a clear hybridization signal when tested on uncultured lymphocytes obtained from normal male donors, while negative results were observed when the test was performed on samples from normal females.

In males, basal epithelial cells from buccal smears showed specific hybridiza-

tion signals, but squamous cells were negative; this was attributed to the poor penetration of the probe into the partially keratinized cells.

In a study of uncultured amniotic cells and chorionic cellular elements, complete concordance between the detection of the Y-specific signals and the sex of the fetus was observed; however, only about half of the analyzed cells were Y-positive in each "positive" sample. When sperm taken from normal fertile men were analyzed, between 35% and 66% of the cells in each sample reacted with the Y-derived probe.

The frequency of Y chromosomal disorders has been investigated by NISH in at least two studies. In 1991, Guttenbach and Schmid investigated the frequency of aneuploidy in eight normal donors and found that the incidence of sperm nuclei with two Y chromosomes varied between 0.1% and 0.5%, with an average frequency of 0.27%, slightly in excess of the frequency (0.1%) of 47,XYY males detected in newborns (Hecht and Hecht, 1987). The difference suggests that either 24,YY spermatozoa are less capable of fertilization than normal sperm (in agreement with the absence of any YY chromosome complements in 2582 hamster eggs fertilized with human spermatozoa as reported by Martin *et al.*, 1982, 1983) or that a double signal may occasionally be given by a single Y chromosome in sperm nuclei.

In the investigation by Guttenbach and Schmid (1991), no correlation between YY chromosomes in sperm and age of the donors was noticed. An average of 50.3% of the sperm contained an X chromosome. The Y chromosome was located in the vicinity of the acrosome in 20.5% of sperm, in the central region in 57.8%, and in the distal region near the neck of the spermatozoon in 21%.

Han *et al.* (1994) have evaluated the frequency of Y chromosome abnormalities in spermatozoa of two 47,XYY subjects using probes for the X and Y chromosomes and, as control, chromosome 17. The overall percentages of X and Y sperm were 47% and 48.4%, respectively. The frequency of Y disomic sperm was not different from that observed in samples from normal individuals.

Only sequences that map in the Y short arm should be used for the prenatal diagnosis of suspected structural abnormalities associated with failure of differentiation of the primordial gonads into testes. By contrast, probes that map on the long arm of the Y chromosome should be used to investigate patients with azoospermia.

The presence of gene(s) controlling human spermatogenesis on the non-fluorescent portion of the Y chromosome (Yq) was first suggested by Tiepolo and Zuffardi (1976). The molecular localization of the AZF (azoospermic factor) locus is assumed to be within the Yq11.23 region. Spermatogenesis appears to be controlled by a Y gene in both mice (Burgoyne, 1987) and *Drosophila* (Brousseau,

1960; Hennig, 1985). Vogt *et al.* (1991), using a fertility gene sequence present in the Y chromosome of *D. hydei*, have screened a pool of human Y-derived sequences and identified seven DNA fragments that map in the pY6H interval, a region that probably contains the AZF gene(s). One sequence (pY6H65) of about 300 kb has an organization reminiscent of the presumed Y fertility gene in *Drosophila*. Studies on isolating the AZF gene(s) could provide valuable probes for NISH testing of patients with primary azoospermia.

Preimplantation Tests

NISH has been successfully applied also in preimplantation genetic diagnosis (PGD). Single blastomeres removed by micromanipulation from early human embryos have been tested using NISH and/or PCR to assess the sex and chromosome complement of the conceptus (Penketh *et al.*, 1989; Handyside *et al.*, 1989, 1990; Roberts *et al.*, 1990b; Grifo, 1992; Griffin *et al.*, 1991, 1992; Chong *et al.*, 1993). FISH, rather than PCR, allowed detection of abnormal numbers of the Y and X chromosomes in preimplantation embryos.

Studies by Griffin *et al.* (1991, 1992) have led to the realization that when single X or Y probes are used to test preimplantation blastomeres, misdiagnoses are relatively frequent due to either a failure of hybridization or the presence of polyploid cells. This can be avoided when both probes are employed simultaneously, and differentially labeled. The advantages of using FISH tests is best illustrated in a study of five couples at risk of producing offspring with an X-linked recessive disease who underwent *in vitro* fertilization (IVF) with a view to selecting the sex of the embryos and transferring only female conceptuses (Delhanty *et al.*, 1993). On the third day postimplantation, one or two cells were removed from the preimplantation embryos and tested by FISH with X- and Y-derived probes. In two couples, no embryos could be transferred due to the detection of an abnormal number of X chromosomes in each blastomere collected from female embryos. In two other cases, two female embryos could be transferred. Some of the remaining embryos were male and/or showed chromosomal abnormalities. In the last case, only one blastomere from a single embryo could be tested, and it had a 45,X chromosome complement.

Most of the X-chromosome abnormalities could not have been detected by PCR, and the FISH approach was essential for the selection of embryos suitable for transplantation. Possibly the most interesting finding documented by Delhanty *et al.* (1993) was the high incidence of X and Y chromosomal disorders detected in this small group of embryos.

However, one of the problems of PGD is that the analysis of a single cell may

not be representative of the whole embryo. Misdiagnosis can also occur when the isolated cell has more than one nucleus (Winston *et al.*, 1991). In a recent investigation, multinucleated blastomeres were detected in about 30% of 230 cleaved but subsequently arrested human embryos, and in about 67% of 21 cleaved embryos, rejected after tests for PGD. In 95% of the embryos, in which mononucleated and multinucleated single cells were analyzed by NISH using Y and X probes, the sex established in the multinucleated cells corresponded to that of the embryo. However, the number of sex chromosomes for multinucleated blastomeres and their distribution in each nucleus varied greatly, indicating their unsuitability for diagnosis of aneuploidy at the preimplantation stage (Munné and Cohen, 1993).

Detection of Chromosomal Abnormalities in Amniotic and Chorionic Villus Cells

Speed and accuracy are the main prerequisites for the prenatal diagnosis of chromosomal disorders in view of the possible outcome of the test and the limited time available if intervention is required.

The analysis by NISH of uncultured amniotic or chorionic cells can only be aimed at the detection of selected numerical chromosomal abnormalities, such as those involving chromosomes 21, 18, 13, X and Y. Aneuploidies only account for 50–70% of all abnormalities detected by conventional cytogenetics, but the interphase test could still be of great value if applied either to mass screening or as a preliminary investigation prior to the results of *in vitro* culture and analysis by conventional cytogenetics. Major limitations of interphase FISH on amniotic fluid or chorionic villus cells are that it requires an invasive procedure to obtain the sample; at present its results are often uninformative. Performed soon after the collection of the samples, it could still give an early indication that the conceptus appears to be normal, at least with regard to major chromosomal disorders. This preliminary information could alleviate maternal anxiety prior to a confirmatory result by conventional methods.

Essential prerequisites for the successful performance of prenatal tests using NISH on uncultured cells are that there should be clearcut results in the majority of cases, and that false positive results should be rare. The first condition implies that only a small number of nuclei should have more or fewer signals than expected.

While the majority of nuclei from freshly collected lymphocytes or uncultured chorionic villi show clear hybridization signals when tested by NISH, only a small proportion of amniotic cells is suitable for analysis (Davies *et al.*, 1994a,b). Technical difficulties have been encountered in particular with chromo-

some 21-derived probes. In 1986, Julien and colleagues reported the first prenatal diagnosis of trisomy 21 on uncultured amniocytes using restriction digested DNA prepared from flow sorted chromosomes 21. However, subsequent investigations performed using chromosome 21 libraries produced unsatisfactory results, mainly because, in cells in interphase, the signals were large and tended to coalesce (Lichter *et al.*, 1988; Pinkel *et al.*, 1988; Kuo *et al.*, 1991; Zheng *et al.*, 1992; Davies *et al.*, 1994a,b).

Kuo *et al.* (1991) used a 21-specific plasmid library and interphase nuclei obtained from cultured amniotic cells grown to a high density, when almost all the cells were viable and in G1 phase. In samples from fetuses with trisomy 21, between 10% and 52% of nuclei showed three signals. The NISH method was less reliable when applied to uncultured amniotic cells.

Attempts at using a repetitive α-satellite specific for the centromeric regions of both chromosomes 21 and 13 (Devilee *et al.*, 1986) have also produced unsatisfactory results (Bartsch and Schwinger, 1991; Weier and Gray, 1992; Davies *et al.*, 1994a,b). This can be attributed to the highly polymorphic nature of the sequences at the centromere of chromosome 21; the hybridization signals are occasionally very weak even when metaphase spreads are tested, and in some individuals, can give a negative signal for the alphoid repeat probe in one of the chromosome 21 centromeres (Verma and Luke, 1992).

In order to circumvent the potential problems of using centromere-specific repeat probes, Klinger *et al.* (1992), Ried *et al.* (1992) and Zheng *et al.* (1992) have more recently compared the results of testing amniotic cells by conventional cytogenetics and FISH on nuclei in interphase, using cosmid probes specific for chromosomes 21, 18, 13, X, and Y. These investigations were performed on samples that had already been tested by conventional tissue culture and cytogenetics and had often been selected to include a variety of chromosomal disorders. Only a minority of the uncultured amniotic cells contained hybridization complexes and only some scorable nuclei showed the expected number of signals when tested with 21-derived probes. The study by Zheng *et al.* (1992) showed three hybridization signals between 34% and 51% of the scorable trisomic cells. In these investigations, the best results were obtained when the amniotic cells were analyzed using contigs over 55 kb long. The frequency of hybridization complexes was lower when single cosmids or YACs were employed.

Similar findings have been reported by Davies *et al.* (1994a,b) when several 21-derived probes, obtained from centromeric sequences, single plasmids or cosmids, contigs or YACs were compared.

The specificity of the 21 library probes was less than optimal because of cross-hybridization signals which could not be suppressed efficiently. When

cosmid D21S18 was tested on normal cultured amniotic samples, between 26% and 70% of the nuclei showed two hybridization complexes; however, several samples showed nuclei with three signals, giving false positive indications of trisomy 21. When tested on a 21-trisomic amniotic sample, 33% of nuclei had three signals, while 35% had two signals; conventional cytogenetic analysis showed no evidence that this fetus was a mosaic.

The YAC probe yGART2 was used to test seven cultured amniocyte samples from normal fetuses: between 33% and 65% of hybridized nuclei showed the expected two signals. Two samples from trisomic fetuses had three signals in 40% and 47% of hybridized nuclei, respectively.

When single contigs were used, the proportion of 21-trisomic cells containing three signals was lower than the percentage of normal cells containing the expected two signals (Davies *et al.*, 1994a,b). This reduction is directly related to the probability that a probe has to hybridize to a single chromosome. If the probability is 80%, the expected percentage of normal nuclei with two signals should be near 64%, while the frequency of "correct" triple signals in trisomic cells is expected to be near 51%, with a small proportion of cells having a double or single signal.

The best results were obtained when two separated, differentially labeled contigs, 242c and cCMP21, were employed. If the two probes are marked with fluorescein and rhodamine, respectively, two double signals, one green and one red, should be seen in most normal nuclei in interphase. In 21-trisomic cells three "doublets" can be observed (Fig. 12). The most prominent feature of the distribution of the hybridization signals was the high proportion (69%) of normal samples without three incorrect signals, while in the remaining samples less than 5% of nuclei showed spurious hybridization complexes.

In the only prospective clinical study performed so far, FISH was utilized to detect chromosomal aneuploidies in 4,500 amniotic cell samples with 21, 18, 13, X, and Y probes (Ward *et al.*, 1993). A sample was considered to be aneuploid when 70% or more scorable nuclei displayed the same abnormal hybridization pattern with a specific probe. The overall detection rate for aneuploidies was 73.3%; that for trisomy 21 was lower (63.3%), since 21 of 60 trisomy samples tested were uninformative, and in five cases, the trisomy was not detected.

Only further prospective trials, using two differentially labeled contigs, can establish whether the diagnosis of Down syndrome (DS) can be performed with a high success rate on uncultured amniotic cells. In the meantime, although the potential of FISH on cells in interphase has been demonstrated, it should not be used as the only diagnostic tool for prenatal diagnostic tests, as recommended by the American College of Medical Genetics in 1993 (Schwartz, invited editorial, 1993, and the policy statement in the American Journal of Human Genetics, 1993).

NISH and Noninvasive Prenatal Tests

The detection of nucleated fetal cells in peripheral maternal blood samples is another area of research in which NISH methods are used.

During the past few years, it has become apparent that despite performing prenatal tests by amniocentesis or chorionic villus sampling on women at risk due to advanced maternal age, the birth incidence of DS has not declined significantly. This is because most DS infants are born to women under 35 years of age, who have a higher pregnancy rate than older women but are not tested because their individual risks are low.

Many attempts have been made to establish new noninvasive procedures based on the detection of fetal nucleated cells present either in maternal peripheral blood samples or in the endocervical canal (see Adinolfi, 1992a,b; Adinolfi *et al.*, 1993, 1994). Three main types of fetal nucleated cell could potentially reach the maternal circulation: syncytiotrophoblastic cellular elements, lymphocytes, and erythroblasts. The total volume of fetal blood present at any time during gestation in the maternal blood is expected to be small—not in excess of 100μl. Thus, enrichment with monoclonal antibodies is required before NISH tests can be performed. At present, most investigators are concentrating their efforts toward the identification of fetal erythroblasts (Bianchi *et al.*, 1990; Bianchi and Klinger, 1993). The identification of the cells is mainly based on FISH using Y- or 21-derived probes (Bianchi *et al.*, 1990; Bianchi and Klinger, 1993; Elias *et al.*, 1992), and occasionally antibodies against fetal hemoglobin (Zheng *et al.*, 1993).

An alternative noninvasive approach is that of detecting fetal cells in endocervical samples collected between 8 and 13 weeks of gestation (Shettles, 1971; Rhine *et al.*, 1977; Griffith-Jones *et al.*, 1992; Adinolfi *et al.*, 1993, 1994). So far, using FISH, fetal cells containing a Y sequence have been detected in transcervical samples obtained from women with male conceptuses. A case of chromosome 18 trisomy was also confirmed (Adinolfi *et al.*, 1993). The prenatal diagnosis of trisomy 21 on transcervical cells collected at about 12 weeks gestation is shown in Fig. 13.

Detection of Mosaicism

The utilization of interphase cytogenetic analysis for the detection of mosaicism has not yet been solved fully because false positive diagnosis of trisomy or monosomy may result from artefacts due to inefficient hybridization of the probes.

A study on the detection of numerical chromosomal abnormalities in neoplastic haematopoietic cells by *in situ* hybridization, Anastasis *et al.* (1990)

proposed a method for establishing the conditions needed to detect mosaicism by FISH on nuclei in interphase. They suggested that diagnosis of monosomy or trisomy should only be made when the percentage of nuclei displaying one or three hybridization signals for autosomal sequences exceeded two standard deviations above the mean of the percentage of cells with a single (false monosomic) or three signals (false trisomic) in control specimens.

Lomax *et al.* (1994) reanalyzed the problem using five centromeric or pericentromeric probes on cultured or uncultured cells from normal or mosaic placental tissues. Although a correct diagnosis was made in most instances, discrepancies were observed between the FISH analysis and the cytogenetic tests. The validity of the suggested approach also depends on the type of probe used and the number of passages of the *in vitro* cultures.

Although no data are yet available, the use of two probes for each chromosome (two differentially labeled contigs) should drastically reduce the frequency of false positive or negative results (Davies *et al.*, 1994b).

Radiation Induced Chromosomal Damage

In 1990, Cremer and colleagues published the results of a pilot study on the feasibility of using NISH to assess chromosomal damage induced by radiation. Human lymphocytes cultured *in vitro* by standard techniques were irradiated with 2, 4, and 8 Gy (neutron dose) of ^{60}Co-γ radiation. Interphase and metaphase spreads from these preparations, and appropriate controls were analyzed for the incidence of abnormalities affecting chromosomes 1 and 7, using specific library probes and a suppression ISH method.

Many nuclei from the irradiated samples showed grossly abnormal staining patterns of chromosomes 1 and 7, including extra domains of variable size indicating radiation-induced mitotic nondisjunction and translocation events. In some nuclei, increased signals were observed and interpreted as evidence of polyploidy.

The number and size of hybridization complexes seen in nuclei that could be analyzed confirmed results of the analysis of the corresponding metaphase spreads. In fact, in agreement with the latter results, interphase response curves suggested a quadratic dependence on the radiation dose. On the basis of the evaluation method employed, about 5% of control, untreated nuclei also exhibited staining patterns and had to be classified as abnormals; this was in contrast with the evaluation of metaphase spreads, where no structural chromosomal abnormalities were observed in normal cells.

These results indicate that NISH analysis of specifically stained interphase chromosomes has potential use for investigating chromosomal abnormalities even in cases of nonoptimal hybridization and background noise from nontargeted sites.

This approach is also suitable for studying damage induced by chemical agents or patients with DNA repair disorders.

Somatic Pairing

With the development of sensitive and specific techniques of NISH, it is now possible to locate individual chromosome pairs in resting cells and to study their movement during the early stages of the cell cycle.

It is generally accepted that interphase chromosomes are restricted to spatial domains (Comings, 1980; Hubert and Bourgeois, 1986; Hilliker and Appels, 1989) and are attached by their centromeres to the nuclear membranes. Under most conditions, the relative fixation of chromosomal domains should result in the separation of homologous pairs (Comings, 1980; Manuelidis, 1985, 1990).

Movement of specific domains during interphase has been demonstrated only rarely (Borden and Manuelidis, 1988; Haaf *et al.*, 1990). Evidence obtained from studies using NISH technology proved that somatic pairing of chromosomes 1 and 17 occurs during interphase in some normal human brain cells (Arnoldus *et al.*, 1989, 1991).

By testing normal human bone marrow, peripheral blood leucocytes, and malignant cells from patients with leukaemia or lymphoma, Lewis *et al.* (1993) have demonstrated pairing of centromeres and p arms of chromosome 15 during interphase. This study was prompted by the observation of an apparent monosomy 15 in tumor cells from some patients with hairy cell leukemia; it became apparent that this resulted from the somatic pairing of chromosomes 15 in interphase.

To demonstrate pairing of 15p and absence of chromosome 15 monosomy, differentially labeled centromeric and 15p specific probe were employed. Pairing could not be detected in amniotic cells, uterine and cervical tissues, and in fibroblasts.

Lewis and colleagues (1993) also observed that the percentage of centromeric pairing of chromosome 15 changed in lymphocytes stimulated by PHA suggesting the hypothesis of intranuclear movement of chromosomes.

NISH AND THE MAPPING OF THE HUMAN GENOME

Current investigations aimed at mapping human genes require a rapid and direct method that allows visualization of specific DNA sequences along each chromosome. This can be achieved by applying NISH to chromosomes in metaphase or interphase.

Radiolabeled probes were employed in early studies, but spatial resolution of the hybridization complexes was imprecise, and several days were required before the autoradiographs could be developed. Furthermore, statistical analysis of the distribution of the silver grains was required.

Counterstaining and banding by conventional staining methods have now been replaced by the use of propidium iodide or DAPI (Adinolfi and Davies, 1994). The introduction of multifluorescence NISH also permits the simultaneous mapping of several differentially labeled probes. The large number of papers dealing with the mapping of the human DNA sequences does not allow us to present a full review of this topic; once again we are forced to limit our exposition to some selected papers.

Metaphase Mapping

One of the first large-scale maps of sequences on the X chromosome was published by Montanaro *et al.* (1991), where 102 YACs were localized in the Xq24-qter region. DNA inserts, purified from YACs by pulsed-field gel electrophoresis were mapped on chromosomes in early metaphase. As expected, DNA sequences more than 300 kb in length were found to be distributed along the entire Xq24-qter region. Further assignment of the sequences was made by comparing the localization of a reporter probe with each YAC DNA. The results showed that *in situ* assignments were accurate enough to place the YACS easily and systematically along the Xq region in "bins" of about 7–10 Mb.

However, the final purpose of mapping sequences is to target genes with known biological activity (Stephens *et al.*, 1990). Here FISH acts as a complementary tool to other molecular techniques that already provide information about the localization of a unique sequence. Recently the gene responsible for X-linked agammaglobilinaemia (XLA) was identified and cloned (Vetrie *et al.*, 1993; Tsukada *et al.*, 1993). This inherited disorder results from abnormal development of B lymphocytes, which are blocked at an early stage of maturation. Using different methodologies, the two groups of investigators were able to clone the gene responsible for the defect and to provide preliminary evidence for its biological function. The physical map of the XLA gene was then confirmed using FISH (Fig. 14).

Several other X-linked genes have now been mapped (or their locations confirmed) using FISH, such as the Duchenne/Becker muscular dystrophy and Hunter genes.

The physical and genetic mapping of chromosome 21 is one of the many aims of the Human Genome Mapping Project. Several hundred YACs that encode sequences concentrated in the q arm of chromosome 21 have already been isolated

(Brownstein *et al.*, 1989; Albertson *et al.*, 1990; Patterson, 1991; Chumakov *et al.*, 1992a,b; Gingrich *et al.*, 1993). Many of the clones used to construct this map were identified using sequence-tagged sites (STSs). In the study by Gingrich *et al.* (1993), the FISH mapping of chromosome 21 was generated with DNA probes derived from YACs isolated by the Joint YAC Screening Effort. The map was compiled using 28 probes that encoded markers already known to be linked to chromosome 21, and centromeric or repeated sequences acting as reference signals. The localization of the fluorescent complexes of each probe was established on metaphase chromosomes in relation to the fraction of chromosome length (FL) from pter. With this approach, 51 YACs and 86 cosmids could be localized on chromosome 21, relative to the known markers employed. One problem encountered in the generation of the FISH map was the inability to obtain hybridization signals with some DNA sequences expected to be linked to chromosome 21. However, the overall map reported by Gingrich *et al.* (1993) was in good agreement with the results of other studies; the only striking ambiguous finding in the FISH map was that the sequence BCE1 seemed to be localized 15 Mb more centromeric than expected.

Another example of the flexibility and advantages of the FISH approach for mapping sequences is the study performed by Inazawa *et al.* (1993), who have localized 342 cosmids on chromosome 17. This chromosome contains several genes whose *de novo* mutations are responsible for inherited disorders such as MDS on 17p13.3; Smith-Magenis syndrome (SMS) on 17p11.2; and Charcot-Marie-Tooth neuropathy type 1 (CMT1A). In recent years, genetic linkage and several regional high-resolution maps have been constructed (Nakamura *et al.*, 1988; Yagel *et al.*, 1990; Borrow *et al.*, 1990, 1991; Ledbetter *et al.*, 1990). Under the experimental conditions employed by Inazawa *et al.* (1993), specific FISH signals could be detected on one or both homologous chromosomes 17 in at least 50% of metaphase spreads examined, and 342 of 452 newly isolated cosmids could be successfully mapped. Since the physical length of chromosome 17 is approximately 85 Mb, the markers analyzed by Inazawa *et al.* (1993) were distributed at an average distance of about 250 kb, but some of the clones clustered in dominant regions. This tendency has been observed also in studies involving chromosomes 3, 6, 8, and 11 (Takahashi *et al.*, 1992; Saito *et al.*, 1992; Emi *et al.*, 1992).

In the study of chromosome 11, 13 known genes, a chromosome-specific DNA repeat and 36 random clones were analyzed by FISH (Lichter *et al.*, 1990). The map position of each probe was expressed as the fraction length (FL) of the total chromosome relative to an arbitrarily chosen fixed reference point (for example, pter). Smaller variations of the FL values were observed when more extended chromosomes were examined.

To assess how well *in situ* maps correlated with positions established by other

techniques, 13 known genes were hybridized by FISH. In all instances but one, the FL value was found to fall within the cytological boundaries defined by previous studies. The exception was the ETS1A oncogene homologue previously reported to map in band 11q23 (Yunis *et al.*, 1989; Budarf *et al.*, 1989). The FL values placed this locus further forward to the telomere in the 11q24 or 11q25 band.

The 36 random clones were also mapped by the NISH procedure and the results confirmed using hybrid cell lines with different deletions of chromosome 11.

An additional 1001 new markers have been localized to five different regions of chromosome 11, using molecular techniques and FISH (Gerhard *et al.*, 1992). A series of radiation-induced somatic cell hybrids was produced that allowed markers within the 11q11–q14 region to be mapped into 11 separate segregation groups.

Several investigators have constructed maps of chromosome 3 by means of hybrid cell deletion panels (Gerber *et al.*, 1988) or by *in situ* hybridization (Atchison *et al.*, 1990; Yamakawa *et al.*, 1991a,b). Deletions or rearrangements of the short arm of chromosome 3 have been reported in nearly all small cell lung carcinomas (SCLC) (Mooibroek *et al.*, 1987; Naylor *et al.*, 1987; Brauch *et al.*, 1990). One of the breakpoints in SCLC maps to the same region as a t(3;8) (p14.2; q24.1) translocation associated with familial renal cell carcinoma (RCC) (Cohen *et al.*, 1979). Chromosome 3 also contains the site of a locus cosegregating with the hereditary tumor syndrome von Hippel-Lindau disease (VHL) (Seizinger *et al.*, 1988; Tory *et al.*, 1989). The autosomal dominant gene for retinitis pigmentosa has been mapped to chromosome 3 (McWilliam *et al.*, 1989), while karyotype analysis of patients with Greig craniopolysyndactyly syndrome, an autosomal dominant disease, has revealed a translocation involving chromosomes 3 and 7 (McKusick, 1986). A fragile site within the 3p14.2 region has been observed and is often associated with rearrangements in a variety of malignancies (Markkanen *et al.*, 1982; Yunis, 1984; Smeets *et al.*, 1986).

In the study published by Haas *et al.* (1993), the probes were prepared from a radiation-induced hybrid, DM1, obtained from a cell line monochromosomal for the human chromosome 3. Fifty six cosmid probes were shown to map between 3p14.3 and 3p22, a region often deleted in SCLC and RCC.

An additional 24 probes were clustered around bands 3p23 and 3p25, a region close to the VHL disease locus. These probes appeared to map near the regions associated with the translocation t(3;8)p14.2; q24.1 detected in some patients with renal carcinoma.

Another eight human chromosome 3p markers, ranging from 500 bp to 4 Kb have been mapped by Heppell-Parton *et al.* (1994) using multicolor FISH. The

results obtained by this approach have resolved previously conflicting data produced by the use of single color FISH methods.

These probes and those investigated by Yamakawa *et al.* (1991a,b) will be very useful in elucidating the genetic alterations present in patients with many inherited disorders, including SCLC, RCC, and VHL syndromes.

The distal region of chromosome 2q contains the locus of the Waardenburg syndrome type I (*WS1*) gene, an autosomal dominant disorder characterized by developmental defects of neural crest cell lineages (Waardenburg, 1951; DiGeorge *et al.*, 1960). The gene responsible for this disease was originally mapped to 2q35–q37.3 after an inversion was observed in one patient (Ishikiriyama *et al.*, 1989), and later to 2q37 on the basis of genetic linkage analyses (Foy *et al.*, 1990; Asher *et al.*, 1991). Recently, some patients with *WS1* have been found to have mutations of the HuP2 (PAX3) gene (Baldwin *et al.*, 1992; Morell *et al.*, 1992; Tassabehji *et al.*, 1992) (see above). Using NISH methods, a total of 25 DNA markers have been located by Lu-Kuo *et al.* (1993) on the distal chromosome 2q region. An important assignment was that of the *PAX3* gene to 2q36.1–q36.2. The gene was found to be deleted in a patient with phenotypic features of *WS1*. The *de novo* deletion (2)(q35q36) and consequent haplo-insufficiency of the *PAX3* product appears to be responsible for the disorder.

Interphase Mapping

Trask *et al.* (1989, 1991) have described two alternative approaches that can be used to order DNA sequences by NISH in interphase nuclei. The first compares the relative distance between probes: For example the order A, B, C can be inferred if the measured distance A–C is equal to or greater than the sum of the distances A–B and B–C. The second is derived by the relative position of three probes hybridized simultaneously and labeled with two fluorochromes. For example, two probes are labeled with red, and one with green fluorescent dyes. The sequence of the signals can either be red–green–red or green–red–red (Fig. 15).

The validity of this approach was confirmed by using five cosmids from a region spanning 800 kb, which includes the factor VIII (F8), glucose-6-phosphate dehydrogenase (G6PD), and color-vision pigment (CV) genes. Probes in the Xq28 regions could be ordered as follows: cen-c1A1-st14c-5′F8-G6PD-18b41-3′ green–green–red-fr7-tel. In this study, the cosmids were from 50 Kb to 2–3 Mb apart (Trask *et al.*, 1989, 1991.

This and other studies (Lawrence *et al.*, 1990; Brandriff *et al.*, 1991; Heng *et al.*, 1992) show that interphase mapping is a straightforward and relatively rapid technique for ordering DNA sequences, but absolute distances are more difficult to

determine than relative order. According to Trask *et al.* (1991), interphase mapping has at least a ten-fold higher resolution for ordering sequences than does the two-color metaphase test (50-100 Kb versus >1 Mb). Two recently developed techniques of cell preparation have led to an even greater resolution. Wiegant *et al.* (1992), using decondensed "halo" chromosomes, have obtained a resolution of 10 Kb, whereas Parra and Windle (1993) have achieved a resolution of 6 Kb using chromosomal DNA that had been stretched on the slide in a technique called direct visual hybridization (DIRVISH) DNA mapping. Fidlerova *et al.* (1994) have described a method utilizing conventionally fixed cytogenetic preparations which are then treated with either formamide or sodium hydroxide in order to release the chromatin. Good signals were obtained with dual labeled probes from within the HLA class II region and this method was found to be useful for resolving the relationships between closely adjacent or overlapping probes.

Highly extended chromatin fibers (ECFs), produced by detergent and high-salt treatment, also provide satisfactory material for ordering YAC contigs (Haaf and Ward, 1994). The protocol for preparing the target DNA is simple and fast, and is suitable for any type of cell, even highly compact haploid sperm nuclei. However, it requires special technical expertise, because when interphase chromatin is extended to the maximum, the hybridization efficiency is low and non-specific fluorescence due to attachment of probe DNA to the glass slides can produce false results.

The diagnostic value of FISH on interphase halo preparations has been evaluated by Tocharoenetanaphol *et al.* (1994) to detect deletions of the dystrophin gene in female carriers. Different probes were employed, including cosmids and YAC clones that contained DNA sequences frequently deleted in DMD patients. The best results were obtained using cosmids; YAC clones, amplified with Alu primers, produced unsatisfactory results. Amplification was achieved in only one of the three YACs tested, where one of 10 exons was amplified. Often, the YAC clones labeled by nick translation exceeded the size of the most frequent deletions.

CANCER AND NISH ANALYSIS OF CHROMOSOMAL DEFECTS

A vast number of papers has been published on the diagnostic value of NISH in patients with premalignant and malignant cancers (Rowley, 1984, 1988; Heim and Mitelman, 1987; Sandberg *et al.*, 1988; Teyssier, 1989; Yunis, 1984; Yunis and Tanzer, 1993). The main aim of these studies is to correlate the numerical and structural chromosomal abnormalities with the diagnosis and prognosis of the

disease. While conventional cytogenetic analysis of cancer cells in metaphase can provide accurate information on the characteristics of even small chromosomal abnormalities, these investigations can only be performed after protracted *in vitro* culture of the isolated cells, which may result in the growth of selected subpopulations. In addition, only a limited number of metaphases will be available for analysis.

NISH methods overcome some of these problems and have the added advantage that single cells (for example, peripheral blood nucleated cells) or tissue sections can be studied (Cremer *et al.*, 1988; Hopman *et al.*, 1990; Poddighe *et al.*, 1992).

Here we discuss only some examples of the application of NISH to elucidate particular aspects of chromosomal disorders in cancer.

In hematology, conventional cytogenetic—and particularly banding—techniques have provided useful information on the characteristics of the chromosomal abnormalities seen in patients with different types of leukemia. Since 1960, the Philadelphia (Ph) chromosome has been shown to be a specific alteration that characterizes chronic myelogenous leukemia (CML) (Nowell and Hungerford, 1960; Rowley, 1973).

This defect results from a translocation involving chromosomes 9 and 22 and the fusion of the proto-oncogene cABL and the "breakpoint cluster region" (BCR) gene. This produces the transcription of a chimeric mRNA of 8 to 85 Kb and the translation of a 310 Kd BCR–ABL fusion protein (Groffen *et al.*, 1984; Shtivelman *et al.*, 1987).

The cytogenetic rearrangement t(9q34;22q11) is observed in more than 90% of CML patients; in the remaining cases, complex translocations are present in addition to those affecting chromosomes 9 and 22. In some cases, the rearrangement involving the two chromosomes may not be apparent when metaphase spreads are analyzed by conventional cytogenetics (Borström, 1981; Heim *et al.*, 1985; De Braekeleer, 1987).

The BCR-ABL fusion gene in cells in metaphase or interphase collected from CML patients can readily be visualized using a two-color FISH preparation (Arnoldus *et al.*, 1990; Tkachuk *et al.*, 1990). The fusion has been detected in all samples investigated, even in cases that appeared cytogenetically negative. As an extension of these studies, Zhang *et al.* (1993) developed several probes using microdissection and PCR amplification which mapped in the 9q34 and 22q11 regions. These probes were then employed to establish the origin of the chromosomal abnormalities in 11 CML patients, nine with various translocations, using FISH. The presence of a variety of complex translocations could be documented unequivocally in the tested CML subjects.

NISH has proved to be a valuable tool to investigate chromosomal defects in other types of leukemia. For example, in a recent study Dohner *et al.* (1993) tested 42 patients with B cell chronic lymphocytic leukemia (B-CLL) and three individuals with prelymphocytic leukemia (B-PLL) using both conventional cytogenetics and NISH. The incidence of total or partial trisomy 12 detected by FISH on cells in interphase was 18% (6 of 42 with B-CLL and 2 of 3 with B-PLL). In four patients the chromosomal abnormalities were observed only when FISH was employed.

In another investigation, chromosome changes in bone marrow and peripheral blood cells were performed by comparing FISH and conventional cytogenetic tests in 13 patients with malignant hematological disorders (Chen *et al.*, 1992). Centromeric probes for chromosomes 1, 6, 7, 8, 9, 12, 13/21, and X were employed. The G-banding results were in accord with the FISH analyses, but, most significantly, FISH tests on nuclei in interphase provided information concerning crucial chromosome abnormalities that were not or could not be detected by cytogenetic tests. The results of this comparative study showed that FISH was clinically valuable for accurate identification of chromosome markers, identification of selected trisomies specific for certain hematological neoplasias, clonal evaluation of cells following sex-mismatched bone marrow transplantation, and residual detection of leukemic cells during clinical remission.

The diagnostic value of using NISH in patients with hematological disorders has been confirmed in many recent reports. Partial or total loss of chromosome 7 is often associated with a variety of myeloid diseases, including childhood chronic myeloproliferative disorders (MPD), myelodysplastic syndromes (MDS) and acute myeloblastic leukemia (AML). MPD is characterized by a preleukemic phase with myelomonocytic proliferation, hepatosplenomegaly, and repeated infections; MDS with monosomy 7 shows a high rate of progression to AML.

An interesting study has been carried out by Baurmann *et al.* (1993) using NISH in interphase and immunohistochemical tests on a group of patients with leukemia and monosomy 7. Monosomy 7 was confirmed in all active cases tested with a specific centromeric probe. While in two patients, conventional cytogenetics suggested that all metaphases were normal for chromosome 7 when tested by FISH, a minority of nuclei was found to be monosomic; in one of these patients a small pericentric chromosome 7-derived marker was also noticed. Monosomy 7 was observed in virtually all myelomonocytic and erythroid cells of another patient with AML and MPD, thus suggesting that the abnormality affected a precursor cell capable of differentiating toward myelomonocytic and erythroid cells, but not lymphocytes.

Kadam *et al.* (1993), using both cytogenetics and FISH on cells in interphase,

investigated two AML patients who did not have demonstrable monosomy 7 when classical cytogenetic methods were used: monosomy 7 was observed in 39.8 and 11%, respectively, of their cells. In some patients with myeloid AML or MDS, granulocytes were also found to be monosomic for chromosome 7 using FISH, thus reflecting the early lineage of the precursor cells affected.

As mentioned, cytogenetic analyses of cells derived from human solid tumors are difficult to perform due to the complexity of the chromosomal changes and the limited number of suitable metaphase spreads. To overcome these limitations, in 1988 Cremer and colleagues explored the possibility of applying NISH to solid tumors using cells in metaphase and interphase. Two glioma cell lines were tested with biotinylated DNA library probes that decorated chromosomes 1, 4, 7, 18, and 22. Numerical changes, deletions, and rearrangements could readily be visualized in metaphase spreads, as well as, early prophase and interphase nuclei. All chromosomes investigated were found to show abnormalities. For example, in one glioma (TC 620) three complete and one metacentric chromosomes 7 (containing the short arm) were present in each cell; in the other glioma (TC 593), four entire chromosomes 7 and a metacentric chromosome containing 7p could be seen in each cell.

NISH methods have been used to study several types of solid malignancy, including cancer of the breast (Devilee *et al.*, 1988); gynecological (Nederlof *et al.*, 1989) and testicular tumors (Giweraman *et al.*, 1989), urinary bladder cancer (Hopman *et al.*, 1988) and prostatic cancer (Brothman and Patel, 1992).

FISH has proved to be particularly useful for investigating the "small round cell tumors," whose diagnosis is particularly difficult because of their undifferentiated character (Selleri *et al.*, 1991b; Giovannini *et al.*, 1992). During the past few years a variety of methods, including immunohistochemical staining, short-term *in vitro* culture, cytogenetics and molecular genetics have been applied to improve diagnosis (Triche and Cavazzana, 1989). Among these tumors, only the primitive mesoectodermal tumors, which include Ewing's sarcoma (ES), show a consistent and unique feature of a translocation between chromosomes 11 and 22—t11;22(q24; q12). Giovannini *et al.* (1992), using FISH, analyzed four primitive neuroectodermal tumor cell lines and cancer cells in interphase obtained from five ES patients, two patients with small osteosarcomas, and one with chronic osteomyelitis. The t(11;22) translocation could be readily detected with FISH in interphase cells from neuroectodermal tumors and in samples from the five ES patients, using the cosmid clones 23.2 and 5.8 bracketing the t(11;22) locus at 11q24.

The direct harvesting of cells from tumor biopsies was found to be preferable for the detection of the translocation in nuclei in interphase, because cells main-

tained in culture for long periods of time showed an increased number of normal diploid cells.

A further example of the potential prognostic value of the application of FISH in solid tumor studies is provided by the work of Taylor *et al.* (1994) in neuroblastoma. Deletions in 1p, N-*myc* amplification, pseudodiploidy or a tetraploid karyotype are predictive of a poor prognosis. Conventional cytogenetic analysis is restricted by a number of factors, including slow cell replication times and very low success rates. FISH using a plasmid probe for N-*myc* (pNB-9), a 35 Kb cosmid mapping close to the consensus deletion point in 1p36.1-2, and an alphoid repeat probe, were all successfully hybridized to imprints of the tumors made directly onto slides, which after simple fixation and pretreatment, were used for *in situ* hybridization. In this way, rapid diagnostic tests providing valuable prognostic information could be performed on neuroblastoma cells in interphase (Taylor *et al.*, 1994).

Additional information on the diagnostic value of NISH for investigating patients with solid tumors can be found in a review by Hopman *et al.* (1990).

EVOLUTION

The relationship between human and primate karyotypes has been extensively investigated to elucidate phylogeny and the process of human evolution. Initially, cytogenetic techniques that allowed only homogeneous staining and comparisons restricted to similarities in number and shape of the chromosomes were employed (Chu and Bender, 1962; Ruffe *et al.*, 1970), but with the development of banding techniques, this research received new impetus and was extended to more species (de Grouchy *et al.*, 1972; Bobrow and Madan, 1973; Dutrillaux, 1979; Seuanez, 1979; Yunis and Prakash, 1982).

The karyotypes of more than 60 species of primates were investigated by Dutrillaux (1979) using all the banding methods available at that time. A very close analogy of chromosome banding was observed between the simians studied and man. Approximately 150 rearrangements were identified and related to the human chromosomes; it was noticed that they varied from one group (suborder, family, genus) to another. For instance, Robertsonian translocations were preponderant among Lemuridae, but nonexistent among Pongidae.

A second phase of these studies continued with the application of radioactive and nonisotopic ISH. Biotin-labeled DNA libraries from flow-sorted human chromosomes were hybridized to metaphase spread preparations of catarrhines, platyrrhines, and prosimians by Wienberg *et al.* (1990).

When a human X chromosome library was used to probe chromosomes of hominoids (*Pan troglodytes* and *Gorilla gorilla*) and lower primates (*Macacca fuscata*, selected *cercopithidae*, *platyhrrines*, and *prosimians*), in all species tested the X chromosome was specifically stained and no translocation of X material to autosomes was observed (Wienberg *et al.*, 1990). This confirmed the suggestion that the X chromosome has been highly conserved during mammalian evolution (Ohno, 1973).

Within the limits of the protocols employed, hybridization signals could not be detected on the X chromosome of some rodents (*Mus musculus* and *Microtus savii*) and a carnivore (*Felis catus*) with the human X-derived probes.

Libraries obtained from human chromosomes 1, 3, 4, 7, and 9 were found to hybridize to individual gorilla and chimpanzee homologues, indicating that these chromosomes have been conserved in their entirety in all three species. When DNA from human chromosomes 5 and 17 was hybridized to gorilla chromosomes the expected rearrangements were observed, showing that the centromere of human chromosome 17, its entire long arm and a small part of the short arm contribute to gorilla chromosome 4, while the short arm was translocated to gorilla chromosome 19 (Wienberg *et al.*, 1990). In a subsequent study (Jauch *et al.*, 1992), chromosome-specific sequences in phages or plasmids, obtained from all 24 flow-sorted human chromosomes, were hybridized by NISH to chromosome spreads prepared from chimpanzee, gorilla, and orangutan. The hybridization patterns unequivocally demonstrated the high degree of chromosomal homology and synteny of the great apes and humans. Relative to human chromosomes, translocations were not observed in great apes, except for the well known fusion origin of human chromosome 2, and the evolutionarily derived reciprocal translocation in gorillas between chromosomes homologous to human chromosomes 5 and 17. In contrast, numerous translocations were detected in the gibbon karyotype, leading to massive reorganization: the 22 human autosomes could be divided into 51 elements to compose the 21 gibbon autosomes.

Radioactive *in situ* hybridization has been applied by Maccarone *et al.* (1992) to investigate the evolution of human chromosome 21. Five human chromosome 21 markers were mapped in marsupials and a monotreme, two major groups of mammals which diverged from eutherians 130–150 million and 150–170 million years ago, respectively. These genes were found to map within two distinct autosomal sites, one containing the superoxide dismutase 1 (SOD1), carbonyl reductase (CBR) and breast cancer estrogen-induced (BCEI) genes, and the other the avian leukaemia E26 viral proto-oncogene (ETS2), and interferon α receptor (INAR) genes, in the marsupials *Macropus eugenii* and *Sminthopsis macroura* and the monotreme *Ornithorhynchus anatinus*. Since these groups of mammals

diverged independently from eutherians, it seems that the two clusters of genes were present in a mammalian ancestor prior to the divergence of the therian and prototherian lineages (Maccarone *et al.*, 1992).

FISH has also been successfully employed to establish chromosomal homologies between *Homo sapiens* and a marmoset, *Callithrix jacchus* (Sherlock, 1993, and unpublished observations). The karyotype of the marmoset was first studied by Egozcue (1968), and shown to have 46 chromosomes: 22 pairs of autosomes, X and Y. Human chromosome-specific library probes (chromosomes 1, 2, 3, 4, 5, 6, 8, 9, 11, 13, 15, 18, 21, X and Y) were hybridized to the marmoset genome to identify corresponding regions. Prebanding with Giemsa-trypsin was also employed to identify individual marmoset chromosomes which were then photographed, destained, and treated for FISH testing. The results showed that four of the human chromosomes, 5, 6, 21, and X, had sequences conserved in a single marmoset chromosome. Probes specific for chromosomes 4, 9, 11, 14, and 18 hybridized to interrupted segments of larger marmoset chromosomes (Fig. 16). Sequences from each of the remaining human chromosomes mapped to more than one marmoset chromosome (Fig. 17). DNA from human chromosome 3 constituted the entire sequence of two acrocentric marmoset chromosomes. Neither of the two alphoid repeats specific for human chromosomes 18 and X were conserved in the marmoset. The results of this study demonstrated that while chromosome homology between *Homo sapiens* and *C. jacchus*, based on banding comparisons, were correct for chromosomes 4, 5, 6, 18, 21, and X, suggested homologies for human chromosomes 1, 2, 3, and 14 (Dutrillaux and Couturier, 1981) were inaccurate.

We have summarized here only some of the studies performed to compare human chromosomes with those from other species, omitting, for example, investigations in mice, an area of intense investigation at the present time.

CONCLUSIONS

From the selected topics discussed in the previous sections, it is clear that the NISH methodologies have made rapid progress and found wide application in several areas of clinical studies and research.

Many diagnostic laboratories are now successfully using these techniques as adjuvants to conventional cytogenetic tests, often exploiting the advantages of commercially available kits that greatly simplify the use of the probes and their hybridization to target DNA.

In the clinical field, perhaps the only doubts are those expressed about the diagnostic value of employing NISH on cells in interphase for the prenatal

detection of major chromosomal disorders (Ledbetter, 1992). Although the accuracy of aneuploid screening by NISH on uncultured amniotic or chorionic cells has improved in recent years, the present view is still that this approach should be used only as a preliminary, rapid test while awaiting the results of cytogenetic tests that may reveal chromosomal abnormalities undetectable by NISH on cells in interphase.

On the other hand, NISH provides essential data in many areas of research, acting, either as a complementary method for gene mapping or as a tool to detect symmetrical portions of DNA sequences in sister chromosomes. In addition to supplying information on longitudinal mapping, NISH allows the lateral (internal, median or external) position of DNA sequences to be established (Baumgartner *et al.*, 1991).

It seems that NISH has avoided the "disappointment phase" that often follows the "excitement" stage of any new method (Ledbetter, 1992) and has "passed with full grades" the tests required for its acceptance as an essential tool in clinical and research investigations.

ACKNOWLEDGMENTS. The authors are grateful to Action Research for financial support for original work quoted in this paper, and to Adrienne Knight for preparing the manuscript.

REFERENCES

Adinolfi, M., 1992a, Fetal nucleated cells in the maternal circulation, in: *Prenatal Diagnosis and Screening* (D.J.H. Brock, C.H. Rodeck, and M.A. Ferguson-Smith, eds.), London pp. 651–662, Churchill Livingstone, Edinburgh.

Adinolfi, M., 1992b, Breaking the blood barrier, *Nature Genet.* **1**:316–318.

Adinolfi, M., 1993, Hunter syndrome: Cloning of the gene, mutations and carrier detection, *Dev. Med. Child Neurol.* **35**:79–85.

Adinolfi, M., and Davies, A.F., 1994, *Non-isotopic In Situ Hybridization: Applications to Clinical Diagnosis and Molecular Genetics*, RG Landes, Austin, Texas.

Adinolfi, M., Davies, A., Sharif, S., Soothill, P., and Rodeck, C., 1993, Detection of trisomy 18 and Y-derived sequences in fetal nucleated cells obtained by transcervical flushing, *Lancet* **342**:403–404.

Adinolfi, M., Soothill, P., and Rodeck, C., 1994, A simple alternative to amniocentesis? *Prenat. Diagn.* **14**:231–233.

Adinolfi, M., Stone, S., and Moralli, D., 1992, Carrier detection of deletions in female relatives of X-linked disorders by nonisotopic *in situ* hybridization, *BioEssays* **14**:421–426.

Albertson, H.M., Abderrahim, H., Cann, H.M., Dausset, J., Le Paslier, D., and Cohen, D., 1990, Construction and characterization of a yeast artificial chromosome library containing seven haploid genome equivalents, *Proc. Natl. Acad. Sci. USA* **87**:4256–4262.

American College of Medical Genetics, 1993, Prenatal interphase fluorescence *in situ* hybridization (FISH) policy statement, *Am. J. Hum. Genet.* **53**:526–527.

Anastasis, J., LeBeau, M.M., Vardiman, J.W., and Westbrook, C.A., 1990, Detection of numerical chromosomal abnormalities in neoplastic hematopoietic cells by *in situ* hybridization with a chromosome-specific probe, *Am. J. Pathol.* **136:**131–139.

Arahata, K., Hoffman, E.P., Kunkel, L.M., Ishihura, S., Tsukahara, T., Ishihara, T., Sunohara, N., Nonaka, I., Ozawa, E., and Sugita, H., 1989, Dystrophin diagnosis: Comparison of dystrophin abnormalities by immunofluorescence and immunoblot analyses, *Proc. Natl. Acad. Sci. USA* **86:**7154–7158.

Arias, S., 1971, Genetic heterogeneity in the Waardenburg syndrome, *Birth Defects Original Article Series* **7:**87–101.

Arnoldus, E.P.J., Peters, A.C.B., Bots, G.T.A.M., Raap, A.K., and Van der Ploeg, M., 1989, Somatic pairing of chromosome 1 centromeres in interphase nuclei of human cerebellum, *Hum. Genet.* **83:**231–234.

Arnoldus, E.P.J., Noordermeer, I.A., Boudewijn Peters, A.C., Voormolen, J.H.C., Bots, G.T.A.M., Raap, A.K., and Van der Ploeg, M., 1991, Interphase cytogenetics of brain tumors, *Genes Chromosomes Cancer* **3:**101–107.

Arnoldus, E.P.J., Wiegant, J., Noordermeer, I.A., Wessels, J.W., Baverstock, G.C., Grosveld, G.C., Vander Ploeg, M., and Rapp, A.K., 1990, Detection of the Philadelphia chromosome in interphase nuclei, *Cytogenet. Cell Genet.* **54:**108–111.

Asher, J.H., and Friedman, T.B., 1990, Mouse and hamster mutants as models for Waardenburg syndrome in humans, *J. Med. Genet.* **27:**618–626.

Asher, J.H., Jr., Morell, R., and Friedman, T.B., 1991, Waardenburg syndrome (WS): The analysis of a single family with a *WSI* mutation showing linkage to RFLP markers on human chromosome 2q, *Am. J. Hum. Genet.* **48:**43–52.

Atchison, L., Cannizzaro, L., Caamano, J., Atchison, M., and Comis, R.L., 1990, Assignment of 35 single-copy and 17 repetitive sequence DNA probes to human chromosome 3: High-resolution physical mapping of seven DNA probes by *in situ* hybridization, *Genomics* **6:**441–450.

Baldini, A., Rocchi, M., Archidiacono, N., Miller, O.J., and Miller, D.A., 1990, A human alpha satellite DNA subset specific for chromosome 12, *Am. J. Hum. Genet.* **46:**784–788.

Baldini, A., Ross, M., Nizetic, D., Vatchvea, R., Lindsay, E.A., Lehrach, H., and Siniscalco, M., 1992, Chromosomal assignment of human YAC clones by fluorescent *in situ* hybridization: Use of single-yeast-colony PCR and multiple labeling, *Genomics* **14:**181–184.

Baldini, A., and Ward, D.C., 1991, *In situ* hybridization banding of human chromosomes with Alu-PCR products: A simultaneous karyotype for gene mapping studies, *Genomics* **9:**770–774.

Baldwin, C.T., Hoth, C.F., Amos, J.A., da Silva, E.O., and Milunsky, A., 1992, An exonic mutation in the HuP2 paired domain gene causes Waardenburg syndrome, *Nature* **355:**637–638.

Barber, L., and Crichter, R., 1994, quoted in Adinolfi, M., and Davies, A., *Non-isotopic In Situ Hybridization: Applications to Clinical Diagnosis and Molecular Genetics*, R.G. Landes, Austin, Texas.

Bartsch, O., and Schwinger, E., 1991, A simplified protocol for fluorescence *in situ* hybridization with repetitive DNA probes and its use in clinical cytogenetics, *Clin. Genet.* **40:**47–56.

Baumgartner, M., Dutrillaux, B., Lemieux, N., Lilienbaum, A., Paulin, D., and Viegas-Pequignot, E., 1991, Genes occupy a fixed and symmetrical position on sister chromatids, *Cell* **64:**761–766.

Baurmann, H., Cherif, D., and Berger, R., 1993, Interphase cytogenetics by fluorescent *in situ* hybridization (FISH) for characterization of monosomy-7-associated myeloid disorders, *Leukemia* **7:**384–391.

Beggs, A.H., Koenig, M., Boyce, F.M., and Kunkel, L.M., 1990, Detection of 98% of DMD/BMD gene deletions by polymerase chain reaction, *Hum. Genet.* **86:**45–48.

Benson, P.F., and Fensom, A.H., 1985, *Genetic Biochemical Disorders*, Oxford University Press, Oxford, England.

Bianchi, D.W., Flint, A.F., Pizzimenti, M.F., Knoll, J.H.M., and Latt, S.A., 1990, Isolation of fetal DNA from nucleated erythrocytes in maternal blood, *Proc. Natl. Acad. Sci. USA* **87:**3279–3283.

Bianchi, D.W., and Klinger, K.W., 1993, Prenatal diagnosis through the analysis of fetal cells in the maternal circulation, in: *Genetic Disorders of the Fetus* (A. Milunsky, ed.), pp. 759–770, The Johns Hopkins University Press, Baltimore.

Bird, T.D., Ott, J., and Giblett, E.R., 1982, Evidence for linkage of Charcot–Marie–Tooth neuropathy to the Duffy locus on chromosome 1, *Am. J. Hum. Genet.* **34**:388–394.

Blennow, E., Telenius, H., Larsson, C., Devos, D., Bajalica, S., Ponder, B.A.J., and Nordenskjold, M., 1992, Complete characterization of a large marker chromosome by reverse and forward chromosome painting, *Hum. Genet.* **90:**371–374.

Bobrow, M., and Madan, K., 1973, A comparison of chimpanzee and human chromosomes, using the Giemsa-11 and other chromosome-banding techniques, *Cytogenet. Cell Genet.* **12:**107–116.

Bonilla, E., Samitt, C.E., Miranda, A.F., Hays, A., Salviati, G., Di Mauro, S., Kunkel, L.M., Hoffman, E.P., and Rowland, L.P., 1988, Duchenne muscular dystrophy: Deficiency of dystrophin at the muscle cell surface, *Cell* **54:**447–452.

Borden, J., and Manuelidis, L., 1988, Movement of the X chromosome in epilepsy, *Science* **242:**1687–1691.

Borrow, J., Black, D.M., Goddard, A.D., Yagle, M.K., Friscaut, A.-M., and Solomon, E., 1991, Construction and regional localization of clones from a NotI linking library from human chromosome 17q, *Genomics* **10:**477–480.

Borrow, J., Goddard, A.D., Sheer, D., and Solomon, E., 1990, Molecular analysis of acute promyelocytic leukemia breakpoint cluster region on chromosome 17, *Science* **249:**1577–1580.

Borström, G.H., 1981, New types of unusual and complex Philadelphia chromosome (Ph^1) translocation in chronic myeloid leukemia, *Cancer Genet. Cytogenet.* **18:**215–220.

Brandriff, B., Gordon, L., and Trask, B., 1991, A new system for high-resolution DNA sequence mapping in interphase pronuclei, *Genomics* **10:**75–82.

Brauch, H., Tory, K., Kotler, F., Gazdar, A.F., Pettingill O., Johnson, B., Graziano, S., Winton, T., Buys, C.H., Sorenson, G.D., Poiesz, B.J., Minna, J.D., and Zbar, B., 1990, Molecular mapping of deletion sites in the short arm of chromosome 3 in human lung cancer, *Genes Chrom. Cancer* **1:**247–255.

Breuning, M.H., Dauwerse, H.G., Fugazza, G., Saris, J.J., Spruit, L., Wijnen, H., Tommerup, N., Vanderhagen, C.B., Imaizumi, K., Kuroki, Y., Vandenboogaard, M.J., Depater, J.M., Marimam, E.C.M., Hamel, B.C.J., Himmelbauer, H., Frischauf, A.M., Stallings, R.L., Beverstock, G.C., Van Ommen, G.J.B., and Hennekam, R.C.N., 1993, Rubinstein–Taybi syndrome caused by submicroscopic deletions within 16p13.3, *Am. J. Hum. Genet.* **52:**249–254.

Brothman, A.R., and Patel, A.M., 1992, Characterization of 10 marker chromosomes in a prostatic cancer cell line by *in situ* hybridization, *Cytogenet. Cell Genet.* **60:**8–11.

Brousseau, G.E., 1960, Genetic analysis of the male fertility factors on the Y chromosome of *Drosophila melanogaster*, *Genetics* **44:**257–274.

Brownstein, B.H., Silverman, G.A., Little, R.D., Burke, D.T., Korsmeyer, S.J., Schlessinger, D., and Olson, M.V., 1989, Isolation of single-copy human genes from a library of yeast artificial chromosome clones, *Science* **244:**1348–1351.

Buckle, V.J., and Craig, I.W., 1986, *In situ* hybridization, in: *Human Genetic Diseases* (K.E. Davies, ed.), pp. 85–100, IRL Press, Oxford, England.

Buckton, K.E., Spowart, G., Newton, M.S., and Evans, H.Y., 1985, Forty-four probands with an additional "marker chromosome," *Hum. Genet.* **69:**353–370.

Budarf, M., Sellinger, B., Griffin, C., and Emanuel, B.S., 1989, Comparative mapping of the constitutional and tumor-associated 11;22 translocations, *Am. J. Hum. Genet.* **45:**128–139.

Bunyan, D.J., Robinson, D.O., Collins, A.L., Cockwell, A.E., Bullman, H.M.S., and Whittaker, P.A.,

1994a, Germline and somatic mosaicism in a female carrier of Duchenne muscular dystrophy, *Hum. Genet.* **93:**541–544.

Bunyan, D.J., Crolla, J.A., Collins, A.L., and Robinson, D.O., 1994b, Fluorescent *in situ* hybridization studies provide evidence for a high level of somatic mosaicism in *de novo* dystrophin gene mutations, *Hum. Genet.* (in press).

Buongiorno-Nardelli, M., and Amaldi, F., 1969, Autoradiographic detection of molecular hybrids between rRNA and DNA in tissue sections, *Nature* **225:**946–947.

Burgoyne, P.S., 1987, The role of the mammalian Y chromosome in spermatogenesis, *Development* **101:**133–141.

Burns, J., Chan, V.T.W., Jonasson, J.A., Fleming, K.A., Taylor, S., and McGee, J.O'D., 1985, Sensitive system for visualizing biotinylated DNA probes hybridized *in situ*: Rapid sex determination of intact cells, *J. Clin. Pathol.* **38:**1085–1092.

Callen, D.F., Eyre, H.J., Ringenbergs, M.L., Freemantle, C.J., Woodroffe, P., and Haan, E.A., 1991, Chromosomal origin of small ring marker chromosomes in man: Characterization by molecular genetics, *Am. J. Hum. Genet.* **48:**769–782.

Callen, D.F., Eyre, H.J., Yip, M.Y., Freemantle, J., and Haan, E.A., 1992, Molecular cytogenetic and clinical studies of 42 patients with marker chromosomes, *Am. J. Med. Genet.* **43:**709–715.

Callen, D.F., Ringenbergs, M.L., Fowler, J.C.S., Freemantle, J., and Haan, E.A., 1990, Small marker chromosomes in man: Origin from pericentric heterochromatin of chromosomes 1, 9, and 16, *J. Med. Genet.* **27:**155–159.

Carey, A.H., Kelly, D., Halford, S., Wadey, R., Wilson, D., Goodship, J., Burn, J., Paul, T., Sharkey, A., Dumanski, J., Nordenskjold, M., Williamson, R., and Scambler, P.J., 1992, Molecular genetic study of the frequency of monosomy 22q11 in DiGeorge syndrome, *Am. J. Hum. Genet.* **51:** 964–970.

Carter, N.P., Ferguson-Smith, M.A., Perryman, M.T., Telenius, H., Pelmear, A.H., Leversha, M.A., Glancy, M.T., Wood, S.L., Cook, K., Dyson, H.M., Ferguson-Smith, M.E., and Willatt, L.R., 1992, Reverse chromosome painting: A method for the rapid analysis of aberrant chromosomes in clinical cytogenetics, *J. Med. Genet.* **29:**299–307.

Chamberlain, J.S., Gibbs, R.A., Ranier, J.E., and Caskey, C.T., 1989, Multiplex PCR for diagnosis of Duchenne muscular dystrophy, in: *PCR Protocols: A Guide To Methods and Applications* (M. Innis, D. Gelfand, J. Sninski, and T. White, eds.), pp. 272–281, Academic Press, New York.

Chance, P.F., Abbas, N., Lensch, M.W., Pentao, L., Roa, B.B., Patel, P.I., and Lupski, J.R., 1994, Two autosomal dominant neuropathies result from reciprocal DNA duplication/deletion of a region on chromosome 17, *Hum. Mol. Genet.* **3:**223–228.

Chance, P.F., Andersom, M.K., Leppig, K.A., Lensch, M.W., Matsunami, N., Smith, B., Swanson, P.D., Odelberg, S., Disteche, C.M., and Bird, T.D., 1993, DNA deletion associated with hereditary neuropathy with liability to pressure palsies, *Cell* **2:**143–151.

Chase, D.S., Morris, A.H., Ballabio, A., Pepper, S., Giannelli, F., and Adinolfi, M., 1986, Genetics of Hunter syndrome: Carrier detection, new mutations, segregation and linkage analysis, *Ann. Hum. Genet.* **50:**349–360.

Chen, Z., Morgan, R., Berger, C.S., and Sandberg, A.A., 1992, Application of fluorescence *in situ* hybridization in hematological disorders, *Cancer Genet. Cytogenet.* **63:**62–69.

Chong, S.S., Kristjansson, K., Cota, J., Handyside, A.H., and Hughes, M.R., 1993, Preimplantation prevention of X-linked disease: Reliable and rapid sex determination of single human cells by restriction analysis of simultaneously amplified ZFX and ZFY sequences, *Hum. Mol. Genet.* **2:**1187–1191.

Choo, K.H., Vissel, B., Brown, R., Filby, R.G., and Earle, E., 1988, Homologous alpha satellite sequences on human acrocentric chromosomes with selectivity for chromosomes 13, 14, and 21:

Implications for recombination between nonhomologues and Robertsonian translocations, *Nucl. Acids Res.* **16:**1273–1284.

Choo, K.H., Vissel, B., and Earle, E., 1989, Evolution of α-satellite DNA on human acrocentric chromosomes, *Genomics* **5:**332–344.

Choo, K.H., Vissel, E.E., and Filby, R.G., 1990, Identification of two distinct subfamilies of alpha-satellite DNA that are highly specific for chromosome 15, *Genomics* **7:**143–151.

Choo, K.H., Vissel, B., Nagy, A., Earle, E., and Kalitsis, P., 1991, A survey of the genomic distribution of alpha satellite DNA on all the human chromosomes, and derivation of a new consensus sequence, *Nucl. Acids Res.* **19:**1179–1182.

Chu, E.H.Y., and Bender, M.A., 1962, Cytogenetics and evolution of primates, *Ann. N.Y. Acad. Sci.* **102:**253–266.

Chumakov, I.M., Rigault, P., Guillou, S., Ougen, P., Bilaut, A., Guasconi, G., Gervy, P., Le Gall, I., Soularue, P., Grinas, L., Bougueleret, L., Bellanne-Chantelot, C., Lacroix, B., Barillot, E., Gesnouin, P., Pook, S., Vaysseix, G., Frelat, G., Schmitz, A., Sambucy, J.-L., Bosch, A., Estivill, X., Weissenbach, J., Vignal, A., Reithman, H., Cox, D., Patterson, D., Gardiner, K., Hattori, M., Sakaki, Y., Ichikawa, H., Ohki, M., Le Paslier, D., Heilig, R., Antonarakis, S., and Cohen, D., 1992*a*, Continuum of overlapping clones spanning the entire human chromosome 21q, *Nature* **359:**380–387.

Chumakov, I.M., Le Gall, I., Billauolt, A., Ougen, P., Soularue, P., Guillou, S., Rigault, P., Bui, H., De Tand, M.-F., Barillot, E., Abderrahim, H., Cherif, P., Berger, R., Le Paslier, D., and Cohen, D., 1992*b*, Isolation of chromosome 21-specific yeast artificial chromosomes from a total human genome library, *Nature Genet.* **1:**222–225.

Cohen, A.J., Li, F.P., Berg, S., Marchetts, D.J., Tsai, S., Jacobs, S.C., and Brown, R.S., 1979, Hereditary renal–cell carcinoma associated with a chromosomal translocation, *N. Engl. J. Med.* **301:**592–595.

Colombi, M., Garadella, R., and Barlati, S., 1988, A frequent HaeIII RFLP of the human fibronectin gene (FN1), *Nucl. Acids Res.* **16:**6761.

Comings, D.E., 1980, Arrangement of chromatin in the nucleus, *Hum. Genet.* **53:**131–143.

Cook, H.J., and Hindley, J., 1987, Cloning of human satellite III DNA: Different components are on different chromosomes, *Nucl. Acids Res.* **6:**3177–3197.

Cooke, H.J., Schmidtke, J., and Gorden, J.R., 1982, Characterization of human Y chromosome repeated sequence and related sequences in higher primates, *Chromosoma* **87:**491–502.

Cremer, T., Landegent, J., Brueckner, A., Scholl, H.P., Schardin, M., Hager, H.D., Devilee, P., Pearson, P., and Van der Ploeg, M., 1986, Detection of chromosome aberrations in the human interphase nucleus by visualization of specific target DNAs with radioactive and nonradioactive *in situ* hybridization techniques: Diagnosis of trisomy 18 with probe L1.84, *Hum. Genet.* **74:** 346–352.

Cremer, T., Lichter, P., Borden, J., Ward, D.C., and Manuelidis, L., 1988, Detection of chromosome aberrations in metaphase and interphase tumor cells by *in situ* hybridization using chromosome-specific library probes, *Hum. Genet.* **80:**235–246.

Cremer, T., Popp, S., Emmerich, P., Lichter, P., and Cremer, C., 1990, Rapid metaphase and interphase detection of radiation-induced chromosome aberrations in human lymphocytes by chromosomal suppression *in situ* hybridization, *Cytometry* **11:**110–118.

Cremer, T., Remm, B., Kharhoush, I., Jauch, A., Wienberg, J., Stelzer, E., and Cremer, C., 1991, Nonisotopic *in situ* hybridization and digital image analysis of chromosomes in mitotitc and interphase cells, *Rev. Europ. Technol. Biomed.* **13:**50–54.

Crolla, J.A., Dennis, N.R., and Jacobs, P.A., 1992, A nonisotopic *in situ* hybridization study of the chromosomal origin of 15 supernumerary marker chromosomes in man, *J. Med. Genet.* **29:** 699–703.

Crolla, J.A., and Llerena, J.C., 1988, A mosaic 45,X.46,X,r(?) karyotype investigated with X and Y centromere-specific probes using a nonautoradiographic *in situ* hybridization technique, *Hum. Genet.* **81**:81–84.

Crolla, J.A., Smith, M., and Docherty, Z., 1989, Identification and characterization of a small marker chromosome using nonisotopic *in situ* hybridization with X and Y specific probes, *J. Med. Genet.* **26**:192–194.

Crolla, J.A., Harvey, J.F., Sitch, F.L., and Dennis, N.R., 1994, Supernumerary marker 15 chromosomes: A clinical, molecular, and FISH approach to diagnosis and prognosis, *Hum. Genet.* (in press).

Curran, M.E., Atkinson, D.L., Ewart, A.K., Morris, C.A., Leppert, M.F., and Keating, M.T., 1993, The elastin gene is disrupted by a translocation associated with supravalvular aortic stenosis, *Cell* **73**:159–168.

Cullen, P., Rodgers, C.S., Callen, D.S., Connolly, V.N., Eyre, H., Fells, P., Gordon, H., Winter, R.M., and Thakker, R.V., 1993, Association of familial Duane anomaly and urogenital abnormalities with a bisatellited marker derived from chromosome 22, *Am. J. Med. Genet.* **47**:925–930.

Davies, A.F., Barber, L., Murer-Orlando, M., Bobrow, M., and Adinolfi, M., 1994a, An improved method for the detection of trisomy 21 in uncultured amniocytes by fluorescence *in situ* hybridization, *Ann. N.Y. Acad. Sci.* **731**:67–72.

Davies, A.F., Barber, L., Murer-Orlando, M., Bobrow, M., and Adinolfi, M., 1994b, FISH detection of trisomy 21 in interphase by the simultaneous use of two differentially labeled cosmid contigs, *J. Med. Genet.* **31**:679–685.

de Grouchy, J., Truleau, C., Roubin, M., and Klein, M., 1972, Evolution caryotypique de l'homme et du chimpanzé: Étude comparative des topographies de bands aprés dénaturation ménagée, *Ann. Genet.* **15**:79–84.

de la Chapelle, A., Herra, R., Koivisto, M., and Aula, P., 1981, A deletion in chromosome 22 can cause Di George syndrome, *Hum. Genet.* **57**:253–256.

De Braekeleer, M., 1987, Variant Philadelphia translocations in chronic myeloid leukemia, *Cytogenet. Cell Genet.* **44**:215–222.

Delhanty, J.D.A., Griffin, D.K., Handyside, A.H., Harper, J., Atkinson, G.H.G., Pieters, M.H.E.C., and Winston, R.M.L., 1993, Detection of aneuploidy and chromosomal mosaicism in human embryos during preimplantation sex determination by fluorescent *in situ* hybridization (FISH), *Hum. Mol. Genet.* **2**:1183–1185.

Den Dunnen, J.T., Grootscholten, P.M., Bakker, E., Blonden, L.A.J., Ginjaar, H.B., Wapenaar, M.C., Van Paassen, H.M.B., Van Broeckhoven, C., Pearson, P.L., and Van Ommen, G.J.B., 1989, Topography of the DMD gene: FIGE and cDNA analysis of 194 cases reveals 115 deletions and 13 duplications, *Am. J. Hum. Genet.* **45**:835–847.

Deng, H.-X., Yoshiura, K., Dirks, R.W., Harada, N., Hirota, T., Tsukamoto, K., Jinno, Y., and Niikawa, N., 1992, Chromosome-band-specific painting: Chromosome *in situ* suppression hybridization using PCR products from a microdissected chromosome band as a probe pool, *Hum. Genet.* **89**:13–17.

Devilee, P., Slagboom, P., Bakker, E., Scholl, H.P., Hager, H.D., Stevenson, A.F.G., Cornelisse, C.J., and Pearson, P.L., 1986, Two subsets of human alphoid repetitive DNA show distinct preferential localization in the pericentric regions of chromosomes 13, 18, and 21, *Cytogenet. Cell Genet.* **41**:193–201.

Devilee, P., Thierry, R.F., and Kievits, T., 1988, Detection of chromosome aneuploidy in interphase nuclei from human primary breast tumors using chromosome-specific repetitive DNA probes, *Cancer Res.* **48**:5825–5830.

DiGeorge, A.M., Olmsted, D.W., and Harley, R.D., 1960, Waardenburg's syndrome, *J. Paediatr.* **57**:649.

Dittrich, B., Robinson, W.P., Knoblauch, H., Buiting, K., Gillessenkaesbach, G., and Horsthemke,

B., 1992, Molecular diagnosis of the Prader–Willi and Angelman syndromes by detection of parent-of-origin specific DNA methylation in 15q11–13, *Hum. Genet.* **90:**313–315.

Dobyns, W.B., Curry, C.Y.R., Hoyme, H.E., Turlington, L., and Ledbetter, D.H., 1991, Clinical and molecular diagnosis of Miller–Dieker syndrome, *Am. J. Hum. Genet.* **48:**584–594.

Dohner, H., Pohl, S., Bulgay-Morschel, M., Stilgenbauer, S., Bentz, M., and Lichter, P., 1993, Trisomy 12 in chronic lymphoid leukemias—a metaphase and interphase cytogenetic analysis, *Leukemia* **7:**516–520.

Driscoll, D.A., Budarf, M.L., and Emanuel, B.S., 1992, A genetic etiology for DiGeorge syndrome: Consistent deletions and microdeletions of 22q11, *Am. J. Hum. Genet.* **50:**924–933.

Duane, A., 1905, Congenital deficiency of abduction associated with impairment of adduction, retraction movements, contractions of the palpebral fissure, and oblique movement of the eye, *Arch. Ophthal.* **34:**133–159.

Dutrillaux, B., 1979, Chromosomal evolution in primates: Tentative phylogy from *Microcebus murinus* (prosimian) to man, *Hum. Genet.* **48:**251–314.

Dutrillaux, B., and Couturier, J., 1981, The ancestral karyotype of Platyrrhine monkeys, *Cytogenet. Cell Genet.* **30:**232–242.

Dyck, P.J., 1993, Neuronal atrophy and degeneration predominantly affecting peripheral sensory and autonomic neurons, in: *Peripheral Neuropathies*, 3rd edition (P.J. Dyck and P.K. Thomas, eds.), pp. 1065–1092, WB Saunders, Philadelphia.

Dyck, P.J., and Lambert, E.H., 1968*a*, Lower motor primary sensory neuron diseases with peroneal muscular atrophy. I. Neurologic, genetic, and electrophysiologic findings in hereditary polyneuropathies, *Arch. Neurol.* **18:**603–618.

Dyck, P.J., and Lambert, E.H., 1968*b*, Lower motor and primary sensory neuron disease with peroneal muscular atrophy. II. Neurologic, genetic, and electrophysiologic findings in various neuronal degenerations, *Arch. Neurol.* **18:**619–625.

Egozcue, J., Perkins, E.M., and Hagemanas, F., 1968, Chromosomal evolution in marmosets, tamarins, and finches, *Folia Primatologica* **9:**81–94.

Elias, G., Price, J., Dockter, M., Wachtel, S., Tharapel, A., and Simpson, J.L., 1992, First trimester prenatal diagnosis of trisomy 21 in fetal cells from maternal blood, *Lancet* **340:**1033.

Emi, M., Takahashi, E., Koyama, K., Okui, K., Oshimura, M., and Nakamura, Y., 1992, Isolation and mapping of 88 new RFLP markers of human chromosome 8, *Genomics* **13:**1261–1266.

Emmerich, P., Loos, P., Jauch, A., Hopman, A.H.N., Wiegant, J., Higgins, M., White, B.N., Ploeg, M., Cremer, C., and Cremer, T., 1989, Double *in situ* hybridization in combination with digitized image analysis: A new approach to study interphase chromosome topography, *Exp. Cell Res.* **181:**126–140.

Epstein, D.J., Malo, D., Vekemans, M., and Gros, P., 1991, Molecular characterization of a deletion encompassing *Splotch* (Sp2H), a mutation affecting development of the mouse neural tube, shows a deletion within the paired homeodomain of Pax-3, *Cell* **67:**767–774.

Ewart, A.K., Morris, C.A., Atkinson, D., Jin, W.S., Sternes, K., Spallone, P., Stock, A.D., Leppert, M., and Keating, M.T., 1993a, Hemizygosity at the elastin locus in a developmental disorder, Williams syndrome, *Nature Genet.* **5:**11–16.

Ewart, A.K., Morris, C.A., Ensing, G.J., Loking, J., Moore, C., Leppert, M., and Keating, M.T., 1993b, A human vascular disorder, supravalvular aortic stenosis, maps to chromosome 7, *Proc. Natl. Acad. Sci. USA* **90:**3226–3230.

Fantes, J.A., Bickmore, W.A., Fletcher, J.M., Ballesta, F., Hanson, I.M., and Van Heyningen, V., 1992, Submicroscopic deletions at the WAGR locus, revealed by nonradioactive *in situ* hybridization, *Am. J. Hum. Genet.* **51:**1286–1294.

Fidlerova, H., Senger, G., Kost, M., Sanseau, P., and Sheer, D., 1994, Two simple procedures for releasing chromatin from routinely fixed cells for fluorescence *in situ* hybridization, *Cytogenet. Cell Genet.* **65:**203–205.

Flomen, R.H., Green, P.M., Bentley, D.R., Giannelli, F., and Green, E.P., 1992, Detection of point mutations and a gross deletion in six Hunter syndrome patients, *Genomics* **13**:543–550.

Foy, C., Newton, V.E., Wellesley, D., Harris, R., and Read, A.P., 1990, Assignment of the locus for Waardenburg syndrome type I to human chromosome 2q37 and possible homology to the splotch mouse, *Am. J. Hum. Genet.* **46**:1017–1023.

Friedrich, U., and Jensen, P.K.A., 1983, Limited use of chromosomal markers in prenatal diagnosis, *Prenat. Diagn.* **3**:355–356.

Gall, J.G., and Pardue, M.L., 1969, Formation and detection of RNA–DNA hybrid molecules in cytological preparations, *Proc. Natl. Acad. Sci. USA* **63**:378–381.

Gandelman, K.Y., Gibson, L., Meyn, M.S., and Yangfeng, T.L., 1992, Molecular definition of the smallest region of deletion overlap in the Wolf–Hirschhorn syndrome, *Am. J. Hum. Genet.* **51**:571–578.

Gerber, M.J., Drabkin, H.A., Firnhaber, C., Miller, Y.E., Scoggin, C.H., and Smith, D.I., 1988, Regional localization of chromosome 3-specific DNA fragments using a hybrid cell deletion panel, *Am. J. Hum. Genet.* **85**:576–580.

Gerhard, D.S., Lawrence, E., Wu, J., Chua, H., Ma, N., Bland, S., and Jones, C., 1992, Isolation of 1001 new markers from human chromosome 11, excluding the region of 11p13-p15.5, and their sublocalization by a new series of radiation-reduced somatic cell hybrids, *Genomics* **13**:1133–1142.

Gingrich, J.C., Shadravan, F., and Lowry, S.R., 1993, A fluorescence *in situ* hybridization map of human chromosome 21 consisting of thirty genetic and physical markers on the chromosome: Localization of 137 additional YAC and cosmid clones with respect to this map, *Genomics* **17**: 98–105.

Giovannini, M., Selleri, L., Biegel, J.A., Scotland, K., Emanuel, B.S., and Evans, G.A., 1992, Interphase cytogenetics for the detection of the t(11;22) (q24; q12) in small round cell tumors, *J. Clin. Invest.* **90**:1911–1918.

Giweraman, A., Hopman, A.H.L., Ramaekers, F.C.S., and Skakkeback, N.E., 1989, Detection of malignant cells in seminal fluid by means of *in situ* hybridization, *Am. J. Path.* **136**:497–504.

Goodfellow, P.N., and Lovell-Badge, R., 1993, SRY and sex determination in mammals, *Ann. Rev. Genet.* **27**:71–92.

Gosden, J., Hanratty, D., Starling, J., Fanter, J., Mitchell, A., and Porteous, D., 1991, Oligonucleotide-primed *in situ* DNA synthesis (PRINS): A method for chromosome mapping, banding, and investigation of sequence organization, *Cytogenet. Cell Genet.* **57**:100–104.

Gould, C.P., Waters, J.J., Mercer, A.M., Challinor, P.R., Hill, S.M., Johnson, R.A., Simpson, P.J., Delhanty, J., and Hulten, M.A., 1992, Limitations of whole chromosome FISH analysis in clinical cytogenetics: Failure of detection of translocated proterminal segments shorter than 2.5Mb, *Eur. Soc. Hum. Genet. Denmark* **78** (abstract).

Goulding, M.D., Chalepakis, G., Deutsch, U., Erselius, J., and Gruss, P., 1991, Pax-3, a novel murine DNA-binding protein expressed during early neurogenesis, *EMBO J.* **10**:1135–1147.

Greenberg, F., Elder, F.F.B., Haffner, P., Northrup, H., and Ledbetter, D., 1988, Cytogenetic findings in a prospective series of patients with DiGeorge anomaly, *Hum. Genet.* **43**:605–611.

Grierson, H.L., and Purtilo, D.T., 1987, Epstein–Barr virus infections in males with the X-linked lymphoproliferative syndrome, *Ann. Intern. Med.* **106**:538–545.

Griffin, D.K., Handyside, A.H., Penkth, R.J.A., Winston, R.M.L., and Delhanty, J.D.A., 1991, Fluorescent *in situ* hybridization to interphase nuclei of human preimplantation embryos with X and Y chromosome-specific probes, *Hum. Reprod.* **6**:101–105.

Griffin, D.K., Wilton, L.J., Handyside, A.H., Winston, R.M.L., and Delhanty, J.D.A., 1992, Dual fluorescent *in situ* hybridization for simultaneous detection of X and Y chromosome-specific probes for the sexing of human preimplantation embryonic nuclei, *Hum. Genet.* **89**:18–22.

Griffith-Jones, M.D., Miller, D., Lilford, R.J., and Scott, J., 1992, Detection of fetal DNA in

transcervical swabs from first trimester pregnancies by gene amplification: A new route to prenatal diagnosis? *Br. J. Obstet. Gynaecol.* **99:**508–511.

Grifo, J.A., 1992, Preconception and preimplantation genetic diagnosis: Polar body, blastomere and trophectoderm biopsy, in: *Micromanipulation of Human Gametes and Embryos* (J. Cohen, H.E. Malter, B.E. Talansky, and J. Grifo, eds.), pp. 223–249, Raven Press, New York.

Groffen, J., Stephenson, J.R., Heisterkamp, N., de Klein, A., Bartram, C.R., and Grosveld, G., 1984, Philadelphia chromosomal breakpoints are clustered within a limited region, bcr, on chromosome 22, *Cell* **36:**93–99.

Guan, X.-Y., Trent, J.M., and Meltzer, P.S., 1993, Generation of band-specific painting probes from a single microdissected chromosome, *Hum. Mol. Genet.* **2:**1117–1121.

Guttenbach, M., and Schmid, M., 1990, Determination of Y chromosome aneuploidy in human sperm nuclei by nonradioactive *in situ* hybridization, *Am. J. Hum. Genet.* **46:**553–558.

Haaf, T., Steinlein, C., and Schmid, M., 1990, Nucleolar transcriptional activity in mouse Sertoli cells is dependent on centromere arrangement, *Exp. Cell Res.* **191:**157–160.

Haaf, T., and Ward, D.C., 1994, High resolution ordering of YAC contigs using extended chromatin and chromosomes, *Hum. Mol. Genet.* **3:**629–633.

Haas, M., Aburatani, H., Stanton, V.P., Jr., Bhat, M., Housman, D., and Ward, D.C., 1993, Isolation and FISH mapping of 80 cosmid clones on the short arm of human chromosome 3, *Genomics* **16:**90–96.

Halford, S., Lindsay, E., Nayudu, M., Carey, A.H., Baldini, A., and Scambler, P.J., 1993, Low-copy-number repeat sequences flank the DiGeorge/velo-cardio-facial syndrome loci at 22q11, *Hum. Mol. Genet.* **2:**191–196.

Han, T.H., Ford, J.H., Flaherty, S.P., Webb, G.C., and Matthews, C.D., 1994, A fluorescent *in situ* hybridization analysis of the chromosome constitution of ejaculated sperm in a 46,XYY male, *Clin. Genet.* **45:**67–70.

Handyside, A.H., Kontogianni, E.H., Hardy, K., and Winston, R.M.L., 1990, Pregnancies from biopsied human preimplantation embryos sexed by Y-specific DNA amplification, *Nature* **344:**768–770.

Handyside, A.H., Pattison, J.K., Penketh, R.J.A., Delhanty, J.D.A., Winston, R.M.L., and Tuddenham, E.G.D., 1989, Biopsy of human preimplantation embryos and sexing by DNA amplification, *Lancet* **ii:**347–349.

Hecht, F., and Hecht, B.K., 1987, Aneuploidy in humans: Dimensions, demography, and dangers of abnormal numbers of chromosomes, in: *Aneuploidy (Part A: Incidence and Etiology)* (B.K. Vig, and A.A. Sandberg, eds.), pp. 9–49, Alan R. Liss, New York.

Heim, S., Billstrom, R., Kristoffersson, U., Maudahl, N., Strombeck, B., and Mitelman, F., 1985, Variant Ph^1 translocations in chronic myeloid leukemia, *Cancer Genet. Cytogenet.* **18:**215–227.

Heim, S., Mitelman, F., 1987, *Cancer Cytogenetics*, Alan R. Liss, New York, **VIII**, 309.

Heng, H.H.Q., Squire, J., and Tsui, L.-C., 1992, High resolution mapping of mammalian genes by *in situ* hybridization to free chromatin, *Proc. Natl. Acad. Sci. USA* **89:**9509–9513.

Hennig, W., 1985, Y chromosome function and spermatogenesis in *Drosophila hydei*, *Adv. Genet.* **23:**179–234.

Heppell-Parton, A.C., Albertson, D.G., Fishpool, R., and Rabbitts, P.H., 1994, Multicolour fluorescence *in situ* hybridization to order small, single-copy probes on metaphase chromosomes, *Cytogenet. Cell Genet.* **66:**42–47.

Herrington, C.S., and McGee, J.O'D., 1990, Interphase cytogenetics, *Neurochem. Res.* **15:**467–474.

Higgins, M.J., Wang, H., Shthromas, I., Haliotis, T., Roder, J.C., Holden, J.J.A., and White, B.N., 1985, Organization of a repetitive human 1.8 kb KpnI sequence localized in the heterochromatin of chromosome 15, *Chromosoma* **93:**77–86.

Hill, R.E., Ravor, J., Hogan, B.L., Ton, C.C., Saunders, G.F., Hanson, I.M., Prosser, J., Jordan, T., Hastie, N.D., and van Heyningen, V., 1991, Mouse small eye results from mutations in a paired-

like homeobox-containing gene [published erratum appears in Nature, 1992, 355:750], *Nature* **354:**522–525.

Hilliker, A.J., and Appels, R., 1989, The arrangement of interphase chromosomes: Structural and functional aspects, *Exp. Cell Res.* **185:**297–318.

Hoffman, E.P., Brown, R.H., and Kunkel, L.M., 1987, Dystrophin: The protein product of the Duchenne muscular dystrophy locus, *Cell* **51:**919–928.

Hopman, A.H.N., Ramaekers, F.C.S., Raap, A.K., Beck, J.L.M., Devilee, P., van der Ploeg, M., and Vooijs, G.P., 1988, *In situ* hybridization as a tool to study numerical chromosome aberrations in solid bladder tumors, *Histochem.* **89:**307–316.

Hopman, A.H.N., Ramaekers, F.C.S., and Vooijs, G.P., 1990, Interphase cytogenetics of solid tumors, in: *In situ Hybridization. Principles and Practice* (J.M. Polak and J.O'D. McGee, eds.), pp. 165–186, Oxford University Press, Oxford.

Hopman, A.H.N., Wiegant, J., Tesser, G.I., and Van Duijn, P., 1986a, A nonradioactive *in situ* hybridization method based on mercurated nucleic acid probes and sulfhydryl–hapten ligands, *Nucl. Acids Res.* **14:**6471–6488.

Hopman, A.H.N., Wiegant, J., and Van Duijn, P., 1986b, Mercurated probes, a new principle for nonradioactive *in situ* hybridization, *Exp. Cell Res.* **169:**357–368.

Hopman, A.H.N., Wiegant, J., and van Duijn, P., 1986c, A new hybridocytochemical method based on mercurated nucleic acid probes and sulphydryl-hapten ligands. II: Effects of variations in ligand structure on the *in situ* detection of mercurated probes, *Histochem.* **84:**179–185.

Hozier, J., Graham, R., Westfall, T., Sievert, P., and Davis, L., 1994, Preparative *in situ* hybridization: Selection of chromosome region-specific libraries on mitotic chromosomes, *Genomics* **19:** 441–447.

Hsu, L.Y.F., 1986, Prenatal diagnosis of chromosome abnormalities, in: *Genetic Disorders and the Fetus*, (A. Milunsky, ed.), pp. 115–183, Plenum Press, New York.

Hubert, J., and Bourgeois, C.A., 1986, The nuclear skeleton and the spatial arrangement of chromosomes in the interphase nucleus of vertebrate somatic cells, *Hum. Genet.* **74:**1–15.

Hulten, M.A., Gould, C.P., Goldman, A.S.H., and Waters, J.J., 1991, Chromosome *in situ* suppression hybridization in clinical cytogenetics, *J. Med. Genet.* **28:**577–582.

Imaizumi, K., and Kuroki, Y., 1991, Rubinstein–Taybi syndrome with *de novo* reciprocal translocation t(2;16) (p13.3; p13.3), *Am. J. Med. Genet.* **38:**636.

Imaizumi, K., Kurosawa, K., Masuno, M., Tsukuhara, M., and Kuroki, Y., 1993, Chromosome aberrations in Rubinstein–Taybi syndrome, *Clin. Genet.* **43:**215–216.

Inazawa, J., Ariyama, T., Tokino, T., Tanigami, A., Nakamura, Y., and Abe, T., 1994, High resolution ordering of DNA markers by multicolor fluorescent *in situ* hybridization of prophase chromosomes, *Cytogenet. Cell Genet.* **65:**130–135.

Inazawa, J., Saito, H., Ariyama, T., Abe, T., and Nakamura, Y., 1993, High-resolution cytogenetic mapping of 342 new cosmid markers including 43 RFLP markers on human chromosome 17 by fluorescence *in situ* hybridization, *Genomics* **17:**153–162.

Ishikiriyama, S., Tonoki, H., Shibuya, Y., Chin, S., Harada, N., Abe, K., and Niikawa, N., 1989, Waardenburg syndrome type I in a child with *de novo* inversion (2)(q35q37.3), *Am. J. Med. Genet.* **33:**505–507.

Jacobs, P.A., Buckton, K.E., Cunningham, C., and Newton, M., 1974, An analysis of the break points of structural rearrangements in man, *J. Med. Genet.* **11:**50–64.

Jacobs, P.A., Betts, P.R., Cockwell, A.E., Crolla, J.A., MacKenzie, M.J., Robinson, D.O., and Youngs, S.A., 1990, A cytogenetic and molecular reappraisal of a series of patients with Turner's syndrome, *Ann. Hum. Genet.* **54:**209–223.

Jauch, A., Wienberg, J., Stanyon, R., Arnold, N., Tofanelli, S., Ishida, T., and Cremer, T., 1992, Reconstruction of genomic rearrangements in great apes and gibbons by chromosome painting, *Proc. Natl. Acad. Sci. USA* **89:**8611–8615.

John, H.L., Birnstiel, M.L., and Jones, K.W., 1969, RNA–DNA hybrids at the cytological level, *Nature* **223:**912–913.

Johnson, D.H., Kroisel, P.M., Klapper, H.J., and Rosenkranz, W., 1992, Microdissection of a human marker chromosome reveals its origin and a new family of centromeric repetitive DNA, *Hum. Mol. Genet.* **1:**741–747.

Joos, S., Scherthan, H., Speicher, M.R., Schlegel, J., Cremer, T., and Lichter, P., 1993, Detection of amplified DNA sequences by reverse chromosome painting using genomic tumor DNA as probe, *Hum. Genet.* **90:**584–589.

Jorgensen, A.L., Jones, C., Bostock, C.J., and Bak, A.L., 1987, Different subfamilies of alphoid repetitive DNA are present on the human and chimpanzee homologous chromosomes 21 and 22, *EMBO J.* **6:**1691–1696.

Julien, C., Bazin, A., Guyot, B., Forestier, F., and Daffos, F., 1986, Rapid prenatal diagnosis of Down's syndrome with *in situ* hybridization of fluorescent DNA probes, *Lancet* **ii:**863–864.

Kadam, I., Umerani, A., Srivastava, A., Masterson, M., Lamptkin, B., and Raza, A., 1993, Combination of chemical and interphase cytogenetics to investigate the biology of meloid disorders: Detection of marked monosomy 7 in AML, *Leukemia Res.* **17:**365–374.

Kao, F.-T., 1987, Chromosome microdissection and microcloning in human molecular genetics, *Somat. Cell Mol. Genet.* **13:**374–380.

Kao, F.-T., and Yu, J.-W., 1991, Chromosome microdissection and cloning in human genome and genetic disease analysis, *Proc. Natl. Acad. Sci. USA* **88:**1844–1848.

Khalfan, H., Abuknesha, R., Rand-Weaver, M., Price, R.G., and Robinson, D., 1986, Aminomethyl coumarin acetic acid: A new fluorescent labeling agent for proteins, *Histochem. J.* **18:**497–499.

Kievits, T., Dauwerse, J.G., Wiegant, J., Devilee, P., Breuning, M.H., Cornelisse, C.J., van Ommen, G.J.B., and Pearson, P.L., 1990, Rapid subchromosomal localization of cosmids by nonradioactive *in situ* hybridization, *Cytogenet. Cell Genet.* **53:**134–136.

Kirkpatrick, S.J., Kent, C.M., Laxova, R., and Sekhon, G.S., 1992, Waardenburg syndrome type 1 in a child with deletion (2) (q35q36.2), *Am. J. Med. Genet.* **44:**699–700.

Klinger, K., Landes, G., Shook, D., Harvey, R., Lopez, L., Locke, P., Lerner, T., Osathanondh, R., Leverone, B., Houseal, T., Pavelka, K., and Dackowski, W., 1992, Rapid detection of chromosome aneuploidies in uncultured amniocytes by using fluorescence *in situ* hybridization (FISH), *Am. J. Hum. Genet.* **51:**55–65.

Koch, J., Hindkjaer, J., Mogensen, J., Kolvraa, S., and Bolund, L., 1991, An improved method for chromosome-labeling of α satellite DNA *in situ* by using denatured double-stranded DNA probes as primers in a primed *in situ* labeling (PRINS) procedure, *GATA* **8:**171–178.

Koch, J., Hobolt, N., Petersen, G.B., Willard, H.F., Waye, J.S., Gregersen, N., and Bolund, L., 1990, A case of 46,XX,r(X)(p1q1) diagnosed by *in situ* hybridization, *Clin. Genet.* **37:**216–220.

Koch, J.E., Kolvraa, S., Petersen, K.B., Gregersen, N., and Bolund, L., 1989, Oligonucleotide-priming methods for the chromosome-specific labeling of alpha-satellite DNA *in situ*, *Chromosoma* **98:**259–265.

Koch, J., Mogensen, J., Pedersen, S., Fisher, H., Hindkjaer, J., Kolvraa, S., Bolund, L., 1992, Fast one-step procedure for the detection of nucleic acids *in situ* by primer-induced sequence-specific labeling with fluorescein-12-dUTP, *Cytogenet. Cell Genet.* **60:**1–3.

Koenig, M., Beggs, A.H., Moyer, M., Scherpf, S., Heindrich, K., Bettecken, T., Meng, G., Muller, C.R., Lindlof, M., Kaariainen, H., de la Chapelle, A., Kiuru, A., Savontaus, M.-L., Gilgenkrantz, H., Recan, D., Chelly, J., Kaplan, J.-C., Covone, A.E., Archidiacono, N., Romeo, G., Lichti-Gallati, S., Schneider, V., Braga, S., Moser, H., Darras, B.T., Murphy, P., Francke, U., Chen, J.D., Morgan, G., Denton, M., Greenberg, C.R., Wrogemann, K., Blonden, L.A.J., van Paassen, H.M.B., van Ommen, G.J.B., and Kunkel, L.M., 1989, The molecular basis for Duchenne versus Beckler muscular dystrophy: Correlation of severity with type of deletion, *Am. J. Hum. Genet.* **45:**498–506.

Koopman, P., Gubbay, J., Vivian, N., Goodfellow, P., and Lovell-Badge, R., 1991, Male development of chromosomally female mice transgenic for *Sry*, *Nature* **351:**117–121.

Koopman, P., Münsterberg, A., Capel, B., Vivian, N., and Lovell-Badge, R., 1990, Expression of a candidate sex-determining gene during mouse testis differentiation, *Nature* **348:**450–452.

Kozma, R., and Adinolfi, M., 1987, *In situ* hybridization and the detection of biotinylated DNA probes, *Mol. Biol. Med.* **4:**357–364.

Kozma, R., and Adinolfi, M., 1988, *In situ* fluorescence hybridization of Y translocations: Cytogenetic analysis using probes Y190 and Y431, *Clin. Genet.* **33:**156–161.

Kozma, R., Fear, C., and Adinolfi, M., 1988, Fluorescence *in situ* hybridization and Y ring chromosomes, *Hum. Genet.* **80:**95–96.

Kuo, W.-L., Tenjin, H., Segreves, R., Pinkel, D., Golbus, M.S., and Gray, J., 1991, Detection of aneuploidy involving chromosomes 13, 18 or 21 by fluorescence *in situ* hybridization (FISH) to interphase and metaphase amniocytes, *Am. J. Hum. Genet.* **49:**112–119.

Kushnick, T., Irons, T.G., Wiley, J.E., Gettig, E.A., Rao, K.W., and Bowyer, S., 1987, 45X/46,r(X) with syndactyly and severe mental retardation, *Am. J. Med. Genet.* **28:**567–574.

Kuwano, A., Ledbetter, S.A., Dobyns, W.B., Emanuel, B.S., and Ledbetter, D.H., 1991, Detection of deletions and cryptic translocations in Miller–Dieker syndrome by *in situ* hybridization, *Am. J. Hum. Genet.* **49:**707–714.

Kuwano, A., Mutirangura, A., Dittrich, B., Buiting, K., Horsthemke, B., Saitoh, S., Niikawa, N., Ledbetter, S.A., Greenberg, F., Chinault, A.C., and Ledbetter, D.H., 1992, Molecular dissection of the Prader-Willi/Angelman syndrome region (15q-11) by YAC cloning and FISH analysis, *Hum. Mol. Genet.* **6:**417–425.

Lacombe, D., Saura, R., Taine, L., and Battin, J., 1992, Confirmation of assignment of a locus for Rubenstein–Taybi syndrome to 16p13.3, *Am. J. Med. Genet.* **44:**126–128.

Landegent, J.E., Jansen de Wal, N., Baan, R.A., Hoeijmakers, J.H.J., and Van der Ploeg, M., 1984, 2-acetylaminofluorene-modified probes for the indirect hybridochemical detection of specific nucleic acid sequences, *Exp. Cell Res.* **153:**61–72.

Landegent, J.E., Jansen in de Wal, N., Dirks, R.W., Baas, F., and Van der Ploeg, M., 1987, Use of whole cosmid cloned genomic sequences for chromosomal localization by nonradioactive *in situ* hybridization, *Hum. Genet.* **77:**366–370.

Langer, P.R., Waldrop, A.A., and Ward, D.C., 1981, Enzymatic synthesis of biotin-labeled polynucleotides: Novel nucleic acid affinity probes, *Proc. Natl. Acad. Sci. USA* **78:**6633–6637.

Lawrence, J.B., 1990, A fluorescence *in situ* hybridization approach for gene mapping and the study of nuclear organization, in: *Genome Analysis Volume 1: Genetic and Physical Mapping* (K.E. Davies and S.M. Tilghman, eds.), pp. 1–38, Cold Spring Harbor Laboratory Press, Cold Spring Harbor, New York.

Lawrence, J.B., Singer, R.H., and McNeil, J.A., 1990, Interphase and metaphase resolution of different distances within the human dystrophin gene, *Science* **249:**928–932.

Leana-Cox, J., Levin, S., Surana, R., Wulfsberg, E., Kenne, C.L., Raffel, L.J., Sullivan, B., and Schwartz, S., 1993, Characterization of *de novo* duplications in eight patients by using fluorescence *in situ* hybridization with chromosome-specific DNA libraries, *Am. J. Hum. Genet.* **52:**1067–1073.

Lebo, R.V., Lynch, E.D., Bird, T.D., Golbus, M.S., Barker, D.F., O'Connell, P., and Chance, P.F., 1992, Multicolor *in situ* hybridization and linkage analysis order Charcot-Marie-Tooth Type I (CMT1A) gene-region markers, *Am. J. Hum. Genet.* **50:**42–55.

Lebo, R.V., Lynch, E.D., Wiegant, J., Moore, K., Trousine, M., and van der Ploeg, M., 1991, Multicolor fluorescence *in situ* hybridization and pulsed–field electrophoresis dissect CMT1B gene region, *Hum. Genet.* **88:**13–20.

Ledbetter, D.H., 1992, The "colorizing" of cytogenetics: Is it ready for prime time? *Hum. Mol. Genet.* **1:**297–299.

Ledbetter, S.A., Wallace, M.R., Collins, F.S., and Ledbetter, D.H., 1990, Human chromosome 17 NotI linking clones and their use in long-range restriction mapping of the Miller–Dieker chromosome region (MDCR) in 17p13.3, *Genomics* **7:**264–269.

Leitch, A.R., Schwarzacher, T., Jackson, D., and Leitch, I.J., 1994, *In situ hybridization: A practical guide. Royal Microscopical Society Microscopy Handbook No. 27*, Bios Scientific Publishers Ltd., Oxford, England.

Lengauer, C., Speicher, M.R., Popp, S., Jauch, A., Taniwaki, M., Nagaraja, R., Riethman, H.C., Donis-Keller, H., D'Urso, M., Schlessinger, D., and Cremer, T., 1993, Chromosomal bar codes produced by multicolor fluorescence *in situ* hybridization with multiple YAC clones and whole chromosome painting probes, *Hum. Mol. Genet.* **2:**505–512.

Lewis, J.P., Tanke, H.J., Raap, A.K., Beverstock, G.C., and Kluin-Nelemans, H.C., 1993, Somatic pairing of centromeres and short arms of chromosome 15 in the hematopoietic and lymphoid system, *Hum. Genet.* **92:**577–582.

Lichter, L., Chang Tang, C.-J., Call, K., Lewis, K., Evans, G.A., Housman, D., and Ward, D.C., 1990, High-resolution mapping of human chromosome 11 by *in situ* hybridization with cosmid clones, *Science* **247:**64–69.

Lichter, P., Cremer, T., Borden, J., Manuelidis, L., and Ward, D.C., 1988, Delineation of individual chromosomes in metaphase and interphase cells by *in situ* suppression hybridization using recombinant DNA libraries, *Hum. Genet.* **80:**224–234.

Lichter, D., and Ward, D.C., 1990, Is nonisotopic *in situ* hybridization finally coming of age? *Nature* **342:**93–94.

Lindsay, E.A., Halford, S., Wadey, R., Scambler, P.J., and Baldini, A., 1993, Molecular cytogenetic characterization of the DiGeorge syndrome region using fluorescence *in situ* hybridization, *Genomics* **17:**403–407.

Lomax, B.L., Kalousek, D.K., Kuchinka, B.D., Barrett, I.J., Harrison, K.J., and Safavi, H., 1994, The utilization of interphasae cytogenetic analysis for the detection of mosaicism, *Hum. Genet.* **93:**243–247.

Looijenga, L.H.J., Smit, V.T.H.B.M., Wessels, J.W., Mollevanger, P., Oosterhuis, J.W., Cornelisse, C.J., and Devilee, P., 1990, Localization and polymorphism of a chromosome 12-specific α satellite DNA sequence, *Cytogenet. Cell Genet.* **53:**216–218.

Love, D.R., and Davies, K.E., 1989, Duchenne muscular dystrophy: The gene and the protein, *Mol. Biol. Med.* **6:**7–17.

Lovelace, R.E., and Shapiro, H.K. (eds.), 1990, *Charcot-Marie-Tooth disorders: Pathophysiology, molecular genetics, and therapy*, Wiley-Liss, New York.

Lüdecke H.-J., Senger, G., Claussen, U., and Horsthemke, B., 1989, Cloning of defined regions of the human genome by microdissection of banded chromosomes and enzymatic amplification, *Nature* **338:**348–350.

Lu-Kuo, J., Ward, D.C., and Spritz, R.A., 1993, Fluorescence *in situ* hybridization mapping of 25 markers on distal human chromosome 2q surrounding the human Waardenburg Syndrome, Type 1 (*WS1*) locus (*PAX3* gene), *Genomics* **16:**173–179.

Maccarone, P., Watson, J.M., Francis, D., Selwood, L., Kola, I., and Marshall Graves, J.A., 1992, The evolution of human chromosome 21: Evidence from *in situ* hybridization in marsupials and a monotreme, *Genomics* **13:**1119–1124.

Manning, J.E., Hershey, N.D., Brooker, T.R., Pellegrini, M., Mitchell, H.K., and Davidson, N., 1975, A new method of *in situ* hybridization, *Chromosoma* **53:**107–117.

Manuelidis, L., 1985, Individual interphase chromosome domains revealed by *in situ* hybridization, *Hum. Genet.* **71:**288–293.

Manuelidis, L., 1990, A view of interphase chromosomes, *Science* **250:**1533–1540.

Manuelidis, L., and Wu, J.C., 1978, Homology between human and simian repeated DNA, *Nature* **276:**92–94.

Mao, Y., and Cremer, M., 1989, Detection of Duchenne muscular dystrophy carriers by dosage analysis using the DMD cDNA clone 8, *Hum. Genet.* **81:**193–195.

Maraschio, P., Cuoco, C., Gimelli, G., Zuffardi, O., and Tiepolo, L., 1988, Origin and clinical significance of inv dup(15), in: *The Cytogenetics of Mammalian Autosomal Rearrangements* (H. Daniel, ed.), pp. 615–634, Alan R. Liss Inc., New York.

Markkanen, A., Heinonen, K., and Knuutila, S., 1982, Methotrexate-induced increase in gap formation in human chromosome band 3p14, *Hereditas* **96:**317–319.

Martin, R.H., Balkan, W., Burns, K., Rademaker, A.W., Lin, C.C., and Rudd, N.L., 1983, The chromosome constitution of 1000 human spermatozoa, *Hum. Genet.* **63:**305–309.

Martin, R.H., Lin, C.C., Balkan, W., and Burns, K., 1982, Direct chromosomal analysis of human spermatozoa: Preliminary results from 18 normal men, *Am. J. Hum. Genet.* **34:**459–468.

Martin, D., Tucker, D.F., Gorman, P., Sheer, D., Spurr, N.K., and Trowsdale, J., 1987, The human placental alkaline phosphatase gene and related sequences map to chromosome 2 band q37, *Ann. Hum. Genet.* **51:**145–152.

McDermid, H.E., Duncan, A.M.V., Higgins, M.J., Hammerston, J.L., Rector, E., Brasch, K.R., and White, B., 1986, Isolation and characterization of an alpha–satellite repeated sequence from human chromosome 22, *Chromosoma* **94:**228–234.

McKusick, V.A., 1986, The human gene map: The morbid anatomy of the human genome, *Clin. Genet.* **29:**545–588.

McKusick, V.A., 1992, *Mendelian inheritance in man* (tenth edition), The Johns Hopkins University Press, Baltimore, Maryland.

McKusick, V.A., and Neufeld, E.F., 1983, The mucopolysaccharide storage diseases, in: *The Metabolic Basis of Inherited Disease* (J.B. Stanbury, J.B. Wyngaarden, D.S. Fredrickson, J.L. Goldstein, and M.S. Brown, eds.), pp. 751–777, McGraw-Hill, New York.

McWilliam, P., Farrar, G.J., Kenna, P., Bradley, D.G., Humphries, D.G., Sharp, E.M., McConnell, D.J., Lawler, M., Sheits, D., Ryan, C., Stevens, K., Daiger, S.P., and Humphries, P., 1989, Autosomal dominant retinitis pigmentosa (ADRP): Localization of an ADRP gene to the long arm of chromosome 3, *Genomics* **5:**619–622.

Meltzer, P.S., Guan, X.-Y., and Trent, J.M., 1993, Telomere capture stabilizes chromosome breakage, *Nature Genet.* **4:**252–255.

Miller, R.W., Fraumeni, J.F., and Manning, M.D., 1964, Association of Wilms' tumor with aniridia, hemihypertrophy, and other congenital malformations, *N. Engl. J. Med.* **270:**922–927.

Mitchell, A.R., Gosden, J.R., and Miller, D.A., 1985, A cloned sequence, p82H, of the alphoid repeated DNA family found at the centromeres of all human chromosomes, *Chromosoma* **92:** 369–377.

Montanaro, V., Casamassimi, A., D'Urso, M., Yvon, J.-Y., Sazzone, S., Mangeri, S., Santoro, A.M., Molta, S., and delle Valle, G., 1991, *In situ* hybridization to cytogenetic bands of yeast artificial chromosome covering 50% of human Xq24–Xq28 DNA, *Am. J. Hum. Genet.* **48:**183–194.

Mooibroek, H., Ojinga, J., Postmus, P.E., Carritt, B., and Buys, C.H., 1987, Loss of heterozygosity for a chromosome 3 sequence presumably at 3p21 in a small cell lung cancer, *Cancer Genet. Cytogenet.* **27:**361–363.

Morell, R., and Friedman, T.B., Moeljopawiro, S., Hartono, Soewito, and Asher, J.H. Jr., 1992, A frameshift mutation in the HuP2 paired domain of the probable human homolog of murine Pax-3 is responsible for Waardenburg syndrome type 1 in an Indonesian family, *Hum. Molec. Genet.* **1:**243–247.

Mossman, J., Blunt, S., Stephens, R., Jones, E., and Pembrey, M., 1983, Hunter's disease in a girl: Association with X:5 chromosomal translocation disrupting the Hunter gene, *Arch. Dis. Child.* **58:**911–915.

Moyzis, R.K., Albright, K.L., Bartholdi, M.F., Cram, L.S., Deaven, L.L., Hildebrand, C.E., Joste, N.E., Longmire, J.L., Meyne, J., and Schwarzacher-Robinson, T., 1987, Human chromosome-

specific repetitive DNA sequences: Novel markers for genetic analysis, *Chromosoma* **95:** 375–386.

Müller, U., Lalande, M., Disteche, C.M., and Latt, S.A., 1986*a*, Construction, analysis, and application to 46,XY gonadal dysgenesis of a recombinant phage DNA library from flow-sorted human Y chromosomes, *Cytometry* **7:**418–424.

Müller, U., Lalande, M., Donlon, T., and Latt, S.A., 1986*b*, Moderately repeated DNA sequences specific for the short arm of the human Y chromosome are present in XX males and reduced in copy number in an XY female, *Nucl. Acids Res.* **14:**1325–1340.

Müller, U., Fontaine, D., Adinolfi, M., Fraccaro, M., and Lalande, M., 1989, Analysis of complex Y chromosome aberrations using a single DNA probe (Y367), *Cytogenet. Cell Genet.* **50:**161–164.

Munné, S., and Cohen, J., 1993, Unsuitability of multinucleated human blastomeres for preimplantation genetic diagnosis, *Hum. Reprod.* **8:**1120–1125.

Mutirangura, A., Greenberg, F., Butler, M.G., Malcolm, S., Nicholls, R.D., Chakravarti, A., and Ledbetter, D.H., 1993, Multiplex PCR of 3 dinucleotide repeats in the Prader-Willi-Angelman critical region (15q11-q13)—molecular diagnosis and mechanism of uniparental disomy, *Hum. Mol. Genet.* **2:**143–151.

Nakamura, Y., Lathrop, M., O'Connell, P., Leppert, M., Barker, D., Wright, E., Skolnick, M., Kondoleon, S., Litt, M., Lalouel, J.-M., and White, R., 1988, A mapped set of DNA markers for human chromosome 17, *Genomics* **2:**302–307.

Naylor, S.L., Johnson, B.E., Minna, J.D., and Sakaguchi, A.Y., 1987, Loss of heterozygosity of chromosome 3p markers in small cell lung cancer, *Nature* **329:**451–454.

Nederlof, P.M., Robinson, D., Abuknesha, R., Wiegant, J., Hopman, A.H.N., Tanke, H.J., and Rappe, A.K., 1989, Three-color fluorescence *in situ* hybridization for the simultaneous detection of multiple nucleic acid sequences, *Cytometry* **10:**20–27.

Nederlof, P.M., van der Flier, S., Wiegant, J., Raap, A.K., Tanke, H.J., Ploem, J.S., and van der Ploeg, M., 1990, Multiple fluorescence *in situ* hybridization, *Cytometry* **11:**126–131.

Nowell, P.C., and Hungerford, D.A., 1960, A minute chromosome in human chronic granulocytic leukemia, *Science* **132:**1497.

Ohno, S., 1973, Ancient linkage groups and frozen accidents, *Nature* **244:**259–262.

Ohta, T., Tohma, T., Soejima, H., Fukushima, Y., Nagai, T., Yoshiura, K., Jinno, Y., and Niikawa, N., 1993, The origin of cytologically unidentifiable chromosome abnormalities: Six cases ascertained by targeted chromosome-band painting, *Hum. Genet.* **92:**1–5.

Ozcelik, T., Leff, S., Robinson, W., Donlon, T., Lalande, M., Sanjines, E., Schinzel, A., and Francke, U., 1992, Small nuclear ribonucleoprotein polypeptide N(SNRPN), an expressed gene in the Prader–Willi syndrome critical region, *Nature Genet.* **2:**265–269.

Parra, I., and Windle, B., 1993, High resolution visual mapping of stretched DNA by fluorescent hybridization, *Nature Genet.* **5:**17–21.

Partington, M.W., 1964, Waardenburg's syndrome and heterochromia iridium in a deaf school population, *Can. Med. Ass. J.* **90:**1008–1017.

Patel, P.I., 1993, Charcot-Marie-Tooth disease type 1A: Mutational mechanisms and candidate gene, *Curr. Opin. Genet. Devel.* **3:**438–444.

Patterson, D., 1991, Report of the second international workshop on human chromosome 21 mapping, *Cytogenet. Cell Genet.* **57:**167–174.

Penketh, R.J.A., Delhanty, J.D.A., van den Berghe, J.A., Finkelstone, E.M., Handyside, A.H., Malcolm, S., and Winston, R.M.L., 1989, Rapid sexing of human embryos by nonradioactive *in situ* hybridization: Potential for preimplantation diagnosis of X-linked disorders, *Prenat. Diagn.* **9:**489–500.

Pinkel, D., Landegent, J., Collins, C., Fuscoe, J., Segraves, R., Lukas, J., and Gray, J., 1988, Fluorescence *in situ* hybridization with human chromosome-specific libraries: Detection of trisomy 21 and translocations of chromosome 4, *Proc. Natl. Acad. Sci. USA* **85:**9138–9142.

Pinkel, D., Straume, T., and Gray, J.W., 1986, Cytogenetic analysis using quantitative, high sensitivity, fluorescence hybridization, *Proc. Natl. Acad. Sci. USA* **83:**2934–2938.

Plattner, R., Heerema, N.A., Howard-Peebles, P.N., Miles, J.H., Soukup, S., and Palmer, C.G., 1993b, Clinical findings in patients with marker chromosomes identified by fluorescence *in situ* hybridization, *Hum. Genet.* **91:**589–598.

Plattner, R., Heerema, N.A., Yurov, Y.B., and Palmer, C.G., 1993a, Efficient identification of marker chromosomes in 27 patients by stepwise hybridization with alpha-satellite DNA probes, *Hum. Genet.* **91:**131–140.

Poddighe, P.J., Ramaekers, F.C.S., and Hopman, A.H.N., 1992, Interphase cytogenetics of tumors, *J. Pathol.* **166:**215–224.

Polak, J.M., and McGee, J.O'D., (eds.), 1990, *In situ Hybridization. Principles and Practice*. Oxford University Press, Oxford, England.

Prior, T.W., Papp, A.C., Snyder, P.J., Highsmith, W.E., Friedmann, K.J., Perry, T.R., Silverman, L.M., and Mendell, J.R., 1990, Determination of carrier status in Duchenne and Becker muscular dystrophies by quantitative polymerase chain reaction and allele-specific oligonucleotides, *Clin. Chem.* **36:**2113–2117.

Rack, K.A., Harris, P.C., MacCarthy,. A.B., Boone, R., Raynham, H., McKinley, M., Fitchett, M., Towe, C.M., Rudd, P., Armour, J.A.L., Lindenbaum, R.H., and Buckle, V.J., 1993, Characterization of three *de novo* derivative chromosomes 16 by "reverse chromosome painting" and molecular analysis, *Am. J. Hum. Genet.* **52:**987–997.

Rauch, A., Pfeiffer, R.A., Trautmann, U., Liehr, T., Rott, H.D., and Ulmer, R., 1992, A study of ten small supernumerary (marker) chromosomes identified by fluorescence *in situ* hybridization (FISH), *Clin. Genet.* **42:**84–90.

Rhine, S.A., Palmer, C.G., and Thompson, J.F., 1977, A simple alternative to amniocentesis for first trimester prenatal diagnosis, *Birth Defects Original Article Series* **XII:**231–247.

Ried, T., Baldini, A., Rand, T.C., and Ward, D.C., 1992, Simultaneous visualization of seven different DNA probes by *in situ* hybridization using combinatorial fluorescence and digital imaging microscopy, *Proc. Natl. Acad. Sci. USA* **89:**1388–1392.

Ried, T., Mahler, V., Vogt, P., Blonden, L., van Ommen, G.J.B., Cremer, T., and Cremer, M., 1990, Direct carrier detection by *in situ* suppression hybridization with cosmid clones of the Duchenne/Becker muscular dystrophy locus, *Hum. Genet.* **85:**581–586.

Roberts, R.G., Bentley, D.R., Barby, T.G., Manners, E.M., and Bobrow, M., 1990a, Direct diagnosis of carriers of Duchenne and Becker muscular dystrophy by amplification of lymphocyte RNA, *Lancet* **336:**1523–1526.

Roberts, C., Lutjen, J., Krzyminska, U., and O'Neill, C., 1990b, Cytogenetic analysis of biopsied preimplantation mouse embryos: Implications for prenatal diagnosis, *Hum. Reprod.* **5:**197–202.

Robinson, W.P., Wagstaff, J., Bernasconi, F., Baccichetti, C., Artifoni, L., Franzoni, E., Suslak, L., Shih, L.Y., Aviv, H., and Schinzel, A.A., 1993a, Uniparental disomy explains the occurrence of the Angelman or Prader–Willi syndrome in patients with an additional small inv dup(15) chromosome, *J. Med. Genet.* **30:**756–760.

Robinson, W.P., Binkert, F., Gine, R., Vazquez, C., Muller, W., Rosenkranz, W., and Schinzel, A., 1993b, Clinical and molecular analysis of five inv dup(15) patients, *Eur. J. Hum. Genet.* **1:**37–50.

Rowley, J.D., 1973, A new chromosomal abnormality in chronic myelogenous leukemia identified by quinacrine fluorescence and Giemsa staining, *Nature* **423:**290–292.

Rowley, J.D., 1984, Biological implications of consistent chromosome rearrangements in leukemia and lymphoma, *Cancer Res.* **44:**3159–3168.

Rowley, J.D., 1988, Chromosome abnormalities in leukemia, *J. Clin. Oncol.* **6:**194–202.

Ruffe, J., and Colombier, P., 1970, Etude cytogenetique de 4 especes de primates. Comparison avec le caryotype humain, *Anal. Génét.* **13:**3–10.

Saito, S., Okui, K., Tokino, T., Oshimura, M., and Nakamura, Y., 1992, Isolation and mapping of 68 RFLP markers on human chromosome 6, *Am. J. Hum. Genet.* **50:**65–70.

Sandberg, A.A., Turc-Carel, C., and Gemmill, R.M., 1988, Chromosomes in solid tumors and beyond, *Cancer Res.* **48:**1049–1059.

Sanger, W., Grierson, H., Scare, J., Wyandt, H., Pirrucello, S., Fordyce, R., and Purtilo, D., 1990, Partial Xq25 deletion in a patient with X-linked lymphoproliferative disease (XLP), *Cancer Genet. Cytogenet.* **47:**163–169.

Scambler, P.J., 1993, Deletions of human chromosome 22 and associated birth defects, *Curr. Opin. Genet. Devel.* **3:**432–437.

Scambler, P.J., Carey, A.H., Wyse, R.K.H., Roach, S., Dumanski, J.P., Nordenskjold, M., and Williamson, R., 1991, Microdeletions within 22q11 associated with sporadic and familial DiGeorge syndrome, *Genomics* **10:**201–206.

Schinzel, A., 1984, *Catalogue of unbalanced chromosome aberrations in man*, Walter de Gruyter, Berlin, Germany.

Schinzel, A., Schmid, W., Fraccaro, M., Tiepolo, L., Zuffardi, O., Opitz, J.M., Lindsten, J., Zetterqvist, P., Enell, H., Baccichetti, C., Tenconi, R., and Pagon, R.A., 1981, The "Cat Eye syndrome": Dicentric small marker chromosome probably derived from a no. 22 (tetrasomy 22pter→q11) associated with a characteristic phenotype, *Hum. Genet.* **57:**148–158.

Schwartz, S., 1993, Efficacy and applicability of interphase fluorescence *in situ* hybridization for prenatal diagnosis (invited editorial), *Am. J. Hum. Genet.* **52:**851–853.

Schwartz, D.C., and Cantor, C.R., 1984, Separation of yeast chromosome-sized DNAs by pulse field gradient gel electrophoresis, *Cell* **37:**67–75.

Schwartz, C.E., Johnson, J.P., Holycross, B., Mandeville, T.M., Sears, T.S., Graul, E.A., Carey, J.C., Schroer, R.J., Phelan, M.C., Szollar, J., Flannery, D.B., and Stevenson, R.E., 1988, Detection of submicroscopic deletions in band 17p13 in patients with Miller–Dieker syndrome, *Am. J. Hum. Genet.* **43:**597–604.

Schweizer, D., Ambros, P., and Andrle, M., 1978, Modifications of DAPI banding on human chromosomes by prestaining with a DNA-banding oligopeptide antibiotic, distamycin A, *Exp. Cell Res.* **III:**327–332.

Seizinger, B.R., Rouleau, G.A., Ozelius, L.J., Lane, A.H., Farmer, G.E., Lamiell, J.M., Haines, J., Yuen, J.W.M., Clooins, D., Majoor–Krakauer, D., Bonner, T., Mathew, C., Rubenstein, A., Halpern, J., McConkie–Rosell, A., Green, J.S., Trofatter, J.A., Ponder, B.A., Eierman, L., Bowmer, M.I., Schimke, R., Oostra, B., Aronin, N., Smith, D.I., Drabkin, H., Waziri, M.H., Hobbs, W.J., Martuza, R.L., Conneally, P.M., Hsia, Y.E., and Gusella, J.F., 1988, von Hippel–Lindau disease maps to the region of chromosome 3 associated with renal cell carcinoma, *Nature* **332:**268–269.

Selleri, L., Hermanson, G.G., Eubanks, J.H., and Evans, J.A., 1991a, Chromosomal *in situ* hybridization using artificial chromosomes, *Genet. Anal. Techniq. Applic.* **8:**59–66.

Selleri, L., Hermanson, G.G., Eubanks, K.A., and Evans, G.A., 1991b, Molecular localisation of the t(11;22)(q24; q12) translocation of Ewing's sarcoma by chromosomal *in situ* suppressor hybridization, *Proc. Natl. Acad. Sci. USA* **88:**887–891.

Senger, G., Lüdecke, H.-G., Horsthemke, B., and Claussen, U., 1990, Microdissection of banded human chromosomes, *Hum. Genet.* **84:**507–511.

Seuanez, H.N., 1979, *The Phylogeny of Human Chromosomes*, Springer, New York.

Sharp, C.B., Bedford, H.M., and Willard, H.F., 1990, Pericentromeric structure of human X "isochromosomes": Evidence for molecular heterogeneity, *Hum. Genet.* **85:**330–336.

Sherlock, J., 1993, Homology of human and marmoset karyotypes. BSc thesis, University of London, England.

Shettles, L.B., 1971, Use of the Y chromosome in prenatal sex determination, *Nature* **230:**52.

Shtivelman, E., Gale, R.P., Dreazen, O., Berrebi, A., Zaizov, R., Kuboniski, I., Miyoshi, I., and Canaan, E., 1987, ber-abl RNA in patients with chronic myelogenous leukemia, *Blood* **69:** 971–973.

Sinclair, A.H., Berta, P., Palmer, M.S., Hawkins, J.R., Griffiths, B.L., Smith, M.J., Foster, J.W.,

Frischauf, A.-M., Lovell–Badge, R., and Goodfellow, P.N., 1990, A gene for the human sex-determining region encodes a protein with homology to a conserved DNA-banding motif, *Nature* **346:**240–244.

Singer, R.H., Lawrence, J.B., Langevin, G.L., Rashtchian, R.N., Villnave, C.A., Cremer, T., Tesin, D., Manuelidis, L., and Ward, D.C., 1987, Double labeling *in situ* hybridization using non-isotopic and isotopic detection, *Acta Histochem. Cytochem.* **20:**589–999.

Skare, J., Grierson, H., Sullivan, J., Nussbaum, R., Purtilo, D., Sylla, B., Lenoir, G., Reilly, D., White, B., and Milunsky, A., 1989a, Linkage analysis of seven kindreds with the X-linked lymphoproliferative syndrome (XLP) confirms that the XLP locus is near DXS42 and DXS37, *Hum. Genet.* **82:**354–358.

Skare, J., Sullivan, J., and Milunsky, A., 1989b, Mapping the mutation causing the X-linked lymphoproliferative syndrome in relation to restriction fragment length polymorphisms on Xq, *Hum. Genet.* **82:**349–353.

Skare, J., Wu, B.-L., Madan, S., Pulijaal, V., Purtilo, D., Haber, D., Nelson, D., Sylla, B., Grierson, H., Nitowsky, H., Glaser, J., Wissink, J., White, B., Holden, J., Housman, D., Lenoir, G., Wyandt, H., and Milunsky, A., 1993, Characterization of three overlapping deletions causing X-linked lymphoproliferative disease, *Genomics* **16:**254–255.

Skre, H., 1974, Genetic and clinical aspects of Charcot-Marie-Tooth disease, *Clin. Genet.* **6:**98–118.

Smeets, D., Scheres, J., and Justin, T., 1986, The most common fragile site in man is 3p14, *Hum. Genet.* **74:**330.

Spranger, J., 1984, The mucopolysaccharidoses, in: *Principles and Practice of Medical Genetics* (A.H. Emery and D.L. Rimoin, eds.), pp. 1339–1347, Churchill Livingstone, Edinburgh, Scotland.

Stephens, J.C., Cavanaugh, M.L., Gradie, M.I., Mador, M.L., and Kidd, K.K., 1990, Mapping the human genome: Current status, *Science* **250:**237–244.

Stone, S., and Adinolfi, M., 1992, Carrier detection of deletions of the Hunter gene by *in situ* hybridization, *Ann. Hum. Genet.* **56:**93–97.

Sullivan, J.L., Byron, K.S., Brewiter, P.E., Baker, S.M., and Ochs, H.D., 1983, X–linked lympho-proliferative syndrome, *J. Clin. Invest.* **71:**1765–1778.

Takahashi, E., Yamakawa, K., Nakamura, Y., and Hori, T., 1992, A high-resolution cytogenetic map of human chromosome 3: Localization of 291 new cosmid markers by direct R-banding fluorescence *in situ* hybridization, *Genomics* **13:**1047–1055.

Tassabehji, M., Read, A.P., Newton, V.E., Harris, R., Balling, R., Gruss, P., and Strachan, T., 1992, Waardenburg syndrome patients have mutations in the human homologue of the Pax-3 paired box gene, *Nature* **355:**635–636.

Taylor, C.P.F., McGuckin, A.G., Bown, N.P., Reid, M.M., Malcolm, A.J., Pearson, A.D.J., and Sheer, D., 1994, Rapid detection of prognostic genetic factors in neuroblastoma using fluorescence *in situ* hybridization on tumor imprints and bone marrow smears, *Br. J. Cancer* **69:**445–451.

Tchen, P., Fuchs, R.P.P., and Sage, E., 1984, Chemically modified nucleic acids as immunodetectable probes in hybridization experiments, *Proc. Natl. Acad. Sci. USA* **81:**3466–3470.

Telenius, H., Carter, N.P., Bebb, C.E., Nordenskjold, M., Ponder, B.A.J., and Tunnacliffe, A., 1992, Degenerate oligonucleotide-primed PCR: General amplification of target DNA by a single degenerate primer, *Genomics* **13:**718–725.

Teyssier, J.R., 1989, The chromosomal analysis of human solid tumors. A triple challenge, *Cancer Genet. Cytogenet.* **37:**103–125.

Tiepolo, L., and Zuffardi, O., 1976, Localization of the factors controlling spermatogenesis in the nonfluorescent portion of the human Y chromosome long arm, *Hum. Genet.* **34:**119–124.

Tkachuk, D.C., Westbrook, C.A., Andreeff, M., Donlon, T.A., Cleary, M.L., Suryanarayan, K., Homge, M., Redner, A., Gray, J., and Pinkel, D., 1990, Detection of bcr-abl fusion in chronic myelogenous leukemia by *in situ* hybridization, *Science* **250:**559–562.

Tocharoentanaphol, C., Cremer, M., Schrock, E., Blonden, L., Kilian, K., Cremer, T., and Ried, T.,

1994, Multicolor fluorescence *in situ* hybridization on metaphase chromosomes and interphase Halo-preparations using cosmid and YAC clones for the simultaneous high resolution mapping of deletions in the dystrophin gene, *Hum. Genet.* **93:**229–235.

Tommerup, N., Van der Hagen, C.B., and Heiberg, A., 1992, Tentative assignment of a locus for Rubinstein–Taybi syndrome to 16p13.3 by a *de novo* reciprocal translocation, t(7;16)(q34; p13.3), *Am. J. Med. Genet.* **44:**237–241.

Ton, C.T., Hirvonen, H., Miwa, H., Weil, M.M., Monaghan, P., Jordan, T., van Heyningen, V., Hastie, N.D., Meijers-Heijboer, H., Drechsler, M., Royer-Pokora, B., Collins, F., Swaroop, A., Strong, L.C., and Saunders, G.F., 1991, Positional cloning and characterization of a paired box- and homeobox-containing gene from the aniridia region, *Cell* **67:**1059–1074.

Tory, K., Brauch, H., Linehan, M., Barba, D., Oldfield, E., Filling-Katz, M., Seizinger, B., Nakamura, Y., White, R., and Marshall, F.F., 1989, Specific genetic change in tumors associated with von Hippel–Lindau disease, *J. Natl. Cancer Inst.* **81:**1097–1101.

Trask, B.J., 1991, Fluorescence *in situ* hybridization: Application in cytogenetics and gene mapping, *Trends in Genet.* **7:**149–154.

Trask, B.J., Massa, H., Kenwrick, S., and Gitschier, J., 1991, Mapping of human chromosome Xq28 by two–color fluorescence *in situ* hybridization of DNA sequences in interphase cell nuclei, *Am. J. Hum. Genet.* **48:**1–15.

Trask, B., Pinkel, D., and van den Engh, G., 1989, The proximity of DNA sequences in interphase cell nuclei is correlated to genomic distance and permits ordering of cosmids spanning 250 Kb pairs, *Genomics* **5:**710–717.

Triche, J.J., and Cavazzana, A.O., 1989, Pathology in pediatric oncology, in: *Principles and Practice of Paediatric Oncology* (P.A. Pizzo and G. Pophack, eds.), pp. 93–125, JB Lippincott Co., Philadelphia.

Tsukada, S., Saffran, D.C., Rawlings, D.I., Parolini, O., Allen, R.C., Klisak, I., Sparkes, R.S., Kubagawa, H., Mohandas, T., Quan, S., Belmont, J.W., Cooper, M.D., Conley, M.E., and Witte, O.N., 1993, Deficient expression of a B cell cytoplasmic tyrosine kinase in human X-linked agammaglobulinemia, *Cell* **72:**279–290.

Upadhyaya, M., Sarfarazi, M., and Bamforth, J.S., 1986, Localization of the gene for Hunter syndrome on the long arm of the X chromosome, *Hum. Genet.* **74:**391–398.

Urioste, M., Visedo, G., Sanchis, A., Sentis, C., Villa, A., Ludena, P., Hortiguela, J.L., Martinezfrias, M.L., and Fernandezpiqueras, J., 1994, Dynamic mosaicism involving in unstable supernumerary der(22) chromosome in Cat Eye syndrome, *Am. J. Med. Genet.* **49:**77–82.

van Heyningen, V., and Hastie, N.D., 1992, Wilms' tumor: reconciling genetics and biology, *Trends in Genetics* **8:**16–21.

Vance, J.M., Nicholson, G.A., Yamaoka, L.H., Stajich, J., Stewart, C.S., Speer, M.C., Hung, W.Y., Roses, A.O., Barker, D., and Pericak-Vance, M.A., 1989, Linkage of Charcot-Marie-Tooth Neuropathy Type 1a to chromosome 17, *Exp. Neurol.* **104:**186–189.

Verma, R.S., and Luke, S., 1992, Variations in alphoid DNA sequences escape detection of aneuploidy at interphase by FISH technique, *Genomics* **14:**113–116.

Vetrie, D., Vorechovsky, I., Sideras, P., Holland, J., Davies, A., Flinter, F., Hammarstrom, L., Kinnon, C., Levinsky, R., Bobrow, M., Smith, C.I.E., and Bentley, D.R., 1993, The gene involved in X-linked agammaglobulinaemia is a member of the src family of protein-tyrosine kinases, *Nature* **361:**226–233.

Vogt, P., Keil, R., Köhler, M., Lengauer, C., Lewe, D., and Lewe, G., 1991, Selection of DNA sequences from interval 6 of the human Y chromosome with homology to a Y chromosomal fertility gene sequence of *Drosophila hydei*, *Hum. Genet.* **86:**341–349.

Von Hemel, J.O., Eussen, B., Wasby-van Swaay, E., and Oostra, B.A., 1992, Molecular detection of a translocation (Y;11) (q11.2; q24) in a 45,X male with signs of Jacobsen syndrome, *Hum. Genet.* **88:**661–667.

Vooijs, M., Yu, L.-C., Tkakuch, D., Pinkel, D., Johnson, D., and Gray, J.W., 1993, Libraries for each human chromosome, constructed from sorter-enriched chromosomes by using linker-adaptor PCR, *Am. J. Hum. Genet.* **52:**586–597.

Waardenburg, P.J., 1951, A new syndrome combining developmental abnormalities of the eyelids, eyebrows and nose root with pigmentary defects of the iris and head hair and with congenital deafness, *Am. J. Hum. Genet.* **3:**195–253.

Wapenaar, M.C., Kievits, T., Hart, K.A., Abbs, S., Blonden, L.A.J., Den Dunnen, J.T., Grootscholten, P.M., Bakker, E., Verellen-Dumoulin, C., Bobrow, M., Van Ommen, G.J.B., and Pearson, P.L., 1988, A deletion hot spot in the Duchenne muscular dystrophy gene, *Genomics* **2:**101–108.

Warburton, D., 1991, *De novo* balanced chromosome rearrangements and extra marker chromosomes identified at prenatal diagnosis: Clinical significance and distribution of breakpoints, *Am. J. Hum. Genet.* **49:**995–1013.

Ward, B.E., Gersen, S.L., Carelli, M.P., McGuire, N.M., Dackowski, W.R., Weinstein, M., Sandlin, C., Warren, R., and Klinger, K., 1993, Rapid prenatal diagnosis of chromosomal aneuploidies by fluorescence *in situ* hybridization: Clinical experience with 4,500 specimens, *Am. J. Hum. Genet.* **52:**854–865.

Ward, B.E., Gersen, S.L., and Klinger, K.W., 1992, A rapid (and wrong) prenatal diagnosis: Integrated genetics replies, *N. Engl. J. Med.* **320:**1639.

Weier, H.-U., and Gray, J.W., 1992, A degenerate alpha satellite probe, detecting a centromeric deletion on chromosome 21 in an apparently normal human male, shows limitations of the use of satellite DNA probes for interphase ploidy analysis, *Anal. Cellular Path.* **4:**81–86.

Wiegant, J., Kalle, W., Mullenders, L., Brookes, S., Hoovers, J.M.N., Dauwerse, J.G., Van Ommen, G.J.B., and Raap, A.K., 1992, High-resolution *in situ* hybridization using halo preparations, *Hum. Mol. Genet.* **1:**587–591.

Wiegant, J., Wiesjeijer, C.C., Hoovers, J.M.N., Schuuring, E., D'Azzo, A., Vrolijk, J., Tanke, H.J., and Raap, A.K., 1993, Multiple and sensitive fluorescence *in situ* hybridization with rhodamine-fluorescein-, and coumarin-labeled DNAs, *Cytogenet. Cell Genet.* **63:**73–76.

Wienberg, J., Jauch, A., Stanyon, R., and Cremer, T., 1990, Molecular cytotaxonomy of primates by chromosomal *in situ* suppression hybridization, *Genomics* **8:**347–350.

Willard, H.F., 1985, Chromosome-specific organization of human alpha satellite DNA, *Am. J. Hum. Genet.* **37:**524–532.

Willard, H.F., 1990, Molecular cytogenetics of centromeres of human chromosomes, *Chromosomes Today* **10:**47–60.

Willard, H.F., 1992, Centromeres-primary constrictions are primarily complicated, *Hum. Mol. Genet.* **1:**667–668.

Willard, H.F., and Waye, J.S., 1987, Hierarchical order in chromosome-specific human alpha satellite DNA, *Trends in Genetics* **3:**192–198.

Winston, N.J., Braude, P.R., Pickering, S.J., George, M.A., Cant, A., Currie, J., and Johnson, M.H., 1991, The incidence of abnormal morphology and nucleocytoplasmic ratios in 2-, 3- and 5-day human pre-embryos, *Hum. Reprod.* **6:**17–24.

Wu, B.-L., Milunsky, A., Nelson, D., Schmeckpeper, B., Porta, G., Schlessinger, D., and Skare, J., 1993, High-resolution mapping of probes near the X-linked lymphoproliferative disease (XLP) locus, *Genomics* **17:**163–170.

Wyandt, H., Grierson, H., Sanger, W., Skare, J.C., Milunsky, A., and Purtilo, D.J., 1989, Chromosome deletion of Xq25 in an individual with X-linked lymphoproliferative disease, *Am. J. Med. Genet.* **33:**426–430.

Yagel, M.K., Parruti, G., Xu, W., Ponder, B.A.J., and Solomon, E., 1990, Genetic and physical map of the von Recklinghausen neurofibromatosis (NF1) region on chromosome 17, *Proc. Natl. Acad. Sci. USA* **87:**7255–7259.

Yamakawa, K., Morita, R., Takahashi, E., Hori, T., Lathrob, M., and Nakamura, Y., 1991*b*, A genetic linkage map of 41 restriction fragment length polymorphism markers for human chromosome 3, *Genomics* **11**:565–572.

Yamakawa, K., Takahashi, E., Saito, H., Sato, T., Oshimura, M., Hori, T., and Nakamura, Y., 1991*a*, Isolation and mapping of 75 new DNA markers on human chromosome 3, *Genomics* **9**:536–548.

Yunis, J., 1984, Recurrent chromosomal defects are found in most patients with acute nonlymphocytic leukemia, *Cancer Genet. Cytogenet.* **11**:125–137.

Yunis, J.J., Jones, C., Madden, M.T., Lu, D., and Mayer, M.G., 1989, Gene order, amplification, and rearrangement of chromosome band 11q23 in hematologic malignancies, *Genomics* **5**:84–90.

Yunis, J.J., and Prakash, O., 1982, The origin of man: A chromosomal pictorial legacy, *Science* **215**:1525–1530.

Yunis, J.J., and Tanzer, J., 1993, Molecular mechanisms of hematologic malignancies, *Crit. Rev. Oncogen.* **4**:161–190.

Zhang, J., Meltzer, P., Jenkins, R., Guan, X.Y., and Trent, J., 1993, Application of chromosome microdissection probes for elucidation of BCR-ABL fusion and variant Philadelphia chromosome translocations in chronic myelogenous leukemia, *Blood* **12**:3365–3371.

Zheng, Y.-L., Carter N.P., Price, C.M., Colman, S.M., Milton, P.J., Hackett, G.A., Greaves, M.F., and Ferguson–Smith, M.A., 1993, Prenatal diagnosis from maternal blood: Simultaneous immunophenotyping and FISH of fetal nucleated erythrocytes isolated by negative magnetic cell sorting, *J. Med. Genet.* **30**:1051–1056.

Zheng, Y.–L., Ferguson–Smith, M.A., Warner, J.P., Ferguson–Smith, M.E., Sargent, C.A., Carter, N.P., 1992, Analysis of chromosome 21 copy number in uncultured amniocytes by fluorescence *in situ* hybridization using a cosmid contig, *Prenat. Diagn.* **12**:931–943.

Index

Abdominal aortic aneurysm, 172
Acridine orange, 59, 91
Acute myeloblastic leukemia (AML), 230–231
Acute myeloid leukemia, 101
Agouti (*a*) gene, 6, 32–33
Albinism, 8; *see also* Ocular albinism; Oculocutaneous albinism
Alkaline phosphatase, 68
Alkaline phosphatase gene: *see* ALPP gene
ALPI gene, 205
Alport's syndrome, 154
ALPP gene, 205
Alveolar rhabdomyosarcoma, 29
Amethopterin, 52
Amniotic cells, chromosomal abnormalities in, 218–220
Aneuploidies, 218, 220
Angelman syndrome (AS), 16, 199, 203, 208–209
Aniridia, 208
Annuloaortic ectasia, 180
Aortic dilation, 169–172
Associated microfibrial protein (AMP), 159
Autosomal dominant oculocutaneous albinism (OCA), 15
Autosomal inherited disorders, deletions in, 204–209
Autosomal recessive ocular albinism (AROA), 18, 20
Azoospermic factor, 216–217

BAB technique: *see* BrdUrd antibody-binding technique
BCEI gene, 233
B cell chronic lymphocytic leukemia (B-CLL), 230
BCR gene, 229
Beaded fibrils, 166
Becker muscular dystrophy (BMD), 209–211
Beta-adrenergic blockers, 172
Black light irradiation, 64, 67, 68
Blacks, OCA type II in, 16–18
BrdUrd, 47–50, 52, 83–84
  condensation delay and, 83, 88–89, 90
  detection of: *see* BrdUrd antibody-binding technique; Fluorochrome-photolysis-Giemsa staining
  S-phase and, 53–58
BrdUrd antibody-binding (BAB) technique, 48, 70, 73
  condensation and, 96
  described, 68–70
  homolog discordance and, 89–90
  lateral asymmetry and, 91–92
Breakpoint cluster region gene: *see* BCR gene
Breast cancer, 231
Breast cancer estrogen-induced gene: *see* BCEI gene
5-Bromo-2'-deoxyuridine: *see* BrdUrd
Brown (type IV) oculocutaneous albinism (OCA), 19–20

cABL gene, 229
Calcium-binding epidermal growth factor (cbEGF), 163–165, 166, 173–175, 178
Cancer, NISH analysis and, 228–232
Carbonyl reductase gene: *see* CBR gene
Cardiovascular problems, in MFS, 169–173
Cat Eye syndrome (CES), 203–204

Caucasians
OCA type I in, 9, 11
OCA type II in, 16–18
C-bands, 85–86, 92
BrdUrd incorporation in S-phase and, 53–58
chromatin quantification in, 93–95
lateral asymmetry in, 90–91
CBR gene, 233
CCA: *see* Congenital contractural arachnodactyly
Charcot-Marie-Tooth (CMT) disease, 117–145
genetic diagnosis for, 135–139
genetic heterogeneity of, 120
inherited primary peripheral neuropathies related to, 119–120
pathological features of, 118–120
peripheral nerve biology studies and, 133–135
X-linked, 133, 135, 143
Charcot-Marie-Tooth type 1 (CMT1) disease, 118–119, 120, 138
Charcot-Marie-Tooth type 1A (CMT1A) disease, 120
DNA duplication in, 121–122
detection of, 135–138
homology regions and, 122–124
molecular insights and, 139–143
NISH detection of, 214–215
DNA rearrangements in, 141–143
gene dosage as mechanism for, 121–124
homologous recombination in, 140–141
NISH-assisted genome mapping of, 225
PMP22 gene and, 124, 128–129, 142, 143–145
Charcot-Marie-Tooth type 1B (CMT1B) disease, 120, 144, 214
MPZ gene and, 132, 133, 134–135, 143
Charcot-Marie-Tooth type 1C (CMT1C) disease, 120, 214
Charcot-Marie-Tooth type 2 (CMT2) disease, 119, 120
Charcot-Marie-Tooth type 4 (CMT4) disease, 120
Charcot-Marie-Tooth type 4A (CMT4A) disease, 120
Chorionic villus cells, chromosomal abnormalities in, 218–220
Chromatids, 140
lateral asymmetry in, 90–92
Chromatin, 60
BAB technique and, 70
in CMT1A, 141
FPG staining and, 65–67
quantification in R, G- and C-bands, 93–95
Chromosomal abnormalities
NISH detection in cancer, 228–232
NISH detection in interphase, 215–223
NISH detection in metaphase, 194–215
Chromosomal duplications, 197–198
Chromosome *in situ* suppression hybridization (CISS), 191–193
Chromosome microdissection, 193–194, 202
Chronic myelogenous leukemia (CML), 229
c-*kit* gene, 22, 26
CMT: *see* Charcot-Marie-Tooth disease
COLA1 gene, 129
COLA2 gene, 129
Colcemid, 50, 51
Colchicine, 51
Color-vision pigment gene, 227
Condensation, 83, 88–89, 90, 95–99
Congenital contractural arachnodactyly (CCA), 154, 180–181
Cosmid probes, NISH, 190, 193, 206, 219–220, 228
3C pause, 92–93
Cx32 gene, 134–135
CMTX disease and, 133, 135, 143
mutation analysis of, 138–139

dCTP, 52, 58
Deafness
OASD and, 20
WS and, 21, 26, 29, 205
Degenerate primed-polymerase chain reaction (DOP-PCR), 193, 198
Dejerine-Sottas syndrome (DSS), 119–120, 138
MPZ gene and, 133, 134–135, 144
PMP22 gene and, 129
Deletions
in HNPP, 122–124, 138, 139–140, 141, 145, 215
NISH detection of, 204–209
NISH detection of X-linked, 209–214
Deoxyuridylate, 52
Descending thoracic aneurysm, 172
DGS: *see* DiGeorge syndrome
DHI, 6, 34
DHICA, 6–7, 34
Diabetes, 33
3,3'-Diaminobenzidine (peroxidase-DAB), 68
DiGeorge syndrome (DGS), 204, 206
Dihydrofolate reductase, 52
5,6-Dihydroxyindole: *see* DHI

5,6-Dihydroxyindole-2-carboxylic acid: *see* DHICA
3,4-Dihydroxyphenylalanine: *see* DOPA
Dilute (*d*) gene, 32
Direct visual hybridization (DIRVISH) DNA mapping, 228
DNA, 99–100; *see also* Chromatin
  BAB technique and, 68–70
  condensation and, 97
  FPG staining and, 60–65
  NISH detection of: *see* Nonisotopic *in situ* hybridization
  quantification in R, G- and C-bands, 93–95
  rearrangements in CMT1A/HNPP, 141–143
  α-satellite, 190–191
  sn5 satellite, 202
DNA duplication: *see* Charcot-Marie-Tooth type 1A disease, DNA duplication in
DNA replication, 51–53
DNA synthesis; *see also* S-phase
  3C pause and, 92–93
  inhibitors of, 51–53
dNTP, 52
DOPA, 3–6
DOPAchrome, 6
DOPAchrome tautomerase, 6–7, 34
DOPAquinone, 6
Down syndrome, 197, 220, 221
DSS: *see* Dejerine-Sottas syndrome
dTTP, 55
Duane anomaly, 204
Duchenne muscular dystrophy (DMD), 209–211
Dural ectasia, 172
Dynamic bands: *see* Replication bands
Dystopia canthorum, 21, 26–27, 29, 205
Dystrophin gene, 209–210

Ectopia lentis, 154, 168, 172, 178
EGF: *see* Epidermal growth factor
Elastic fibers, 154–161
  composition of, 157–161
  organization and distribution of, 155–157
Elastin, 155, 157–159, 161
Elastin gene, 207
Elaunin fibers, 155
Epidermal growth factor (EGF), 161–166
  calcium-binding, 163–165, 166, 173–175, 178
Epidermal melanin unit, 7
Epidermolysis bullosa, 154
Epstein-Barr virus, 212
ETS1A gene, 226
ETS2 gene, 233
Euchromatin, 70–73, 73, 85–86, 88
Eumelanin, 6
Evolution, 232–234
Ewing's sarcoma (ES), 231
Extended chromatin fibers (ECFs), 228
Extension (*e*) gene, 6, 32
Extracellular matrix (ECM), 153, 154, 161, 167
  MFS and, 174–175, 177

Factor VIII, 143, 227
Factor IX, 174
Familial aniridia, 208
FBN1 gene, 154, 159, 166
  MFS and, 173, 175–177, 180, 181, 182
FBN2 gene, 154, 159, 166, 180–181
FdUrd, 52
Fibrillin, 157, 159, 161–167
  gene structure of, 166
  hybrid motif in, 165–166
  MFS and, 154, 173–177
  MFS-like conditions and, 180–181
  microfibrillar assembly in, 163–165, 166–167
  protein structure in, 161–166
Fibrillin 2, 161, 167, 180–181
FISH: *see* Fluorescence *in situ* hybridization
FLP, 159
Fluorescence *in situ* hybridization (FISH), 138, 191, 194
  cancer analysis and, 230–231, 232
  deletions detected with, 205, 206, 207–208
  DNA duplications detected with, 121, 214
  evolution traced with, 234
  genome mapping and, 224–227, 228
  marker chromosomes detected with, 199, 202
  mosaicism detected with, 222
  prenatal tests and, 217, 218, 219, 220, 221
  translocations and isochromosomes detected with, 197–198
  X-linked deletions detected with, 211, 214
Fluorochrome-photolysis-Giemsa (FPG) staining, 47–48, 59–68, 70, 73, 100
  alteration of BrdUrd-substituted chromatin in, 65–67
  condensation and, 96
  homolog discordance and, 89–90
  lateral asymmetry and, 91–92
  photolysis of BrdUrd-substituted DNA in, 60–65

5-Fluorouracil (5-FU), 52
Forward chromosome painting, 193
FPG staining: *see* Fluorochrome-photolysis-Giemsa staining
FU-FdUrd, 58

G-bands, 47–101
  BrdUrd incorporation in S-phase and, 53–58
  chromatin quantification in, 93–95
  distinctive features of, 99–100
  homolog discordance in, 88–90
  inactive X-chromosome and, 87–88
  juxtacentromeric area in, 85
  lateral asymmetry in, 90–92
  noncongruency in, 73–77
  patterns of, 70–73
  telomeric region of, 86–87
GBG bands, 48, 58, 70–72, 71, 73, 75–76, 83–84, 85–86
  chromatin and, 93
  condensation and, 97
  telomeric area and, 87
GBI bands, 87
Gene dosage, CMT1A and, 121–124
Genome mapping, 223–228
Germicidal lamp irradiation, 67
Glaucoma, 168
Gliomas, 231
α Globin gene, 142
β Globin gene, 142
Glucose-6-phosphate dehydrogenase (G6PD) gene, 227
G^1 phase, 51
G^2 phase, 51, 92–93
Greig craniopolysyndactyly syndrome, 226
G^1/S transition, 52–55, 90
GTG bands, 48, 50, 58, 73, 75–76, 77, 85–86, 100
  chromatin and, 95
  condensation and, 96, 97
  idiograms of, 84–85
  inactive X-chromosome and, 87

Hair color
  melanin and, 2, 7
  piebaldism and, 21
Hearing loss: *see* Deafness
Hereditary motor and sensory neuropathy type I (HNSNI): *see* Charcot-Marie-Tooth disease type 1
Hereditary motor and sensory neuropathy type II (HNSNII): *see* Charcot-Marie-Tooth disease type 2
Hereditary motor and sensory neuropathy type III (HNSNIII): *see* Dejerine-Sottas syndrome
Hereditary neuropathy with liability to pressure palsies (HNPP), 119
  deletions in, 122–124, 138, 139–140, 141, 215
  DNA rearrangements in, 141–143
  PMP22 gene and, 128–132, 144, 145
Hermansky-Pudlak syndrome, 31
Heterochromatin, 85–86
Heterochromia iridis, 26
Heteroduplex analysis, 138
Hirschsprung's disease, 26
Histone H1, 141
HNPP: *see* Hereditary neuropathy with liability to pressure palsies
Hoechst 33258, 60–65, 67, 68
Homolog discordance in replication bands, 88–90
Homologous recombination, 140–141
Hot saline treatment, in FPG, 65
Human Genome Mapping Project, 224
Hunter syndrome, 212
Hybrid motif, 165–166

Idiograms, 84–85, 97
ilv gene, 140
Inactive X-chromosome, 87–88
INAR gene, 233
Indole-5,6-quinone, 6
Inherited primary peripheral neuropathies, 119–120
  PMP22 gene and, 128–132
Interferon α receptor gene: *see* INAR gene
Interphase
  NISH detection of chromosomal abnormalities in, 215–223
  NISH genome mapping in, 227–228
Intestinal alkaline phosphatase gene: *see* ALPI gene
In vitro fertilization, 217–218
Isochromosomes, NISH detection of, 195–198

Jacobsen syndrome, 197
Joint YAC Screening Effort, 225
Juxtacentromeric area in replication bands, 85

Kallmann's syndrome, 20
KDR gene, 24, 26
KIT gene, 22–26
Klein-Waardenburg syndrome: *see* Waardenburg syndrome type III

Langer-Giedion syndrome, 209
Lateral asymmetry in replication bands, 90–92
Learning disabilities, 172
LeucoDOPAchrome, 6
leu gene, 140
Leukemia, 101, 229–231
Leukoderma, 21
Light microscopy (LM), 68, 70

Marfan's syndrome (MFS), 154, 168–182
  clinical features of, 168–172
  clinical management of, 172–173
  conditions similar to, 180–181
  fibrillin mutations in, 154, 173–177
  intrafamily varibility in, 178–180
Marker chromosomes, 198–204
Melanin, 2–8
Melanoblasts, 2–3
Melanocytes, 2–8
  development disorders in, 21–29
  function disorders in, 8–20
Melanocyte-stimulating hormone (MSH), 32, 33
Melanosomes, 3
Metaphase
  NISH detection of chromosomal disorders in, 194–215
  NISH genome mapping in, 224–227
  replication bands and, 51, 54, 83, 97
Metaphyseal chondrodysplasia, 154
metF gene, 140
Methotrexate, 50, 52–53, 58
MFS: *see* Marfan's syndrome
Mice
  cloned genes affecting pigmentation in, 30–34
  white spotting in, 22, 26
Microfibril associated glycoprotein (MAGP), 159
Microfibril associated protein (MAP), 159
Microfibrillar diseases, 153–182; *see also* Fibrillin; Microfibrils; specific diseases
Microfibrils, 154–161
  assembly in fibrillin, 163–165, 166–167
  composition of, 157–161
  organization and distribution of, 155–157
Microphthalmia (*mi*) gene, 29, 31–32
Miller-Dieker syndrome (MDS), 205–206
MITF gene, 29, 31–32
Mitotic phase, 50, 51, 53, 58, 83
Mitral-aortic-skin-skeletal (MASS) phenotype, 180
Mitral valve prolapse, 171, 178, 180
Mononucleosis, 212
Monosomy 7, 230–231
Moroccan Jews, OCA type I in, 15
Morphologic bands, 47–101; *see also* G bands; R bands
  patterns of compared with replication bands, 73–84
Mosaic exons, 166
Mosaicism, 221–222
Mottled (*mo*) gene, 30
MPZ gene
  CMT1B and, 132, 133, 134–135, 143
  DSS and, 133, 134–135, 144
  mutation analysis of, 138–139
Mucopolysaccharidosis II (MPSII): *see* Hunter syndrome
Mutation analysis, of CMT-associated genes, 138–139
Myelin basic protein (MBP), 135
Myelin protein zero gene: *see MPZ* gene
Myelodysplastic syndromes, 230
Myeloproliferative disorders, 230–231
Myopia, 168, 178

Nettleship-Falls (X-linked recessive) type ocular albinism (OA1), 20
Neural crest
  melanocytes in, 2
  piebaldism and, 21–22
  WS and, 26
Neuroblastoma, 232
NISH: *see* Nonisotopic *in situ* hybridization
Nonisotopic *in situ* hybridization (NISH), 187–235
  cancer and, 228–232
  deletions detected with, 204–209
  DNA duplications detected with, 214–215
  evolution traced with, 232–234
  genome mapping and, 223–228
  isochromosomes detected with, 195–198
  marker chromosomes detected with, 198–204
  mosaicism detected with, 221–222
  prenatal tests and, 215–221

Nonisotopic *in situ* hybridization (NISH) (*cont.*)
probes used in, 190–194
radiation-induced damage detected with, 222–223
somatic pairing detected with, 223
translocations detected with, 195–198
X-linked deletions detected with, 209
Nystagmus, 15

OA1: *see* X-linked recessive ocular albinism
OA1 gene, 20
OASD: *see* X-linked ocular albinism and deafness
OCA: *see* Oculocutaneous albinism
Ocular albinism
autosomal recessive, 18, 20
X-linked recessive, Nettleship-Falls type, 20
Oculocutaneous albinism (OCA), 1
autosomal dominant, 15
type I, tyrosinase-deficient, 8–15
type II, tyrosinase positive, 15–19
type IV, brown, 19–20
Oxytalan fibers, 155

Paired box genes, 27–28
Pallid (*pa*) gene, 30–31
Patch (*Ph*) gene, 26
Pax-3 gene, 27–29, 205, 227
PCR: *see* Polymerase chain reaction
PDGFRA gene, 24, 26
Pearl (*pe*) gene, 31
Pelizaeus-Merzbacher disease, 143
P gene, 15–19
Pheomelanin, 6, 15
Philadelphia chromosme, 229
pHY2.1 probe, NISH, 215
Piebaldism, 21–26
Pigmentation disorders, 1–34; *see also* specific disorders
cloned genes affecting in mouse, 30–34
melanocyte development in, 21–29
melanocyte function in, 8–20
Pigmentation system, 2–8
Plasmid probes, NISH, 190
PLP gene, 143
PMP22 gene, 134
CMT1A and, 124, 128–129, 142, 143–145
DSS and, 129
HNPP and, 128–132, 144, 145
mutation analysis of, 138–139
Poliosis, 21
Polymerase chain reaction (PCR), 138, 139, 141, 188–189, 193–194
degenerate-primed, 193, 198
deletions detected with, 207, 209
marker chromosomes detected with, 202
prenatal tests and, 217
reverse-transcription, 209, 211
translocations and isochromosomes detected with, 195
Prader-Willi syndrome (PWS), 16, 90
deletions in, 208–209
SMCs in, 199, 203
Preimplantation tests, 217–218
Prelymphocytic leukemia (B-PLL), 230
Premature termination codons (PTC), 175–176
Premelanosomes, 3
Prenatal tests, 215–221
Preparative *in situ* hybridization (pre-ISH), 194
Presynchronization, in S-phase, 52
Primary cardiomyopathy, 172
Probes, NISH, 190–194
Prophase, 51, 52, 97
Prostatic cancer, 231
Protrusio acetabulae, 172
Puerto Ricans, OCA type I in, 15
Pulmonary artery dilation/dissection, 171–172
Pulsed-field gel electrophoresis (PFGE), 138
PWS: *see* Prader-Willi syndrome

Radiation-induced chromosome damage, 222–223
R-bands, 47–101
BrdUrd incorporation in S-phase and, 53–58
chromatin quantification in, 93–95
distinctive features of, 99–100
homolog discordance in, 88–90
inactive X-chromosome and, 87–88
juxtacentromeric area in, 85
lateral asymmetry in, 90–92
noncongruency in, 73–77
patterns of, 70–73
telomeric region of, 86–87
RBG bands, 48, 58, 70–72, 79–82, 83–84, 85–86, 100
chromatin and, 93, 95
condensation and, 97
lateral asymmetry and, 91
noncongruency with RHG bands, 73–77
telomeric area and, 86–87
RBI bands, 86, 87
Release, in S-phase, 52, 54

Renal cell carcinoma (RCC), 226
Replication asynchrony, 88–90
Replication bands, 47–101
  condensation and, 83, 88–89, 90, 95–99
  homolog discordance in, 88–90
  inactive X-chromosome and, 87–88
  juxtacentromeric area in, 85
  lateral asymmetry in, 90–92
  patterns of, 70–73
  patterns of compared with morphologic bands, 73–84
  telomeric region of, 86–87
Restriction fragment length polymorphism (RFLP), 205, 206
Retinal detachment, 168
Retinal pigmentation, 20
Retinitis pigmentosa, 143–144, 226
Reverse chromosome painting, 193, 198
Reverse-transcription-polymerase chain reaction (RT-PCR), 209, 211
R/G transition, 52–53, 72, 100
  BrdUrd incorporation in S-phase and, 53–58
  3C pause and, 92–93
  homolog discordance and, 90
  inactive X-chromosome and, 87–88
RHG bands, 75–76, 85–86, 100
  chromatin and, 95
  condensation and, 96, 97
  idiograms of, 84–85
  inactive X-chromosome and, 87
  noncongruency with RBG bands, 73–77
Rhodopsin gene, 143–144
Ribonucleotide reductase, 52
Rubenstein-Taybi syndrome (RTS), 207–208

α-Satellite DNA, 190–191
sn5 Satellite DNA, 202
Scanning electron microscopy (SEM), 64
Schmid form of metaphyseal chondrodysplasia, 154
Schwann cell defects, in CMT, 118, 120, 135
Scoliosis, 168, 180
Sex-related Y gene: *see* SRY gene
Silver (*si*) gene, 34
Single-strand conformation polymorphism, 138
Skeletal system, in MFS, 168–169
Skin pigmentation
  melanin and, 7
  piebaldism and, 21
Slaty (*slt*) gene, 33–34
Small cell lung carcinomas, 226, 227
SMCs: *see* Supernumerary marker chromosomes
Smith-Magenis syndrome (SMS), 209, 225
SOD1 gene, 233
Somatic pairing, 223
Southern blotting, 138
  deletions detected with, 207
  marker chromosmes detected with, 202, 203
  X-linked deletions detected with, 209
S-phase
  BrdUrd incorporation and, 53–58
  3C pause in, 92–93
  homolog discordance and, 90
  replication bands and, 48, 51–53, 83
  synchronization techniques in, 51–52
Splotch (*Sp*) gene, 27–28, 205
Spontaneous aniridia, 208
Spontaneous pneumothorax, 172
SRY gene, 195
Striae disease, 172, 178
Structural bands: *see* Morphologic bands
Supernumerary marker chromosomes (SMCs), 198–204
Superoxide dismutase 1 gene: *see* SOD1 gene
Supravalvular aortic stenosis, 207
Synchronization, in S-phase, 52

T-bands, 97
TBP culture method: *see* Thymidine-BrdUrd culture method
TDY gene, 195
Telomeric region of replication bands, 86–87
Testicular differentiation gene: *see* TDY gene
Testicular tumors, 231
TGF: *see* Transforming growth factor
Thalassemia, 142
THG bands, 95
thr gene, 140
Thymidine-BrdUrd permutation (TBP) culture method, 47–48, 73, 84, 100, 101
  homolog discordance and, 89–90
  R/G transition and, 87, 88
  S-phase and, 55–58
Thymidylate, 52
Thymidylate synthetase, 52
Tigroid retinal pigmentation, 20
Tomaculous neuropathy: *see* Hereditary neuropathy with liability to pressure palsies
Topoisomerase I (Topo I), 194
Topoisomerase II (Topo II), 141

Transforming growth factor-β1 (TGF-β1), 165, 166
Translocations, NISH detection of, 195–198
Transmission electron microscopy (TEM), 64, 68, 70, 96
Trembler mouse, 128
Tricuspid valve prolapse, 171
Trisomy 18, 221
Trisomy 21, 219–220, 221
Tropoelastin, 157
TRP-1, 19, 33
TRP-2, 33–34
Turner syndrome, 197
Type I (tyrosine-deficient) oculocutaneous albinism (OCA), 8–15
Type IA oculocutaneous albinism (OCA), 9, 10, 11
Type IB oculocutaneous albinism (OCA), 9, 10, 11
Type II (tyrosine-positive) oculocutaneous albinism (OCA), 15–19
Type IV (brown) oculocutaneous albinism (OCA), 19–20
TYR gene, 9–15
Tyrosinase-related protein: *see* TRP-1
Tyrosine, melanin production and, 3–6
TYRP gene, 19–20

Ultraviolet (UV) light
  FPG staining and, 61–67
  melanin protection from, 2
Uridine, 69
Urinary bladder cancer, 231

von Hippel-Lindau disease (VHL), 226, 227

Waardenburg syndrome (WS), 21, 26–29
  deletions in, 204–205
  Pax-3 gene and, 27–29, 205, 227
Waardenburg syndrome type I (WS1), 26, 28–29, 205, 227
Waardenburg syndrome type II (WS2), 26, 29, 205
Waardenburg syndrome type III (WS3), 26–27, 28–29
WAGR locus, 208
White spotting, in mice, 22
Williams syndrome, 207
Wilms' tumor gene: *see* WT1 gene
Wolf-Hirschhorn syndrome, 209
WS: *see* Waardenburg syndrome
WT1 gene, 208

X-linked agammaglobulinaemia (XLA), 224
X-linked Charcot-Marie-Tooth (CMTX) disease, 133, 135, 143
X-linked deletions, 209–214
X-linked ichthyosis, 20
X-linked lymphoproliferative (XLP) disease, 212–214
X-linked ocular albinism and deafness (OASD), 20
X-linked (Nettleship-Falls type) recessive ocular albinism (OA1), 20
XYY males, 216

YAC chromosome, 20
YAC probes, NISH, 190, 193, 206, 219–220, 224–225, 228
Yellow-red pheomelanins, 15
Yp probes, NISH, 195–197